Establishing an evidence-based foundation for the integration of emerging technologies in 3D GIScience

by

Ian Lochhead

Master of Science, Simon Fraser University, 2017

Bachelor of Arts, Simon Fraser University, 2015

Thesis Submitted in Partial Fulfillment of the
Requirements for the Degree of
Doctor of Philosophy

in the
Department of Geography
Faculty of Environment

SIMON FRASER UNIVERSITY

Summer 2022

Declaration of Committee

Name:	**Ian Lochhead**
Degree:	**Doctor of Philosophy (Geography)**
Title:	**Establishing an evidence-based foundation for the integration of emerging technologies in 3D GIScience**
Committee:	**Chair:** **Nadine Schuurman** Professor, Geography
	Nick Hedley Supervisor Associate Professor, Geography
	Arzu Çöltekin Committee Member Professor, Institute for Interactive Technologies FHNW University of Applied Sciences and Arts Northwestern Switzerland
	Brian Fisher Committee Member Professor, Interactive Arts & Technology
	Peter Keller Examiner Professor, Geography
	Vincent Tourre External Examiner Associate Professor, Ambiances Architectures Urbanitès (AAU-CRENAU) ENSA/Ecole Centrale de Nantes, France

Ethics Statement

The author, whose name appears on the title page of this work, has obtained, for the research described in this work, either:

a. human research ethics approval from the Simon Fraser University Office of Research Ethics

or

b. advance approval of the animal care protocol from the University Animal Care Committee of Simon Fraser University

or has conducted the research

c. as a co-investigator, collaborator, or research assistant in a research project approved in advance.

A copy of the approval letter has been filed with the Theses Office of the University Library at the time of submission of this thesis or project.

The original application for approval and letter of approval are filed with the relevant offices. Inquiries may be directed to those authorities.

Simon Fraser University Library
Burnaby, British Columbia, Canada

Update Spring 2016

Abstract

Geography is increasingly reliant on modern technology and rapid technological advancements have inspired novel uses of these technologies for geospatial applications. Geographic Information Systems (GISs) themselves, the backbone of contemporary geospatial analyses, were once considered a novel technology in search of an application, and it was not until Geographic Information Science (GIScience) established the science of GIS that GIS earned its legitimacy as a scientific tool. In many ways, emerging geospatial technologies (EGTs), or technologies that have only recently been adopted for geospatial applications (i.e., data capture, analysis, or delivery), are experiencing the same challenges as early GISs. EGTs such as Structure from Motion (SfM) and Extended Reality (XR) have experienced increased adoption in the geospatial realm despite uncertainty surrounding their use and usefulness as spatially rigorous 3D GIScience tools. There is a need for the 3D GIScience that supports the use of these EGTs as legitimate scientific tools. In this dissertation, five manuscripts are presented: 1) a novel SfM workflow and a series of performance benchmarks quantifying the impact that camera, camera settings, lighting, and capture strategy have on 3D data accuracy; 2) an assessment of a SfM workflow in a simulated temperate benthic environment and the impact that underwater camera equipment has on 3D data accuracy; 3) an evaluation of temperate marine SfM performance and the opportunity for XR based 3D data visualizations of complex morphology; 4) a discussion on the design and development of immersive virtual environments for geospatial visual analytics and the interpretation of 3D spatial data sets, and; 5) an immersive mental rotations test to evaluate the impact that virtual reality based visualizations and 3D virtual environments have on mental rotation task performance. These five manuscripts explore and evaluate SfM and XR as EGTs for 3D data capture, visualization, and analysis. This research endeavors to strengthen the empirical foundation supporting the use of these EGTs as legitimate geospatial technologies for 3D GIScience and geospatial visual analytics.

Keywords: 3D GIScience; 3D Geovisualization; Emerging Geospatial Technology; Spatial Ability; Structure from Motion; Virtual Reality

Dedication

To all those who supported me along the way

Acknowledgements

Thank you to my supervisor, Nick Hedley for your help and support throughout this journey. I am grateful that our paths crossed – your passion for what you do changed my life. And of course, thank you for swimming in that cold, dark, and dirty fish tank when a broken leg kept me from capturing my own data.

Thank you to my committee for your guidance and your commitment to ensuring my progress despite these challenging times.

Thank you to the past members of the Spatial Interface Research Lab - Sam, Ruslan, and Sonja. Thank you to the Department of Geography and all those who I worked with along the way.

To my wife and kids, your love and encouragement means the world to me. Thank you.

Table of Contents

List of Tables

List of Figures

Chapter 1.

Introduction

1.1. Foreword

This dissertation focuses on the use of emerging geospatial technologies (EGTs) in contemporary 3D geographic information science (GIScience), examining structure from motion (SfM) photogrammetry and extended reality (XR) interfaces as spatially rigorous 3D GIScience tools.

Crucially, this dissertation addresses a considerable challenge facing EGT use, as while EGTs receive increased attention with rising popularity across an array of geospatial applications, there is a need for commensurate 3D GIScience that allows us to understand how established subfields of GIScience play out in an EGT world. The adoption of EGTs for geospatial applications should not be driven by a *because we can* mindset but must be supported by empiricism for EGT use to be anything more than technological novelty. In this dissertation, presented through applied work and demonstrated through empiricism, I highlight how EGT use is not just about the technology but the GIScience within it.

The research presented in this dissertation was significantly influenced by the context of an internship I held, as the result of a MITACS-funded collaboration between the Spatial Interface Research Lab, and Ocean Wise and the Vancouver Aquarium. These organizations sought out research partners to study underwater SfM and the prospect of implementing underwater SfM to monitor glass sponge morphology in temperate marine environments. This internship, as advertised, was the epitome of a technology driven research project: led by a desire to *apply* a novel technology (SfM) to produce compelling 3D data outputs, rather than a desire to *understand* the capabilities of the spatial data acquisition technology and to evaluate the quality of spatial data products that resulted. This was a good example of how 3D data generation methods (such as SfM) have rapidly gained popularity across a wide range of spatial characterization domains (such as Earth science, urban characterization, ecological monitoring, archaeology), to produce compelling 3D data products. However, this trend has resulted in a wide range of unique implementations, with limited or highly variable

consideration of representational veracity. These considerations are fundamental in GIScience and geovisualization and should be at the foundation of integrating new 3D data, visualization, and interactive methods with spatial reality capture - both within and outside of GIScience itself.

This dissertation is not focused solely on SfM but applies a GIScience perspective to SfM and other emerging methods to critically assess the performance of an EGT and highlight how – as part of evolving 3D GIScience methods – well-intended (but unsophisticated) 3D data acquisition workflow decisions can translate to inaccurate characterizations and outcomes. Simply adopting new 3D data generation methods (such as SfM) to generate data without understanding what that data represents is of little scientific value and the advertised approach of the MITACS proposal misses critical opportunities to address questions surrounding 3D spatial characterization and representational veracity. We can also see across several literatures, that acritical visualization of 3D data in emerging 3D visualization interface platforms also misses key opportunities to generate experience from which new theory and conceptual models may inform other EGTs (XR interfaces) for 3D spatial data visualization. These deeper engagements are important to reveal the collective potential for SfM and XR to mediate the representation and interpretation of complex spatial phenomena.

In many ways, this dissertation explores the differences between the *use* and *usefulness* of EGTs. Much like Goodchild (1992) sought to legitimize the use of geographic information systems (GISs) in supporting other sciences through the science of GIS (i.e., GIScience), there is a need to legitimize the use of EGTs in GIScience. EGT *use* without the science supporting it may not be that *useful* for GIScience. As the MITACS internship was written, it would have almost certainly determined that a SFM workflow can produce 3D models of glass sponges in temperate marine environments. In other words, that SfM can be *used* to generate 3D data. However, it is unlikely that that internship would have determined the *usefulness* of SfM as a glass sponge monitoring tool, as the internship was not designed to develop the science – to assess 3D data quality or understand the impact that idiosyncratic sets of variables have on SfM-based 3D data quality – supporting SfM use. In other words, it would not have proven that SfM is *useful*.

The objective of this dissertation was to establish an empirically grounded foundation for the *use* of EGTs (namely SfM and XR) as *useful* 3D GIScience tools. While the MITACS internship was written to explore the possibility of 3D data capture in temperate waters, it was not the technology itself, nor the act of 3D data capture, that was of value to Ocean Wise and the Vancouver Aquarium. The true value lay in understanding what these technologies can and cannot do – in the accuracy of the 3D data products and the ability to monitor changing glass sponge morphology through time. This then not only requires accurate 3D data, but effective 3D visualizations and analytical frameworks for 3D data exploration and interpretation, as what is done with the data can be just as important as the data itself.

EGTs can be *used* by almost anyone to capture, visualize, and analyze geospatial phenomena. However, I ask, "what is the point in capturing 3D data or developing 3D visualizations if they are not implemented or developed effectively?" Simply *using* EGTs does not make them *useful*. The MITACS internship epitomized this; the applied use of an EGT is not inherently useful. In this dissertation I unpack the use of SfM and XR, significantly informed by my experiences with the MITACS internship, to elucidate the usefulness of these EGTs. Here it is in the ability to generate highly accurate 3D data characterizing complex 3D phenomena, to affect the human ability to perceive and mentally manipulate 3D phenomena, and to extend the space of analytical practice through immersive, interactive, and experiential interfaces. While SfM-based 3D models and novel XR-based visualizations have gained popularity in a changing, technology enabled, geospatial economy, photorealism and immersion must not be confused for accuracy and effectiveness. As EGTs, SfM and XR hold significant potential as 3D GIScience tools. This dissertation serves to strengthen an empirical foundation that supports their use as useful EGTs for 3D GIScience.

1.2. Emerging Geospatial Technologies

Technology and geography have become inextricably linked. Every geospatial data function, from data capture, storage, and operation to analysis and communication can be performed with, and is increasingly reliant on, the support of modern geospatial technology. Furthermore, geospatial technologies have become intertwined with virtually all aspects of human activity, from problem solving, decision making, and simulation to the discovery and explanation of the Earth's environmental and social

systems (Dangermond & Goodchild, 2020). While these technologies have and will continue to shape the relationship between humans, geospatial data, and the world around us, rapid technological advancement and the constant, unpredictable evolution of the social, economic, political, and environmental contexts in which geospatial technologies are applied will inevitably contribute to the emergence of new geospatial technologies, and new uses for those technologies, that help to address the modern geospatial challenges facing humanity (Dangermond & Goodchild, 2020).

The concept of *geospatial technology* describes a wide-range of technological tools that are not necessarily geospatial by design, but are useful in the collection, processing, or analysis of geospatial data (Fagin et al., 2020). These technologies, starting with those first used to digitize maps and Earth images, have evolved over the last half century (Dangermond & Goodchild, 2020). EGTs on the other hand, are the *location-based* tools that have only recently been embraced for geospatial applications, regardless of whether they are new technologies (Fagin et al., 2020). While this definition adopts location-based as a defining feature of EGTs, *location-based* invokes expectations regarding global positioning system (GPS) sensors when not all EGTs are equipped with such features. Location is a fundamental component of EGTs, and of geospatial data in general, however describing EGTs as location-based tools does a disservice to the EGTs that are *spatially rigorous* but are not explicitly location-based.

EGTs can be broadly classified, according to their geospatial data function, as those which are used for data analysis, data capture, or data delivery; however, these classifications are not mutually exclusive and one piece of emerging technology can perform multiple data functions (Fagin et al., 2020). EGTs can be further categorized according to type into seven different EGT categories: autonomous and semi-autonomous vehicles, Global Navigation Satellite System (GNSS) services, web-mapping technologies, laser scanning services, location-based services (LBS), virtual reality (VR), and peripheral devices (Fagin et al., 2020). While these classifications and categories were useful for characterizing EGTs in the survey conducted by Fagin et al. (2020), their schema does not, nor does it pretend to, qualify every EGT, and at the same time identifies technology that has long past the emergence stage. This then raises questions as to what qualifies any given piece of technology as an *emerging* geospatial technology.

1.3. Emerging Technology

Defining a given technology as an emerging technology elicits ideations of a technological breakthrough, yet technology need not be new to be recognized as emergent. In an evaluation of major innovation studies, a set of key foundational elements qualifying any given technology as emerging technology were identified; these elements are: radical novelty, (relatively) fast growth, coherence, prominent impact, and uncertainty and ambiguity (Rotolo et al., 2015) (Figure 1.1). Rotolo et al. (2015) used these elements to craft their definition of emerging technology as:

> "…a relatively fast growing and radically novel technology characterized by a certain degree of coherence persisting over time and with the potential to exert a considerable impact on the socio-economic domain(s) which is observed in terms of the composition of actors, institutions and the patterns of interactions among those, along with the associated knowledge production processes. Its most prominent impact, however, lies in the future and so in the emergence phase is still somewhat uncertain and ambiguous."

Each of the five key elements are prominently featured in this definition of emerging technology. However, in unpacking each component, it is evident that technology can entre, or re-entre, the emergent stage at any point in its lifecycle. For a technology to be radically novel it does not need to be new, but rather have a new purpose, function, or use; for it to exhibit relatively fast growth it can experience an increase in the number of actors involved, the quantity of funding received, the total knowledge produced, or the volume of products or services generated; for it to have coherence the technology cannot be purely conceptual but has already established a community of practice with unifying internal characteristics that stand up to external forces; for it to have a prominent impact it can lead to the creation or transformation of industry, produce wide-ranging benefits for diverse actors, or exert economic influence; and, perhaps most importantly, there is uncertainty and ambiguity surrounding its future potential, what will come of its use, and whether it will result in unintended or undesirable outcomes (Rotolo et al., 2015).

With this unpacked definition of emerging technology in mind, it is conceivable that any spatially rigorous technology, already in existence or yet to be conceived, could become an EGT. Of the seven EGT categories identified by Fagin et al. (2020), none explicitly refers to a technology with a singular purpose that has not evolved over time.

This technological evolution is a necessary step towards technological novelty, which in turn paves the way for growth, coherence, impact, and uncertainty. This dissertation explores structure from motion (SfM) photogrammetry and extended reality (XR) technology, two EGTs that are not *new* technologies but are novel, fast growing, coherent technologies that have had a prominent impact on geospatial data capture and visualization despite the uncertainty that surrounds their usefulness and future potential in 3D GIScience.

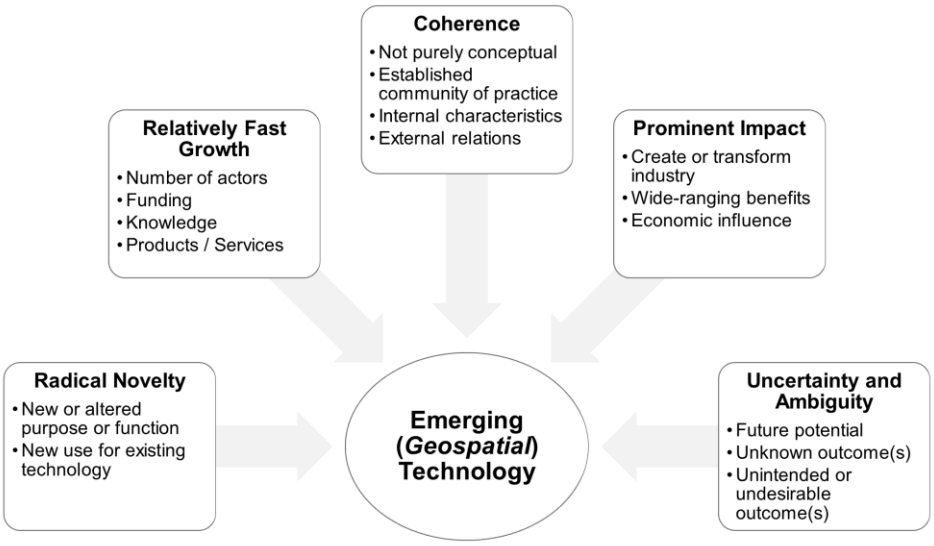

Figure 1.1 Emerging technology is characterized by its novelty, fast growth, coherence, impact, and uncertainty and ambiguity. EGTs are emerging technologies with a geospatial data function, including data capture, storage, operation, analysis, and visualization.

1.4. Structure from Motion (SfM) Photogrammetry

Photogrammetry allows for the measurement of features by analyzing overlapping photographs that provide alternate perspectives of those features. Based on the fundamentals of trigonometry, the technique was first realized and instituted by a French Army surveyor conducting a ground-based topographical survey in the 1850s; while the term “photogrammetry” was later introduced by a German architect (Luhmann & Robson, 2006; McCarthy, 2014). Photogrammetry represents a passive form of remote sensing that enables 3D reconstruction of the shape and location of features

using a single image (single image photogrammetry), two images (stereophotogrammetry), or multiple images (multi-image photogrammetry) (Luhmann & Robson, 2006). The 3D spatial attributes of target features are determined by reconstructing rays from each camera location through the perspective centre to each image point, requiring both the intrinsic orientation parameters of the camera as well as its 3D location (extrinsic parameters) at the time the photographs were captured (Luhmann & Robson, 2006; Remondino et al., 2012). The intrinsic and extrinsic parameters of each camera are defined through camera calibration, a process that distinguishes the stereophotogrammetric approach from that of multi-image photogrammetry (Luhmann & Robson, 2006).

Multi-image photogrammetry (more commonly known as structure from motion or SfM) enables 3D reconstruction and measurement of features from two or more 2D images. SfM emerged in the 1990s with the arrival of digital photogrammetry, and owes much of its existence to the computer vision community and the feature-matching algorithms introduced during the 1980s (McCarthy, 2014; Westoby et al., 2012). While the photogrammetric community favors geometric quality over automation, those from computer vision stressed the importance of automation and auto-calibration, features characteristic of modern SfM software packages (Remondino et al., 2012). Several SfM software solutions have emerged since the mid-2000s, making multi-image photogrammetry accessible and attractive to a wide-range of research disciplines (McCarthy, 2014).

SfM exhibits all the characteristics of an emerging technology. While the arrival of SfM in the 1990s established its place as an EGT for spatial data capture, the release of modern SfM software packages in the mid/late 2000s drove rapid growth and solidified its EGT status. These user-friendly software packages stimulated new professional and academic applications, leading to a consistent period of growth that was only disrupted by a global pandemic (Figure 1.2). However, it is the uncertainty and ambiguity that surrounds these “black-box” software packages - which effortlessly transform 2D photographs into 3D data – and their role in GIScience that are of particular interest.

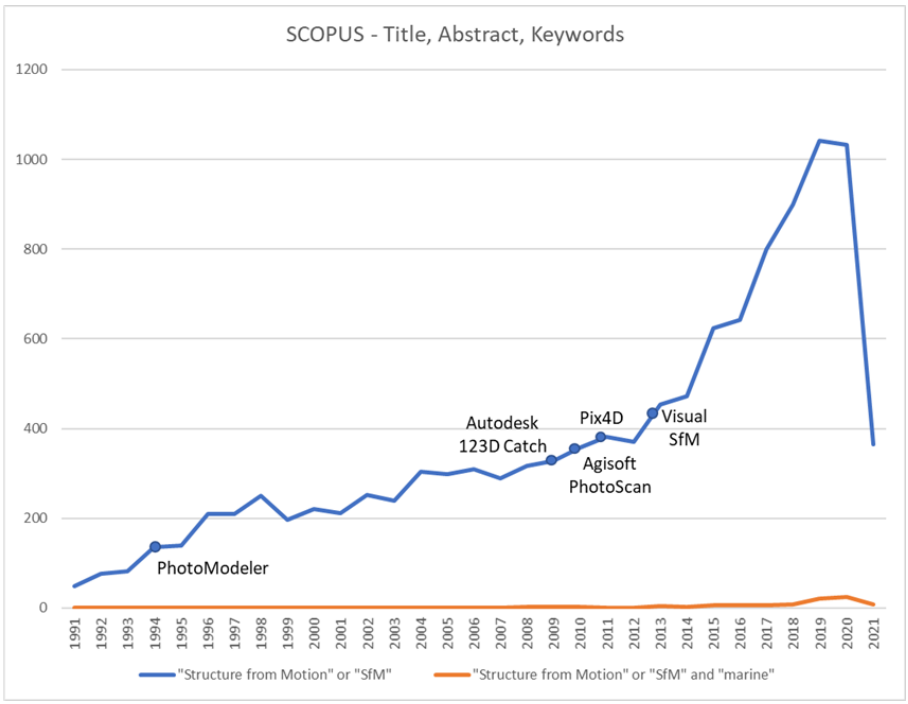

Figure 1.2 **The results of a Scopus database search (May 25, 2021) for article titles, abstracts, or keywords containing "structure from motion" or "SfM" as well as for "structure from motion" or "SfM" and "marine." While there appears to be consistent growth in relevant literature throughout the 1990s and 2000s, the introduction of user-friendly SfM software in the late 2000s and early 2010s spurred rapid growth in SfM related publications. Marine applications did not follow the same growth curve, and only in the late 2010s was there an uptick in publications referencing marine SfM.**

The accuracy of SfM-based 3D data is directly correlated to the quality of the photographs that are used to generate that data. For the terrestrial applications that have dominated the research literature, high-quality photographs are relatively easy to capture. However, for the marine applications that have emerged more recently, as SfM workflows are implemented to produce 3D characterizations of benthic phenomena, the addition of water between camera and subject presents challenges for high-quality photography; water refracts and attenuates light and is seldom devoid of sediment and other debris. While it is not impossible to generate high-quality photographs that produce high-quality 3D data in terrestrial or marine applications, the attention given to SfM workflows is seldom sufficient to quantify accuracy as a product of those workflows. It is quite easy to capture an overlapping collection of photographs and generate 3D data yet understanding precisely how the chosen workflow impacts SfM data quality is not so simple. For SfM to become a useful GIScience tool for documenting the

morphometry of complex 3D phenomena, further research which explores the relationship between data capture strategy and data accuracy is required. SfM practitioners must be intentional with their SfM workflows and must understand the implications that idiosyncratic sets of variables have on the quality of their 3D data products.

1.5. Extended Reality (XR)

Extended reality (XR) is an umbrella term that describes virtual reality (VR), augmented reality (AR), and mixed reality (MR) technologies. The XR moniker has gained traction throughout academia and industry despite the stark differences that exist between each of the constituent technologies. Milgram & Kishino (1994) introduced the *virtuality continuum* as a taxonomy for what was then a growing collection of visual displays – all of which would now be considered XR. At opposing ends of their continuum are real environments – composed entirely of real objects – and virtual environments – composed solely of virtual objects. Mixed reality – composed of real and virtual objects – occupies the middle ground between real and virtual and can be further subdivided into AR and AV (augmented virtuality) according to the proportions of real and virtual objects. While the continuum considers AR to be a form of MR, modern discourse considers AR and MR to be different technologies, where AR simply superimposes virtual objects anywhere in real space and MR enables meaningful interactions between real and virtual objects according to a shared spatial reference frame (Çöltekin et al., 2020; Hedley, 2017). Regardless of the technology or how we refer to it, we are amid a period of rapid growth in XR applications.

XR technologies are EGTs. VR, AR, and MR are all currently experiencing a period of rapid growth (Figure 1.3); new uses are constantly emerging, there is an established community of practice, and XR has had a significant impact on the geospatial community. However, many questions regarding the future role of XR, what it enables, who it best suited for, and how and where it should be applied remain unanswered. While the release of new VR and MR consumer hardware in 2016 solidified XR as an EGT, it is the applied research that will determine the usefulness of XR for geospatial applications.

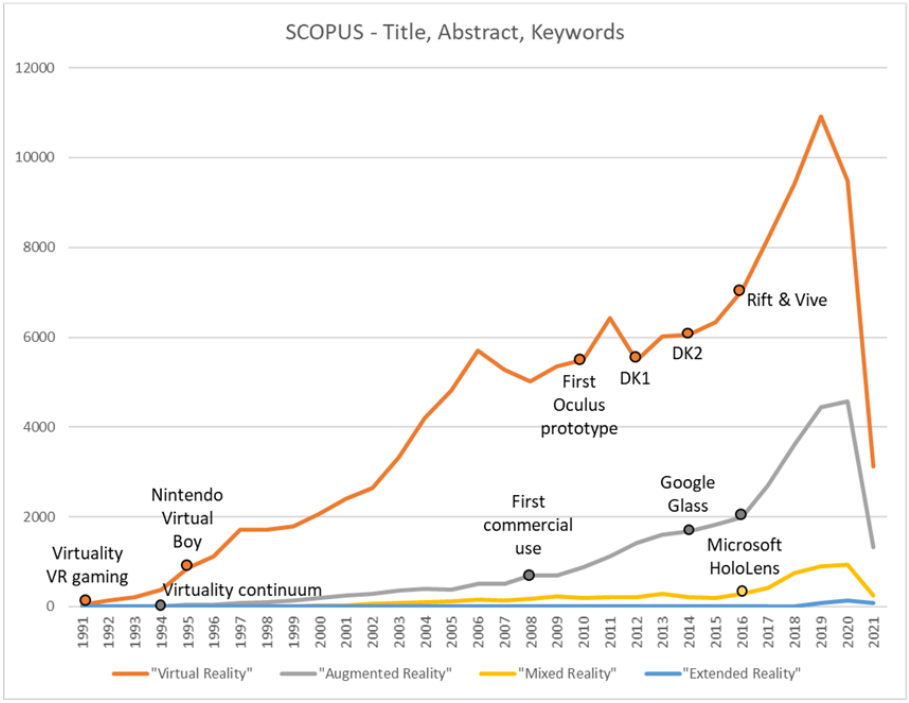

Figure 1.3 A Scopus database search (May 25, 2021) for article titles, abstracts, or keywords containing virtual reality, augmented reality, mixed reality, or extended reality. The release of key pieces of XR technology are noted for reference.

XR technology has the power to change the relationship between people, data, and geospatial phenomena. However, while the immersive, situated, and collaborative experiences enabled by these technologies may be powerful, what proves transformative for one user may be confusing, uncomfortable, or unnecessary for the next. User studies should therefore be at the forefront of geospatial XR research, exploring the affordances and limitations of XR technologies for 3D geospatial data visualization and analysis, and evaluating the design of XR interfaces to ensure that they are usable and useful. Furthermore, while XR may be a convenient and popular term, it is critical that we acknowledge that the individual pieces of technology (VR, AR, and MR) that constitute XR are not one and the same; research on XR design, the impact of XR, or XR applications may unnecessarily limit our awareness of the use, user, data, and technology combinations and their impact on geospatial data visualization and analysis.

1.6. The Opportunity for Emerging Technologies in 3D GIScience

SfM and XR are EGTs that will have a significant impact on geospatial data collection, delivery, and analysis. Recent innovations in both SfM and XR technologies have inspired novel applications and rapid growth across academia, industry, and society in general, influencing the way 3D (geospatial) phenomena are characterized and visualized. Yet the extent of their role in the future of 3D GIScience remains very much unknown. While sensationalistic product launches, such as Apple's RealityKit Object Capture, promise 'lifelike' 3D models that can be integrated into XR applications, there are critical questions that must be asked to uncover the true value that these technologies hold as rigorous 3D GIScience tools. The opportunity for 3D GIScience lies in defining that rigor, understanding what geospatial data can be collected, how accurately that data can be collected, and how visualizing and analyzing that data using XR technology impacts our ability to perceive and comprehend 3D spatial phenomena. This dissertation presents two research efforts centered around EGTs and 3D GIScience: 1) high-accuracy and high-resolution *3D data capture* – investigated through a remote and challenging underwater application; and 2) XR-based *3D data visualization and analysis* – focused on spatial ability (mental rotation) as mediated by XR technology, and the design of immersive virtual environments (VEs) for geospatial visual analytics.

As an EGT, SfM has revolutionized 3D data capture. User friendly SfM workflows and software packages allow non-experts to rapidly convert 2D photographs and videos into photorealistic 3D models. This ease of access and ease of use has resulted in rapid growth and new applications in domains that recognize the value in generating the 3D data that may once have been inaccessible; including surveys documenting the structure of coral reefs (Bennecke et al., 2016; Casella et al., 2017; Gutierrez-Heredia et al., 2016; Pizarro et al., 2017), reconstructing ancient shipwrecks (Balletti et al., 2016; Beltrame & Costa, 2017; McCarthy & Benjamin, 2014) and human built structures (Balletti et al., 2015; De Reu et al., 2013; McCarthy, 2014), and mapping dynamic landscapes (Dietrich, 2016; Javernick et al., 2014; Kalacska et al., 2017). However, photorealism is not synonymous with accuracy, which is fundamental to many 3D GIScience applications, and it is critical that practitioners define the level of accuracy necessary to properly characterize the phenomena within the context of their analysis, that they understand the potential for any given workflow to deliver that accuracy, and

that they understand how idiosyncratic variables (e.g., camera settings and lighting) impact their ability to produce accurate models. Addressing the uncertainty and ambiguity that surrounds the *accuracy* of SfM is a critical step in the adoption of SfM for spatially rigorous 3D GIScience.

XR technologies have emerged as advanced (geo)visualization interfaces with the potential to transform 3D GIScience. With XR, (3D) spatial data is no longer constrained by the 2D confines of conventional desktop interfaces, but can be visualized and analyzed through interactive, experiential, immersive, situated, and collaborative interfaces. XR has proven useful in the visualization and analysis of geological features for mine exploration (Antoniou et al., 2020) and virtual fieldwork (Zhao et al., 2019), for exploring marine ecosystems (Hruby et al., 2019) and coastal futures (Rydvanskiy & Hedley, 2020), for experiencing virtual simulations in situ (Hedley & Lonergan, 2012; Lochhead & Hedley, 2018; Lonergan & Hedley, 2015), and for communicating historical narratives (Pulver et al., 2020; Romano & Hedley, 2021) While VR, AR, and MR technologies have been the subject of many research projects over the last several decades, the ability for these technologies to transform widespread 3D GIScience practice (or any domain for that matter) was restricted by their limited accessibility. However, the democratization of XR technologies over the last decade has inspired new uses and users for XR and provided an unprecedented ability to advance the science supporting XR's utility within 3D GIScience. Yet, just because we can does not mean we should - as the who, what, where, when, and whys of XR in 3D GIScience remain largely unanswered.

This dissertation presents a compilation of manuscripts inspired by an expressed desire to create 3D models of glass sponge bioherms. However, it is not the models themselves but an awareness for what the 3D data that constitutes those models represents and what can and cannot be done with that data that transforms EGT use into EGT usefulness. The opportunity for SfM and XR (as EGTs) in 3D GIScience rests in developing the science that validates and focuses their use as spatially rigorous 3D data capture workflows and 3D visualization interfaces, addressing some of the persistent research challenges (e.g., data quality, data collection, human factors, and design challenges (Çöltekin et al., 2017)) that plague geovisualization.

1.7. Geovisualization and Spatial Knowledge

Geovisualization draws from the approaches of scientific visualization, cartography, image analysis, information visualization, exploratory data analysis, and GIS in formulating the 'theory, methods, and tools for visual exploration, analysis, synthesis, and presentation of geospatial data' (MacEachren & Kraak, 2001). The primary objectives of geovisualization are to encourage the formation of knowledge through visual exploration and analysis of geospatial data, and to provide the tools necessary to subsequently retrieve, synthesize, and use that knowledge (MacEachren & Kraak, 2001). While maps also offer the opportunity to engage with reality through the exploration and filtering of geospatial data (Kraak & Fabrikant, 2017), the heightened levels of interaction available through geovisualization differentiate it from traditional cartography (Çöltekin et al., 2017; Dykes et al., 2005). In the absence of direct physical interaction with real environments, mediated interactions through geovisualizations offer an opportunity to generate knowledge about those environments (Sharlin et al., 2009). This spatial knowledge can include information about the location, size, distance, direction, shape, connectivity, overlap, dimensionality, or hierarchy of spatial phenomena and can be called upon for a range of spatial tasks, including wayfinding and imagining places and reasoning with mental models of those places (Montello & Raubal, 2012).

The acquisition of spatial knowledge, or mental representations of space, is distinguished as landmark, route, or survey knowledge derived from real-world experiences, map use, or a combination thereof (Thorndyke & Hayes-Roth, 1982). While some spatial tasks may have once required perceptual-motor experiences only possible through direct real-world interaction (Montello & Raubal, 2012), the acquisition and use of spatial knowledge can now be learned through interaction with contemporary 3D geovisualizations utilizing EGTs; for example, SfM for spatial data acquisition and XR for immersive geovisualization. The 3D data generated through modern SfM workflows enables rapid characterization of spatial phenomena and XR interfaces provide an immersive, experiential means of interacting with that data. Considerable research efforts have focused on spatial knowledge acquisition as it relates to navigation and wayfinding (e.g. Huang et al., 2012; König et al., 2021; Lokka & Çöltekin, 2019; Morganti, 2018), however, wayfinding is not the only use for spatial knowledge, which is more broadly utilized to understand the world around us (Tversky, 2018).

At a time when the nature of mainstream GIScience data generation has been rapidly adopting and advancing 3D spatial characterization methods (such as SfM and other forms of 'reality capture'), this thesis aims to demonstrate and explore their workflows and applied potential. EGT-based geovisualizations, like maps, are characterizations of reality, and like maps, they must provide accurate information to be useful (Mark et al., 1999). However, regardless of their accuracy, there is no guarantee that spatial knowledge will be acquired through geovisualization use, as learning from visualizations has been shown to be impacted by factors such as visualization type and spatial ability (Höffler, 2010). Therefore, the acquisition of useful spatial knowledge from geovisualizations implementing SfM derived data products and XR interfaces is contingent on an awareness of SfM data quality, of the implications that SfM workflows have on data quality, of XR-based geovisualization design and development, and of the context in which XR-based geovisualizations may be beneficial.

1.8. Research Questions and Objectives

1.8.1. Research Questions

Emerging Data Collection Workflows and their Implications

- How accurately can terrestrial SfM workflows characterize the morphology of discrete phenomena?
- How accurately can underwater SfM workflows characterize the morphology of discrete phenomena?
- What implications do SfM workflow parameters (e.g., camera, camera settings, camera position/configuration, and lighting) have for the accuracy of the 3D data product?

Emerging Data Display and Analysis Technologies and their Implications

- How can XR technology be leveraged to help visualize the structure of complex 3D phenomena?
- What impact does XR technology have on (geo)visualization use and usefulness?
- What is the relationship between XR technology and the human factors which dictate geovisualization use and usefulness?
- What impact does XR technology have on the characterization of spatial ability (specifically mental rotation task performance)?

- Are mental rotation tasks performed more accurately and/or more rapidly with stereo 3D stimuli than with 2D images of those 3D stimuli?
- What impact does background complexity (i.e., information intensity) have on mental rotation task performance?
- What role do multidisciplinary design heuristics serve in the development of XR-based visual analytics applications?

1.8.2. Research Objectives

- Study the evolving practice of 3D spatial data acquisition, analysis, and visualization – enabled by EGTs – and their implications for modern 3D GIScience.
- Explore the capabilities of SfM workflows for morphometric monitoring in terrestrial and temperate marine environments.
- Design, develop, and quantify the performance of a SfM workflow for discrete phenomena in temperate marine environments.
- Explore the capabilities of emerging interface technologies (i.e., XR), demonstrating how they may transform the spaces in which we conduct GIScience practice and geovisual analysis.
- Investigate the perceptual, experiential, and task capabilities of emerging interface technologies by gathering preliminary empirical evidence through the design, development, and deployment of an immersive mental rotations test.
- Assess the perceptual and experiential implications of emerging 3D interface technologies for applied geospatial research, practice, and social integration.
- Curate and showcase a multidisciplinary set of design heuristics which inform the design and development of VR-based visual analytics environments.

1.9. How this Dissertation Contributes to the Utility of Emerging Geospatial Technology in 3D GIScience and Visual Analytics

EGTs are characterized by their use in the collection, processing, or analysis of geospatial data. SfM photogrammetry and XR interfaces are two key examples of EGTs that, despite the uncertainty and ambiguity that surrounds them, have experienced rapid growth, have developed a community of practice, and have had a prominent impact through novel use, purpose, or function. This dissertation strives to address the uncertainty and ambiguity that surrounds their use, examining the usefulness of SfM for

3D data capture and XR for 3D data visualization and analysis. While the resultant 3D *digital twins* and *realistic* 3D experiences may be driving the popularity of these geospatial technologies, their *usefulness* is highly dependent on an ability to quantify their capacity to accurately characterize spatial phenomena and positively impact our perception and comprehension of the 3D spatial phenomena at hand. The objective of this dissertation is not to disprove or discredit SfM or XR as geospatial technologies, but rather to address some of the underlying questions that must be answered to validate their *usefulness* for 3D GIScience.

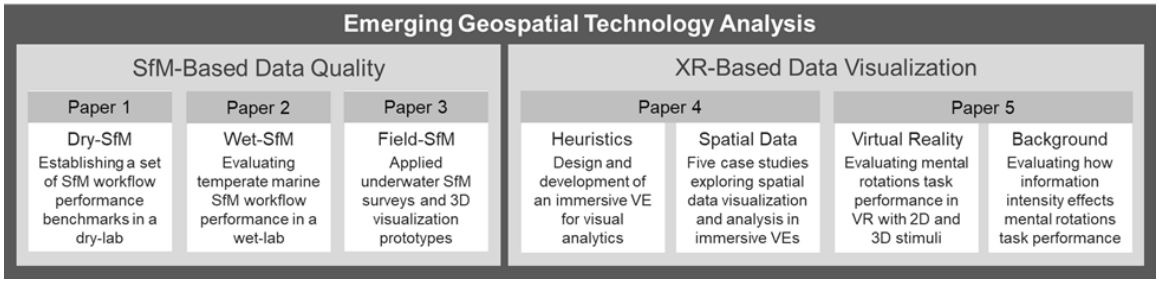

Figure 1.4 This collection of research presents an analysis of SfM for 3D spatial data acquisition and XR interface technologies for 3D spatial data visualization and analysis.

Through a collection of five manuscripts (Figure 1.4), this dissertation investigates the utility of SfM photogrammetry and XR technology - two EGTs - for 3D GIScience and 3D visual analytics. This collection of manuscripts explores multiple facets of 3D GIScience and 3D visual analytics, focusing not only on one piece of emerging technology, GIScience activity, or analytical process, but on the capacity for emerging technology to transform the way 3D spatial phenomena are characterized, perceived, and understood.

The first three manuscripts document the design, development, testing, and implementation of an underwater SfM workflow. The focus of these manuscripts is not on SfM and the algorithms that convert 2D images into 3D data, but rather on the impact that variable SfM workflows (i.e., photograph and video acquisition strategies) have on the quality of the 3D data product. The first manuscript establishes a set of performance benchmarks for multiple SfM workflows in a controlled, dry-lab environment. The second manuscript, informed by the performance benchmarks established in the dry-lab, implements and evaluates select SfM workflows in a wet-lab environment simulating the temperate marine conditions typical of those experienced in the field. The third

manuscript then reports on the SfM workflow performance in the field and introduces a set of XR prototypes for 3D data visualization and analysis. These three manuscripts not only produce 3D data characterizing the marine phenomena of interest, but through the SfM workflow performance benchmarks, they establish a clear understanding of data quality and the impact that SfM workflow parameters have on data quality.

Having established an awareness of variable SfM workflows and their implications on 3D data quality, the focus of this research then shifts to XR interfaces and their use in 3D data visualization and analysis. The fourth manuscript presents an immersive virtual environment for visual analytics and discusses the use of multidisciplinary design heuristics in the design and development of XR (specifically VR) interfaces for the visual exploration and analysis of geospatial data. In the quest for new spatial knowledge, XR interfaces provide an alternative spatial data experience – enabling methods of exploration and interaction not possible through conventional interfaces. While the fourth manuscript explores how these spatial data interfaces may be designed to promote spatial knowledge transfer, the fifth manuscript explores how this new spatial data experience impacts our ability to understand spatial data. This fifth manuscripts reports on the design, development, and deployment of the immersive mental rotations test (IMRT), a new implementation of the well-established MRT, adapted to immersive visualization environments; so that we may move into immersive XR information spaces, equipped with interface-appropriate empirical assessment tools with which to document and evaluate the spatial cognitive outcomes of visualization use.

While these manuscripts may at first seem widely spread across the spectrum of GIScience, they represent critical locations on a continuum of research examining the capacity for EGTs (i.e., SfM and XR) to accurately characterize spatial phenomena in 3D, to support the analysis of 3D spatial data using interactive, experiential, and immersive interfaces, and to affect our perception and cognition of those phenomena through immersive 3D visualization.

1.9.1. The Manuscripts

The first manuscript (Chapter 2) introduces an underwater SfM data capture platform designed and developed for surveying glass sponge colonies in Howe Sound, BC. As the first of three related manuscripts (dry-lab, wet-lab, and field-based) in this

dissertation, this research provides a set of dry-lab performance benchmarks utilizing different cameras, camera settings, lighting conditions, and image capture strategies. These performance benchmarks were a critical first step towards understanding the capacity for SfM to capture the annual small scale (mm – cm) changes in glass sponge morphometry. While SfM has been applied to underwater studies of benthic ecosystems in tropical waters, research quantifying SfM performance in temperate marine environments is limited.

The second manuscript (Chapter 3) presents a series of wet-lab analyses of SfM performance in a controlled marine environment indicative of the field conditions expected at depths > 20 m. The performance benchmarks provided by the dry-lab research in the first manuscript informed the design of the wet-lab study presented here. SfM performance in the wet-lab was compared to SfM performance on dryland, quantifying the impact that the temperate marine environment and the multimedia (air, glass, and water) interface of the underwater camera housing had on SfM accuracy. Additionally, as underwater data capture is limited by the amount of time SCUBA divers can spend at depth, a series of analyses were performed with fewer camera positions and alternate camera configurations to identify an optimal SfM survey workflow for subsequent field-based surveys.

The third manuscript (Chapter 4) documents a series of SfM surveys of two glass sponge colonies in Howe Sound, BC. These surveys were intended to be the first of two sets in an analysis of temporal changes in glass sponge morphology. Unfortunately, a second set of SfM surveys were never conducted. Nevertheless, this manuscript presents an analysis of the 3D data products that were created, contrasting those produced from photographs with those from extracted video frames, and explores how the resultant data products can be used to transform conventional monitoring efforts, supplanting 2D photographs and videos with interactive 3D visualizations and analyses. A collection of XR interfaces were developed to showcase how these interfaces could be used by marine ecologists monitoring glass sponge morphology.

The fourth manuscript (Chapter 5) showcases the development of an immersive virtual environment for visual analytics (IVEVA) and discusses the multidisciplinary set of design heuristics that were utilized during the development process. These design heuristics, curated from cartography, human-computer interaction (HCI), and XR

development, played an integral role in the development of IVEVA as an extension to the space in which 3D GIScience and visual analytics are conducted. While XR interfaces have garnered attention for their ability to immerse users within one-to-one representations of reality, XR represents an opportunity to connect users with 3D spatial data in experiential, interactive, and analytical virtual environments. IVEVA presents five case studies, selected to highlight the challenges associated with different spatial phenomena and spatial data formats, and a collection of analytical tools for real-time data analysis and simulation.

Finally, the fifth manuscript (Chapter 6) introduces the Immersive Mental Rotations Test (IMRT), an adaptation of the traditional 2D paper-and pencil mental rotations test (MRT) used to assess spatial ability (see Peters et al., 1995; Shepard & Metzler, 1971; Vandenberg & Kuse, 1978). While spatial ability tests such as the MRT are commonly used by researchers to assess the spatial ability of those using (3D) geovisualizations, as spatial ability (e.g., mental rotation) has been found to have an impact on the use and usefulness of (3D) geovisualizations, applying a 2D test to evaluate the utility of 3D visualizations developed for XR interfaces appeared incongruous. The IMRT was created and deployed to evaluate *mental rotation* task performance when those tasks are conducted in VR with stereo 3D stimuli and 2D images of those stimuli. Furthermore, this manuscript evaluates the effect that background complexity (i.e., information intensity) has on IMRT performance and discusses the effect that biological sex, learning, and angular disparity may have on IMRT performance.

In summary, this dissertation examines SfM and XR as EGTs for 3D spatial data acquisition, visualization, and analysis in GIScience. Demonstrating and documenting workflow and feasibility is certainly part of this. However, the key contributions that this dissertation aims to make to an evolving GIScience, that extend beyond just the technology are: to critically assess the ability of emerging data acquisition methods to adequately represent complex spatial phenomena; to critically reflect on the design rationale for immersive visualization environments; and, to develop new methods with which to empirically elucidate the spatial cognitive outcomes of spatial stimuli in immersive spaces, as GIScience stands on the threshold of XR.

To this end, the first three manuscripts present in-depth analyses of SfM workflow performance and the implications that idiosyncratic workflow variables have on 3D data quality; the fourth manuscript discusses the design and development of an immersive virtual environment and explores VR-based spatial data visualization and analysis through a collection of 3D data driven case studies; and the fifth manuscript presents the IMRT as a contemporary test of individual spatial ability. Each of these manuscripts represents an innovative and important contribution to 3D GIScience, addressing some of the uncertainty and ambiguity that surrounds SfM and 3D spatial data quality, and XR and spatial data visualization and analysis. While the ability to generate 3D data using SfM workflows and to visualize that data using XR interfaces was never in question, the quality of the 3D data and the utility of XR interfaces were.

Through these targeted engagements of SfM and XR, this dissertation aims to contribute knowledge and experience to evolving GIScience, by documenting and critically reflecting upon experiences of spatial reality capture in applied science, demonstrating the GIScience implications of technology and workflow, the spatial representation outcomes that result, how they might be ported into immersive spaces, how geovisualization objectives and design heuristics combine into anticipated spatial information experiences and capability, and how new empirical frameworks are needed, as a basis for new frontiers of 3D GIScience using XR.

References

Antoniou, V., Bonali, F. L., Nomikou, P., Tibaldi, A., Melissinos, P., Mariotto, F. P., Vitello, F. R., Krokos, M., & Whitworth, M. (2020). Integrating virtual reality and gis tools for geological mapping, data collection and analysis: An example from the metaxa mine, santorini (Greece). *Applied Sciences (Switzerland)*, *10*(23), 1–27. https://doi.org/10.3390/app10238317

Balletti, C., Beltrame, C., Costa, E., Guerra, F., & Vernier, P. (2016). 3D reconstruction of marble shipwreck cargoes based on underwater multi-image photogrammetry. *Digital Applications in Archaeology and Cultural Heritage*, *3*(1), 1–8. https://doi.org/10.1016/j.daach.2015.11.003

Balletti, C., Guerra, F., Scocca, V., & Gottardi, C. (2015). 3D integrated methodologies for the documentation and the virtual reconstruction of an archaeological site. *International Archives of the Photogrammetry, Remote Sensing and Spatial Information Sciences - ISPRS Archives*, *40*(5W4), 215–222. https://doi.org/10.5194/isprsarchives-XL-5-W4-215-2015

Beltrame, C., & Costa, E. (2017). 3D survey and modelling of shipwrecks in different underwater environments. *Journal of Cultural Heritage*, 3–9. https://doi.org/10.1016/j.culher.2017.08.005

Bennecke, S., Kwasnitschka, T., Metaxas, A., & Dullo, W.-C. (2016). In situ growth rates of deep-water octocorals determined from 3D photogrammetric reconstructions. *Coral Reefs*, *35*(4), 1227–1239. https://doi.org/10.1007/s00338-016-1471-7

Casella, E., Collin, A., Harris, D., Ferse, S., Bejarano, S., Parravicini, V., Hench, J. L., & Rovere, A. (2017). Mapping coral reefs using consumer-grade drones and structure from motion photogrammetry techniques. *Coral Reefs*, *36*(1), 269–275. https://doi.org/10.1007/s00338-016-1522-0

Çöltekin, A., Bleisch, S., Andrienko, G., & Dykes, J. (2017). Persistent challenges in geovisualization – a community perspective. *International Journal of Cartography*, *9333*, 1–25. https://doi.org/10.1080/23729333.2017.1302910

Çöltekin, A., Lochhead, I., Madden, M., Christophe, S., Devaux, A., Pettit, C., Lock, O., Shukla, S., Herman, L., Stachoň, Z., Kubíček, P., Snopková, D., Bernardes, S., & Hedley, N. (2020). Extended reality in spatial sciences: A review of research challenges and future directions. *ISPRS International Journal of Geo-Information*, *9*(7). https://doi.org/10.3390/ijgi9070439

Dangermond, J., & Goodchild, M. F. (2020). Building geospatial infrastructure. *Geo-Spatial Information Science*, *23*(1), 1–9. https://doi.org/10.1080/10095020.2019.1698274

De Reu, J., Plets, G., Verhoeven, G., De Smedt, P., Bats, M., Cherretté, B., De Maeyer, W., Deconynck, J., Herremans, D., Laloo, P., Van Meirvenne, M., & De Clercq, W. (2013). Towards a three-dimensional cost-effective registration of the archaeological heritage. *Journal of Archaeological Science*, *40*(2), 1108–1121. https://doi.org/10.1016/j.jas.2012.08.040

Dietrich, J. T. (2016). Riverscape mapping with helicopter-based Structure-from-Motion photogrammetry. *Geomorphology*, *252*, 144–157. https://doi.org/10.1016/j.geomorph.2015.05.008

Dykes, J., Maceachren, A. M., & Kraak, M.-J. (2005). Exploring Geovisualization. In J. Dykes, A. M. Maceachren, & M.-J. Kraak (Eds.), *Exploring Geovisualization* (1st Editio, pp. 3–19). Pergamon.

Fagin, T. D., Wikle, T. A., & Mathews, A. J. (2020). Emerging Geospatial Technologies in Instruction and Research: An Assessment of U.S. and Canadian Geography Departments and Programs. *Professional Geographer*, *72*(4), 631–643. https://doi.org/10.1080/00330124.2020.1777573

Goodchild, M. F. (1992). Geographical Information Science. *International Journal of Geographic Information Systems*, *6*(1), 31–45.

Gutierrez-Heredia, L., Benzoni, F., Murphy, E., & Reynaud, E. G. (2016). End to End Digitisation and Analysis of Three-Dimensional Coral Models, from Communities to Corallites. *PLoS ONE*, *11*(2). https://doi.org/10.1371/journal.pone.0149641

Hedley, N., & Lonergan, C. D. (2012). Controlling Virtual Clouds and Making It Rain Particle Systems in Real Spaces Using Situated Augmented Simulation and Portable. *International Archives of the Photogrammetry, Remote Sensing and Spatial Information Sciences - ISPRS Archives*, *39*(B2), 113–117. https://doi.org/10.5194/isprsarchives-XXXIX-B2-113-2012

Hedley, Nick. (2017). Augmented Reality. In D. Richardson, N. Castree, M. F. Goodchiild, A. Kobayashi, W. Liu, & R. A. Marston (Eds.), *International Encyclopedia of Geography* (pp. 1–13). John Wiley & Sons, Ltd. https://doi.org/doi:10.1201/9780849375477.ch213\r10.1201/9780849375477.ch213

Höffler, T. N. (2010). Spatial ability: Its influence on learning with visualizations-a meta-analytic review. *Educational Psychology Review*, *22*(3), 245–269. https://doi.org/10.1007/s10648-010-9126-7

Hruby, F., Ressl, R., & de la Borbolla del Valle, G. (2019). Geovisualization with immersive virtual environments in theory and practice. *International Journal of Digital Earth*, *12*(2), 123–136. https://doi.org/10.1080/17538947.2018.1501106

Huang, H., Schmidt, M., & Gartner, G. (2012). Spatial Knowledge Acquisition with Mobile Maps, Augmented Reality and Voice in the Context of GPS-based Pedestrian Navigation: Results from a Field Test. *Cartography and Geographic Information Science*, *39*(2), 107–116. https://doi.org/10.1559/15230406392107

Javernick, L., Brasington, J., & Caruso, B. (2014). Modeling the topography of shallow braided rivers using Structure-from-Motion photogrammetry. *Geomorphology*, *213*, 166–182. https://doi.org/10.1016/j.geomorph.2014.01.006

Kalacska, M., Chmura, G. L., Lucanus, O., Bérubé, D., & Arroyo-Mora, J. P. (2017). Structure from motion will revolutionize analyses of tidal wetland landscapes. *Remote Sensing of Environment*, *199*, 14–24. https://doi.org/10.1016/j.rse.2017.06.023

König, S. U., Keshava, A., Clay, V., Rittershofer, K., Kuske, N., & König, P. (2021). Embodied Spatial Knowledge Acquisition in Immersive Virtual Reality: Comparison to Map Exploration. *Frontiers in Virtual Reality*, *2*(March), 1–23. https://doi.org/10.3389/frvir.2021.625548

Kraak, M. J., & Fabrikant, S. I. (2017). Of maps, cartography and the geography of the International Cartographic Association. *International Journal of Cartography*, *3*(sup1), 9–31. https://doi.org/10.1080/23729333.2017.1288535

Lochhead, I., & Hedley, N. (2018). Mixed reality emergency management: bringing virtual evacuation simulations into real-world built environments. *International Journal of Digital Earth*, *0*(0), 1–19. https://doi.org/10.1080/17538947.2018.1425489

Lokka, I. E., & Çöltekin, A. (2019). Toward optimizing the design of virtual environments for route learning: empirically assessing the effects of changing levels of realism on memory. *International Journal of Digital Earth*, *12*(2), 137–155. https://doi.org/10.1080/17538947.2017.1349842

Lonergan, C., & Hedley, N. (2015). Navigating the future of tsunami risk communication: using dimensionality, interactivity and situatedness to interface with society. *Natural Hazards*, *78*(1), 179–201. https://doi.org/10.1007/s11069-015-1709-7

Luhmann, T., & Robson, S. (2006). Introduction. In *Close Range Photogrammetry : Principles, Techniques and Applications* (pp. 1–30). Whittles Publishing. https://ebookcentral-proquest-com.proxy.lib.sfu.ca/lib/sfu-ebooks/detail.action?docID=3417309.

MacEachren, A. M., & Kraak, M.-J. (2001). Research Challenges in Geovisualization. *Cartography and Geographic Information Science*, *28*(1), 3–12. https://doi.org/10.1559/152304001782173970

Mark, D. M., Freksa, C., Hirtle, S. C., Lloyd, R., & Tversky, B. (1999). Cognitive models of geographical space. *International Journal of Geographical Information Science*, *13*(8), 747–774. https://doi.org/10.1080/136588199241003

McCarthy, J. (2014). Multi-image photogrammetry as a practical tool for cultural heritage survey and community engagement. *Journal of Archaeological Science*, *43*(1), 175–185. https://doi.org/10.1016/j.jas.2014.01.010

McCarthy, J., & Benjamin, J. (2014). Multi-image Photogrammetry for Underwater Archaeological Site Recording: An Accessible, Diver-Based Approach. *Journal of Maritime Archaeology*, *9*(1), 95–114. https://doi.org/10.1007/s11457-014-9127-7

Milgram, P., & Kishino, F. (1994). A Taxonomy of Mixed Reality Visual Displays. *IEICE (Institute of Electronics, Information and Communication Engineers) Transactions on Information and Systems*, *Special Issue on Networked Reality*.

Montello, D. R., & Raubal, M. (2012). Functions and applications of spatial cognition. *Handbook of Spatial Cognition.*, 249–264. https://doi.org/10.1037/13936-014

Morganti, F. (2018). Enacting space in virtual reality: A comparison between Money's Road Map test and its virtual version. *Frontiers in Psychology*, *9*(DEC), 1–9. https://doi.org/10.3389/fpsyg.2018.02410

Peters, M., Laeng, B., Latham, K., Jackson, M., Zaiyouna, R., & Richardson, C. (1995). A Redrawn Vandenberg and Kuse Mental Rotations Test. Different Versions and Factors That Affect Performance. *Brain and Cognition*, *28*, 39–58.

Pizarro, O., Friedman, A., Bryson, M., Williams, S. B., & Madin, J. (2017). A simple, fast, and repeatable survey method for underwater visual 3D benthic mapping and monitoring. *Ecology and Evolution*, *7*(6), 1770–1782. https://doi.org/10.1002/ece3.2701

Pulver, Y., Merz, C., Koebel, K., Scheidegger, J., & Çöltekin, A. (2020). Telling engaging interactive stories with extended reality (xr): Back to 1930s in zurich's main train station. *ISPRS Annals of the Photogrammetry, Remote Sensing and Spatial Information Sciences*, *5*(4), 171–178. https://doi.org/10.5194/isprs-Annals-V-4-2020-171-2020

Remondino, F., Pizzo, S. Del, Kersten, T. P., Troisi, S., Metrology, O., Kessler, B., & Fbk, F. (2012). Low-Cost and Open-Source Solutions for Automated Image Orientation – A Critical Overview. In M. Ioannides, D. Fritsch, J. Leissner, R. Davies, F. Remondino, & R. Caffo (Eds.), *Progress in Cultural Heritage Preservation 4th International Conference, EuroMed 2012* (pp. 40–54). Springer, Berlin, Heidelberg. https://doi.org/https://doi-org.proxy.lib.sfu.ca/10.1007/978-3-642-34234-9

Romano, S., & Hedley, N. (2021). Daylighting Past Realities: Making Historical Social Injustice Visible Again Using HGIS-Based Virtual and Mixed Reality Experiences. *Journal of Geovisualization and Spatial Analysis*, *5*(1). https://doi.org/10.1007/s41651-021-00077-8

Rotolo, D., Hicks, D., & Martin, B. R. (2015). What is an emerging technology? *Research Policy*, *44*(10), 1827–1843. https://doi.org/10.1016/j.respol.2015.06.006

Rydvanskiy, R., & Hedley, N. (2020). 3d geovisualization interfaces as flood risk management platforms: Capability, potential, and implications for practice. *Cartographica*, *55*(4), 281–290. https://doi.org/10.3138/CART-2020-0003

Sharlin, E., Watson, B., Sutphen, S., Liu, L., Lederer, R., & Frazer, J. (2009). A tangible user interface for assessing cognitive mapping ability. *International Journal of Human-Computer Studies*, *67*(3), 269–278. https://doi.org/10.1016/j.ijhcs.2008.09.014

Shepard, R., & Metzler, J. (1971). Mental rotation of three-dimensional objects. *Science*, *171*(3972), 701–703.

Thorndyke, P. W., & Hayes-Roth, B. (1982). Differences in Spatial Knowledge Acquired and Navigation from Maps. *Cognitive Psychology*, *589*(14), 560–589.

Tverksy, B. (2018). Levels and structure of spatial knowledge. *Cognitive Mapping: Past, Present and Future*, 24–43. https://doi.org/10.4324/9781315812281-3

Vandenberg, S. G., & Kuse, A. R. (1978). Mental rotations, a group test of three-dimensional spatial visualization. *Perceptual and Motor Skills*, *47*(2), 599–604. https://doi.org/10.2466/pms.1978.47.2.599

Westoby, M. J., Brasington, J., Glasser, N. F., Hambrey, M. J., & Reynolds, J. M. (2012). “Structure-from-Motion” photogrammetry: A low-cost, effective tool for geoscience applications. *Geomorphology*, *179*, 300–314. https://doi.org/10.1016/j.geomorph.2012.08.021

Zhao, J., Wallgrün, J. O., LaFemina, P. C., Normandeau, J., & Klippel, A. (2019). Harnessing the power of immersive virtual reality - visualization and analysis of 3D earth science data sets. *Geo-Spatial Information Science*, *22*(4), 237–250. https://doi.org/10.1080/10095020.2019.1621544

Chapter 2.

Dry-Lab Benchmarking of a Structure from Motion Workflow Designed to Monitor Marine Benthos in Three Dimensions

This paper is published in The Photogrammetric Record.

Citation Details: Lochhead, I. and Hedley, N. (2021), Dry-lab benchmarking of a structure from motion workflow designed to monitor marine benthos in three dimensions. Photogram Rec, 36: 224-251. https://doi.org/10.1111/phor.12370

Abstract

Structure from motion (SfM) has emerged as a popular method for characterizing marine benthos (seabed organisms), particularly in clear, tropical waters. However, there are many environmentally sensitive benthic organisms inhabiting temperate waters, including the reef-forming glass sponges of the north-east Pacific Ocean. Broader questions are raised, not just about whether SfM is a capable spatial data acquisition and ecological characterization method in temperate waters; but whether a systematic assessment of capture methods in dry and wet laboratory conditions reveals critical relationships between SfM parameters, data products and their implications for underwater surveys. This paper, the first of two empirical assessments, reports on a series of dry-lab tests quantifying the impact that lighting, camera type, camera settings and capture strategy have on data accuracy. These tests provide a crucial accuracy baseline for subsequent wet-lab and field-based surveys, revealing that photographs captured from a controlled and stable platform produce superior data products. While the measurable differences were small, they may be critical for accurate change detection in temperate environments.

Keywords: 3D modelling, structure from motion, data quality, marine ecology, glass sponge morphometry

2.1. Introduction

In this work, the authors evaluate the accuracy and variability of the 3D data products generated through structure from motion (SfM) photogrammetry and the implications for modelling marine benthos – in this case, reef-forming glass sponges (phylum Porifera: class Hexactinellida). Glass sponge reefs constitute a unique and ecologically important marine habitat exclusive to the north-east Pacific Ocean. Unfortunately, the remote locations and extreme depths of these reef structures pose a significant challenge for those attempting to monitor glass sponge health. The emergence of SfM-based photogrammetry as a high-precision, cost-effective and accessible method to characterize marine environments shows significant potential for glass sponge research. However, the cold, dark and deep waters of the north-east Pacific Ocean present significantly different challenges to the SfM workflow than the warm, shallow tropical environments documented within much of the benthic SfM research literature. Furthermore, that research has not systematically addressed the impact that camera settings and capture strategy have on the quality of the resultant model.

The research presented in this paper represents the first phase of a three-phase (dry-lab, wet-lab and field-based) research paradigm designed to establish the data science supporting the utilization of SfM to characterize the 3D structure of temperate marine phenomena. The data quality benchmarks established through the dry-lab tests documented in this paper delineate what features can be resolved and the impact that idiosyncratic sets of variables (for instance, equipment, environment, and subject matter) have on derived SfM data quality. While these dry-lab tests may seem out of place, they serve a critical role to inform wet-lab research reported in a subsequent paper, which in turn informs applied field-based research characterizing glass sponges in situ. While proceeding directly to field-based surveying would have undoubtedly generated 3D data quickly, there was a critical opportunity to develop the spatial data science behind this method, asking questions about the representational veracity of SfM as a tool for underwater ecological surveys.

2.1.1. A Brief Primer on Glass Sponges

The Western Canadian glass sponge reefs are considered a key structural habitat for their uniqueness, sensitivity and influential role in maintaining ecosystem dynamics (Fisheries and Oceans Canada, 2010). They support a variety of marine fauna including bryozoans, gastropods, crustaceans, echinoderms and fish (Chu & Leys, 2010; Krautter et al., 2001; Marliave et al., 2009). As filter-feeders, they remove waterborne bacteria with 95% efficiency, are a potentially important carbon sink (Kahn et al., 2015) and their siliceous skeletons represent a substantial silica sink (Chu et al., 2011). The ecological productivity of these reefs attracts many commercial fisheries, resulting in an estimated 253 tons of coral and sponge bycatch between 1996 and 2002 (Leys et al., 2007) and widespread reports of reef damage (Conway et al., 2007; Conway et al., 2001; Conway et al., 2005; Cook et al., 2008; Krautter et al., 2001). Fisheries and Oceans Canada (2010) introduced fisheries closures to protect sensitive reef habitats and ongoing research efforts are attempting to quantify glass sponge growth rates and their capacity to recover from anthropogenic damage.

The growth rate of reef-forming glass sponges is believed to be 1 to 10 cm per year. However, only five of the 12 known studies documenting annual growth contain primary observations, of which only three address reef-building sponges. Austin et al. (2007) approximated annual growth at 10 cm per year based on measurements made using a series of marked photographs collected over a four-year period; Kahn et al. (2016) reported 1 to 3 cm per year (7 to 9 cm per year for projections) based on images collected between 2005 and 2014; and Levings & McDaniel (1974) discovered a 60-cm-long sponge growing on an underwater telephone cable that had been submerged for 52 years. There is an inherent lack of accuracy and precision in these growth rate quantifications, as Levings and McDaniel (1974) collected a sponge of unknown age and both Austin et al. (2007) and Kahn et al. (2016) quantified 3D growth based on 2D photographs that were assumed to provide the same perspective at different points in time. New methods of 3D data capture are required that can accurately and precisely quantify morphometric change, thereby providing a basis for long-term, repeated measurements of glass sponges through time. SfM photogrammetry shows great potential in this regard; however, it is imperative for glass sponge ecology that SfM methods are supported by data science and a firm understanding of data quality.

2.1.2. Underwater SfM

SfM is a photogrammetric method that resolves the 3D structure of a scene from multiple overlapping 2D photographs. Unlike traditional photogrammetry, the scene geometry, camera position and camera orientation parameters are extracted simultaneously and automatically through image matching and bundle adjustment (Westoby et al., 2012). SfM emerged during the 1990s with the advent of digital photogrammetry, owing much of its existence to the computer vision community and the feature-matching algorithms introduced during the 1980s (McCarthy & Benjamin, 2014; Westoby et al., 2012). While the photogrammetric community favored geometric quality over automation, those from computer vision stressed the importance of automation and auto-calibration (Remondino et al., 2012), which are features characteristic of the modern SfM software (such as VisualSFM, PhotoModeler, Agisoft Metashape/PhotoScan and Pix4D) that made SfM accessible and attractive to a range of research disciplines (McCarthy, 2014). The emergence of user-friendly SfM software democratized what once demanded significant temporal, financial and intellectual resources (Beltrame & Costa, 2017), providing experts across a wide range of domains with a simple, low-cost method for documenting, measuring and visualizing various phenomena.

SfM photogrammetry also eased the burden imposed by the awkward equipment and technical workflows of traditional photogrammetry, resulting in a surge of underwater SfM research touting SfM's ability to capture and represent complex marine environments. Recent publications document the use of SfM for bathymetric surveying (Abadie et al., 2018), marine archaeology (Beltrame & Costa, 2017; McCarthy & Benjamin, 2014; Skarlatos et al., 2012), ecological monitoring (Fukunaga et al., 2019), morphometric analyses (Gutierrez-Heredia et al., 2016; Lavy et al., 2015; Napolitano et al., 2019), benthic mapping and classification (Bayley et al., 2019; Burns et al., 2015; Leon et al., 2015; Pizarro et al., 2017) and monitoring temporal change (Bennecke et al., 2016; Piazza et al., 2018). For ecological analyses of marine benthos, SfM represents a non-destructive, non-invasive method of documentation that reduces the time spent in the field and enables objective interpretation (Piazza et al., 2018).

However, the 3D data product is only a model of reality, the accuracy and precision of which can be difficult to ascertain in the often-challenging conditions and

remote locations of many underwater environments. While the accuracy and precision of 3D SfM data has been studied by comparing derived data to reference objects of known dimension (for example, Lavy et al., 2015; Raoult et al., 2017), it cannot be assumed that employing the same camera and lens combination to capture a similar number of photographs will produce results of comparable accuracy and precision. Other factors, such as the photograph capture strategy, camera settings and the lighting conditions have a direct impact on photograph, and therefore model, quality. Furthermore, in an underwater environment the characteristics of the object being surveyed (such as color, orientation and surroundings), the physical characteristics of the water (for example, visibility, optical noise, light absorption and color loss), the conditions on the day of the survey (weather, wind and currents) and the dive-time limitations are key considerations (Menna et al., 2018; Semaan & Salama, 2019). Simply collecting photographs and processing them with user-friendly SfM software may produce a 3D model, but that model is not necessarily the greatest 3D representation that is achievable given the available equipment.

Establishing data quality benchmarks for SfM workflows, both underwater and on dry land, is an important element of research efforts designed to characterize the morphology of benthic organisms in situ. Figueira et al. (2015) established a set of benchmarks at the colony scale, capturing images in a shallow pool, and at the patch scale, capturing images along a transect of rocky subtidal reef, to inform others about the importance of selecting a workflow that matches the application. Similarly, Lavy et al. (2015) assessed the accuracy of coral models derived from underwater photographs, and contrived geometric shapes and plasticine models, derived from photographs and extracted video frames, to highlight the effect that complex, irregular shapes can have on model accuracy. Both studies reflect the need for research that unpacks the effects of methodological choices on SfM data quality.

This study evaluates the quality of 3D SfM data generated from photographs and videos captured in a dry-lab with two different cameras, using different camera settings and different lighting conditions to quantify the variable accuracy of SfM workflows. With an annual growth rate estimated at 1 to 10 cm per year, recurrent surveys of glass sponges must be accurate and precise enough to detect centimeter- or millimeter-scale changes in morphology. As the first stage of a dry-lab, wet-lab and field research paradigm, this paper describes the dry-lab design and testing methods, providing a

performance baseline for the SfM workflow. The aim is to support the underwater survey and 3D SfM work of others in the marine ecology community by providing these benchmarks.

2.2. Materials and Methods

The materials and methods presented in the following subsections, while discussed in the context of a dry-lab test, were selected and designed to handle the challenging underwater conditions of the north-east Pacific Ocean. Ultimately, the equipment and methodology described here will be used by a dive team at depths of 20 to 25 meters.

2.2.1. The Platform

A custom SfM data capture platform, named HEXYZ-1 (Figure 2.1), was designed to overcome the challenging currents and lighting conditions typical of glass sponge habitats and offers a repeatable method of data capture not possible with scuba divers alone. HEXYZ-1 maintains camera stability and course (thus camera-to-object distance) during underwater data collection and provides a world-stabilized light source (shadows cast are unchanged over time). The hexagonal structure was constructed from a series of 1-inch (25-mm) square tube aluminum bars, coupled by molded nylon connectors and reinforced by aluminum plates. Suspended from a hexagonal plate mounted to the top of HEXYZ-1 is an adjustable camera armature that rotates around the central axis. Attached to the armature is an adjustable camera platform and tilting tripod head. The combined adjustability of the armature, camera platform and tripod head provide a high degree of camera maneuverability within HEXYZ-1. Fully assembled, HEXYZ-1 measures 2.44 m wide (vertex to vertex) by 1.7 m tall and weighs approximately 25 kg.

Figure 2.1 HEXYZ-1: A data capture platform designed for underwater SfM surveying in temperate waters.

2.2.2. Lighting

The natural light available at 20 to 25 meters depth is insufficient for high-quality photography and an artificial light source must be provided. Seven artificial light sources were created by mounting extra-wide beam LED dive lights (BigBlue AL1200XWP) within hemispherical housings. The semi-opaque housings helped diffuse the light and reduce shadowing.

Lighting Tests

The optimal position and intensity of the lights was determined by evaluating the accuracy of the SfM data product generated under five different lighting configurations (Test 1 to Test 5; Figure 2.2). Each light assembly was attached directly to the HEXYZ-1 frame or the camera armature. The number of lights, their location within HEXYZ-1 and their lumen output are presented in Table 2.1 for each of the five tests.

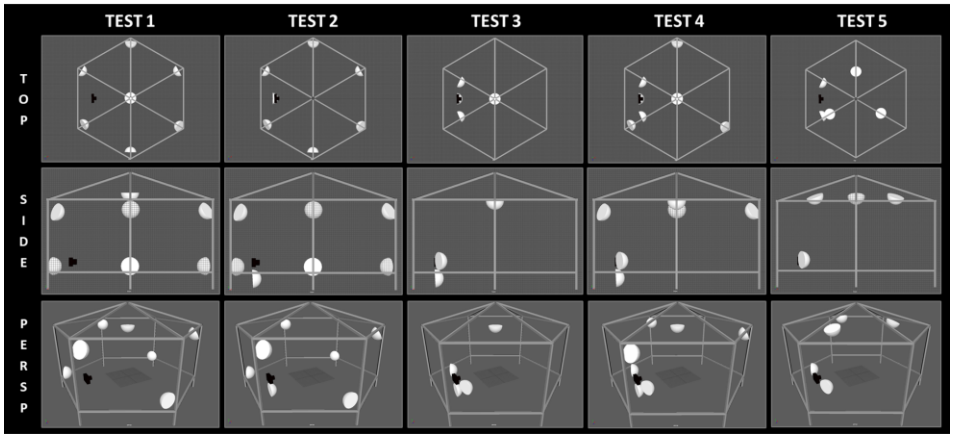

Figure 2.2 **The location of each light within HEXYZ-1 is indicated by the white circles/domes. Top, side, and perspective views are provided for clarity.**

Table 2.1 **Light test configuration and lumen output.**

Light Test	Number of Lights	Lumen Output			
		Centre	Top	Bottom	Camera
Test 1	7	600	600	600	600
Test 2	7	-	600	600	150
Test 3	4	300	-	-	150
Test 4	7	300	300	-	150
Test 5	5	-	300	-	150

The test subject for the light tests was a small glass sponge skeleton (approximately 21 cm in height). The glass sponge was collected from the field by a Howe Sound Research Group dive team and was dried in the laboratory before being mounted on a stable base that held the skeleton in an upright position. The mounted skeleton was then placed on a wooden box (40 cm × 35 cm × 25 cm) located at the centre of HEXYZ-1 and 168 photographs (24 photographs from each of seven encircling paths of fixed height and distance) were captured for each light test using a Sony Alpha α6500 mirrorless digital camera fitted with a Sony E PZ 16 to 50 mm F3.5 to 5.6 OSS (Optical SteadyShot) lens (referred to as the Sony A6500). All photographs used a 30

mm focal length, f/5.0 aperture, ISO 640 and 1/60 s shutter speed. A wooden block, with rulers affixed to two sides, served as a reference object of known dimensions.

The photographs from each light test were imported into Agisoft PhotoScan Professional (V1.4.0) and processed individually. For each test, image alignment was performed using the high-accuracy setting, pair preselection was disabled, and camera calibration was performed automatically. Once aligned, scale bars were created by positioning markers on easily identifiable points on the reference object and their positions were manually adjusted within each aligned image. The sparse point cloud was then trimmed to remove points beyond the extent of the wooden box and photograph alignment was optimized prior to dense cloud and mesh construction. Dense cloud construction was performed using the high-quality setting and depth filtering was set to aggressive. Each mesh was built as an arbitrary surface of high polygon count using the dense clouds.

Five distinct features on the glass sponge skeleton were measured using a digital caliper, including the diameter of the osculum (the large aperture through which water is expelled) and the dimensions of select tubular processes (Figure 2.3). Each feature was measured twice and the average of the two measurements was recorded as the measured value. For each light test, features on the 3D SfM model were measured using the ruler tool in PhotoScan. The measured value represents an average of two measurements.

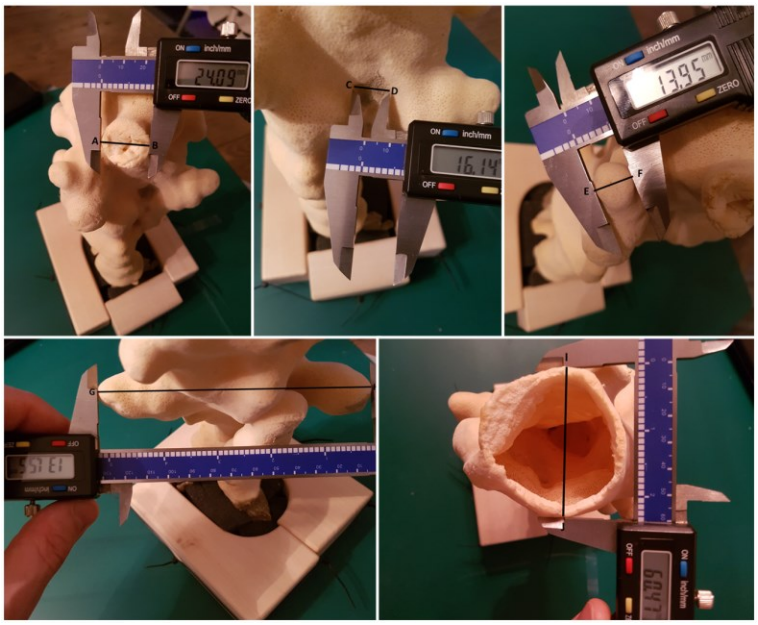

Figure 2.3 **Digital calipers were used to measure select structural features of the glass sponge skeleton.**

The glass sponge skeleton was only used for the light tests and not the camera tests described in subsequent sections. Collecting precise measurements of the glass sponge skeleton proved challenging and helped to demonstrate the difficulty associated with manual measurement of complex structures in the field.

2.2.3. Cameras

The camera tests were conducted using the Sony A6500 and a GoPro HERO6 Black. The Sony A6500 was chosen primarily due to the availability of an underwater dive housing; however, this is a highly rated digital camera appropriate for SfM data capture. Action cameras, largely GoPro models, are often cited by researchers employing SfM workflows for terrestrial and marine surveying (for example, Gutierrez-Heredia et al., 2016; Raoult et al., 2016; Thoeni et al., 2014; Van Damme, 2015). The GoPro HERO6 Black was selected to gauge the appropriateness of an action camera for underwater SfM-based surveying and ecological monitoring.

The Wide field of view (FOV) mode was utilized for all GoPro photography and videography despite the presence of radial lens distortion in the resultant photographs and videos. It has been shown that the radial distortion of GoPro cameras is largely offset during underwater photography, presenting no issues for camera auto-calibration

(Van Damme, 2015). As these dry-lab tests served to inform subsequent underwater testing and fieldwork, the Wide FOV mode was maintained for the dry-lab tests and the fisheye camera type was defined in PhotoScan during the camera auto-calibration stage.

Best practices suggest that photographs, as compared to frames extracted from video, provide superior results for SfM modelling. Both photographs and video were collected using the methodology and settings described in the following subsections.

Photographs

The primary method of data capture generated five circular sets of 36 photographs by rotating the HEXYZ-1 mounted camera around the test subject in 10° increments (Figure 2.4). The first three sets of photographs were captured with the camera's lens positioned 35 cm from the centre of the test subject. The camera was perpendicular to the ground surface in the first set, at a 45° angle in the second and at a 35° angle in the third. For the fourth and fifth sets the camera was positioned 60 cm from the centre of the test subject. The camera was perpendicular to the ground surface for the fourth set of photographs and angled at 45° for the fifth set. Two additional camera tests mirrored this methodology using a handheld camera, while two others utilized photographs captured from random positions within HEXYZ-1.

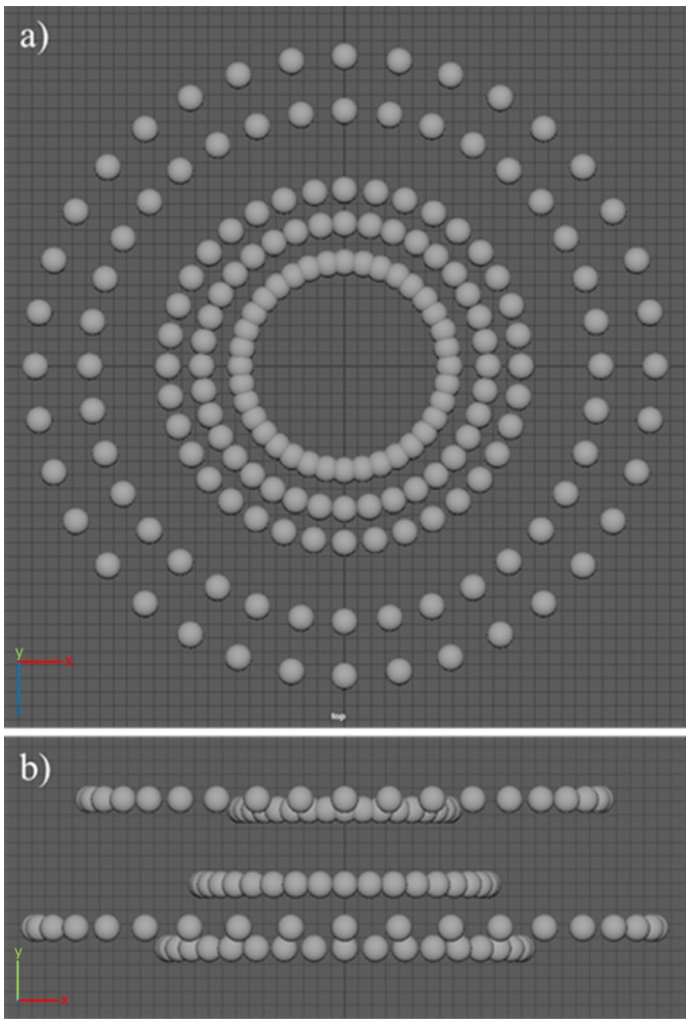

Figure 2.4 **Five circular sets of photographs were collected of the test subject. Each circle represents the camera's position around the test subject. (a) Top view, showing the 10° separation in camera positions. (b) Side view.**

The camera tests were also designed to evaluate the effect that different camera settings have on SfM model accuracy. For the photographs captured with the GoPro HERO6 Black, only one ISO/aperture/shutter configuration was used; however, three different ISO/aperture/shutter combinations were tested with the Sony A6500 (Table 2.2). While low ISO speed settings should be used to minimize noise (Agisoft LLC, 2018), ISO values lower than 400 resulted in photographs which were too dark for processing. To eliminate camera movement caused by human contact when capturing photographs, GoPro's smartphone application (Capture) was utilized for all GoPro tests and a two-second delay timer was employed for all Sony A6500 tests.

Table 2.2 Cameras and settings – photographs.

Camera	Pixel count	File Type	ISO	Relative aperture	Shutter speed (s)	Focal length	35mm equivalent
GoPro HERO6 Black	12 MP	RAW & JPEG	400	f/2.8	1/125	3 mm	15 mm
Sony A6500	24 MP	RAW & JPEG	400	f/3.5	1/60	16 mm	24 mm
Sony A6500	24 MP	RAW & JPEG	640	f/3.5	1/60	16 mm	24 mm
Sony A6500	24 MP	RAW & JPEG	Auto	Auto	Auto	16 mm	24 mm

The GoPro RAW photographs were too noisy for meaningful SfM processing. Therefore, new sets of photographs were collected in the JPEG format. Each of the photographs collected with the Sony A6500 were simultaneously captured in ARW (Sony's RAW format) and JPEG format. The ARW files were converted to TIFFs using Sony's Image Data Converter (Version 5.1.00.04270). No postprocessing was completed on any of the photographs.

Videos

In each video test, the camera was positioned along the same five pathways introduced earlier. However, instead of manually moving the armature in 10° increments, each video was captured with the armature in continuous motion, requiring approximately 60 seconds to complete each of the five passes. The camera settings used for video capture are presented in Table 2.3.

Table 2.3 Cameras and settings – videos.

Camera	Pixel count	Frame rate	File type	ISO
GoPro HERO6 Black	3840 x 2160	4k 24p60M	MP4	400
Sony A6500	3840 x 2160	4k 30 fps	MP4	Auto

Individual frames were manually extracted from each of the MP4 video files using VLC Media Player (Version 3.0.4). The images were extracted at a rate of approximately 10° of armature rotation, providing an evenly distributed image set consistent with the

photograph-based approach. The individual frames were saved as PNG files. As with the photographs, five sets of 36 images (180 total) constituted one complete test.

Camera Calibration

The camera calibration parameters for each of the described tests were assigned automatically by PhotoScan. While in situ self-calibration is critical to applications demanding high-accuracy results (Shortis, 2019), the underwater field site where a subsequent phase of this research was conducted presented several challenges to in situ calibration. First, with HEXYZ-1 in place on the seafloor there was limited available space with which to perform calibration activities while avoiding damage to the glass sponge. Second, dive times were limited to approximately 20 minutes for initial dives and decreased significantly with each successive dive: a choice was made to prioritize data collection over calibration activities. 2D calibration objects were included to assist with auto-calibration, and the authors acknowledge the potential for systematic errors in this approach. However, the ultimate test of the accuracy of the chosen workflow is the validation of measurements (Shortis, 2019), which are relied on to quantify accuracy.

2.2.4. Test Subjects

An assemblage of wooden blocks and a gaming die (dice) served as the test subjects for the camera tests. While a glass sponge skeleton is more representative of the living glass sponges that will be encountered in the field, minimizing manual measurement error was critical at this stage. The wooden blocks and die provided the easily measurable structures necessary to ensure accuracy and precision.

Wooden Blocks

Three wooden blocks were assembled as a crude representation of the structure of a glass sponge (Figure 2.5). While the natural color and texture of the wood is similar to that of the glass sponge skeleton, the shorter of the blocks was painted white to assess the impact that color and texture have on the quality of the model. These wooden blocks, two of natural color and one painted white, were used for all camera tests.

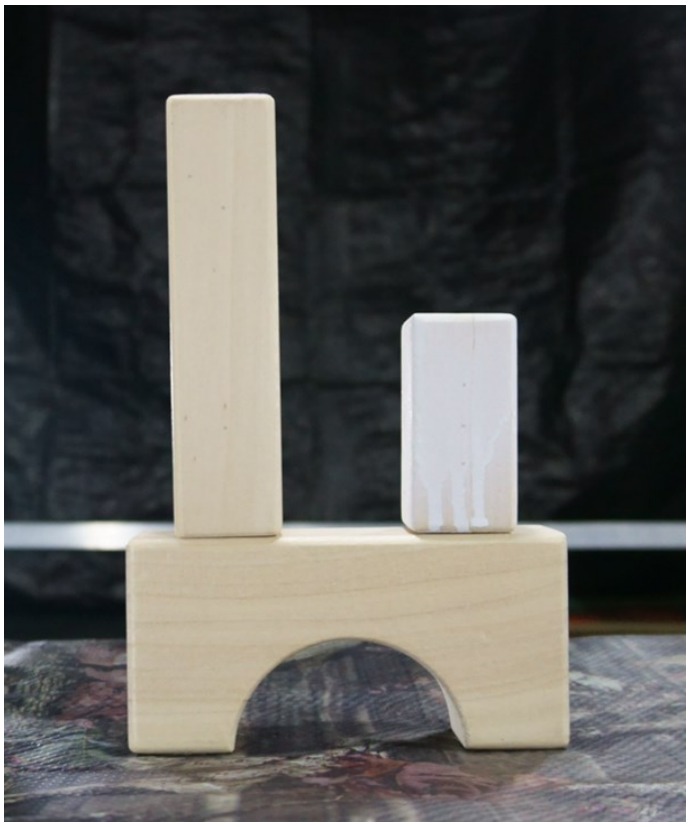

Figure 2.5 Three wooden blocks provided a simple, easily measurable 3D structure for SfM accuracy analyses. The taller block (left) maintained its natural wood texture while the shorter block (right) was painted white.

A series of circular impressions were made in each vertical block using an 8 mm pointed centre punch. The resultant line segments (a–b, b–c, d–e, …), as well as the block dimensions (side 1, side 2, …), were measured using a digital caliper (Figure 2.6). Each measurement was made twice and an average of the two measurements was recorded as the measured value.

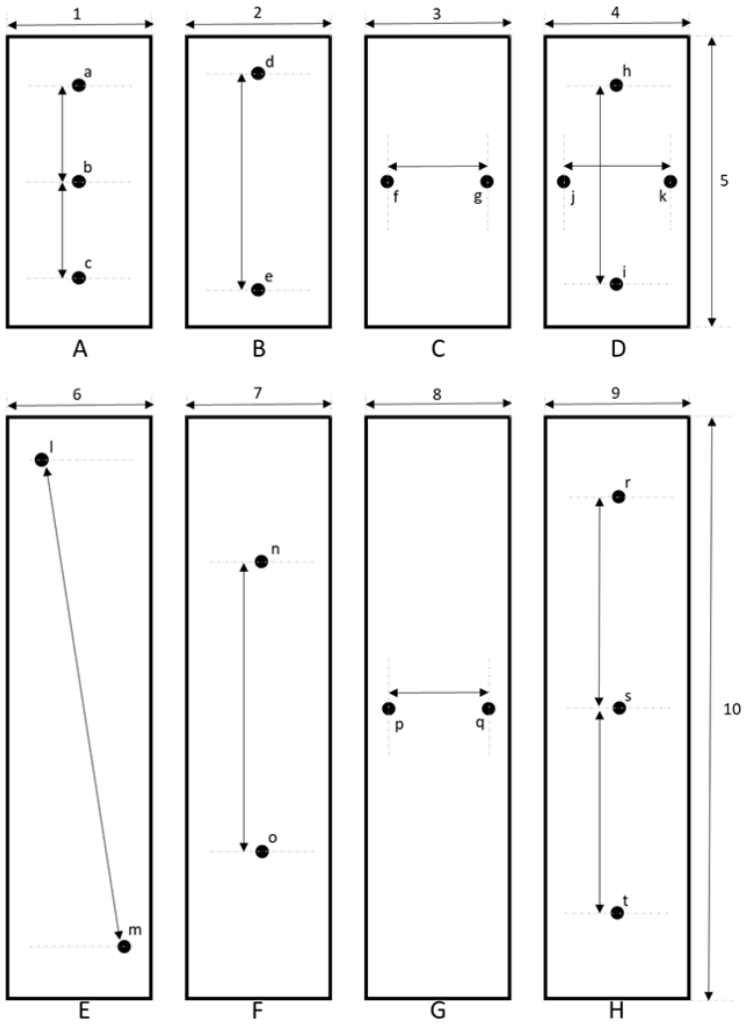

Figure 2.6 **Impressions in each block yielded easily measurable line segments (a-b, b-c, ...). The width of each block face (1, 2, 3, ...) was also measured. The upper row illustrates the locations of the impressions and the faces of the white block, and the lower row does the same for the natural block.**

Gaming Die

A white gaming die was placed on top of the natural-colored wooden block in selected camera tests to represent a change (simulated glass sponge growth) in the physical structure of the test subject. The resultant models (with the gaming die) would then be compared to other models (without the gaming die) to evaluate the accuracy with which this simulated growth is modelled. As the objective of the greater research project is to capture morphometric changes of glass sponges, it was important to gauge the accuracy with which this change (the addition of the die) could be modelled.

2.2.5. Camera Tests

The combination of different cameras, camera settings, test subjects and capture methodologies resulted in 18 camera tests. The lighting configuration from Light Test 1 was utilized for each test, with each light charged to full capacity before each test to avoid reduced lumen output resulting from partially charged batteries. All photographs and videos were captured in a room devoid of other light sources.

The wooden blocks were affixed to a wooden box (40 cm × 35 cm × 25 cm) wrapped in a camouflage tarp (tarpaulin). The tarp served to simulate some of the irregular complexity present on the seafloor, but also helped replicate the contrast between a living glass sponge and the seafloor. An additional block, with rulers on two sides and two axes, served as a reference object of known dimension. The wooden box, complete with blocks and reference object, was placed on the floor in the centre of HEXYZ-1 (Figure 2.7).

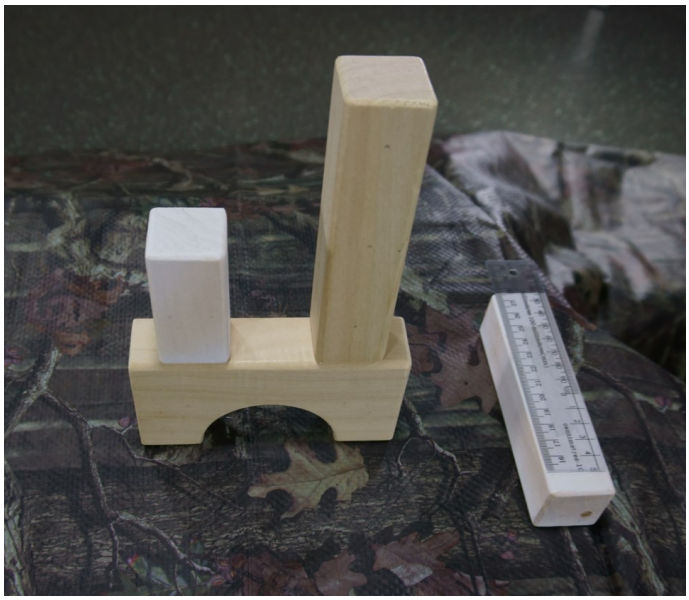

Figure 2.7 The wooden blocks, reference object, and box utilized for all camera tests.

The Sony A6500 was utilized in camera tests 1 to 12 and the GoPro in camera tests 13 to 18. The specifics of each camera test are outlined in Table 2.4. The addition of the die effectively resulted in duplicate (paired) camera tests (thus camera tests 1 and 4, 2 and 5, 3 and 6, and so on use the same configurations and camera settings and only differ by the presence of the gaming die). This duplication provided a simple

indicator of repeatability and enabled the change detection analysis by providing paired camera tests that differ only in the test subject (one includes the die, and one does not).

Table 2.4 SfM Test scenarios.

	Scenario		Camera and Settings									
Camera Test	Test subject	Lights (lumens x light #)	Camera movement	Camera	Focal length (mm)	Focal length (35 mm equiv.)	Format	File format	Pixel count	ISO	Aperture	Shutter Speed
Test 1	Blocks	600 x 7	Rig	Sony	16	24	Image	TIFF	6000x 4000	640	3.5	1/60
Test 2	Blocks	600 x 7	Rig	Sony	16	24	Image	TIFF	6000x 4000	400	3.5	1/60
Test 3	Blocks	600 x 7	Rig	Sony	16	24	Image	TIFF	6000x 4000	Auto	Auto	Auto
Test 4	Blocks & die	600 x 7	Rig	Sony	16	24	Image	TIFF	6000x 4000	640	3.5	1/60
Test 5	Blocks & die	600 x 7	Rig	Sony	16	24	Image	TIFF	6000x 4000	400	3.5	1/60
Test 6	Blocks & die	600 x 7	Rig	Sony	16	24	Image	TIFF	6000x 4000	Auto	Auto	Auto
Test 7	Blocks	600 x 7	Rig	Sony	16	24	Video	PNG	3840x 2160	Auto	3.5	1/50
Test 8	Blocks & die	600 x 7	Rig	Sony	16	24	Video	PNG	3840x 2160	Auto	3.5	1/50
Test 9	Blocks	600 x 7	Handheld (Rig Pattern)	Sony	16	24	Image	TIFF	6000x 4000	400	3.5	1/60
Test 10	Blocks & die	600 x 7	Handheld (Rig Pattern)	Sony	16	24	Image	TIFF	6000x 4000	400	3.5	1/60
Test 11	Blocks	600 x 7	Handheld (Random)	Sony	16	24	Image	TIFF	6000x 4000	400	3.5	1/60
Test 12	Blocks & die	600 x 7	Handheld (Random)	Sony	16	24	Image	TIFF	6000x 4000	400	3.5	1/60

Test 13	Blocks & die	600 x 7	Rig	GoPro	3	15	Image	JPEG	4000x 3000	400	2.8	1/125
Test 14	Blocks & die	600 x 7	Rig	GoPro	3	15	Video	PNG	3840x 2160	400	2.8	Auto
Test 15	Blocks & die	600 x 7	Rig	GoPro	3	15	Image	JPEG	4000x 3000	Auto	2.8	1/125
Test 16	Blocks	600 x 7	Rig	GoPro	3	15	Image	JPEG	4000x 3000	400	2.8	1/125
Test 17	Blocks	600 x 7	Rig	GoPro	3	15	Video	PNG	3840x 2160	400	2.8	Auto
Test 18	Blocks	600 x 7	Rig	GoPro	3	15	Image	JPEG	4000x 3000	Auto	2.8	1/125

2.2.6. 3D Model Construction

The photographs (still photographs or extracted video frames) from each test were imported into Agisoft PhotoScan Professional (V1.4.0). Each set of photographs was aligned using the high-accuracy setting and pair preselection was disabled. Two scale bars, aligned to two different axes, were created from four manually placed markers and image alignment was improved with the optimize tool. A dense point cloud was constructed using the high-quality setting and depth filtering was set to aggressive. All points representing features other than the test subject were removed, and erroneous points were deleted manually. A mesh was constructed with the polygon count set to high and a texture was then created. The workflow and settings were identical for each of the tests. A 3D point cloud was exported as a final step.

2.2.7. 3D Model Measurement

The block faces and line segments were measured within PhotoScan using the ruler tool. Each measurement was made twice, the average of which defined the measured value. Some of the impressions were not visible within the untextured meshes, therefore all measurements were made using the textured models.

2.2.8. Point Cloud Analysis

The point clouds from each of the paired camera tests were imported into CloudCompare (Version 2.10.1) to assess the accuracy with which each SfM workflow could detect structural change (the addition of the die). In each analysis, the point cloud from the camera test without the gaming die served as the reference cloud to which the cloud with the gaming die would be compared. Each set of point clouds was roughly aligned and then finely registered before computing the cloud-to-cloud distance. The maximum cloud-to-cloud absolute distance ($D_{[C2C]}$) was recorded as the change measurement, which was then compared to the measurement of the real die ($D_{[REAL]}$) attained with a digital caliper.

2.2.9. Statistical Analysis

The variability between camera tests was analyzed using a univariate analysis of variance (one-way ANOVA), with the absolute value of the line segment measurement error functioning as the independent variable. The absolute value of the error was utilized so as to not reduce the average error value with positive and negative measurement errors.

The line segment measurement error was calculated as the difference between the real-world caliper measurement ($M_{[REAL]}$) and the digital model measurement collected from within PhotoScan ($M_{[SfM]}$). The difference from $M_{[REAL]}$ is expressed as a percentage of difference Δ as follows:

$$\Delta = ((M_{|REAL|} - M_{|SFM|}) / M_{|REAL|}) * 100$$

Microsoft Excel was used to document each of the measurements and for the statistical analyses.

2.3. Results

The test results are presented in the following subsections. The light tests served only to inform the lighting configuration for the camera tests.

2.3.1. Light Tests

A textured, high-resolution 3D model with minimal excluded or erroneous structures was successfully generated for each of the light tests (Figure 2.8). No variations in the physical structure of these models were apparent upon visual inspection; however, there were color variations, with test 1 producing a texture most representative of the glass sponge skeleton. Highlights from the SfM processing results are presented in Table 2.5.

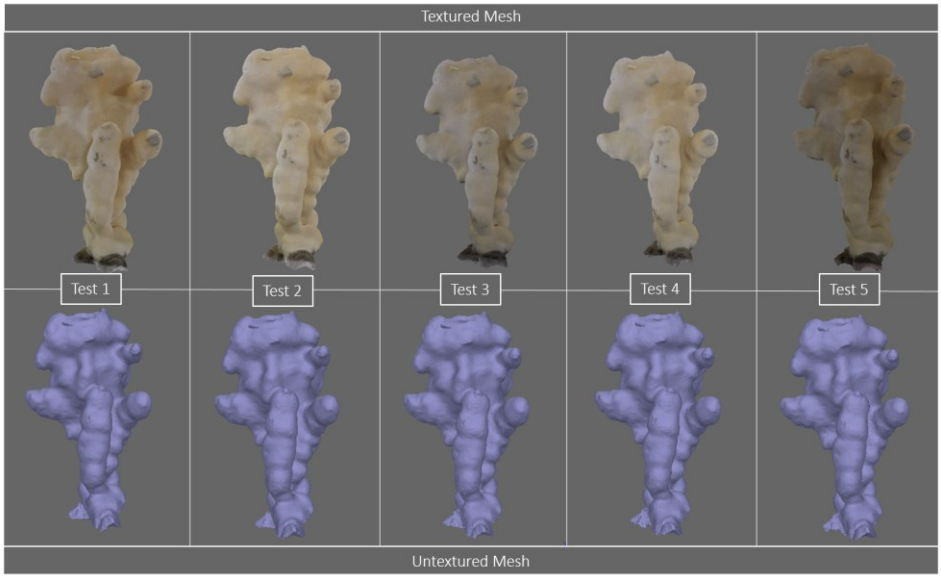

Figure 2.8 The textured and untextured meshes produced for each light test.

Table 2.5 Light tests - SfM processing results.

Light test	Cameras (aligned)	Sparse cloud (points)	Dense cloud (points)	Mesh (faces)	RMS error (mm)	Reprojection error (pixels)	Resolution (mm/pixel)	Scale bar error (mm)
Test 1	168 (168)	104 000	10 029 000	2 006 000	0.171	1.14	0.049	0.000
Test 2	168 (168)	82 000	10 910 000	2 182 000	0.203	1.15	0.048	0.015
Test 3	168 (168)	76 000	10 559 000	2 112 000	0.233	1.28	0.049	0.043
Test 4	168 (168)	84 000	10 293 000	2 059 000	0.154	1.02	0.049	0.094
Test 5	168 (168)	75 000	9 135 000	1 827 000	0.208	1.32	0.050	0.029

Each of the models appears visually similar and their accuracy was assessed by comparing the line segment measurements of the real glass sponge skeleton to those of the 3D models within PhotoScan (Table 2.6). While both methods are subject to systematic errors, accuracy was based on linear measurements rather than surface area and volume measurements (such as foil-wrap and wax-drip) that are themselves subject to error, and high-accuracy alternatives (for example, laser scanning) were not available (Figueira et al., 2015). The difference between the real measurements and the model measurements are reported as the modelling error in Figure 2.9. A univariate analysis of variance (one-way ANOVA) using the absolute value of line segment measurement error as the independent variable, revealed a statistically significant difference between the test results ($F(4,20) = 4.829$, $p = 0.007$).

Table 2.6 Line segment measurements (mm) for the glass sponge skeleton and SfM models

Line segment	Caliper measurement	Light test 1	Light test 2	Light test 3	Light test 4	Light test 5
A - B	24.09	24.05	23.06	23.70	23.60	23.45
C – D	16.14	16.30	16.65	16.60	16.75	16.65
E – F	13.95	13.85	14.45	13.50	13.75	13.70
G – H	131.55	130.95	132.40	131.95	131.05	131.70
I – J	60.47	60.50	59.75	60.25	59.75	59.95

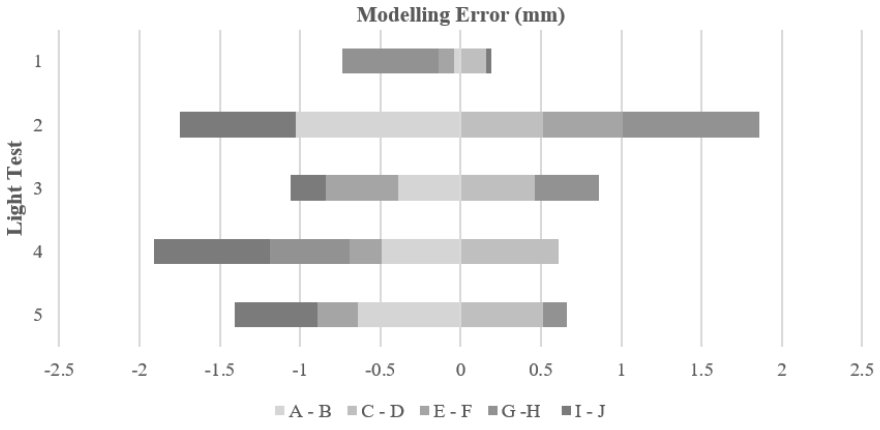

Figure 2.9 A comparison of the cumulative positive and negative modelling error across each of the light tests.

The light configuration from light test 1 was applied to each of the camera tests, as there was a statistically significant difference between the measurement error across light tests, with light test 1 producing the lowest mean error (0.19 mm), having the smallest error range (0.76 mm) and producing the model with the most representative texture.

2.3.2. Camera Tests

SfM Processing Results

Each of the 18 camera tests produced a complete 3D model of the wooden block assemblage. Test 3 was the only test in which all the cameras were not successfully aligned. Selected SfM processing results are presented in Table 2.7.

Table 2.7 Camera tests - SfM processing results.

Camera test	Cameras (aligned)	Sparse cloud (points)	Dense cloud (points)	Mesh (faces)	RMS error (mm)	Reprojection error (pixel)	Resolution (mm/pixel)	Scale bar error (mm)
Test 1	180 (180)	80662	2 053 753	410 750	0.198	2.00	0.232	0.005
Test 2	180 (180)	85 120	2 004 466	400 892	0.283	2.73	0.104	0.082
Test 3	180 (156)	94 197	1 831 379	366 275	0.218	2.10	0.190	0.173
Test 4	180 (180)	111 803	1 980 031	396 006	0.218	2.05	0.198	0.090
Test 5	180 (180)	114 036	1 977 517	395 503	0.222	2.12	0.180	0.068
Test 6	180 (180)	112 693	1 969 524	393 904	0.217	2.15	0.177	0.035
Test 7	180 (180)	116 710	718 559	180 000	0.205	1.27	0.268	0.074
Test 8	180 (180)	125 380	723 415	180 000	0.200	1.24	0.224	0.019
Test 9	180 (180)	129 175	1 513 312	302 662	0.237	2.15	0.282	0.024
Test 10	180 (180)	107 025	2 148 420	429 684	0.383	3.66	0.192	0.051
Test 11	180 (180)	111 625	766 633	180 000	0.258	2.26	0.189	0.138
Test 12	180 (180)	116 609	1 584 318	316 863	0.418	3.64	0.181	0.085
Test 13	180 (180)	112 833	254 654	180 000	0.198	1.40	0.695	0.015
Test 14	180 (180)	104 880	279 361	180 000	0.219	1.04	0.499	0.001
Test 15	180 (180)	106 847	233 752	180 000	0.196	1.33	0.530	0.018

Test 16	180 (180)	111 320	223 198	180 000	0.199	1.42	0.668	0.026
Test 17	180 (180)	109 395	235 524	180 000	0.201	1.02	0.637	0.203
Test 18	180 (180)	106 831	205 710	180 000	0.198	1.37	0.617	0.020

The precision of PhotoScan's image alignment, dense point cloud and mesh production were evaluated by repeating camera tests 1, 2 and 3 three times each (thus Test 1 was repeated three times as Tests 1.1, 1.2 and 1.3). The photographs used in these tests were collected in bursts of three photographs so that each camera location generated three photographs simultaneously; the first photograph from each camera location was applied to Test x.1, the second to Test x.2 and the third to Test x.3. The SfM processing results from these tests are presented in Table 2.8. The repeated tests produced consistent results; however, while the photographs in Test 3.2 were successfully aligned, the sparse point cloud was not representative of the subject and a dense point cloud could not be built. Multiple attempts to align these photographs were unsuccessful despite their similarity to the photographs in Tests 3.1 and 3.3.

Table 2.8 Camera tests - SfM processing results for repeated camera tests.

Camera Test	Cameras (Aligned)	Sparse Cloud (Points)	Dense Cloud (Points)	Mesh (Faces)	RMS Error (mm)	Reprojection Error (pix)	Resolution (mm/pix)	Scale Bar Error (mm)
Test 1.1	180 (180)	81 388	2 086 671	417 334	0.189	1.94	0.228	0.085
Test 2.1	180 (180)	87 220	2 040 225	408 045	0.190	1.92	0.179	0.119
Test 3.1	180 (180)	108 953	1 911 328	382 265	0.157	1.64	0.198	0.100
Test 1.2	180 (180)	81 261	2 127 459	425 491	0.188	1.94	0.227	0.121
Test 2.2	180 (180)	87 078	2 018 622	403 724	0.190	1.93	0.179	0.088
Test 3.2	180 (180)	104 391	-	-	-	-	-	-
Test 1.3	180 (180)	86 905	2 090 883	418 176	0.190	1.92	0.223	0.088
Test 2.3	180 (180)	93 506	2 068 333	413 666	0.192	1.92	0.173	0.007
Test 3.3	180 (180)	117 468	1 905 326	381 065	0.158	1.62	0.188	0.078

SfM Measurements

The differences between $M_{[REAL]}$ and $M_{[SfM]}$ are reported as the cumulative positive and negative modelling error in Figure 2.10. A univariate analysis of variance (one-way ANOVA) using the absolute value of line segment measurement error as the independent variable, revealed a statistically significant difference between test results ($F(17,360) = 4.365$, $p = 3.41 \times 10^{-8}$). Performing the same analysis of variance on the repeated camera tests (including camera tests 1 to 3 in the analysis) revealed no statistically significant difference between the results of the repeated tests (Test 1: $F(3,80) = 0.389$, $p = 0.761$, Test 2: $F(3,80) = 0.194$, $p = 0.900$, Test 3: $F(2,60) = 1.538$, $p = 0.223$).

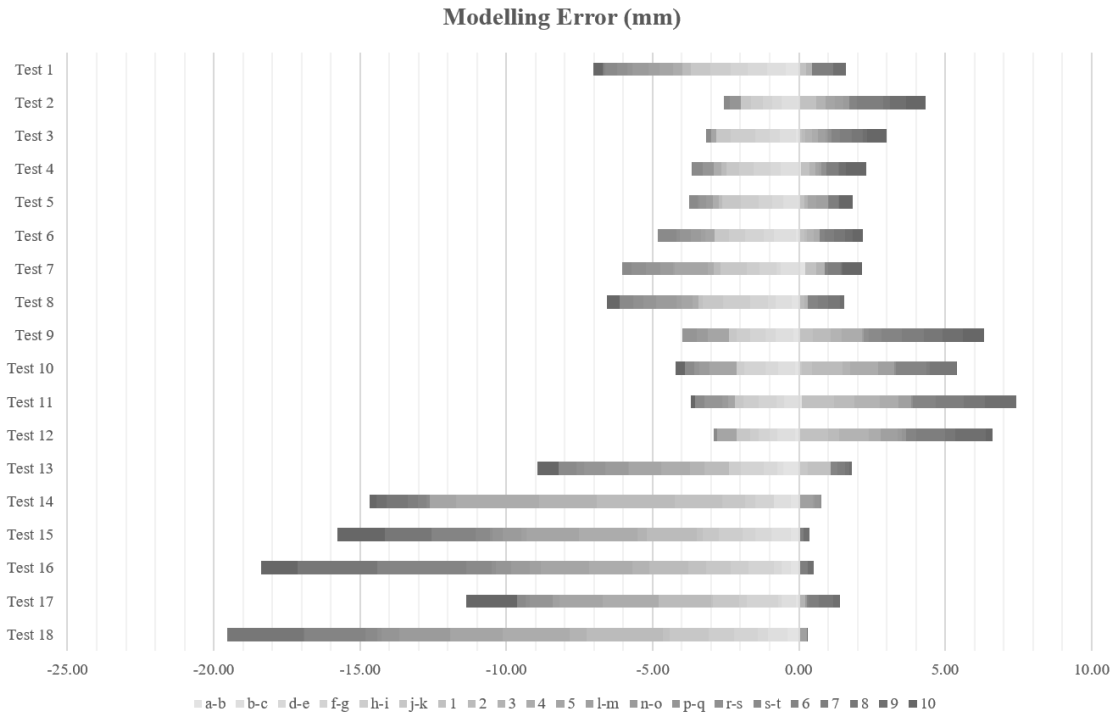

Figure 2.10 A comparison of the cumulative positive and negative modelling error across each of the camera tests.

While the statistical analysis indicates that there is a statistically significant difference in the accuracy of the 3D models generated under the different parameters of the test configurations, the analysis provides no information regarding which tests were accurate and which were not. Across all camera tests, the difference between $M_{[REAL]}$ and $M_{[SfM]}$ ranged from −8.83% to +3.17% (Figure 2.11). For the camera tests conducted with the Sony A6500, the measurement difference was −6.05% to +3.17%, with the

frames extracted from video tests ranging from −4.99% to +1.59% and the photograph tests from −6.05% to +3.17%. For the camera tests conducted with the GoPro, there was a −8.83% to +2.30% difference in measurement, with those models produced from extracted video frames ranging from −8.26% to +1.38% and −8.83% to +2.30% for those from photographs.

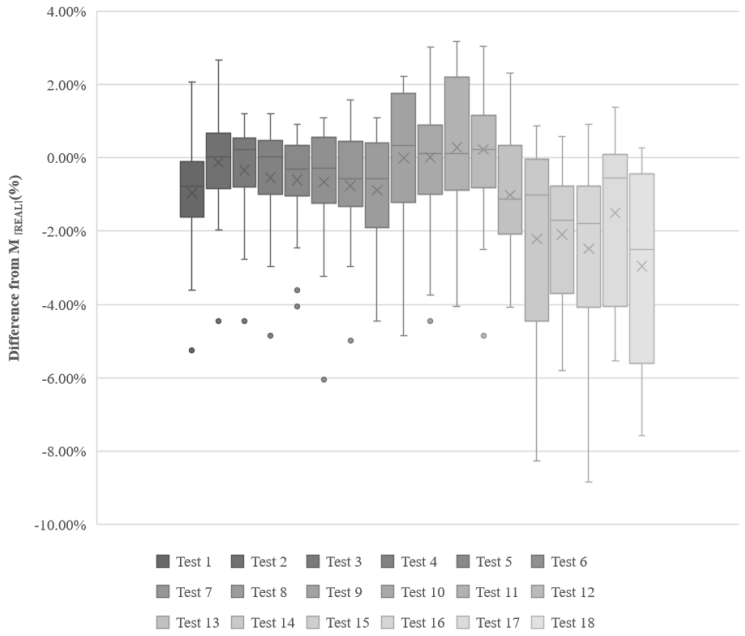

Figure 2.11 The distribution of measurement accuracy across all camera tests.

To assess the impact that the color of the block had on model accuracy, the measurement accuracy was subdivided into those measurements made on the white block and those on the natural block (Figure 2.12). Overall, the accuracy distribution across all tests is not that dissimilar, with the difference between $M_{[REAL]}$ and $M_{[SfM]}$ ranging from −8.26% to +3.17% for the white block and −8.83% to +3.05% for the natural block. However, for the natural block measurements in tests 1 to 6 (HEXYZ-1 mounted Sony A6500 photographs), the difference between $M_{[REAL]}$ and $M_{[SfM]}$ is less variable than other tests, ranging from −1.96% to +1.60%.

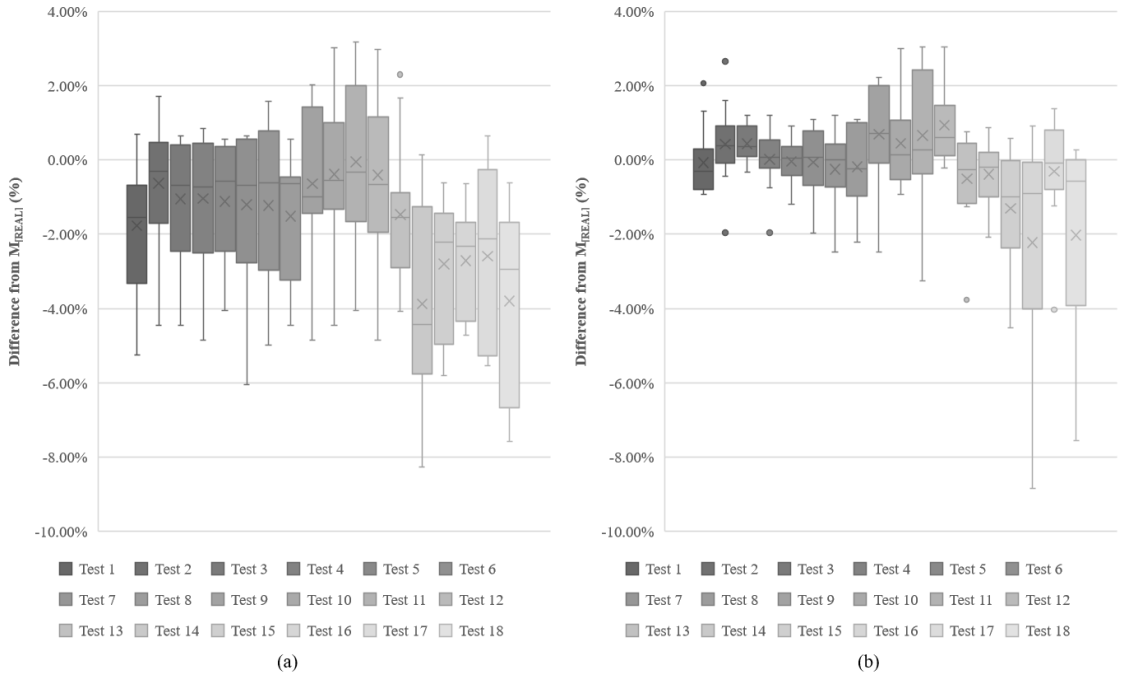

Figure 2.12 The distribution of measurement accuracy across all camera tests. Measurement accuracy is subdivided into the white block (a) and the natural block (b).

The measurement accuracy graphs reveal a difference between the accuracy of those models made using the Sony A6500 and those using the GoPro, as well as those made of the white block and those of the natural block. Addressing the Sony A6500 and GoPro models separately with a one-way ANOVA, comparing the absolute values of line segment measurement error as the independent variable, reveals that there was a statistically significant difference between the test results for the Sony A6500 ($F(11,240) = 2.483$, $p = 0.006$) but not for the GoPro ($F(5,120) = 1.156$, $p = 0.335$). An analysis of the measurement error across all Sony A6500 white block tests ($F(11,120) = 1.386$, $p = 0.188$) and natural block tests ($F(11,108) = 1.503$, $p = 0.141$) reveals that there is not a statistically significant difference between the measurement errors within each group of tests. This suggests that the variability within the Sony A6500 tests is the result of block color and not camera settings, which presents challenges for ecological studies of organisms having uniform color or texture.

2.3.3. Point Cloud Analysis

A cloud-to-cloud (C2C) comparison of the dense point clouds from each paired test configuration was used to determine the change measurement accuracy. The dense point clouds from the camera tests without the gaming die served as the reference data to which the camera test with the gaming die were compared. Each analysis generated an absolute distance point cloud (Figure 2.13), of which the maximum distance calculation should be equal to the size of the die. The accuracy of the distance estimate (the difference between the $D_{[C2C]}$ and $D_{[REAL]}$) for each test configuration pair is presented in Figure 2.14. Across all test pairs, the difference ranged from −5.17% to +4.89%, with the most accurate configuration providing an underestimate of 2.54% (equal to 0.37 mm).

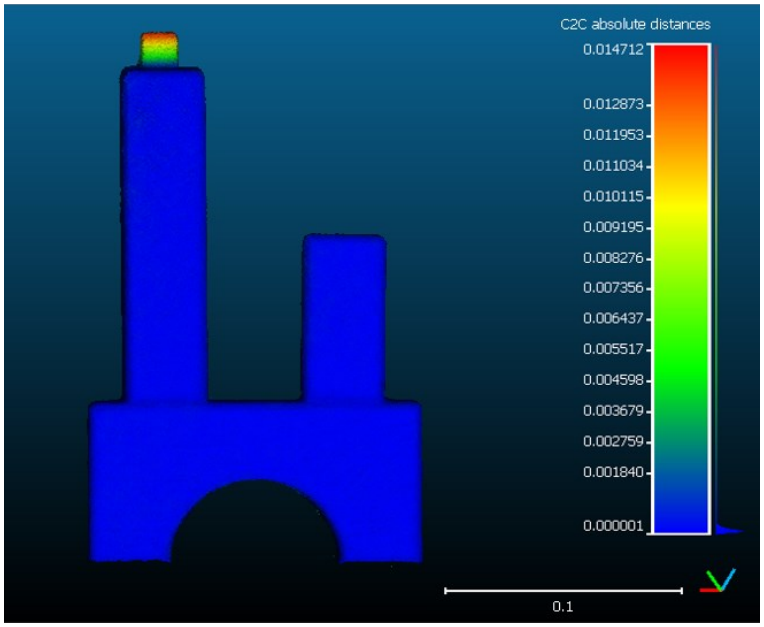

Figure 2.13 Structural change (the addition of the die) was evaluated with cloud-to-cloud distance analyses.

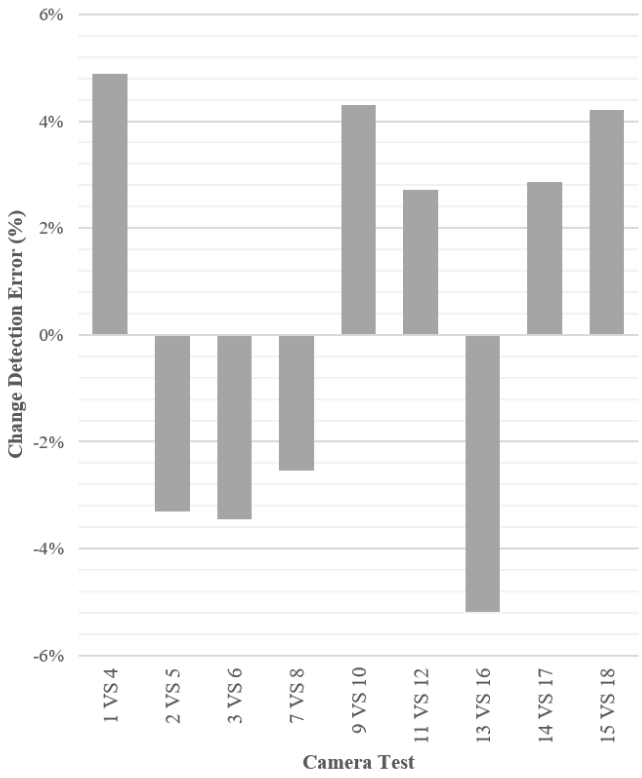

Figure 2.14 A comparison of the cloud-to-cloud change detection accuracy across test pairs.

2.4. Discussion

This research provides an assessment of the effect that lighting, camera type and settings, and capture methodology have on the accuracy of 3D models created from photographs and videos captured in a dry-lab. These dry-lab analyses were designed to establish a set of SfM data quality benchmarks that would inform the design of subsequent wet-lab research and, ultimately, the temporal evaluation of glass sponge morphology in situ. The slow growth rate of glass sponges, coupled with the inherent difficulties associated with underwater photography in temperate marine environments necessitates a thorough understanding of the critical features that can be resolved, how accurately they can be resolved, and the impact that environmental and workflow variability have on SfM data quality. While SfM has proven to be a valuable 3D modelling tool across many disciplines, including studies of benthic organisms and ecosystems, the authors wonder whether the documented accuracy of the SfM models in those studies represents the greatest accuracy that can be achieved given the equipment

used. This research strives to challenge and further develop the data science supporting SfM-based surveying, both in a temperate marine environment and beyond.

Overall, the −8.83% to +3.17% (or −3.07 to 1.09 mm) difference from $M_{[REAL]}$ obtained in this study is comparable to similar studies addressing the accuracy of SfM for modelling marine benthos. Figueira et al. (2015) assessed the level of error achieved with high-resolution SfM models of complex structures at the coral-colony scale by comparing SfM data to laser scanning data. Their analyses included 10 coral colonies and six different morphologies, ranging in size from 15 to 50 cm diameter. Images were captured using a 24 MP Sony NEX-7 camera with a 16 mm f/2.8 wide-angle lens in a waterproof housing fitted with a dome port. Each coral colony was photographed approximately 120 times in a 1.2-m-deep pool. The image capture strategy included two circular passes at 1 m, 60 cm and 30 cm and two perpendicular arcs over each coral colony. Accuracy was calculated by comparing laser scans of each coral colony to the averaged SfM model derived from a set of SfM models. The SfM models were accurate within 1.3 to 2.5 mm of the laser scan data; however, there was significant spatial variation in that accuracy measurement, and SfM-derived surface rugosity values varied from laser scan data by as much as 38%.

Lavy et al. (2015) quantified the volume and surface area of six cubical cardboard boxes (of varying sizes) and seven playdough models (of varying shape and posture) using both still photographs and images extracted from video, from four different cameras (Canon G11, Canon S100, GoPro HERO3+ and LG Nexus 5). True volume and surface area values were determined by measuring the boxes, and the volume of the playdough models was determined by water displacement. Approximately 50 images of each object were uploaded to Autodesk 123D Catch for SfM processing, using reference objects for scale. The results showed a linear relationship between the measured and the SfM-derived measures of volume and surface area, indicating constant relative accuracy regardless of object size. However, the volume and surface area measures for the cardboard boxes were slightly overestimated by the SfM workflow. The true volume of the playdough models differed from the SfM model by −4.2% to 3.4% for all shapes other than an arch (+13.3%). When the orientation of the playdough model was changed, the SfM-derived volumes differed from the true volume by −4.2% to 5.0%. The surface area and volume estimates derived from the Nexus 5 images produced the best results (1.1% and 1.3% errors, respectively), while the

extracted video clips from the Canon S100 produced a surface area error of 1.4% and a volume error of 4.1%.

The present paper builds on these prior studies, not only addressing the differences in accuracy between cameras and between test subjects but also addressing the accuracy of the camera as a function of its settings and how it was used, highlighting the implications of these choices for future SfM applications. While the Sony A6500 was accurate to within −4.06% to 3.17% of the real-world linear measurements in one test, it was also accurate within −2.46% to 0.90% in another; the only difference between the two tests being that the former used photographs captured with a handheld camera whereas with the latter the camera was mounted on HEXYZ-1. While the statistical analysis suggests that this difference is not significant, under the context of slow annual glass sponge growth, its difference and accuracy are very important when characterizing slow growth.

The 3D growth and extended projections of certain glass sponges prove difficult for accurate growth measurement (Kahn et al., 2016). The high-density 3D point clouds of SfM offer a possible solution to this problem. The mean value of the measurement errors generated for each camera test was primarily less than 1 mm (Figure 2.15). While the wooden blocks used for these tests served to simplify measurement, their simple shape is not representative of glass sponge structure and shape has been shown to play an influential role in SfM accuracy (Lavy et al., 2015). Nonetheless, some basic conclusions can be drawn from this research about the camera and the data capture strategy.

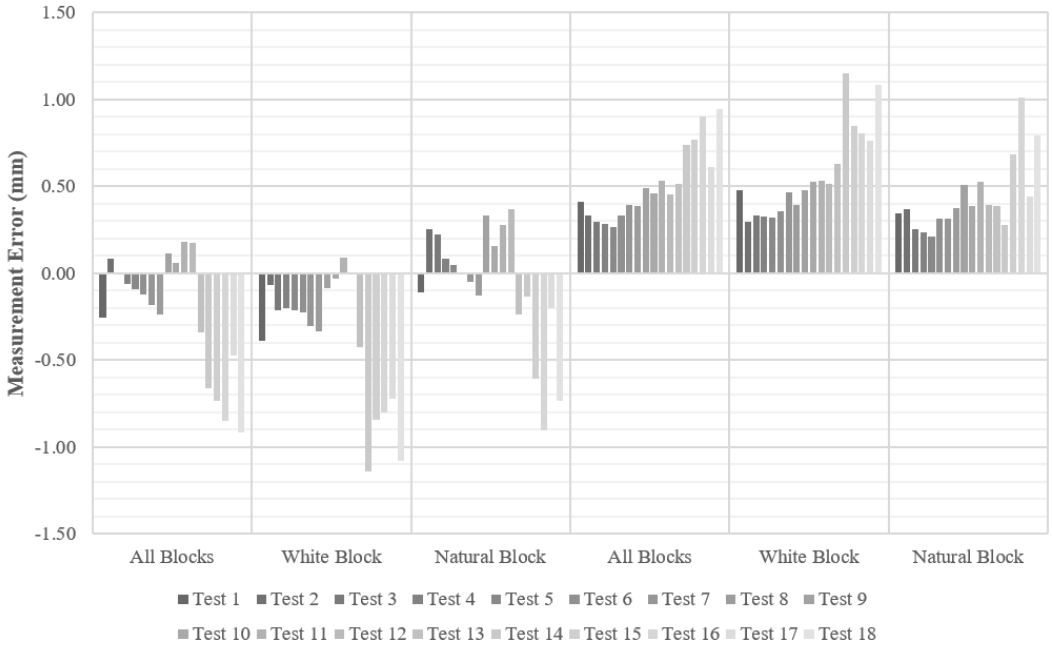

Figure 2.15 The mean measurement error for each camera test. The three left-hand columns represent the mean value, while the three right-hand columns represent the mean of the absolute value, of error measurements.

2.5. Conclusion

This research was designed to provide a set of SfM data quality benchmarks and to evaluate HEXYZ-1's performance in a controlled, dry-lab setting. Additionally, the work hoped to highlight how variability in the chosen data capture methodology has a direct impact on data quality. For marine ecologists and others considering SfM-based modelling in challenging and untested environments, it is critical to understand what is, and what is not, possible given the chosen workflow and available equipment. In these tests, the Sony A6500 produced higher accuracy models than the GoPro HERO6. This was expected, as the Sony A6500 is a superior camera that provides greater performance and pixel density. Furthermore, higher accuracy models were produced with the camera mounted to the HEXYZ-1 armature, which provides a stable platform for the camera, eliminating any motion caused by handheld photography. Surprisingly, there were minimal differences between the mean value of absolute accuracy measurements for the 3D models generated from photographs and those from video; however, the range of measurement accuracy was greater for the video tests than the camera tests. While photographs did produce slightly better results, the ability to generate accurate

models from video is advantageous, as data capture in the field is limited by the amount of time that can be spent underwater, and video capture is significantly quicker. The different ISO speed settings of the A6500 tests had minimal impact on measurement accuracy. This does not suggest that any ISO will suffice, as the test subject was well illuminated and did not necessitate the higher ISO values which would introduce noise. The results of the C2C absolute distance analyses were surprising, with each test pair proving accurate within 1 mm and the Sony A6500 video tests providing the most accurate change measurement. This helps support the case for video data capture by scuba divers.

This paper builds on prior research efforts quantifying the accuracy of SfM modelling in the context of marine benthos by teasing out the influence that lighting, camera settings and capture strategy have on the accuracy of the resultant SfM model. The results of the dry-lab study indicate a statistically significant difference between the accuracy of the SfM models generated using a Sony A6500 digital camera and a GoPro HERO6 Black action camera, but not between Sony A6500 tests modelling simple wooden blocks of the same color. However, statistical significance aside, the tests suggest that a well-illuminated test subject, a stable camera platform and photographs collected with a low ISO value will produce higher accuracy SfM models with less variability in measurement error. These results demonstrate that the accuracy of SfM modelling efforts are not only influenced by the type of camera, but by the camera's settings and the method of data capture.

The results of this study are limited by the chosen quality control measures. Camera calibration was performed automatically within PhotoScan rather than manually with a calibration grid. While reference markers and scale bars were implemented to assist with quality control, model accuracy relies on these limited, 2D measures and risks the influence of systematic errors associated with auto-calibration. Ultimately, 3D model accuracy was evaluated through repeated measurements of easily identifiable features made across the multiple axes of the wooden blocks, which was deemed sufficient for this study given the limitations that would be imposed on underwater camera calibration within the confines of HEXYZ-1. Furthermore, the simple structure of the wooden blocks, while they helped to reduce the manual measurement errors associated with the complex structure of the glass sponge skeleton, are not representative of most benthic species to which the presented methodology may be

applied. However, the dry-lab tests and rudimentary shapes were critical in the authors' ability to understand the performance of this workflow prior to moving into a wet-lab. Future iterations of this research should explore camera calibration options and incorporate more complex shapes, perhaps 3D printing objects of known dimension with identifiable features and provisions for the addition of projections simulating growth.

Overall, HEXYZ-1 provides a stable, well-illuminated platform for repeated data capture that has proven to provide 3D accuracy sufficient for monitoring glass sponge growth. However, these results do not confirm that this methodology will return the same results underwater. Subsequent phases of this research translate the workflow from a dry-lab into a wet-lab, modelling a more complex structure and quantifying the accuracy of the resultant SfM models, and then to the field to quantify changes in glass sponge morphology over time. While the results of this study may suggest that accurate, high-resolution modelling of glass sponges may be possible in situ, the complexities introduced by the marine environment and the multi-media (air–glass–water) interface of an underwater housing may impact the ability to replicate the dry-lab results. Furthermore, while the results of video tests proved promising, photographs provided superior results and further investigation into the performance of SfM modelling using fewer photographs, as well as different camera position configurations, should be assessed.

Acknowledgements

This work was supported by Mitacs through the Mitacs Accelerate Program in partnership with Ocean Wise and the Vancouver Aquarium. The authors would also like to acknowledge the SFU Faculty of Science Machine Shop for their help fabricating HEXYZ-1.

References

Abadie, A., Boissery, P., & Viala, C. (2018). Georeferenced underwater photogrammetry to map marine habitats and submerged artificial structures. The Photogrammetric Record, 33(164), 448–469. https://doi.org/10.1111/phor.12263

Agisoft LLC. (2018). Agisoft PhotoScan User Manual - Professional Edition, Version 1.4 (p. 119). http://www.agisoft.com/pdf/photoscan-pro_1_4_en.pdf

Austin, W. C., Conway, K. W., Barrie, J. V., & Krautter, M. (2007). Growth and morphology of a reef-forming glass sponge, Aphrocallistes vastus (Hexactinellida), and implications for recovery from widespread trawl damage. Porifera Research: …, 139–145. http://www.poriferabrasil.mn.ufrj.br/iss/09-book/pdf/Austin et al - Growth and morphology of Aphrocallistes vastus.pdf

Bayley, D. T. I., Mogg, A. O. M., Koldewey, H., & Purvis, A. (2019). Capturing complexity: field-testing the use of 'structure from motion' derived virtual models to replicate standard measures of reef physical structure. PeerJ, 7, e6540. https://doi.org/10.7717/peerj.6540

Beltrame, C., & Costa, E. (2017). 3D survey and modelling of shipwrecks in different underwater environments. Journal of Cultural Heritage, 3–9. https://doi.org/10.1016/j.culher.2017.08.005

Bennecke, S., Kwasnitschka, T., Metaxas, A., & Dullo, W.-C. (2016). In situ growth rates of deep-water octocorals determined from 3D photogrammetric reconstructions. Coral Reefs, 35(4), 1227–1239. https://doi.org/10.1007/s00338-016-1471-7

Burns, J., Delparte, D., Gates, R., & Takabayashi, M. (2015). Integrating structure-from-motion photogrammetry with geospatial software as a novel technique for quantifying 3D ecological characteristics of coral reefs. PeerJ, 3, e1077. https://doi.org/10.7717/peerj.1077

Chu, J. W. F., & Leys, S. P. (2010). High resolution mapping of community structure in three glass sponge reefs (Porifera, Hexactinellida). Marine Ecology Progress Series, 417, 97–113. https://doi.org/10.3354/meps08794

Chu, J. W. F., Maldonado, M., Yahel, G., & Leys, S. P. (2011). Glass sponge reefs as a silicon sink. Marine Ecology Progress Series, 441, 1–14. https://doi.org/10.3354/meps09381

Conway, K., Barrie, J., Hill, P., Austin, W., & Picard, K. (2007). Mapping sensitive benthic habitats in the Strait of Georgia, coastal British Columbia: deep-water sponge and coral reefs. In Geological Survey of Canada, Current Research (Vols. 2007-A2). https://doi.org/10.1002/9780470344620.fmatter

Conway, K. W., Krautter, M., Barrie, J. V., & Neuweiler, M. (2001). Hexactinellid sponge reefs on the Canadian continental shelf: A unique “living fossil.” In Geoscience Canada (Vol. 28, Issue 2, pp. 71–78).

Conway, Kim W., Barrie, J. V., & Krautter, M. (2005). Geomorphology of unique reefs on the western Canadian shelf: Sponge reefs mapped by multibeam bathymetry. Geo-Marine Letters, 25(4), 205–213. https://doi.org/10.1007/s00367-004-0204-z

Cook, S. E., Conway, K. W., & Burd, B. (2008). Status of the glass sponge reefs in the Georgia Basin. Marine Environmental Research, 66, S80–S86. https://doi.org/10.1016/j.marenvres.2008.09.002

Department of Fisheries and Oceans Canada. (2010). Pacific Region Coral and Sponge Conservation Strategy 2010-2015. In Oceans, Habitat and Species at Risk Oceans Program. Fisheries and Oceans Canada.

Figueira, W., Ferrari, R., Weatherby, E., Porter, A., Hawes, S., & Byrne, M. (2015). Accuracy and precision of habitat structural complexity metrics derived from underwater photogrammetry. Remote Sensing, 7(12), 16883–16900. https://doi.org/10.3390/rs71215859

Fukunaga, A., Burns, J., Craig, B., & Kosaki, R. (2019). Integrating Three-Dimensional Benthic Habitat Characterization Techniques into Ecological Monitoring of Coral Reefs. Journal of Marine Science and Engineering, 7(2), 27. https://doi.org/10.3390/jmse7020027

Gutierrez-Heredia, L., Benzoni, F., Murphy, E., & Reynaud, E. G. (2016). End to End Digitisation and Analysis of Three-Dimensional Coral Models, from Communities to Corallites. PLoS ONE, 11(2). https://doi.org/10.1371/journal.pone.0149641

Kahn, A. S., Vehring, L. J., Brown, R. R., & Leys, S. P. (2016). Dynamic change, recruitment and resilience in reef-forming glass sponges. Journal of the Marine Biological Association of the United Kingdom, 96(02), 429–436. https://doi.org/10.1017/S0025315415000466

Kahn, A. S., Yahel, G., Chu, J. W. F., Tunnicliffe, V., & Leys, S. P. (2015). Benthic grazing and carbon sequestration by deep-water glass sponge reefs. Limnology and Oceanography, 60(1), 78–88. https://doi.org/10.1002/lno.10002

Krautter, M., Conway, K. W., Barrie, J. V., & Neuweiler, M. (2001). Discovery of a “Living Dinosaur”: Globally unique modern hexactinellid sponge reefs off British Columbia, Canada. Facies, 44, 265–282. https://doi.org/10.1007/BF02668178

Lavy, A., Eyal, G., Neal, B., Keren, R., Loya, Y., & Ilan, M. (2015). A quick, easy and non-intrusive method for underwater volume and surface area evaluation of benthic organisms by 3D computer modelling. Methods in Ecology and Evolution, 6(5), 521–531. https://doi.org/10.1111/2041-210X.12331

Leon, J. X., Roelfsema, C. M., Saunders, M. I., & Phinn, S. R. (2015). Measuring coral reef terrain roughness using “Structure-from-Motion” close-range photogrammetry. Geomorphology, 242, 21–28. https://doi.org/10.1016/j.geomorph.2015.01.030

Levings, C. D., & McDaniel, N. G. (1974). A unique collection of baseline biological data: benthic invertebrates from an underwater cable across the Strait of Georgia (Issue Mi). http://www.dfo-mpo.gc.ca/Library/52321.pdf

Leys, S. P., Mackie, G. O., & Reiswig, H. M. (2007). The Biology of Glass Sponges. Advances in Marine Biology, 52(06), 1–145. https://doi.org/10.1016/S0065-2881(06)52001-2

Marliave, J. B., Conway, K. W., Gibbs, D. M., Lamb, A., & Gibbs, C. (2009). Biodiversity and rockfish recruitment in sponge gardens and bioherms of southern British Columbia, Canada. Marine Biology, 156(11), 2247–2254. https://doi.org/10.1007/s00227-009-1252-8

McCarthy, J. (2014). Multi-image photogrammetry as a practical tool for cultural heritage survey and community engagement. Journal of Archaeological Science, 43(1), 175–185. https://doi.org/10.1016/j.jas.2014.01.010

McCarthy, J., & Benjamin, J. (2014). Multi-image Photogrammetry for Underwater Archaeological Site Recording: An Accessible, Diver-Based Approach. Journal of Maritime Archaeology, 9(1), 95–114. https://doi.org/10.1007/s11457-014-9127-7

Menna, F., Agrafiotis, P., & Georgopoulos, A. (2018). State of the art and applications in archaeological underwater 3D recording and mapping. Journal of Cultural Heritage, 33, 231–248. https://doi.org/10.1016/j.culher.2018.02.017

Napolitano, R., Chiariotti, P., & Tomasini, E. P. (2019). Preliminary assessment of Photogrammetric Approach for detailed dimensional and colorimetric reconstruction of Corals in underwater environment. 2018 IEEE International Workshop on Metrology for the Sea; Learning to Measure Sea Health Parameters, MetroSea 2018 - Proceedings, 39–45. https://doi.org/10.1109/MetroSea.2018.8657835

Piazza, P., Cummings, V., Lohrer, D., Marini, S., Marriott, P., Menna, F., Nocerino, E., Peirano, A., & Schiaparelli, S. (2018). Divers-operated underwater photogrammetry: Applications in the study of Antarctic benthos. International Archives of the Photogrammetry, Remote Sensing and Spatial Information Sciences - ISPRS Archives, 42(2), 885–892. https://doi.org/10.5194/isprs-archives-XLII-2-885-2018

Pizarro, O., Friedman, A., Bryson, M., Williams, S. B., & Madin, J. (2017). A simple, fast, and repeatable survey method for underwater visual 3D benthic mapping and monitoring. Ecology and Evolution, 7(6), 1770–1782. https://doi.org/10.1002/ece3.2701

Raoult, V., David, P. A., Dupont, S. F., Mathewson, C. P., O'Neill, S. J., Powell, N. N., & Williamson, J. E. (2016). GoPros as an underwater photogrammetry tool for citizen science. PeerJ, 4, e1960. https://doi.org/10.7717/peerj.1960

Raoult, V., Reid-Anderson, S., Ferri, A., & Williamson, J. (2017). How Reliable Is Structure from Motion (SfM) over Time and between Observers? A Case Study Using Coral Reef Bommies. Remote Sensing, 9(7), 740. https://doi.org/10.3390/rs9070740

Remondino, F., Pizzo, S. Del, Kersten, T. P., Troisi, S., Metrology, O., Kessler, B., & Fbk, F. (2012). Low-Cost and Open-Source Solutions for Automated Image Orientation – A Critical Overview. In M. Ioannides, D. Fritsch, J. Leissner, R. Davies, F. Remondino, & R. Caffo (Eds.), Progress in Cultural Heritage Preservation 4th International Conference, EuroMed 2012 (pp. 40–54). Springer, Berlin, Heidelberg. https://doi.org/https://doi-org.proxy.lib.sfu.ca/10.1007/978-3-642-34234-9

Semaan, L., & Salama, M. S. (2019). Underwater Photogrammetric Recording at the Site of Anfeh, Lebanon. In J. K. McCarthy, J. Benjamin, T. Winton, & W. van Duivenvoorde (Eds.), 3D Recording and Interpretation for Maritime Archaeology (pp. 67–87). Springer International Publishing. https://doi.org/10.1007/978-3-030-03635-5_5

Shortis, M. (2019). Camera Calibration Techniques for Accurate Measurement Underwater. In J. K. McCarthy, J. Benjamin, T. Winton, & W. van Duivenvoorde (Eds.), 3D Recording and Interpretation for Maritime Archaeology (pp. 11–27). Springer International Publishing. https://doi.org/10.1007/978-3-030-03635-5_2

Skarlatos, D., Demestiha, S., & Kiparissi, S. (2012). An 'Open' Method for 3D Modelling and Mapping in Underwater Archaeological Sites. International Journal of Heritage in the Digital Era, 1(1), 1–24.

Thoeni, K., Giacomini, A., Murtagh, R., & Kniest, E. (2014). A comparison of multi-view 3D reconstruction of a rock wall using several cameras and a Laser scanner. International Archives of the Photogrammetry, Remote Sensing and Spatial Information Sciences - ISPRS Archives, 40(5), 573–580. https://doi.org/10.5194/isprsarchives-XL-5-573-2014

Van Damme, T. (2015). Computer Vision Photogrammetry for underwater archaeological site recording in a low-visibility environment. International Archives of the Photogrammetry, Remote Sensing and Spatial Information Sciences - ISPRS Archives, 40(5W5), 231–238. https://doi.org/10.5194/isprsarchives-XL-5-W5-231-2015

Westoby, M. J., Brasington, J., Glasser, N. F., Hambrey, M. J., & Reynolds, J. M. (2012). "Structure-from-Motion" photogrammetry: A low-cost, effective tool for geoscience applications. Geomorphology, 179, 300–314. https://doi.org/10.1016/j.geomorph.2012.08.021

Chapter 3.

Evaluating the 3D Integrity of Underwater Structure from Motion Workflows

This paper is published in *The Photogrammetric Record*.

Citation Details: Lochhead, I. and Hedley, N. (2022), Evaluating the 3D Integrity of Underwater Structure from Motion Workflows. Photogram Rec, 37: 35-60. https://doi.org/10.1111/phor.12399

Abstract

Structure from motion (SfM) is an accessible and non-intrusive method of 3D data capture popular for tropical coral reef surveying. In the northeast Pacific Ocean, where there are many environmentally sensitive benthic organisms whose morphology and function are equally important, SfM surveys are less commonly studied. Temperate waters pose unique challenges to SfM workflows, which must be systematically unpacked to understand their impact on data quality and veracity. This uncertainty raises broader questions concerning SfM as a spatial data acquisition and ecological characterization method in temperate waters, and whether a systematic workflow assessment reveals vital relationships between SfM implementation parameters, 3D data products, and their implications for other underwater SfM surveys. This paper, the second of two empirical assessments, reports on a series of wet-lab and dryland tests quantifying the impact that temperate waters, underwater cameras, and photograph quantity and configuration have on SfM accuracy. These tests provided crucial accuracy benchmarks informing subsequent field-based surveys and revealed that underwater SfM workflows can generate highly accurate 3D models in temperate waters.

Keywords: 3D modelling, benthic monitoring, data quality, glass sponge, marine ecology, structure-from-motion

3.1. Introduction

The biogenic glass sponge reefs (phylum Porifera: class Hexactinellida) of the northeast Pacific Ocean are unique, fragile, and ecologically important, providing a key structural habitat for several fish and invertebrate species (Fisheries and Oceans Canada, 2010). However, the functional integrity of these ecosystems is currently threatened by a collection of anthropogenic, climatic, and environmental factors (Marliave, 2015), the impact of which is difficult to monitor without cost-effective and informative ecological indicators of glass sponge reef health. While structural complexity is known to influence biodiversity, productivity, and survivorship in biogenic habitats (Gratwicke & Speight, 2005) such as glass sponge reefs, traditional two-dimensional (2D) methods of measurement may fail to adequately characterize the three-dimensional (3D) complexities of habitat structure. Furthermore, these methods can be difficult, time consuming and produce highly variable results; or are destructive, thereby limiting the information that can be deduced from such studies (Abdo et al., 2006; Cocito et al., 2003). Accurate methods of 3D characterization are needed to improve our knowledge of glass sponge ecology, to assist with coastal monitoring efforts, and to facilitate informed marine management policy decision making.

Structure from motion (SfM) photogrammetry can be used to characterize 3D structure from multiple overlapping 2D photographs. SfM workflows provide a user-friendly, high-accuracy, and non-intrusive method of 3D data capture that has made them popular across many research domains. This includes bathymetric surveying (Abadie et al., 2018), marine archaeology (Beltrame & Costa, 2017; McCarthy & Benjamin, 2014; Skarlatos et al., 2012), ecological monitoring (Fukunaga et al., 2019), morphometric analyses (Gutierrez-Heredia et al., 2016; Lavy et al., 2015; Napolitano et al., 2019; Palma et al., 2018; Prado et al., 2019), benthic mapping and classification (Bayley et al., 2019; Burns et al., 2015; Leon et al., 2015; Pizarro et al., 2017), and temporal change detection (Bennecke et al., 2016; Olinger et al., 2019; Piazza et al., 2018) – including low resolution models of glass sponges intended for visualization purposes (Kahn et al., 2016). Such successful underwater applications suggest that a similar SfM workflow could be equally effective and relevant in an assessment of glass sponge reef health, considering sponge reefs provide structural and ecological functions analogous to the coral reefs which dominate the research literature. However, the

comparatively cold, dark, and nutrient rich waters of the northeast Pacific Ocean present several challenges absent from many studies documenting the accuracy and precision of SfM workflows.

High quality 3D SfM models hinge on high-quality datasets (photographs or video). However, unlike terrestrial photography, underwater photography is impacted by light attenuation and scattering as natural or artificial light passes through the water column; the influence of each is determined by factors such as water temperature, salinity, water chemistry, and particulates (Jaffe, 1990; Mobley, 1994). Furthermore, waterproof camera housings introduce a multimedia interface (air, glass, and water), with each medium possessing different refractive indices, that impacts the transmission of light and leads to geometric distortion and measurement inaccuracies (McCarthy & Benjamin, 2014; Sarakinou et al., 2016). However, the use of a hemispheric dome port has proven to reduce refraction and increase the SfM software's ability to align photographs (Bruno et al., 2011; McCarthy & Benjamin, 2014) and the radiometric qualities of the photographs have been found to have minimal impact on the geometric qualities of the resultant SfM model (Sarakinou et al., 2016).

While the published SfM research literature has previously addressed the accuracy of SfM modelling (e.g., Lavy et al., 2015; Raoult, Reid-Anderson, Ferri, & Williamson, 2017; Troisi, Del Pizzo, Gaglione, Miccio, & Testa, 2015) and reported creative approaches to SfM-based surveying (Pizarro et al., 2017), any conclusions concerning 3D data quality drawn from these studies may not hold true in temperate waters. Research which builds upon the existing SfM, and underwater survey work is needed to support SfM-based 3D modelling for temperate marine ecology. This paper reports on the second phase of a three-phase research program (1. dry-lab, 2. wet-lab, and 3. field work) designed to establish foundational temperate marine SfM data quality benchmarks. Our dry-lab research (see Lochhead & Hedley, 2021) evaluated the performance of HEXYZ-1 and our SfM workflow in a controlled dry environment, establishing an optimal lighting configuration and a set of performance benchmarks for different cameras, camera settings, and photograph/video capture strategies. By contrast, the wet-lab research presented in this manuscript evaluates the effect that (simulated) low light levels and cold, turbid conditions - typical of temperate marine environments and glass sponge habitats – have on the performance of our SfM

workflow. Subsequent field-based activities (see Lochhead & Hedley, 2020) were informed by our dry-lab and wet-lab research.

There were three main objectives for this research: 1. to assess the performance of a custom-made SfM data capture platform (named HEXYZ-1) in a controlled underwater environment; 2. to compare the results of wet-lab SfM surveys against their dryland equivalents and use manual measurements to quantify the performance of the underwater SfM workflow, and; 3. to determine the optimal number and configuration of photographs so as to maximize model accuracy while accounting for the temporal constraints (approximately 20-minutes per dive) imposed by subsequent field-based data collection at depths of 20-25 meters. The wet-lab research discussed in this manuscript was an essential step in this research program, as it was informed by our initial dry-lab system and SfM workflow performance tests (Lochhead & Hedley, 2021) and informed subsequent field-based surveys of glass sponge morphology (Lochhead & Hedley, 2020). This approach not only delivers an operable field survey architecture, but also establishes the data science and data quality benchmarks necessary to understand SfM performance in temperate marine environments.

The equipment and workflow presented here were selected and designed to facilitate underwater photography and video capture for 3D SfM-based modelling of glass sponges and glass sponge colonies in Howe Sound, BC at depths > 20 m. Our workflow was intentionally designed to provide a set of SfM performance benchmarks for glass sponge colonies (up to 0.20 m3) prior to designing larger more difficult SfM-based surveys of glass sponge reefs and bioherms. While portions of this workflow may be onerous and impractical for field research (such as manual repositioning of cameras), the rigor was fundamental to manipulate, test, and understand how idiosyncratic sets of variables impact data quality.

The wet-lab research presented in this paper specifically evaluates the performance of underwater SfM in a simulated temperate marine environment and highlights the ramifications that photograph quantity and camera formation have on the accuracy of SfM surveys conducted in temperate waters; however, the results of these tests have practical implications for any SfM-based survey of isolated objects. In combination with the prior dry-lab phase evaluating SfM data quality under various lighting configurations and camera settings (Lochhead & Hedley, 2021) this research

served to inform subsequent field-based surveys of individual glass sponge colonies (Lochhead & Hedley, 2020). The three phases of this research project provide a foundation for the design of SfM surveys in temperate marine environments and for future surveys of glass sponge reefs and bioherms.

3.2. Materials and Methods

To assess workflow performance prior to data capture in the open ocean, photographs of an ornamental aquarium coral were captured both underwater (wet-lab) and on land (dryland). While the morphology of the ornamental coral does not match that of the reef-building glass sponges of interest, the structural complexities are sufficiently similar for the purpose of SfM performance analyses. The following subsections describe the materials and methods used for this study.

3.2.1. SfM Data Capture Platform

A custom-made SfM data capture platform named HEXYZ-1 (Figure 3.1) was constructed to provide camera stability, world-stabilized lighting, and a repeatable data capture strategy. HEXYZ-1 serves to minimize the impact that variable imaging strategies, diver experience levels, and underwater currents have on photograph quality and therefore SfM data products and morphometric analyses. HEXYZ-1 is constructed from 1-inch (25mm) square aluminum tubes linked by a nylon connector system that is reinforced with aluminum plates. An adjustable camera armature, which pivots around HEXYZ-1's central axis, is suspended from a hexagonal plate mounted to the top of the structure. Affixed to an adjustable platform on the vertical section of the armature is a tilting tripod head. The combined adjustability of the armature's components offers a wide range of camera positioning options within the confines of HEXYZ-1. When assembled, HEXYZ-1 weighs approximately 25 kg and measures 2.44 m wide (from vertex to vertex) by 1.7 m tall.

Figure 3.1 HEXYZ-1, a custom-made underwater imaging platform.

3.2.2. Lighting

Attached to HEXYZ-1 are seven extra-wide beam LED dive lights with a maximum output of 1200 lumens each. Each light is encased by a semi-opaque, hemispherical housing that diffuses the light and softens any shadows cast on the target object. The staggered positioning of the lights was determined through a series of dry-lab SfM tests (Lochhead & Hedley, 2021).

The amount of available natural light reaching the benthic zone is influenced by absorption and scattering, which vary according to water depth and the physical properties of the water column (Sarakinou et al., 2016). As the light conditions in the open ocean can vary significantly according to the weather, time of day, time of year, turbidity levels, etc. an artificial light source was required to ensure optimal lighting conditions for high-quality photographs. The photographs in this study were captured at night, within a large, semi-opaque fabric building, while making a concerted effort to minimize natural and artificial light pollution.

3.2.3. Camera and Housing

All photographs were captured with a Sony Alpha α6500 mirrorless digital camera outfitted with a Sony E PZ 16-50 mm F3.5-5.6 OSS (Optical SteadyShot) lens (referred to as the Sony A6500). The camera lens was set to a 16 mm focal length, an

aperture of f/3.5, a 400 ISO, and a 1/60 shutter speed. The same settings were used for underwater and dryland photography. Underwater photographs were taken with the Sony A6500 camera mounted inside an Aquatica A6500 Underwater Housing equipped with an 8-inch dome port, the use of which is known to reduce refraction and improve image alignment during SfM processing (Bruno et al., 2011; McCarthy & Benjamin, 2014). Either the camera or the underwater housing (with camera) could be mounted directly to the quick-release tripod head on the armature. A two-second shutter release delay was utilized to ensure that the camera and armature were at rest before the photographs were captured.

The radial distortion introduced by the hemispherical dome port was not of concern for this study, as the chosen SfM software (Agisoft PhotoScan – now Agisoft Metashape) can resolve the optical characteristics of the lens from the photographs without the added step of pre-calibration (Burns et al., 2015; McCarthy & Benjamin, 2014). While pre-calibration is advised (McCarthy & Benjamin, 2014), preliminary tests revealed it to have little impact on model accuracy; therefore, camera calibration and optimization were completed by PhotoScan, and pre-calibration was not conducted for future tests.

3.2.4. Test Environments

This study required both a wet-lab for underwater photography and a space for dryland photography. These two test environments were provided by a semi-permanent fabric building located at the Fisheries and Oceans Canada Centre for Aquaculture and Environmental Research in West Vancouver, BC.

A saltwater tank within the building served as the wet-lab and the ground surface beside it afforded a location for dryland photography (Figure 3.2). In the wet-lab, HEXYZ-1 was lowered into the centre of the tank where a team member, outfitted with a wetsuit and dive mask, activated all the lights before manually moving the armature into the positions required for each photograph. The water level within the tank was kept level with the top of HEXYZ-1, allowing the team member in the tank to stand with their head above water. The water within the tank was provided by a slow but constant feed from the bottom of Burrard Inlet. On dryland, HEXYZ-1 was placed on level ground and

the team member followed the same protocols for moving the armature and capturing photographs of the test subject. The two test environments are presented in Figure 3.3.

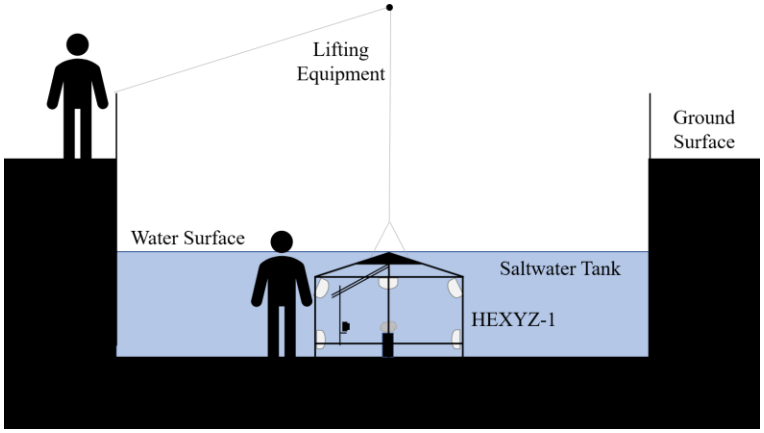

Figure 3.2 **A saltwater tank served as the wet-lab in this study. Dryland photographs were captured with HEXYZ-1 on the ground surface adjacent to the tank.**

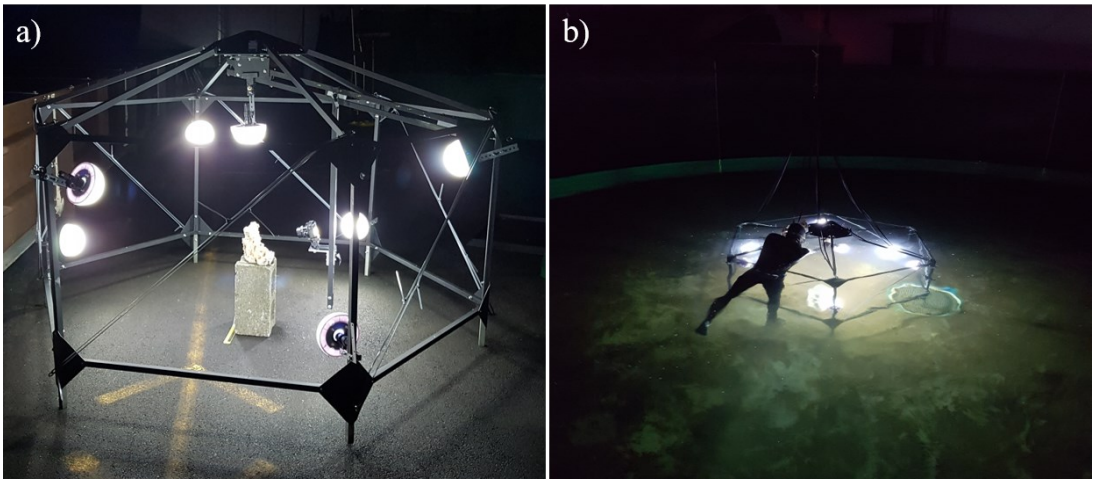

Figure 3.3 **SfM Test Environments. a) Dryland testing. b) Underwater testing (wet-lab).**

3.2.5. Test Subject

An ornamental aquarium coral served as the test subject for the wet-lab and dryland tests (Figure 3.4). The rigid, complex structure of the ornamental coral, while not representative of reef forming glass sponge morphology, provided a measurable 3D structure considered suitable for this study.

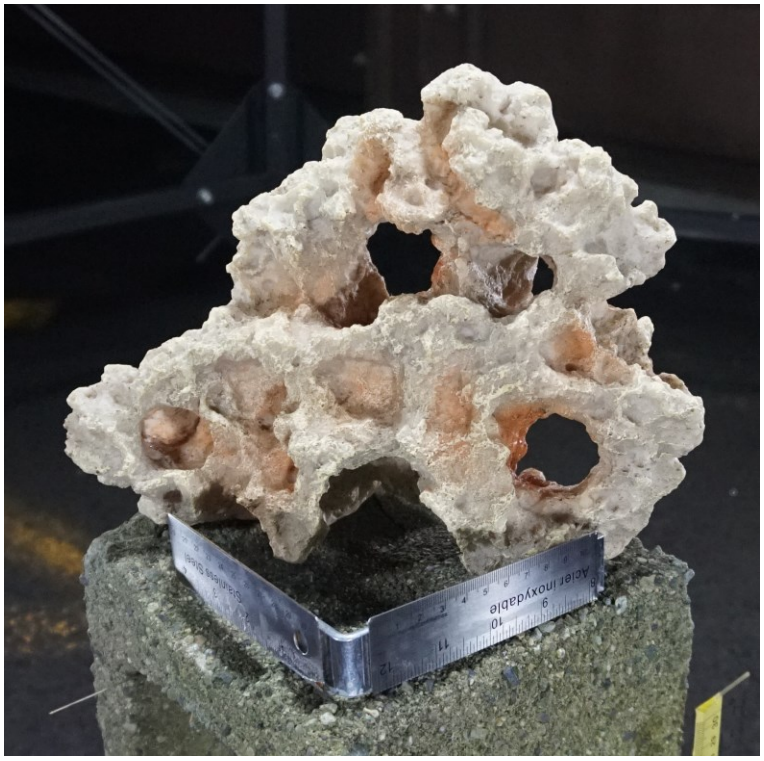

Figure 3.4 An ornamental aquarium coral served as the test subject for wet-lab and dryland SfM tests. Rulers served as a reference object of known dimension.

Pairs of easily identifiable physical features on each of the primary surfaces of the ornamental coral were selected for measurement. This provided six measurable line segments (e.g., A-B, C-D, …) from 12 physical features (Figure 3.5). Line segments were selected to include features of varying lengths, directions, and surface characteristics (i.e., recessed or protruded). Each of the line segments was measured using a digital caliper and recorded as the true value ($M_{[REAL]}$) for that feature.

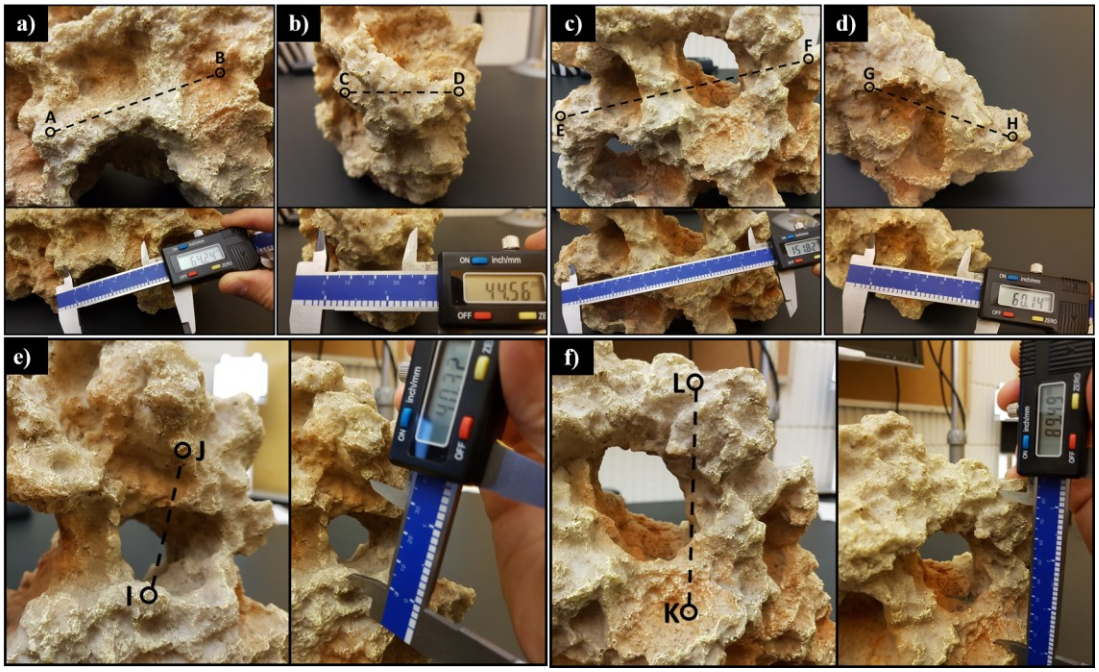

Figure 3.5 Six measurable line segments were generated from 12 identifiable features on the surface of an ornamental coral.

3.2.6. Photograph Acquisition

The photograph capture methodology was identical for the wet-lab and dryland tests. The ornamental coral was placed on a cement block located in the centre of HEXYZ-1. Three rulers affixed to a rigid steel bracket were placed next to the coral (see Figure 3.4), serving as a reference object with known dimensions. The camera (or camera and underwater housing) was then attached to HEXYZ-1's armature and manually maneuvered into the start position. The shutter button was then manually triggered, a photograph was captured, and the armature was moved to the next position. This process was repeated until a complete set of 180 photographs was collected from five circular sets (three inner sets and two outer sets) of 36 photographs (Figure 3.6). Approximately eight minutes were required to collect each circular set of photographs; however, on dryland, each circular set required approximately five minutes. The three-minute time differential is a function of the operator, outfitted only with a dive mask, having to periodically come up for air when collecting photographs in the wet-lab.

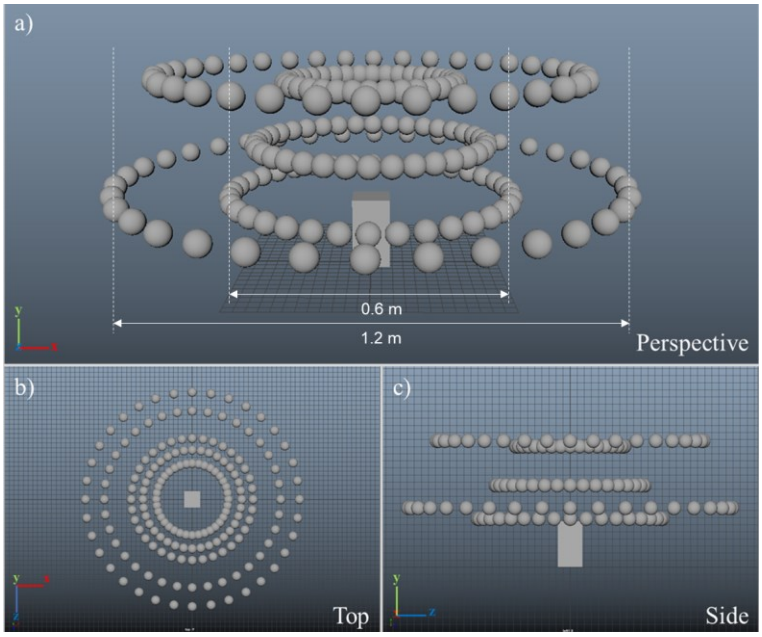

Figure 3.6 **Camera locations for SfM processing. Each sphere indicates a camera location – the ornamental coral was positioned on top of the cinder block in the centre (cube).**

As time is a limiting factor in underwater data collection, the 180 photographs from the dryland and wet-lab tests were processed as 26 unique SfM tests, providing 13 test sets (i.e., a wet-lab and dryland pair). Each test was performed under the same lighting conditions and camera settings (Table 3.1); however, each test set incorporated a different number of photographs and camera formations. As fewer photographs require less time underwater, and as dive time (limited to approximately 20-minutes)is the primary factor restricting underwater data collection efforts in the field, the effect that reduced photograph quantity and alternate photograph configuration have on 3D model accuracy was evaluated.

Table 3.1 **Camera Settings and Lighting Configuration for Dryland and Wet-Lab SfM tests**

Camera	Camera Settings							Lighting (lumens x number of lights)
	Focal Length (mm)	35 mm equivalent (mm)	ISO	Aperture	Shutter Speed (s)	Format	MP	
Sony A6500	16	24	400	f/3.5	1/60	ARW	24	600 x 7

Camera formations were structured so that photographs from each circular set were located every 10-degrees (180 photographs), 20-degrees (90 photographs), 30-degrees (60 photographs), and 40-degrees (45 photographs). The variable spacing also produced variable levels of photograph overlap, which was calculated as the overlapping visible surface area of a centrally located sphere visible from adjacent camera locations (this calculation is an estimate based on intended camera positions and their perspective of a spherical target – not the actual camera locations and their perspective of the irregular ornamental coral). The percentage of horizontal overlap decreased with the number of photographs for the three inner sets of photographs (180: 92.1%, 90: 84.3%, 60: 76.5%, 45: 68.7%) and the two outer sets (180: 93.2%, 90: 86.4%, 60: 79.6%, 45: 72.8%). Vertical photograph overlap was 76.5% between adjacent photographs in the inner sets and 79.6% between those in the outer sets. For each test, other than those including a complete set of 180 photographs, variations (i.e., V1, V2, …) of those tests were created by purposefully excluding select photographs from each of the five circular sets. For example, the 90 photograph SfM tests include: V1 with photographs located in 20-degree increments starting at the 0-degree position, V2 with photographs every 20-degrees starting at the 10-degree position, and V3 which staggers the alignments across the five circular sets of photographs. Those tests with 60 and 45 photographs include four and five variations respectively due to the overall reduction in photographs and the increased availability of starting positions. Staggering the circular sets of photographs served to balance the distribution of photographs around the central target. While staggering had no impact on the horizontal overlap between photographs it did slightly decrease the vertical overlap between adjacent (but now offset) photographs; however, the act of staggering photographs did increase the average overlap between triangulated groups of photographs (90: +0.9%, 60: +1.5%, 45: +2.8%). Examples of the alternate camera formations are presented in Figure 3.7.

For each camera position, photographs were simultaneously captured in the ARW (Sony's RAW equivalent) and JPEG file format. ARW files were converted to TIFF files with Image Data Converter Version 5.1.00.04270 (Sony, 2017). JPEG files were only used for visual reference.

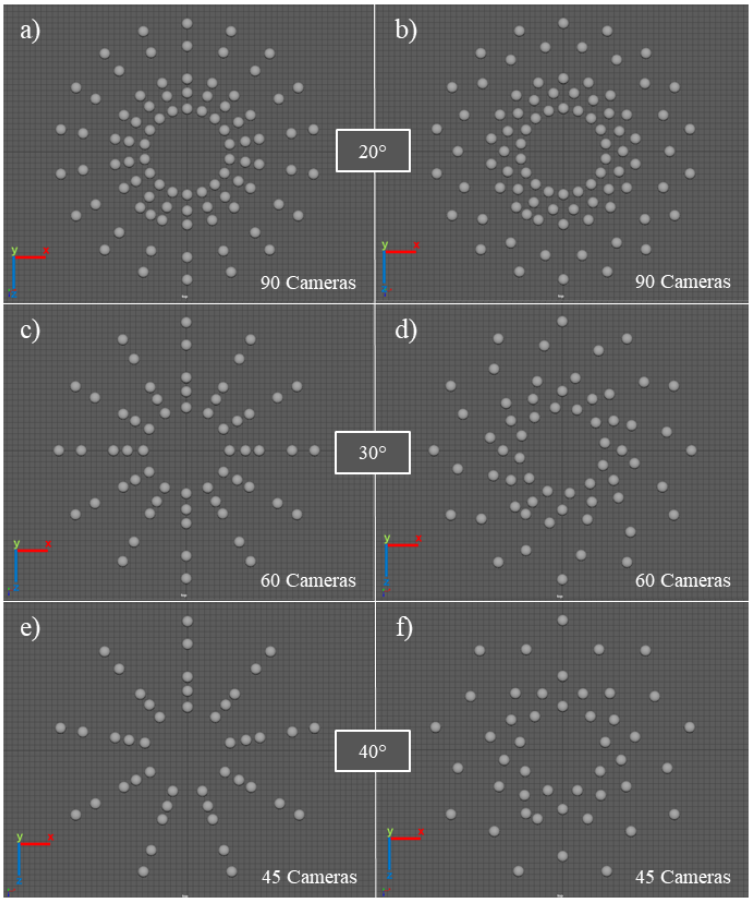

Figure 3.7 Examples of the alternative camera formations for the SfM Tests. (a, c, e) Aligned camera locations. (b, d, f) Staggered camera locations.

3.2.7. Camera Calibration

The camera calibration parameters for the SfM tests were assigned automatically within PhotoScan. While we acknowledge the importance of in situ self-calibration for applications demanding high accuracy results (Shortis, 2019), the unique challenges imparted by the benthic field site where subsequent phases of this research were conducted made in situ self-calibration impractical; this includes the limited free space within HEXYZ-1 from which to perform calibration activities and the limited dive time (approximately 20 minutes - less for subsequent dives) available to perform data collection. As such, a decision was made to prioritize data collection over in situ calibration. To assist the auto-calibration process, 2D calibration objects (rulers) were included around the ornamental coral. The potential for systematic errors associated with this workflow is acknowledged by the authors. However, despite the error risks, the accuracy of whichever workflow is chosen ultimately hinges on the validation of

measurements (Shortis, 2019) - which are used to quantify the accuracy of the data in this study.

As the calibration parameters were automatically adjusted for each SfM test, and were not reassigned from one test to another, there was inherent variability in the adjusted values. However, there were similarities in the adjusted values within the collection of dryland tests and within the wet-lab tests. For example, the within group variability in the adjusted focal length for the collection of dryland (M = 4028.82, SD = 7.09) and wet-lab tests (M = 3915.88, SD = 12.82) was minimal (apart from individual outliers in each) while there was greater variability between the two collections. A similar pattern was observed for each adjusted parameter; however, there was greater variability in the adjustments made for the wet-lab tests than there was for the dryland tests.

3.2.8. SfM Processing

The photographs for each of the 26 SfM tests were imported into Agisoft PhotoScan Professional (Version 1.4.0) as TIFF files. This version of the software, rather than newer versions under the Agisoft Metashape name, was utilized to maintain consistency with preliminary SfM workflow analyses that were conducted prior to the software updates. For each test, the images were aligned using the high-accuracy setting, without pair preselection, and camera calibration was performed automatically. Six markers were manually added to the reference objects in the aligned photographs and three scale bars, along three axes, were created using those markers. The position of each marker was then manually adjusted in each photograph, image alignment was optimized, and the extent of the sparse point cloud was reduced to the extent of the cinder block prior to dense point cloud construction. The dense point clouds were created under the high-accuracy setting with aggressive depth filtering. The resultant point clouds were manually cleaned to eliminate all points not representing the ornamental coral itself. Meshes were constructed with the polygon count set to high and a texture map was produced. As a final step, both a dense point cloud and a textured mesh were exported for each SfM test.

3.2.9. 3D Model Measurement

The 3D textured mesh from each SfM test was measured within PhotoScan using the Ruler tool. Each of the line segments was measured twice and an average of the two measurements was recorded as the measured value ($M_{[SfM]}$). Measurements were made using the textured meshes, as the physical features defining the points at the end of each line segment were not identifiable using the 3D mesh alone.

3.2.10. Point Cloud Analysis

Dense point clouds from each SfM test set (i.e., the equivalent wet-lab and dryland tests) were imported into CloudCompare (Version 2.10.1) to identify differences in point cloud density and point cloud composition. Point cloud densities were calculated as the number of neighbors within a local neighbourhood radius of 0.5 mm. The mean point cloud density from each SfM test served as a comparator between tests. Point cloud density, while it is a function of the surface characteristics (e.g., color, shade, and uniformity) of the subject, was of interest here as the structural complexity of the ornamental coral (and subsequently the glass sponges in the field) can only be resolved if there are enough points to accurately characterize those features. However, greater point density does not equate to greater accuracy and was only used to compare wet-lab and dryland results.

Differences in the composition of test set point clouds were evaluated by roughly aligning and then finely registering each set of dense point clouds to calculate the cloud-to-cloud (C2C) absolute distance. The resulting absolute distance point clouds for the wet-lab data sets were then filtered to exclude points with an absolute distance > 0.5 mm. For each wet-lab test, the number of points in the original point cloud was compared to the number in the filtered point cloud, producing a percentage value for wet-lab points with an absolute distance < 0.5 mm.

3.2.11. Statistical Analysis

The performance of the wet-lab SfM tests was assessed on an absolute basis (against manual measurements) and a relative basis (against dryland tests) to both

quantify the accuracy of our underwater SfM workflow and the impact that water and the underwater housing (i.e., the air-glass-water interface) have on SfM data quality.

For each of the line segment measurements made on the 3D models ($M_{[SfM]}$), the difference from the true measurement ($M_{[REAL]}$) is expressed as a dimension (mm) and as a percentage of difference (($M_{[SfM]}$ - $M_{[REAL]}$) / ($M_{[REAL]}$)) *100). A univariate analysis of variance (one-way ANOVA), using the absolute value of the line segment measurement error, was used to identify statistical differences (α = 0.05) between SfM tests. The absolute value of the measurement error was utilized to eliminate the reduction in average error caused by offsetting positive and negative error values (both values are presented in Table III). Differences between SfM test sets were evaluated using a Mann-Whitney U Test (α = 0.05).

All measurement data was compiled and examined within Microsoft Excel.

3.3. Results

3.3.1. SfM Processing Results

A complete, textured 3D model was produced in 17 of the 26 SfM tests (10 dryland tests and seven wet-lab tests). All cameras were successfully aligned in nine dryland tests and one wet-lab test (the 180 camera tests were the only successfully aligned test set). In general, as the camera count decreased the software increasingly struggled to align the full complement of cameras – especially for the wet-lab tests. For the SfM tests with > 60 cameras, the tendency was for the software to fail to align isolated images, whereas those tests with < 60 cameras failed to create a point cloud of closed geometry. In the 60 camera tests, the cameras were well aligned for dryland tests, however, wet-lab tests were not well aligned, either missing groups of cameras in close proximity or failing to produce closed point clouds.

Dryland tests produced sparse and dense point clouds containing a greater number of points and a mesh with a greater number of polygons than wet-lab tests in every test set (Figure 3.8). Omitting failed tests, the dryland tests generated 176.28 – 239.69% more sparse points and 35.38 – 97.33% more dense points and polygons than their wet-lab equivalents. Overall, the total number of points and polygons decreased as the total number of cameras, and the overlap between cameras, decreased, with the 45

camera tests failing to produce a dense point cloud from the limited number of sparse points on all but two occasions. Select results from the SfM tests are presented in Table 3.2 (rows containing cells without values indicate tests which failed to produce a dense point cloud).

Reprojection error, which is a stronger indicator of photogrammetric model quality than the number points and polygons, was less for dryland tests than wet-lab and tends to decrease with the reduction in the number of cameras across all tests other than 90 V2, where the dryland test generated anomalous error values. 90 V2 Dry also produced a larger scale bar measurement error (0.8 mm) than the average (0.04 mm) across completed dryland tests. While the scale bar measurement error provides a measure of photogrammetric accuracy compared to an object of known dimension, 3D model quality was ultimately determined from a series of line segment measurements.

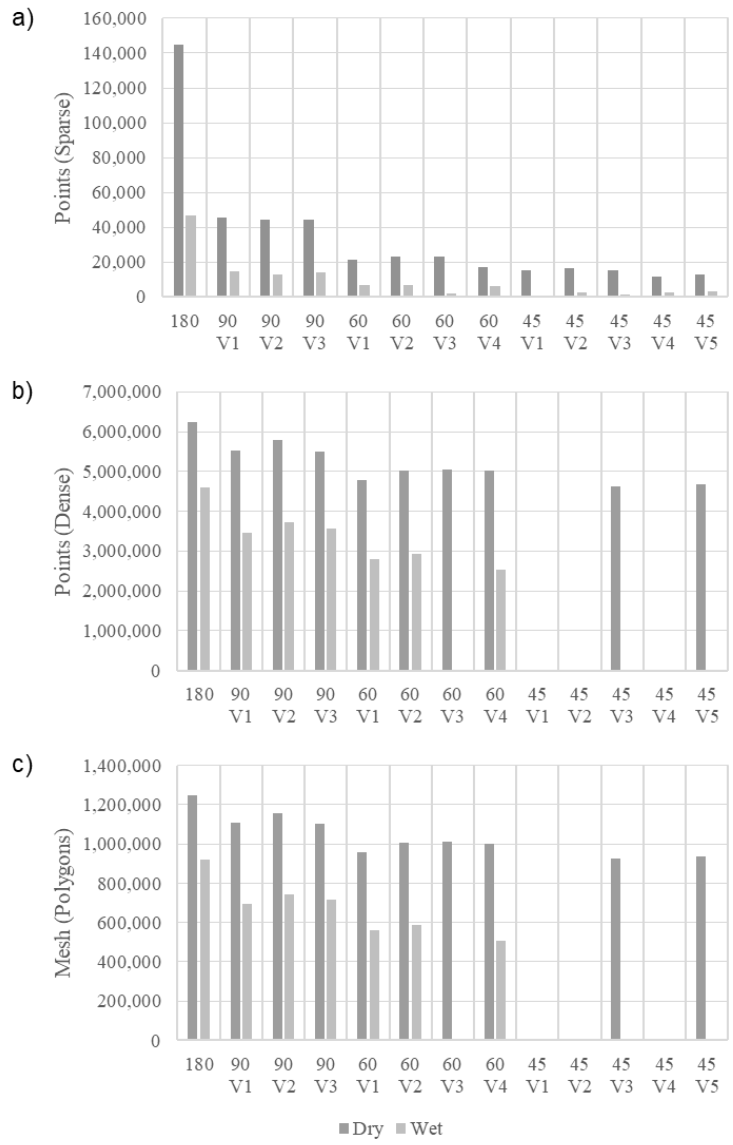

Figure 3.8 **A comparison of the a) sparse point clouds, b) dense point clouds, and c) mesh faces (polygons) generated for each of the dryland and wet-lab SfM tests.**

Table 3.2 **SfM Tests – Processing Results**

SfM Test	Cameras (Aligned)	Sparse Cloud	Dense Cloud	Mesh (Faces)	RMS Error	Reprojection Error (pix)	Resolution (mm/pix)	Scale Bar Error (mm)
180 Dry	180(180)	144,783	6,236,443	1,247,287	0.142	0.977	0.106	0.06
180 Wet	180(180)	47,060	4,606,569	921,312	0.183	1.390	0.105	0.004
90 V1 Dry	90(90)	45,690	5,536,444	1,107,287	0.120	0.836	0.100	0.05
90 V1 Wet	90(79)	14,701	3,462,617	692,522	0.179	1.220	0.105	0.01
90 V2 Dry	90(90)	44,662	5,790,170	1,158,034	0.582	2.750	0.099	0.80
90 V2 Wet	90(83)	13,148	3,715,732	743,145	0.161	1.260	0.107	0.06

90 V3 Dry	90(90)	44,487	5,504,234	1,100,845	0.113	0.838	0.102	0.02
90 V3 Wet	90(79)	14,319	3,570,276	714,055	0.185	1.290	0.105	0.04
60 V1 Dry	60(59)	21,645	4,782,695	956,538	0.104	0.756	0.100	0.05
60 V1 Wet	60(46)	6,680	2,796,820	559,364	0.130	1.150	0.107	0.16
60 V2 Dry	60(60)	23,281	5,023,872	1,004,774	0.104	0.731	0.097	0.02
60 V2 Wet	60(42)	6,936	2,924,872	584,974	0.141	1.150	0.106	0.15
60 V3 Dry	60(60)	22,912	5,052,719	1,010,543	0.096	0.728	0.097	0.06
60 V3 Wet	60(14)	2,190	-	-	-	-	-	-
60 V4 Dry	60(60)	17,066	5,015,202	1,003,040	0.125	0.887	0.098	0.01
60 V4 Wet	60(46)	6,177	2,541,580	508,316	0.153	1.200	0.107	0.09
45 V1 Dry	45(43)	15,263	-	-	-	-	-	-
45 V1 Wet	45(4)	876	-	-	-	-	-	-
45 V2 Dry	45(42)	16,630	-	-	-	-	-	-
45 V2 Wet	45(23)	2,864	-	-	-	-	-	-
45 V3 Dry	45(45)	15,168	4,623,695	924,738	0.105	0.730	0.097	0.06
45 V3 Wet	45(6)	1,711	-	-	-	-	-	-
45 V4 Dry	45(38)	11,976	-	-	-	-	-	-
45 V4 Wet	45(17)	2,422	-	-	-	-	-	-
45 V5 Dry	45(45	13,000	4,688,720	937,743	0.528	2.370	0.097	0.02
45 V5 Wet	45(45)	3,336	-	-	-	-	-	-

3.3.2. SfM Measurements

Line segment measurements for $M_{[SfM]}$ and $M_{[REAL]}$ are presented in Table 3.3. The differences between $M_{[SfM]}$ and $M_{[REAL]}$ values are presented as the cumulative negative and positive modelling error in Figure 3.9. A one-way ANOVA, using the absolute value of the modelling errors, determined that there was a statistically significant difference between the SfM tests ($F(12,65) = 3.848$, $p = 0.00019$).

Expressed as a percentage, the difference between $M_{[SfM]}$ and $M_{[REAL]}$ for individual line segment measurements ranged from -2.60 to +1.21% for all dryland tests and -5.07 to +0.60% for all wet-lab tests. The average line segment error for all dryland SfM tests ranged from -2.00 to +0.28% and from -1.26% to -0.05% for all wet-lab tests. Using the absolute value of the measurement error, dryland tests ranged from +0.23 to + 2.00% and wet-lab tests from +0.26% to +1.31%. SfM tests 60 V2 Dry and 180 Wet produced the smallest average error (-0.05%) and 60 V2 Dry the smallest average absolute error (0.23%).

Table 3.3 SfM Test Line Segment Measurements

	Line Segment Measurements (mm)						Measurement Error			
	A - B	C - D	E - F	G - H	I - J	K- L	Mean (mm)	Mean (%)	|Mean| (mm)	|Mean| (%)
$M_{[SfM]}$ (Caliper)	64.24	44.56	151.82	60.14	40.32	89.49	-	-	-	-
180 Dry	64.00	44.30	151.20	60.20	40.40	89.50	-0.16	-0.18	0.21	0.28
180 Wet	64.20	44.50	151.40	60.40	40.40	89.10	-0.09	-0.05	0.21	0.26
90 V1 Dry	64.20	44.30	151.40	60.20	40.10	89.30	-0.18	-0.26	0.20	0.30
90 V1 Wet	64.10	44.00	150.50	60.30	40.30	89.10	-0.38	-0.43	0.43	0.52
90 V2 Dry	62.90	43.40	148.50	58.90	39.80	87.90	-1.53	-2.00	1.53	2.00
90 V2 Wet	64.30	42.50	151.40	60.40	40.30	89.30	-0.39	-0.77	0.50	0.95
90 V3 Dry	64.00	44.30	151.60	60.10	40.20	89.70	-0.11	-0.21	0.18	0.28
90 V3 Wet	64.10	43.60	151.50	60.10	40.20	89.50	-0.26	-0.49	0.26	0.49
60 V1 Dry	64.00	44.30	151.30	60.10	40.00	89.40	-0.24	-0.38	0.24	0.38
60 V1 Wet	64.20	42.70	151.90	60.50	40.20	89.80	-0.21	-0.59	0.46	0.92
60 V2 Dry	64.10	44.70	151.70	60.20	40.10	89.60	-0.03	-0.05	0.13	0.23
60 V2 Wet	63.90	43.30	151.20	60.00	40.10	89.90	-0.36	-0.68	0.50	0.83
60 V3 Dry	64.10	44.00	151.50	60.20	39.90	89.40	-0.24	-0.45	0.26	0.49
60 V3 Wet	-	-	-	-	-	-	-	-	-	-
60 V4 Dry	64.10	44.30	151.40	60.30	40.00	89.50	-0.16	-0.27	0.22	0.36
60 V4 Wet	63.70	42.30	151.50	-	40.20	89.60	-0.63	-1.26	0.67	1.31
45 V1 Dry	-	-	-	-	-	-	-	-	-	-
45 V1 Wet	-	-	-	-	-	-	-	-	-	-
45 V2 Dry	-	-	-	-	-	-	-	-	-	-
45 V2 Wet	-	-	-	-	-	-	-	-	-	-
45 V3 Dry	64.20	45.10	151.80	60.50	40.20	89.70	0.16	0.28	0.21	0.40
45 V3 Wet	-	-	-	-	-	-	-	-	-	-
45 V4 Dry	-	-	-	-	-	-	-	-	-	-
45 V4 Wet	-	-	-	-	-	-	-	-	-	-
45 V5 Dry	64.00	44.00	151.90	60.20	39.80	89.40	-0.21	-0.48	0.26	0.53
45 V5 Wet	-	-	-	-	-	-	-		-	-

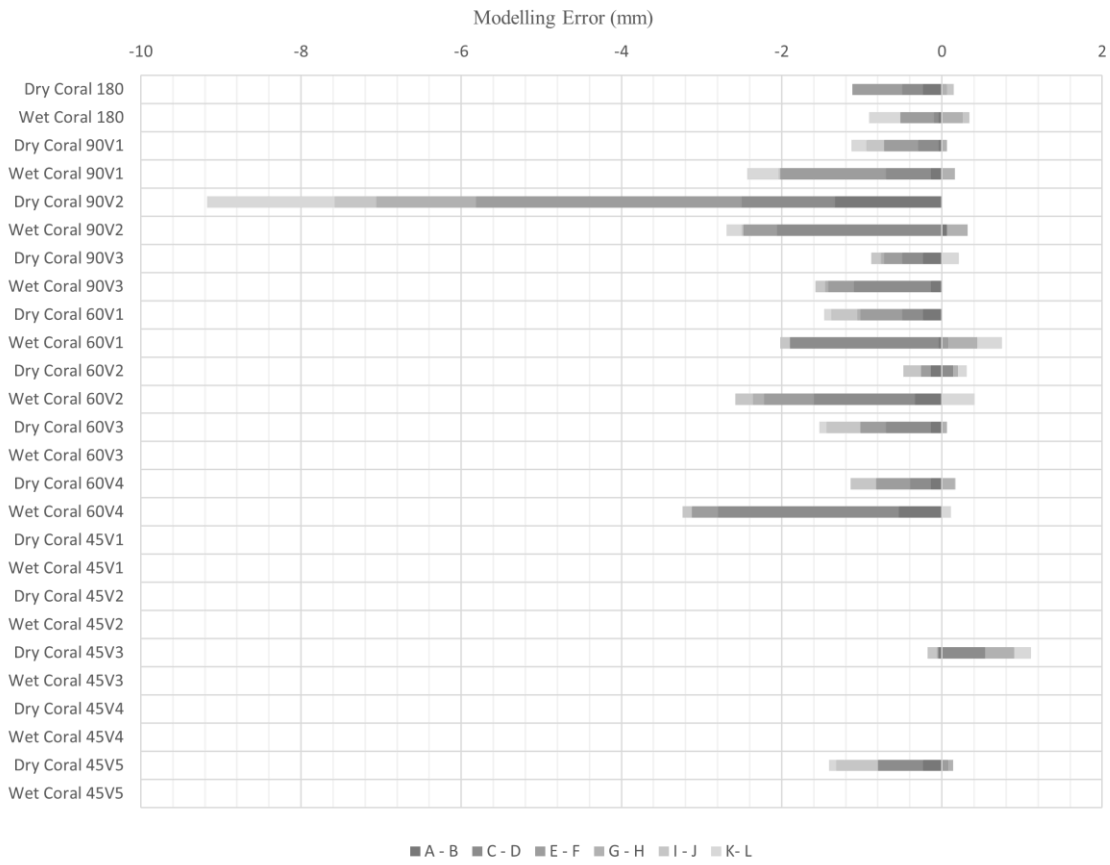

Figure 3.9 The cumulative negative and positive modelling error (difference between $M_{[SfM]}$ and $M_{[REAL]}$) for each SfM test.

There was not a significant difference (Mann-Whitney, $\alpha = 0.05$) between the dryland and wet-lab test sets for six of the seven test scenarios (180, 90 V1, 90 V3, 60 V1, 60 V2, and 60 V4) in which both the dryland and wet-lab tests were successful. However, there was a significant difference between the results of test scenario 90 V2, although that difference is believed to be the product of a modelling error.

3.3.3. Point Cloud Analysis

The number of points within a local neighbourhood radius of 0.5 mm ranged from 20.56 (60 V1 Wet) to 36.43 (90 V2 Dry). For each SfM test set, the wet-lab test produced a dense point cloud with a lower mean point density and a more negatively skewed frequency distribution (Figure 3.10). The degree to which the frequency distribution was negatively skewed increased as the number of cameras and the overlap between cameras decreased for both dryland and wet-lab tests. Point cloud density also

decreased, for each test other than for test 90 V2 Dry, as the number of cameras decreased (Figure 3.11).

The reduction in point cloud density from dryland to wet-lab increased as the number of cameras decreased, with 180 camera tests differing by 11.16%, and 90 and 60 camera tests differing by an average of 26.02% and 34.03% respectively. Within each test environment, reducing the total number of cameras from 180 to 90 reduced the mean point cloud density by an average of 4.08% for dryland and 20.19% for wet-lab, and from 90 to 60 cameras by an average of 8.16% for dryland and 18.37% for wet-lab.

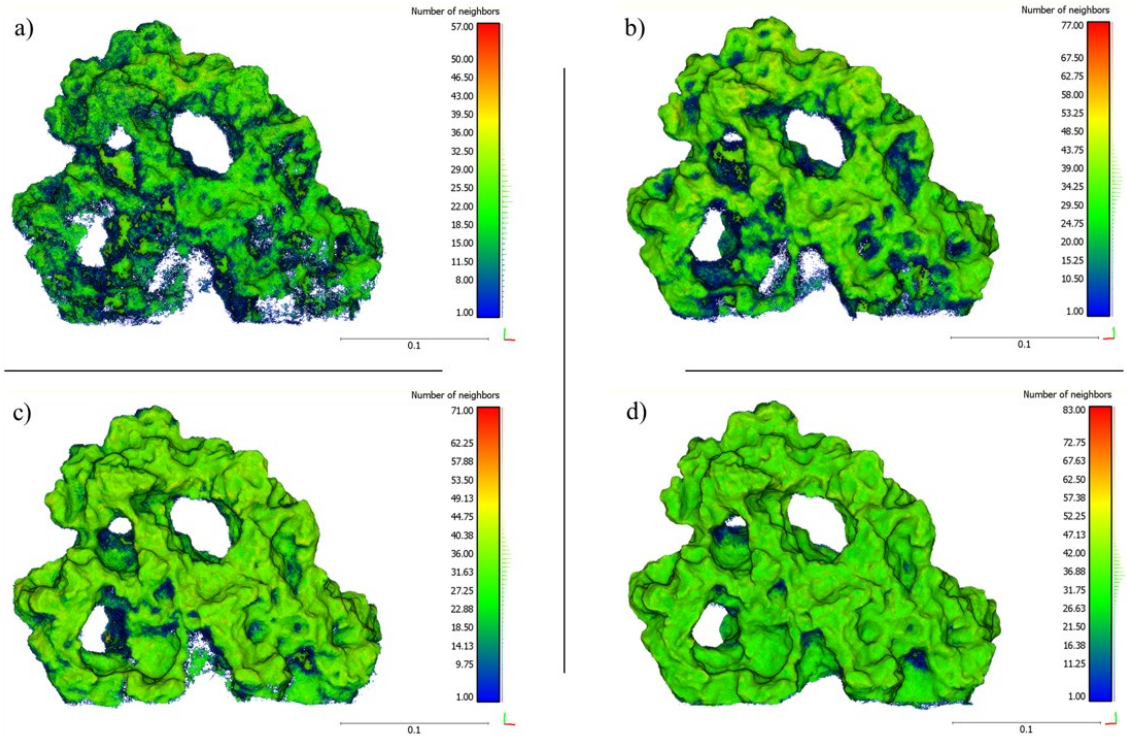

Figure 3.10 Point cloud density, calculated as the number of neighbors within a 0.5 mm radius, for a) 60V1 Wet, b) 180 Wet, c) 60V1 Dry, and d) 180 Dry.

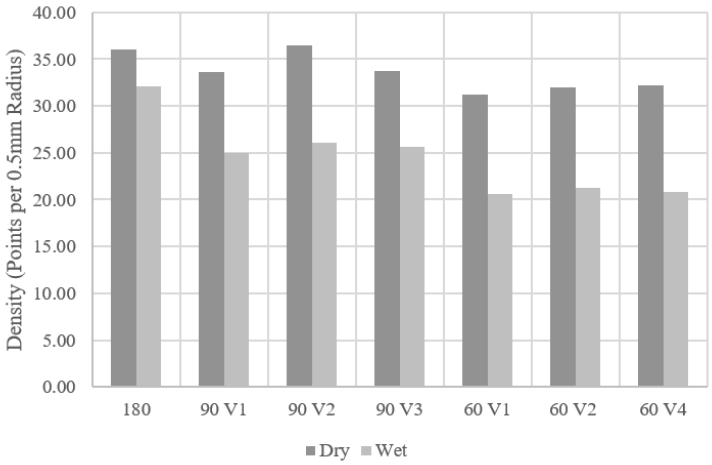

Figure 3.11 Mean point cloud density for successful dryland and wet-lab SfM tests.

The calculated C2C absolute distance between SfM test sets reveals significant differences between tests utilizing different numbers of cameras and different configurations of cameras (Figure 3.12). SfM test sets utilizing a greater number of cameras tended to produce point clouds that were more similar than those with fewer cameras (Figure 3.13); however, there were variations with changes in camera configuration. The percentage of wet-lab dense point cloud points that were within a 0.5 mm absolute distance of their dryland equivalent ranged from 22.10% (60 V4 Wet) to 88.77% (180 Wet). The mean C2C absolute distance ranged from 0.33 mm (180 Wet) to 1.85 mm (60V4 Wet).

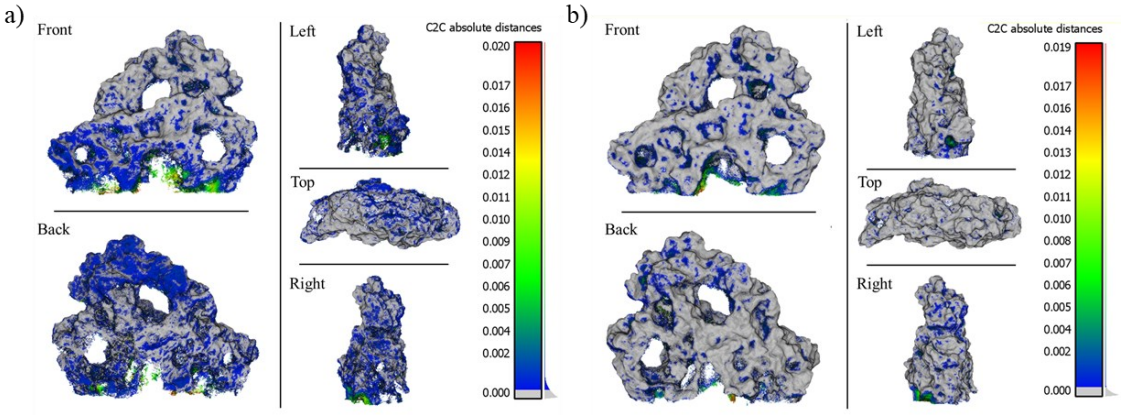

Figure 3.12 Cloud-to-cloud absolute distance calculation for a) 60V1 and b) 180 SfM tests. The grey areas represent points having a C2C distance < 0.5 mm. (Units: meters)

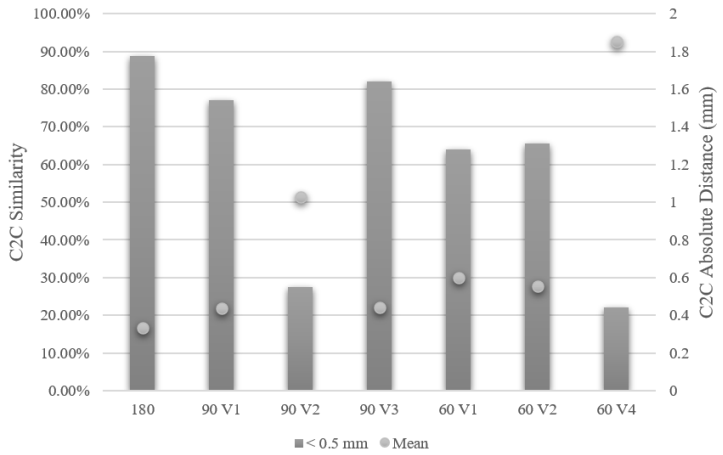

Figure 3.13 SfM test C2C comparison. The C2C similarity for each SfM test is plotted on the primary y-axis and the mean C2C absolute distance on the secondary y-axis.

3.4. Discussion

This study evaluates the performance of an underwater SfM workflow, designed to monitor temporal changes in the morphology of benthic organisms in the northeast Pacific Ocean, using absolute and relative measures. Through processing different quantities and configurations of dryland and wet-lab photographs of an ornamental aquarium coral using Agisoft PhotoScan, we gained insight into both the capacity of our workflow to generate accurate 3D models of complex structures and the impact that dark, temperate waters have on SfM accuracy. This series of SfM tests provided important performance benchmarks prior to an applied study of glass sponge morphology in the open ocean. As dive time, and thus data collection, is constrained by depth, identifying the quantity and configuration of photographs required to maximize SfM performance was critical. While underwater SfM workflows have proven to be a relatively low-cost, simple, and informative method of documenting the 3D structure of benthic organisms in tropical regions, this wet-lab study, as well as prior dry-lab research (Lochhead & Hedley, 2021), were necessary steps preceding subsequent field surveys (see Lochhead & Hedley, 2020).

Our analysis compared the 3D data products of 13 wet-lab and dryland test sets based on their SfM processing results, their absolute modelling error, and their relative similarity. Seven of the 13 test sets produced a complete 3D data product, as one 60 photograph and all five 45 photograph wet-lab tests failed to align enough photographs

to produce a dense point cloud. Overall, a greater number of points and polygons were generated from dryland tests than wet-lab tests, and from those tests containing more photographs; however, while greater numbers of points and polygons are encouraging, they mean little without some form of validation. Scale bar error estimates and reprojection error provide some insight into the photogrammetric quality of the data, yet the scale bar error range from successful tests was estimated at 0.0047 mm to 0.16 mm and reprojection error was < 0.3 mm; such small errors would suggest that all test configurations would be sufficient for tracking glass sponge growth. Further scrutiny was required to confirm accuracy across all tests, as a simple visual inspection of the final 3D data products (Figure 3.14) suggested significant differences among tests.

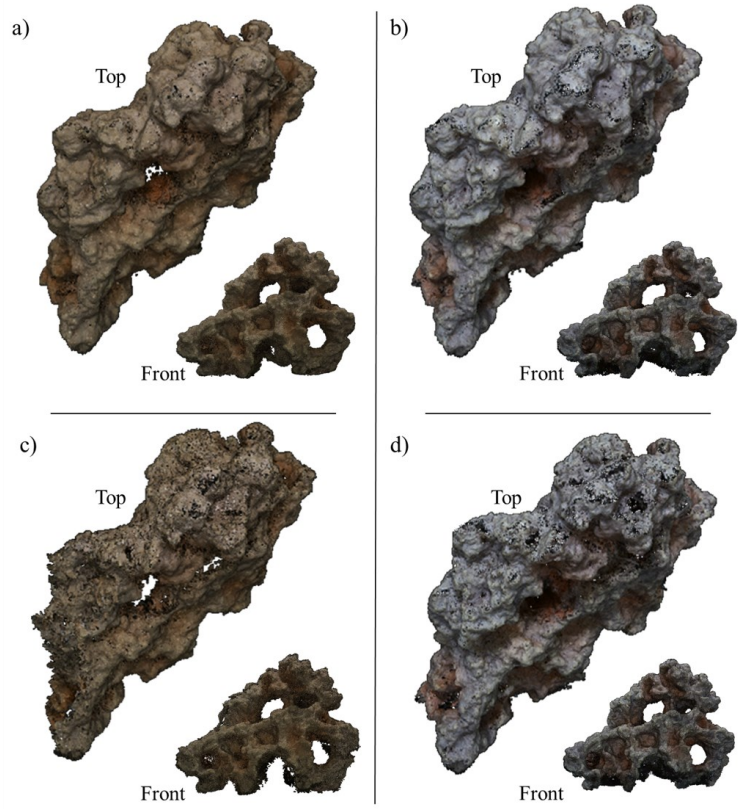

Figure 3.14 Colored dense point clouds for the a) 180 Wet, b) 180 Dry, c) 60V4 Wet, and d) 60V4 Dry SfM tests.

A comparison of line segment measurements from each 3D SfM model to the absolute measurement of that feature obtained with a digital caliper provided additional information about the accuracy of the 3D models from each SfM test. Individual line segment measurements differed from reality by -2.60% to +1.21% for all dryland tests

and -5.07 to +0.60% for all wet-lab tests, and the mean value of absolute measurement error by +0.23 to + 2.00% for dryland and +0.26% to +1.31% for wet-lab (although the erroneous values of 90 V2 Dry negatively skew the dryland data). At the higher end of the accuracy spectrum are the 180 dryland and wet-lab tests, in which average measurement error was -0.18% and -0.05%, and the average of the absolute value of measurement error was 0.28% and 0.26% respectively. While this linear measurement accuracy is sufficiently high to characterize the documented linear growth estimates (1-10 cm $year^{-1}$) for glass sponges (Austin et al., 2007; Kahn et al., 2016; Levings & McDaniel, 1974; Leys & Lauzon, 1998), benthic organisms experience 3D growth that is not best characterized by a series of 2D measurements.

Through a series of point cloud analyses, we were able to identify clear differences between dense point clouds from within and between each of the dryland and wet-lab SfM tests. In both test environments, tests with a greater quantity of photographs produced greater mean point densities and a more normal point cloud frequency distribution than tests containing fewer photographs. With each subsequent reduction in photograph quantity the frequency distribution became more negatively skewed; this negative skew was also evident when comparing wet-lab tests to their dryland equivalents. When we relate this trend in point densities to the trend in mean absolute measurement error (Figure 3.15), we see that in a dryland environment the reduction in point density has minimal impact on measurement error, increasing mean error from 0.28% (180 Dry) to 0.36% (average of 60 Dry tests). However, in the wet-lab tests, where the mean measurement error was less with 180 photographs than on dryland (0.26%), the error increases to 1.02% (average of 3 successful 60 Wet tests).

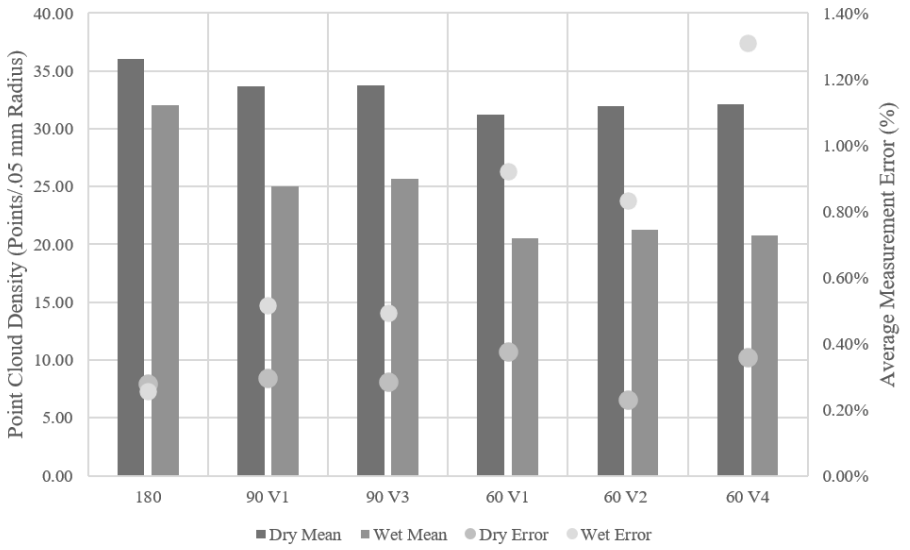

Figure 3.15 Dense point cloud density and average measurement error for dry and wet-lab SfM tests.

The line segment measurement approach that was applied to evaluate the 3D accuracy of this studies SfM modelling workflow was designed to align with the linear glass sponge growth estimates documented in the research literature, but also to highlight the limitations associated with linear measurements of a 3D organism such as a glass sponge and the significant opportunity presented by SfM modelling. This choice, however, makes it difficult to draw direct comparisons between the outcomes from this study and those quantifying other morphological characteristics (e.g., surface area and volume – see Olinger et al., 2019; Prado et al., 2021). Furthermore, the 3D accuracy of SfM modelling is influenced by variables such as the chosen equipment, data capture strategy, data format, and the variable physical properties of the subject (e.g., sponge) and the context (e.g., location, water properties, and light) in which it is surveyed (Lochhead and Hedley, 2021; Capra et al. 2015; Lavy et al. 2015; Thoeni et al. 2014; Kersten and Lindstaedt 2012), making the performance or suitability of a technique (i.e., SfM) hard to overtly express without careful consideration of context.

Overall, individual wet-lab SfM measurements from this study were within 0.1 – 2.06 mm (or 0.01 – 5.07%) of $M_{[REAL]}$. Figueira et al. (2015) documented 1.3 – 2.5 mm overall accuracy when comparing their SfM models of coral colonies to laser-scan data and Lavy et al. (2015) reported a volume underestimate of 1.4% and overestimates of 1.72%, 2.96%, and 5.44% for four marine sponges when comparing SfM volume

estimates to water displacement measurements. The results of this study appear to align with those obtained by others, suggesting that the SfM workflow developed for monitoring glass sponges in situ can produce accurate 3D models from underwater photographs captured in temperate, albeit controlled, conditions. However, with a mean measurement error of 0.05% and a mean absolute measurement error of 0.26%, the 180 Wet SfM test performed exceptionally well. While 3D models, as accurate as what is reported in the research literature, were successfully generated with as few as 60 underwater photographs, those tests containing 90 and 180 photographs produced higher density point clouds with less measurement error.

This study was conducted to explore the potential for SfM-based surveys to monitor the changing morphology of glass sponges in the northeast Pacific Ocean. Currently, manual measurements and visual inferences from photographs and videos provide estimates of these changes, but lack the accuracy and precision required to document the small scale (mm and cm) changes typical of glass sponges. HEXYZ-1 was developed to overcome the challenges presented by temperate marine environments, proving that a controlled, repeatable SfM workflow could provide the accuracy and precision required to document small scale change. However, HEXYZ-1 was designed only for colony-scale analyses of glass sponges (up to approximately 0.2 m^3) and not for reef-scale analyses of the ecologically important glass sponge reefs and bioherms. Our decision to start small was intentional; selected to identify what is ultimately possible with isolated colonies prior to developing a reef-scale SfM workflow. The lessons learned in our dry-lab ((Lochhead & Hedley, 2021) and wet-lab tests highlight the challenges associated with underwater surveying (e.g., time constraints, lighting, and camera stability) and their implications for 3D model accuracy. This research represents an important and necessary step towards monitoring glass sponge morphology in 3D.

3.5. Conclusions

The primary objective of this study was to develop the data science informing SfM data capture in temperate marine environments. SfM surveying is more nuanced than simply collecting photographs or videos. Therefore, we found it prudent that we establish a clear set of data quality benchmarks prior to collecting field-based data: assessing the performance of HEXYZ-1 in a marine setting, quantifying the performance

of our SfM workflow in cold, dark temperate waters, and identifying the relationship between the number of photographs, camera formation, and 3D model accuracy. These distinct wet-lab tests provided an essential basis to inform field-based surveys (see Lochhead & Hedley, 2020) and enabling informed decisions regarding the balance between data requirements, data quality, and survey efficiency.

This study confirmed that HEXYZ-1 is well equipped to provide camera stability and world-stabilized artificial light in a temperate marine environment. The SfM workflow performed exceptionally well, providing 3D data of comparable quality to that produced on dryland, but only when 180 photographs were processed. While reducing the number of photographs would decrease data collection time and lessen the burden imposed on SCUBA divers, the consequent reduction in data quality, particularly regarding point cloud density, associated with fewer photographs is problematic for accurate studies of 3D morphology over time.

This paper looks to build on prior research efforts addressing SfM performance in marine environments. This research contributes to future SfM-based surveys in temperate marine environments (for glass sponges and other benthic species), offering a proven underwater capture strategy and a set of underwater SfM performance benchmarks specific to cold, dark temperate marine conditions. Furthermore, by reducing photograph quantity and staggering camera formations to maximize photograph overlap, this research explores and documents the trade-off between data quality and survey efficiency. While these tests were conducted in a controlled environment and not the open ocean, the scarcity of natural light and the cold temperate waters were indicative of the field conditions for which this research was designed. Under those conditions, there was a statistically significant difference between the accuracy of the SfM models generated under each test scenario. However, the accuracy of the line segment measurements from these tests, even with only 60 photographs, would be enough to monitor annual growth at a rate of 1 – 10 cm $year^{-1}$. The reduction in point cloud density and C2C similarity associated with a reduced number of photographs on the other hand, may have implications for tracking other morphological characteristics such as surface area and volume.

Limitations of this study include the line segment measurements used to quantify 3D data accuracy and the absence of extracted video frames. Line segments served

their role for linear measurements, yet the 3D growth of an organism is difficult to properly quantify using line segments. Future studies should include volume and surface area accuracy assessments, perhaps using simple shapes and more complex coral or sponge models of known dimension. Our analysis of the impact that different quantities and configurations of photographs have on model accuracy was designed to identify ways to reduce data collection time in accordance with restricted SCUBA dive times at depths up to 30 m. We excluded extracted 4K video frames from our analysis, despite the fact that video capture is significantly quicker than photography, as extracted video frames from our camera (3840 x 2160 pixels) do not provide the recommended highest resolution (Agisoft LLC, 2018) output of our digital camera (6000 x 4000 pixels), and prior SfM research reports lower resolution 3D models (Bennecke et al., 2016; Hollick et al., 2013) and less accurate 3D measurements (Lochhead & Hedley, 2021) from lower resolution images. Nevertheless, extracted video frames may have provided a useful comparator for this study, as field-based data collection did necessitate the use of 4K video (Lochhead & Hedley, 2020).

This paper provides contextual benchmarks to support the applied fieldwork of others, as well as our own. The next phase of this research employed these benchmarks to inform our field-based activities deploying HEXYZ-1 in the northeast Pacific Ocean (see Lochhead & Hedley, 2020). Future research efforts will look to capture sets of photographs, collected approximately six months apart, to quantify temporal changes in glass sponge morphology. We hope that this wet-lab phase and the overall research project will help inform future SfM research efforts in temperate marine environments and improve the research community's knowledge of glass sponge ecology.

Acknowledgements

This work was supported by Mitacs (IT10019) through the Mitacs Accelerate Program in partnership with Ocean Wise and the Vancouver Aquarium. We would like to acknowledge the SFU Faculty of Science Machine Shop for their help fabricating HEXYZ-1 and Fisheries and Ocean Canada's Centre for Aquaculture and Environmental Research for allowing us to use their facilities.

References

Abadie, A., Boissery, P., & Viala, C. (2018). Georeferenced underwater photogrammetry to map marine habitats and submerged artificial structures. The Photogrammetric Record, 33(164), 448–469. https://doi.org/10.1111/phor.12263

Abdo, D. A., Seager, J. W., Harvey, E. S., McDonald, J. I., Kendrick, G. A., & Shortis, M. R. (2006). Efficiently measuring complex sessile epibenthic organisms using a novel photogrammetric technique. Journal of Experimental Marine Biology and Ecology, 339(1), 120–133. https://doi.org/10.1016/j.jembe.2006.07.015

Agisoft LLC. (2018). Agisoft PhotoScan User Manual - Professional Edition, Version 1.4 (p. 119). http://www.agisoft.com/pdf/photoscan-pro_1_4_en.pdf

Austin, W. C., Conway, K. W., Barrie, J. V., & Krautter, M. (2007). Growth and morphology of a reef-forming glass sponge, Aphrocallistes vastus (Hexactinellida), and implications for recovery from widespread trawl damage. Porifera Research: …, 139–145. http://www.poriferabrasil.mn.ufrj.br/iss/09-book/pdf/Austin et al - Growth and morphology of Aphrocallistes vastus.pdf

Bayley, D. T. I., Mogg, A. O. M., Koldewey, H., & Purvis, A. (2019). Capturing complexity: field-testing the use of ‘structure from motion’ derived virtual models to replicate standard measures of reef physical structure. PeerJ, 7, e6540. https://doi.org/10.7717/peerj.6540

Beltrame, C., & Costa, E. (2017). 3D survey and modelling of shipwrecks in different underwater environments. Journal of Cultural Heritage, 3–9. https://doi.org/10.1016/j.culher.2017.08.005

Bennecke, S., Kwasnitschka, T., Metaxas, A., & Dullo, W.-C. (2016). In situ growth rates of deep-water octocorals determined from 3D photogrammetric reconstructions. Coral Reefs, 35(4), 1227–1239. https://doi.org/10.1007/s00338-016-1471-7

Bruno, F., Bianco, G., Muzzupappa, M., Barone, S., & Razionale, A. V. (2011). Experimentation of structured light and stereo vision for underwater 3D reconstruction. ISPRS Journal of Photogrammetry and Remote Sensing, 66(4), 508–518. https://doi.org/10.1016/j.isprsjprs.2011.02.009

Burns, J. H. R., Delparte, D., Gates, R. D., & Takabayashi, M. (2015). Utilizing underwater three-dimensional modeling to enhance ecological and biological studies of coral reefs. International Archives of the Photogrammetry, Remote Sensing and Spatial Information Sciences - ISPRS Archives, 40(5W5), 61–66. https://doi.org/10.5194/isprsarchives-XL-5-W5-61-2015

Capra, A., Dubbini, M., Bertacchini, E., Castagnetti, C., & Mancini, F. (2015). 3D reconstruction of an underwater archaeological site: Comparison between low-cost cameras. International Archives of the Photogrammetry, Remote Sensing and Spatial Information Sciences - ISPRS Archives, 40(5W5), 67–72. https://doi.org/10.5194/isprsarchives-XL-5-W5-67-2015

Cocito, S., Sgorbini, S., Peirano, A., & Valle, M. (2003). 3-D reconstruction of biological objects using underwater video technique and image processing. Journal of Experimental Marine Biology and Ecology, 297(1), 57–70. https://doi.org/10.1016/S0022-0981(03)00369-1

Department of Fisheries and Oceans Canada. (2010). Pacific Region Coral and Sponge Conservation Strategy 2010-2015. In Oceans, Habitat and Species at Risk Oceans Program. Fisheries and Oceans Canada.

Figueira, W., Ferrari, R., Weatherby, E., Porter, A., Hawes, S., & Byrne, M. (2015). Accuracy and precision of habitat structural complexity metrics derived from underwater photogrammetry. Remote Sensing, 7(12), 16883–16900. https://doi.org/10.3390/rs71215859

Fukunaga, A., Burns, J., Craig, B., & Kosaki, R. (2019). Integrating Three-Dimensional Benthic Habitat Characterization Techniques into Ecological Monitoring of Coral Reefs. Journal of Marine Science and Engineering, 7(2), 27. https://doi.org/10.3390/jmse7020027

Gratwicke, B., & Speight, M. R. (2005). The relationship between fish species richness, abundance and habitat complexity in a range of shallow tropical marine habitats. Journal of Fish Biology, 66(3), 650–667. https://doi.org/10.1111/j.0022-1112.2005.00629.x

Gutierrez-Heredia, L., Benzoni, F., Murphy, E., & Reynaud, E. G. (2016). End to End Digitisation and Analysis of Three-Dimensional Coral Models, from Communities to Corallites. PLoS ONE, 11(2). https://doi.org/10.1371/journal.pone.0149641

Hollick, J., Moncrieff, S., Belton, D., Woods, A. J., Hutchison, A., & Helmholz, P. (2013). Creation of 3D Models from Large Unstructured Image and Video Datasets. ISPRS - International Archives of the Photogrammetry, Remote Sensing and Spatial Information Sciences, XL-1/W1(May), 133–137. https://doi.org/10.5194/isprsarchives-xl-1-w1-133-2013

Jaffe, J. S. (1990). Computer Modeling and the Design of Optimal Underwater Imaging Systems. IEEE Journal of Oceanic Engineering, 15(2), 101–111. https://doi.org/10.1109/48.50695

Kahn, A. S., Vehring, L. J., Brown, R. R., & Leys, S. P. (2016). Dynamic change, recruitment, and resilience in reef-forming glass sponges. Journal of the Marine Biological Association of the United Kingdom, 96(02), 429–436. https://doi.org/10.1017/S0025315415000466

Kersten, T. P., & Lindstaedt, M. (2012). Image-Based Low-Cost Systems for Automatic 3D Recording and Modelling of Archaeological Finds and Objects. In C. R. Ioannides M., Fritsch D., Leissner J., Davies R., Remondino F. (Ed.), Progress in Cultural Heritage Preservation. EuroMed 2012. Lecture Notes in Computer Science: Vol. 7616 LNCS (pp. 1–10). Springer, Berlin, Heidelberg. https://doi.org/10.1007/978-3-642-34234-9_1

Lavy, A., Eyal, G., Neal, B., Keren, R., Loya, Y., & Ilan, M. (2015). A quick, easy and non-intrusive method for underwater volume and surface area evaluation of benthic organisms by 3D computer modelling. Methods in Ecology and Evolution, 6(5), 521–531. https://doi.org/10.1111/2041-210X.12331

Leon, J. X., Roelfsema, C. M., Saunders, M. I., & Phinn, S. R. (2015). Measuring coral reef terrain roughness using “Structure-from-Motion” close-range photogrammetry. Geomorphology, 242, 21–28. https://doi.org/10.1016/j.geomorph.2015.01.030

Levings, C. D., & McDaniel, N. G. (1974). A unique collection of baseline biological data: benthic invertebrates from an underwater cable across the Strait of Georgia (Issue Mi). http://www.dfo-mpo.gc.ca/Library/52321.pdf

Leys, S. P., & Lauzon, N. R. J. (1998). Hexactinellid sponge ecology: Growth rates and seasonality in deep water sponges. Journal of Experimental Marine Biology and Ecology, 230(1), 111–129. https://doi.org/10.1016/S0022-0981(98)00088-4

Lochhead, I., & Hedley, N. (2020). 3D Modelling in Temperate Waters: Building Rigs and Data Science to Support Glass Sponge Monitoring Efforts in Coastal British Columbia. The International Archives of the Photogrammetry, Remote Sensing and Spatial Information Sciences, XLIII-B2-2(B2), 969–976. https://doi.org/10.5194/isprs-archives-XLIII-B2-2020-969-2020

Lochhead, I., & Hedley, N. (2021). Dry-lab benchmarking of a structure from motion workflow designed to monitor marine benthos in three dimensions. The Photogrammetric Record, phor.12370. https://doi.org/10.1111/phor.12370

Marliave, J. (2015). Cloud Sponge, Aphrocallistes vastus (Porifera: Hexactinellida), fragment healing and reattachment. Canadian Field-Naturalist, 129(4), 399–402.

McCarthy, J., & Benjamin, J. (2014). Multi-image Photogrammetry for Underwater Archaeological Site Recording: An Accessible, Diver-Based Approach. Journal of Maritime Archaeology, 9(1), 95–114. https://doi.org/10.1007/s11457-014-9127-7

Mobley, C. D. (1994). Radiative Transfer: Across the surface. Light and Water: Radiative Transfer in the Natural Waters, 159–161.

Napolitano, R., Chiariotti, P., & Tomasini, E. P. (2019). Preliminary assessment of Photogrammetric Approach for detailed dimensional and colorimetric reconstruction of Corals in underwater environment. 2018 IEEE International Workshop on Metrology for the Sea; Learning to Measure Sea Health Parameters, MetroSea 2018 - Proceedings, 39–45. https://doi.org/10.1109/MetroSea.2018.8657835

Olinger, L. K., Scott, A. R., McMurray, S. E., & Pawlik, J. R. (2019). Growth estimates of Caribbean reef sponges on a shipwreck using 3D photogrammetry. Scientific Reports, 9(1), 1–12. https://doi.org/10.1038/s41598-019-54681-2

Palma, M., Casado, M. R., Pantaleo, U., Pavoni, G., Pica, D., & Cerrano, C. (2018). SfM-based method to assess gorgonian forests (Paramuricea clavata (Cnidaria, Octocorallia)). Remote Sensing, 10(7), 1–21. https://doi.org/10.3390/rs10071154

Piazza, P., Cummings, V., Lohrer, D., Marini, S., Marriott, P., Menna, F., Nocerino, E., Peirano, A., & Schiaparelli, S. (2018). Divers-operated underwater photogrammetry: Applications in the study of Antarctic benthos. International Archives of the Photogrammetry, Remote Sensing and Spatial Information Sciences - ISPRS Archives, 42(2), 885–892. https://doi.org/10.5194/isprs-archives-XLII-2-885-2018

Pizarro, O., Friedman, A., Bryson, M., Williams, S. B., & Madin, J. (2017). A simple, fast, and repeatable survey method for underwater visual 3D benthic mapping and monitoring. Ecology and Evolution, 7(6), 1770–1782. https://doi.org/10.1002/ece3.2701

Prado, E., Cristobo, J., Rodríguez-Basalo, A., Ríos, P., Rodríguez-Cabello, C., & Sánchez, F. (2021). In situ Growth Rate Assessment of the Hexactinellid Sponge Asconema setubalense Using 3D Photogrammetric Reconstruction. Frontiers in Marine Science, 8(February), 1–16. https://doi.org/10.3389/fmars.2021.612613

Prado, E., Sánchez, F., Rodríguez-Basalo, A., Altuna, Á., & Cobo, A. (2019). Analysis of the population structure of a gorgonian forest (Placogorgia sp.) using a photogrammetric 3D modeling approach at Le Danois Bank, Cantabrian Sea. Deep-Sea Research Part I: Oceanographic Research Papers, 153(September). https://doi.org/10.1016/j.dsr.2019.103124

Raoult, V., Reid-Anderson, S., Ferri, A., & Williamson, J. (2017). How Reliable Is Structure from Motion (SfM) over Time and between Observers? A Case Study Using Coral Reef Bommies. Remote Sensing, 9(7), 740. https://doi.org/10.3390/rs9070740

Sarakinou, I., Papadimitriou, K., Georgoula, O., & Patias, P. (2016). Underwater 3D modeling: Image enhancement and point cloud filtering. International Archives of the Photogrammetry, Remote Sensing and Spatial Information Sciences - ISPRS Archives, 41(July), 441–447. https://doi.org/10.5194/isprsarchives-XLI-B2-441-2016

Shortis, M. (2019). Camera Calibration Techniques for Accurate Measurement Underwater. In J. K. McCarthy, J. Benjamin, T. Winton, & W. van Duivenvoorde (Eds.), 3D Recording and Interpretation for Maritime Archaeology (pp. 11–27). Springer International Publishing. https://doi.org/10.1007/978-3-030-03635-5_2

Skarlatos, D., Demestiha, S., & Kiparissi, S. (2012). An 'Open' Method for 3D Modelling and Mapping in Underwater Archaeological Sites. International Journal of Heritage in the Digital Era, 1(1), 1–24.

Thoeni, K., Giacomini, A., Murtagh, R., & Kniest, E. (2014). A comparison of multi-view 3D reconstruction of a rock wall using several cameras and a Laser scanner. International Archives of the Photogrammetry, Remote Sensing and Spatial Information Sciences - ISPRS Archives, 40(5), 573–580. https://doi.org/10.5194/isprsarchives-XL-5-573-2014

Troisi, S., Del Pizzo, S., Gaglione, S., Miccio, A., & Testa, R. L. (2015). 3D models comparison of complex shell in underwater and dry environments. International Archives of the Photogrammetry, Remote Sensing and Spatial Information Sciences - ISPRS Archives, 40(5W5), 215–222. https://doi.org/10.5194/isprsarchives-XL-5-W5-215-2015

Chapter 4.

3D Data Science and XR Applications to Support Glass Sponge Monitoring in Coastal British Columbia

This is an extended version of the paper published in The International Archives of the Photogrammetry, Remote Sensing and Spatial Information Sciences.

Citation Details: Lochhead, I., & Hedley, N. (2020). 3D Modelling in Temperate Waters: Building Rigs and Data Science to Support Glass Sponge Monitoring Efforts in Coastal British Columbia. International Archives of the Photogrammetry, Remote Sensing and Spatial Information Sciences - ISPRS Archives, 43(B2), 969–976. https://doi.org/10.5194/isprs-archives-XLIII-B2-2020-969-2020

Abstract

Structure from motion (SfM) has emerged as a popular method of characterizing marine benthos in tropical marine environments and could be of tremendous value to glass sponge monitoring and management efforts in the Northeast Pacific Ocean. However, temperate marine environments present a unique set of challenges to SfM workflows, and the combined impact that cold, dark, and turbid waters have on the veracity of SfM derived data must be critically evaluated in order for SfM to become a meaningful tool for ongoing glass sponge research. This paper discusses the design, development, testing, and deployment of an innovative underwater SfM workflow for generating high-resolution 3D models in temperate marine environments and explores the development and use of XR interfaces for visual analyses of the resultant data. This multi-phase research project (dry-lab, wet-lab, and field), while possibly seen as unconventional, was designed to innovate in three ways. First to build an operational data capture platform to support low-cost SfM-based seafloor surveys. Second, to enable systematic isolation and evaluation of SfM data capture parameters and their implications for representational veracity and data quality. And finally, to explore how XR interfaces can be used to visualize, manipulate, and interpret 3D glass sponge data in 3D. The challenges and outcomes from a series of field surveys conducted in Howe Sound, BC, one of which serves as the first of two data sets in a temporal analysis of 3D morphometric change, are also

discussed. This research demonstrates that accurate, high-resolution morphometric characterization, of all benthic species and habitats, is dependent on a range of equipment, procedural, and environmental variables. It is also intended to share our applied problem-solving path to successful 3D capture and 3D visualization backed up by robust data science.

Keywords: 3D Underwater Modelling, Photogrammetry, Structure-from-Motion, 3D Visualization, Extended Reality, Temperate Marine Ecology, Glass Sponges

4.1. Introduction – The Significance of Glass Sponges and the Challenges of Underwater Three-Dimensional Monitoring

The glass sponge reefs found throughout the western Canadian continental shelf are considered a key structural habitat due to their uniqueness, delicacy, and role in maintaining ecosystem dynamics (Fisheries and Oceans Canada, 2010). As filter-feeders, they remove waterborne bacteria with 95% efficiency, are a potentially important carbon sink (Kahn et al., 2015), and their siliceous skeletons provide a significant silica sink (Chu et al., 2011). Glass sponge reefs support a variety of marine fauna, including bryozoans, gastropods, crustaceans, echinoderms, and fish (most notably, several species of rockfish) (Chu & Leys, 2010; Krautter et al., 2001; Marliave et al., 2009). This ecological productivity attracts many commercial fisheries, resulting in an estimated 253 tons of coral and sponge bycatch between 1996 and 2002 (Leys et al., 2007) and widespread reports of damage (K. Conway et al., 2007; K. W. Conway et al., 2001; Kim W. Conway et al., 2005; Cook et al., 2008; Krautter et al., 2001). Consequently, Fisheries and Oceans Canada closed fisheries in coastal waters known to contain these sensitive reef habitats (2010), thereby protecting these ecosystems as researchers continue to assess reef health and their ability to adapt to environmental and anthropogenic influences. However, effective monitoring efforts are inhibited by insufficient pragmatic indicators of glass sponge reef function - stemming from their relative inaccessibility and a reliance on traditional 2D metrics that are subjective, time consuming, prone to error, and provide an inadequate characterization of the complex, 3D structure of glass sponges. Accurate characterization of this 3D complexity through time is critical for assessing and monitoring the health of glass sponge reef ecosystems,

improving coastal monitoring efforts, and implementing informed marine management policies.

Habitat complexity is a critical attribute of underwater ecosystems, as kelp forests, coral reefs, and glass sponge reefs support a variety of marine fish and invertebrates, and higher levels of structural complexity are linked to increased biodiversity, productivity, and survivorship (Connell & Jones, 1991; Gratwicke & Speight, 2005). While traditional 2D metrics (e.g., percent cover or maximum relief) fail to sufficiently characterize habitat structural complexity, more recent methods (e.g., LiDAR), which can provide high-resolution, 3D characterizations, come with significant costs that place them out of reach for many researchers and monitoring organizations (J. H. R. Burns et al., 2015; Wedding et al., 2008). However, structure from motion (SfM) photogrammetry has emerged as a popular alternative for documenting the 3D structure of marine benthos, particularly in clear, tropical waters.

4.1.1. The Rise of SfM in Marine Ecology

SfM, or multi-image photogrammetry, is a photogrammetric approach enabling 3D reconstruction and measurement from two or more overlapping 2D images. SfM emerged in the 1990s with the arrival of digital photogrammetry and owes much of its existence to the computer vision community and the feature-matching algorithms introduced during the 1980s (McCarthy, 2014; Westoby et al., 2012). While the photogrammetric community favors geometric quality over automation, those from computer vision stressed the importance of automation and auto-calibration, features characteristic of modern SfM software packages (Remondino et al., 2012) such as VisualSFM, Agisoft Metashape (formerly PhotoScan), and Pix4D. While these user-friendly interfaces make 3D reconstruction from a collection of 2D photographs quite simple, they are often criticized as being black-boxes, due to their level of automation and lack of transparency (McCarthy & Benjamin, 2014; Remondino et al., 2012; Smith et al., 2016; Van Damme, 2015).

Nevertheless, the usefulness and accuracy of SfM workflows are documented throughout bathymetric surveying (Abadie et al., 2018), marine archaeology (Beltrame & Costa, 2017; McCarthy & Benjamin, 2014; Skarlatos et al., 2012), ecological monitoring (Fukunaga et al., 2019), morphometric analyses (Gutierrez-Heredia et al., 2016; Lavy et

al., 2015; Napolitano et al., 2019), benthic mapping and classification (Bayley et al., 2019; J. Burns et al., 2015; Leon et al., 2015; Pizarro et al., 2017), and temporal change detection (Bennecke et al., 2016; Piazza et al., 2018). The successful nature of these studies would suggest a significant opportunity to apply the SfM workflow to an ecological assessment of glass sponges and sponge reefs in the Northeast Pacific Ocean, particularly given the structural and ecological parallels that exist between glass sponge reefs and coral reefs. However, there is a lack of published SfM research in temperate marine environments - where the collective impact of cold, dark, nutrient-rich waters on photograph, and by extension, SfM data quality is unknown.

4.1.2. 3D Data Visualization

The use of 3D data, including the 3D point clouds derived from SfM surveying, continues to become increasingly popular throughout academia and industry. In architecture, archaeology, biology, ecology, earth science, and geography for example, 3D SfM data sets provide a temporal snapshot of the 3D structural characteristics and relationships of real-world phenomena; however, that data is often visualized, manipulated, and analyzed using 2D displays (i.e., using desktop computers), which may thereby restrict the full value of the data and the information that can be extracted from it (Zhao et al., 2019). Extended reality (XR) interfaces – a catchall term used to describe virtual reality (VR), mixed reality (MR), and augmented reality (AR) interfaces – afford many unique opportunities to data visualization which preserve the dimensionality of the phenomena and provide intuitive methods of interaction that enable perceptual experiences resembling physically being in the field or holding the phenomena in hand. While remote access to 3D scale models of physical phenomena provides valuable opportunities for researchers to analyze their 3D data sets, as well as for teaching and training purposes (Kharroubi et al., 2019), it is the capacity of XR technologies to enable users to transcend their own physical limitations by exploring novel and often impossible places, perspectives, relationships, and scenarios that makes XR so powerful.

The recent surge in popularity of 3D data and 3D visual interfaces has largely been driven by the democratization of enabling technologies and not a newfound awareness of their individual and combined potential to affect our perception and comprehension of 3D phenomena. After all, the first head-mounted display (HMD) which surrounded users with perspective 2D images that changed according to user's

head movements in order to provide the illusion of 3D, was created by Ivan Sutherland in the 1960s (Sutherland, 1968). While the device was crude by today's standards, requiring a ceiling mounted mechanical head position sensor to track user movement, it effectively created the illusion of 3D and contributed to the subsequent decades of research and development (a comprehensive overview is provided by Jerald (2015)) behind the technology we see today. Modern HMDs, tablets, and smartphones have ushered in a new wave of XR research and development exploring their practical use in 3D data visualization.

XR technologies are fundamentally transforming the way in which geospatial data is generated and consumed, offering new methods of visualization and interaction, and new spaces for representation and engagement (Çöltekin et al., 2020; Hedley, 2017). The ongoing democratization of the prerequisite XR technologies has resulted in studies exploring the use of MR interfaces to improve spatial skills through the use of augmented 3D maps (Carbonell Carrera & Bermejo Asensio, 2016), to visualize floods and watershed dynamics (Zhang et al., 2020), for temporal visualization of archaeological excavations (Papadopoulou et al., 2020), and for geography fieldwork learning (Wang et al., 2017), to name just a few. Concurrently, VR has been explored as an immersive visualization and analytics tool for 3D earth science data (Zhao et al., 2019), geohazard assessment, (Havenith et al., 2019), and environmental preference evaluation (Birenboim et al., 2019) and is effective in motivating spatial training activities (Carbonell-Carrera & Saorín, 2017) and for conducting traditionally field-based training activities (Levin et al., 2020). Research shows that MR technologies offer improved learning and recall performance (Valimont et al., 2007), reduced cognitive load (Baumeister et al., 2017), and positive learning experiences (Turan et al., 2018), while immersive VR experiences can elicit a sense of presence that can enhance engagement and motivation resulting in higher level cognitive processing (Detyna & Kadiri, 2020), and can accelerate research efforts through rapid site visits, data quantification, and data integration (Zhao et al., 2019). However, when not designed properly – accounting for hardware limitations such as the restricted field-of-view of HMDs – these technologies can increase the cognitive load placed on the user (Baumeister et al., 2017), and VR can overwhelm and distract the user, thereby detracting from their learning experience (Makransky et al., 2019).

4.1.3. Developing a Rig for Operational SfM and Critical Benchmarking

The first objective of this study was to develop a SfM data capture workflow, supported by a preliminary sequence of data quality analyses conducted in a dry and wet-lab, that can be used to monitor changes to the complex, 3D morphology of glass sponges and glass sponge reefs in temperate marine environments. Given the annual growth rate of glass sponges is documented at 1-10 cm/year (Austin et al., 2007; Kahn et al., 2016), 3D models derived from biannual SfM surveys needs to be sufficiently accurate to detect sub-centimeter changes.

Our approach focuses on a systematic analysis of survey parameters that are commonly reported or undertaken idiosyncratically to understand how camera type, camera settings, lighting, capture strategy, and underwater environments impact the veracity of SfM-derived 3D data. By implementing a systematic program of SfM benchmarking in controlled dry lab and wet lab conditions, we were able to establish a robust and informative context that provided a basis to understand the imaging and geomorphometric capacity of our workflow to resolve object morphology and features across a range of granularities, and to provide a basis for understanding the impact of combined equipment and environmental variability in the field.

4.1.4. Developing XR Applications for the Visual Analysis of Glass Sponge Data

Our second objective was to develop a collection of XR interfaces which would enable interactive, immersive, and collaborative visual analyses of the resultant 3D glass sponge data. Traditional methods of visualizing SfM derived data include desktop-based 3D viewers – either within the SfM software itself or through other third-party solutions (e.g., CloudCompare and MeshLab) – and static 2D graphics and data sets characterizing 3D phenomena. Our focus here was on developing XR interfaces that preserve the 3D nature of the data, allowing for intuitive interaction, exploration, or immersion within that data, and providing an opportunity for collaborative visual analyses.

4.2. Equipment and Benchmarking

The glass sponges selected for this study are located off the west coast of Bowen Island, BC at a depth of 20-30 meters. These sites can experience strong currents, turbid waters, and low light levels; therefore, it was determined that providing camera and light stability would be critical to high-quality data capture. The following subsections describe the equipment and workflow benchmarking phases of this project, which provided critical data sets quantifying the performance of our SfM workflow in both a dry and wet-lab environment, and the first portion of the field work phase.

4.2.1. Data Capture Platform

The custom-built data capture rig (HEXYZ-1, named for the sponge species, the shape of rig, and acknowledging the objective of deriving 3D geometry) was designed to deliver camera stability, a controlled and repeatable data capture strategy, and a world stabilized light source (Figure 4.1). An adjustable camera armature, extending from and rotating around the apex of HEXYZ-1's one-inch square tube aluminum frame, offered a stable, circular pathway for photograph and video capture. Seven extra-wide beam LED dive lights (BigBlue Model AL1200XWP), one at each of HEXYZ-1's six vertices (staggered high and low) and one at its apex, were attached to the frame within semi-opaque housings. This lighting configuration offered consistent, soft lighting that could be controlled (using 150, 300, 600, or 1200 lumen settings) to suit environmental conditions and prevented hard showing and over or under exposure.

Figure 4.1 **A custom designed data capture platform (HEXYZ-1) was constructed to provide camera stability, repeatability, and consistent, world-stabilized lighting in temperate marine environments.**

4.2.2. Camera Equipment

Two different camera types were utilized in this research; a Sony Alpha α6500 mirrorless digital camera equipped with a Sony E PZ 16-50mm F3.5-5.6 OSS (Optical SteadyShot) lens, and a GoPro HERO6 Black action camera. Both cameras were used in the dry-lab phase of this project, but only the Sony A6500 camera, mounted within an Aquatica A6500 underwater housing equipped with an 8-inch dome port, was used in the wet-lab and field phases.

The Sony A6500 was selected due to the availability of an underwater housing and as a highly rated digital camera suitable for SfM data capture. The GoPro HERO6 Black was chosen to evaluate the aptness of action cameras for SfM-based modelling, as action cameras, largely GoPro models, are often cited in the SfM research literature (e.g., Gutierrez-Heredia et al., 2016; Raoult et al., 2016; Thoeni, Giacomini, Murtagh, & Kniest, 2014; Van Damme, 2015). While the GoPro used here was significantly less expensive than the combined cost of the Sony A6500 and underwater housing, financial savings may come at the expense of data quality, which would limit the usefulness of action cameras in benthic surveys endeavoring to monitor small-scale (centimeter or less) morphometric changes.

Documented best practices indicate that photographs, as compared to frames extracted from video, provide superior SfM modelling results. Photographs and videos were collected in this study to calculate performance disparity. Sony A6500 photographs were captured in the ARW format and converted to TIFFs for processing, whereas GoPro photographs, while captured in the RAW and JPEG format, were only processed as JPEGs due to problems with the quality of the RAW files. Individual frames from each 4K video were manually extracted as PNG files using VLC Media Player.

4.2.3. SfM Processing

Images from each of the SfM tests and surveys described throughout this paper were processed using Agisoft PhotoScan Professional (V1.4.0). In each instance, images were aligned using the high accuracy setting, markers were placed where reference object were visible, and a minimum of two scalebars were created using the reference objects (rulers) located by each subject, and image alignment was optimized using the optimize tool. Dense point clouds were then created using the high-quality setting and depth filtering was set to aggressive. Point clouds were then cleaned to remove erroneous points and high-polygon count meshes were created, as necessary. Dense point clouds were exported for analysis in CloudCompare.

4.2.4. Phase One: Dry-lab Benchmarks

The objective of the first phase of this research project was to identify the optimal lighting configuration and which combination of camera type, camera settings, and data capture strategy resulted in the highest accuracy data (Lochhead and Hedley, in press). Five different lighting tests were conducted to assess the impact that a different number, configuration, and lumen output of lights had on model accuracy. Each test included 168 photographs of a glass sponge skeleton collected with the Sony A6500 (30mm focal length, f/5.0 aperture, ISO 640, and 1/60 shutter speed) mounted to HEXYZ-1. 3D model accuracy was determined by comparing linear measurements of five distinct features made within PhotoScan to those collected from the sponge skeleton using a digital caliper. The lighting configuration (shown in HEXYZ-1 Figures throughout) provided the smallest measurement error and was therefore applied to all subsequent tests.

Much of the research in phase one focused on identifying SfM data quality and data quality variability resultant from purposefully selected combinations of camera types, camera settings, data format, and data capture strategies utilizing HEXYZ-1 (Figure 4.2). These combinations yielded nine unique test configurations. Each test contained a total of 180 photographs (or 180 images extracted from videos), that provided either a unique perspective of the test subject in 10-degree increments along five encircling pathways (Figure 4.3), or a unique perspective collected from random positions within the confines of HEXYZ-1. An assemblage of wooden blocks of known dimension served as the test subject for these tests, rather than the glass sponge skeleton, in order to overcome imprecise manual measurements of a complex, irregular structure. SfM data quality was again determined by comparing linear SfM model measurements to real-world measurements. Overall, this battery of tests revealed that the Sony A6500 produced higher accuracy models than the GoPro, that having the Sony A6500 mounted to HEXYZ-1 (as opposed to being handheld) resulted in higher accuracy models, and that there was little difference between the mean measurement errors of tests containing photographs and those containing images extracted from videos.

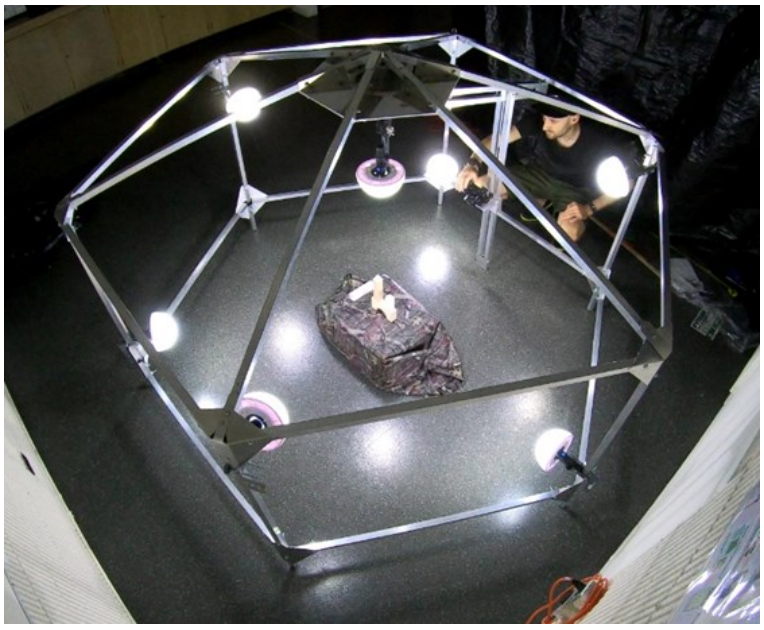

Figure 4.2 Dry-lab tests evaluated SfM data quality resulting from photographs and videos collected using different cameras, camera settings, light configurations, and with and without the stability of HEXYZ-1.

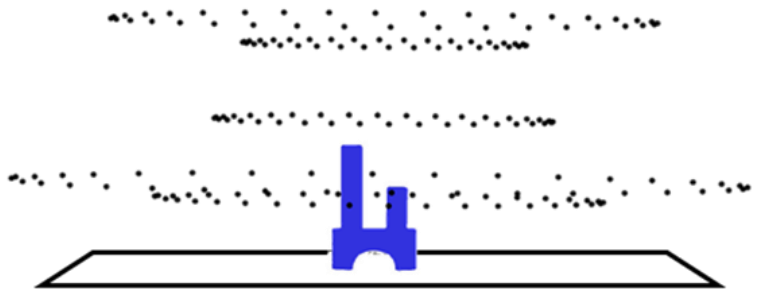

Figure 4.3 **180 images provided 360-degree coverage of the test subject. Images were captured from camera positions (black points) arranged in five halos around target objects (blue). This image shows a side perspective of the five halos of camera positions and target object.**

4.2.5. Phase Two: Wet-lab Benchmarks

The objective of the second phase of this project was to evaluate the highest accuracy workflow from phase one in a controlled wet-lab, thereby quantifying the impact that a cold, dark marine environment has on SfM data quality (Lochhead and Hedley, in review). 180 photographs of an ornamental coral were collected underwater and on dryland with the Sony A6500 (16 mm, f/3.5, 400 ISO, and 1/60 shutter speed) mounted to HEXYZ-1 and using the data capture strategy depicted in Figure 4.3. Underwater photographs, captured from within a large saltwater holding tank, and dryland photographs, captured from beside that tank were both collected after sunset and from within the confines of semi-permanent fabric building located at the Fisheries and Oceans Canada Centre for Aquaculture and Environmental Research in West Vancouver, BC (Figure 4.4).

Data quality was again determined by comparing the accuracy of a series of linear measurements made within PhotoScan to manual measurements made using a digital caliper. These tests revealed that, using the presented workflow, SfM models generated from underwater images can be as accurate as those generated from dryland images; in fact, the underwater photographs in this test produced a model of slightly higher overall accuracy (0.26% (wet) versus 0.28% (dry) difference – calculated as the mean of the absolute value of all measurement errors). However, that level of accuracy was only obtained when all 180 photographs were processed, as tests including 90, 60, and 45 photographs (processed in different configurations) resulted in greater measurement errors than those containing the complete set of photographs.

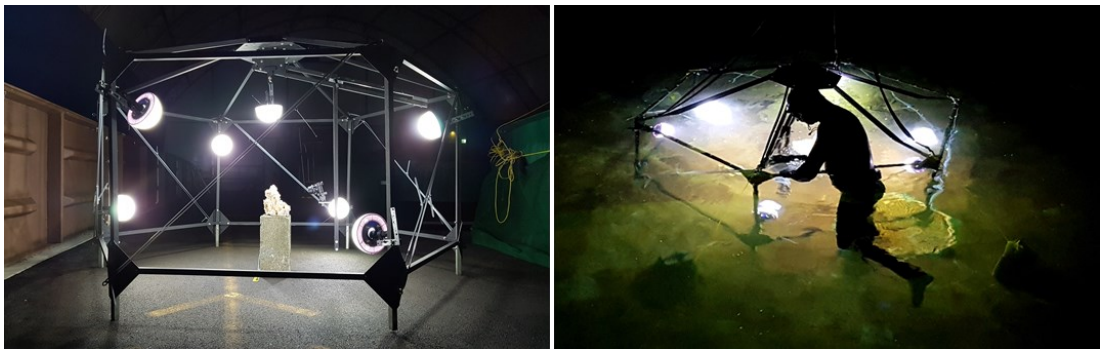

Figure 4.4 **The quality of SfM data sets, derived from photographs collected in a dryland (left) and wet-lab (right) environment, were evaluated to quantify the impact of a dark, cold water marine environment.**

4.2.6. Phase 3: Glass Sponge Surveys

The workflow and data quality benchmarks delivered through phase one and two of this research project served to both guide the design and define the capacity of a SfM data capture strategy capable of monitoring the health and morphology of temperate marine ecosystems (specifically glass sponge reefs). Phase three of this research takes the next step towards the goal of informed reef-scale surveying in temperate waters by applying our workflow in the field. Photographs and videos of individual glass sponges were captured during a series of field surveys conducted off the coast of Bowen Island, BC (49°23'19.0" N 123°24'38.2" W) at a depth of 20-25 meters. All photographs and videos were collected using a Sony A6500 mounted within an Aquatica housing fitted with an 8" dome port (photographs: 16 mm, f/3.5, 400 ISO, and 1/60 shutter speed, video: 4K). All field surveys conducted with HEXYZ-1 utilized the lighting configuration presented in phases one and two (seven lights each producing 600 lumens). The specifics of each survey are presented in the following subsections. All SCUBA diving activities were conducted by members of the Howe Sound Research Group and their affiliates.

Survey 1

HEXYZ-1 was deployed from a small research vessel, lowered onto the seafloor, and then moved into position over a glass sponge by two divers; a small lift bag was utilized to support the weight of HEXYZ-1 as it was moved into place. Four marked stakes (for image alignment) and three scale markers (for model scaling) were driven into the seafloor surrounding the glass sponge. A total of 32 photographs (one circular

pass) were collected with the camera attached to HEXYZ-1's armature (Figure 4.5). All equipment, other than the marked stakes, was collected at the conclusion of this survey.

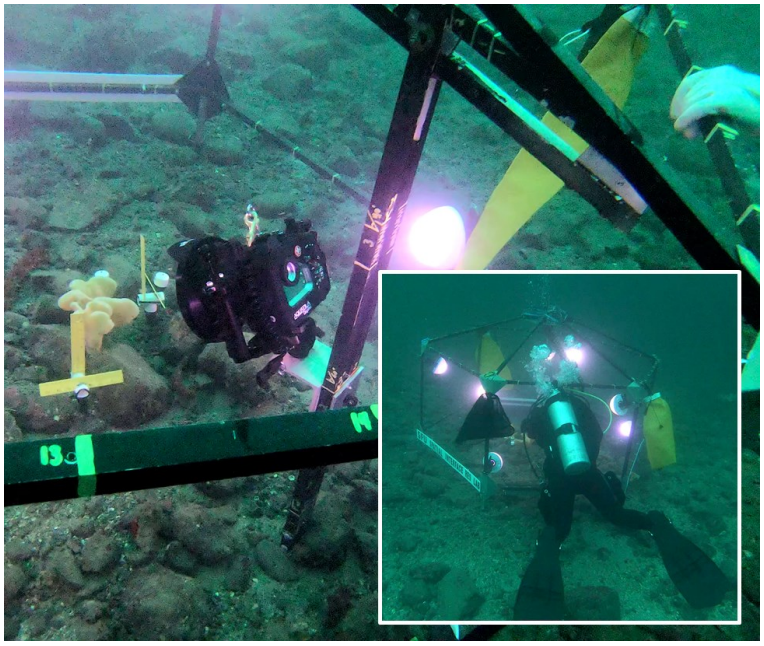

Figure 4.5 **Underwater data collection was performed by the Howe Sound Research Group, a division of Ocean Wise. Three sets of photographs or three videos of a glass sponge were collected from different positions and perspectives.**

Survey 2

HEXYZ-1 was not deployed for this survey, in which two sets of photographs were collected manually by an underwater photographer. Scale bars were again placed around the glass sponge for reference. The first dive generated 67 photographs of the glass sponge, illuminated by a single camera mounted wide beam dive light (800 lumens), and the second dive yielded 73 photographs, illuminated this time by a single BigBlue extra-wide beam dive light (1200 lumens). The photographer was asked to collect sets of photographs encircling the glass sponge in a manner like that delivered by HEXYZ-1. All reference objects were collected at the end of this dive.

Survey 3

HEXYZ-1 was again deployed from the research vessel by a team of divers, only this time the intended glass sponge could not be located. HEXYZ-1, the marked stakes, and the scale bars were instead placed around a different, smaller glass sponge. 36

photographs were collected in one circular path; however, none of those photographs contained enough of the glass sponge to be useful for 3D reconstruction. Only the camera and dive lights were collected at the conclusion of this survey.

Survey 4

Returning the following day, and with HEXYZ-1 and the reference objects already on site, the dive lights were installed, and 75 photographs were captured from two paths encircling the glass sponge at different heights above the seafloor. Only the camera and dive lights were collected at the conclusion of this survey.

HEXYZ-1 remained on site for approximately three weeks, as divers were unable to safely return to the site due to poor weather conditions.

Survey 5

Having yet to successfully generate a complete data set, it was decided that videos, rather than photographs, would be collected to overcome the time limitations introduced by successive dives at depths of 20-25 meters. Three videos were collected for this survey, each video encircling the glass sponge at different heights and providing a different perspective. All equipment, other than the stakes, was collected at the end of this survey. A total of 189 frames were extracted from these videos.

4.2.7. 3D Visualization Development

The 3D point clouds generated through each of the underwater surveys provide high-resolution 3D characterizations of a living glass sponge. A set of 3D applications were developed using Unity, a popular multi-platform game engine, to provide interactive, immersive, and collaborative methods of engaging with these 3D glass sponge point clouds. The interface development workflow is discussed in the following subsections.

Data Processing

The dense point clouds generated within PhotoScan were saved in the LAS and XYZ file format. While various 3D files can be exported directly from PhotoScan, none are natively supported by Unity. However, Point Cloud Free Viewer, a free asset from the Unity Asset Store, generates 3D point clouds during Unity runtime from OFF files.

The LAS and XYZ point clouds from Surveys 4 and 5 were converted to OFF files using either MeshLab or a combination of CloudCompare and MeshLab. These files were then saved to the appropriate Unity project folder, Point Cloud Free Viewer created a 3D GameObject (a fundamental component of a Unity Scene) at runtime, and the resultant GameObject was used to create a Prefab Asset (a stored version of the GameObject created at runtime). This Prefab version of the point cloud can then be included in any subsequent Unity Scene or Project outside of runtime. The point clouds contained within the MR and VR prototypes are scale models of the glass sponges surveyed in Howe Sound.

Mixed Reality

MR development was conducted using Unity (Version 2019.2.13f1) and Vuforia Engine (Version 8.5.9), a popular MR development package fully supported through Unity's XR Settings. This MR application was developed for Android and installed on a Samsung Galaxy S10e. The application is an image-based MR application, whereby a predefined image target is detected and tracked by Vuforia Engine using the device's camera. 3D content is thereby displayed on the device's screen so long as the device's camera has the image target within view. This provides the user with full control over the physical relationship between the device and the image target - by manually manipulating the position and orientation of the device, image target, or both - to control when, what, and how 3D content is displayed on the device's screen. This tangible form of MR offers the visual, spatial, and sensorimotor cues, akin to holding the real object itself, which promote visual knowledge acquisition (Shelton & Hedley, 2004).

Functionally, this MR application allows the user to control which 3D models are displayed, make linear measurements of those models, and inspect structural characteristics of those models using a series of cut planes. The application contains point clouds from Surveys 4 and 5, as well as a Cloud-to-Cloud (C2C) Distance point cloud which highlights the physical differences between the two survey results. Linear measurements are made by manipulating the position of two spheres, which are embedded within the 3D content and between which distance is calculated, through touchscreen inputs and adjustments to the device position relative to the image target itself. Three cut planes, one for each the axis (X, Y, and Z), bisect the point clouds using an occlusion shader.

Virtual Reality

VR development was also conducted using Unity and the Oculus VR SDK contained within Unity's XR Settings. Additional VR packages utilized in development include the Oculus Integration (Version 15.0) and the Virtual Reality Toolkit (VRTK) (Version 3.3.0). The VRTK offers plug and play VR development solutions incorporating assets from the Oculus Integration (e.g., player, camera, and controller prefabs) and its own solutions to player movement and interaction within the virtual environment (VE). This VE was built for the Oculus Quest, an all-in-one VR platform which uses built-in sensors and Oculus Insight Tracking to convert real-world movement into VR movement with room-scale tracking.

This VE was designed to simulate a boardroom, lab, or other common office space in which various forms of digital data can be presented for both visual analyses and simple morphometric assessments. The VE includes the 3D points clouds from Surveys 4 and 5, display screens containing the images and videos from which those models were generated, statistical outputs from SfM processing, and simple measurement and inspection tools. Users can pick up and manipulate the point clouds, make linear and volumetric measurements of them using real-time computational tools, and arrange cut planes for cross sectional analyses. Users can freely move about the VE using VRTK's teleportation system or the can simply walk about, relying on the room-scale tracking functionality of the Oculus Quest to track and translate their real-world movement.

Finally, the VE was designed to be both an individual experience, in which single users can access the VE, and a collaborative experience, in which multiple users can simultaneously access the VE and interact with each other and the data in real-time. Collaboration is enabled through Photon Unity Networking 2 (PUN 2) Free, a Unity Package offered by Exit Games, which allows up to 20 concurrent users (located anywhere with a wireless network) to access the networked application through the Photon Cloud.

4.3. Results and Discussion

4.3.1. 3D Models

A variety of SfM workflows have proven to be beneficial for marine surveying across a range of research disciplines. As a low-cost, non-intrusive, and relatively rapid method of 3D data capture, SfM has gained significant popularity. Yet temperate marine applications are not as commonly reported as those in tropical environments, and questions remained about SfM performance in challenging temperate environments. The objective of this research was to assess the impact of some of those challenges and develop a SfM workflow suitable for monitoring glass sponges in Howe Sound, BC.

Phase one and two of this research project provided those performance benchmarks, defining the capacity of our workflow under ideal conditions as well as in a cold, dark, and turbid marine environment. However, data collection in the field presented an additional set of logistical and methodological challenges which ultimately resulted in five disparate data sets.

The photographs and extracted images resulting from each of the five surveys were processed within PhotoScan using the parameters discussed above. Select results are presented in Table 1. No image enhancements or color correction procedures were performed on any of the photographs.

Table 4.1 SfM Field Survey Statistics

Survey	Images (Aligned)	Ground Resolution (mm/pix)	RMS Reprojection Error (pix)	Scale Bar Error (meters)
1	32 (32)	0.215	1.17	0.0004
2A	67 (65)	0.286	1.66	0.00002
2B	73 (72)	0.25	2.44	0.0002
3	36 (0)	-	-	-
4	75 (67)	0.174	1.27	0.00009
5	189 (189)	0.383	1.22	0.0002

The first deployment of HEXYZ-1 (Survey 1), while data was collected, was intended to evaluate the logistics of HEXYZ-1's deployment and data collection efforts. Survey 2 provided two valuable data sets containing manually collected photographs, the results of which could be compared to HEXYZ-1 collected data to identify differences resultant from lighting and camera control. Unfortunately, Survey 3 could not relocate the original glass sponge, and while a new sponge was identified, this survey did not produce a usable data set. Survey 4 did produce two circular sets of images using HEXYZ-1, but due to time constraints imposed by repeated dives at depths of 20-25 meters, did not produce a third set of images completing the intended data set. Survey 5 generated a set of three videos - having to settle for the lesser quality but more rapid video format to generate the intended set of data providing three perspectives - of the glass sponge.

For each survey, measurements of an additional scale marker, that was included in the survey but not utilized for model scaling, were made within PhotoScan to provide an approximation of model accuracy. The measurement made in Survey 1, despite the limited number of photographs processed, was only 1 mm less than the true distance value. The measurements made for Survey 2 was 1 cm over the true distance, and a measurement could not be made in Survey 2B due to excessive point cloud noise (Figure 4.6). In both instances, the single dive light provided an insufficient and unstable light source that resulted in points which could not be removed using PhotoScan's aggressive depth filtering. Survey 3 did not produce a 3D model. The measurement made in Survey 4 was equivalent to the true distance, and in Survey 5 only differed by 1 mm.

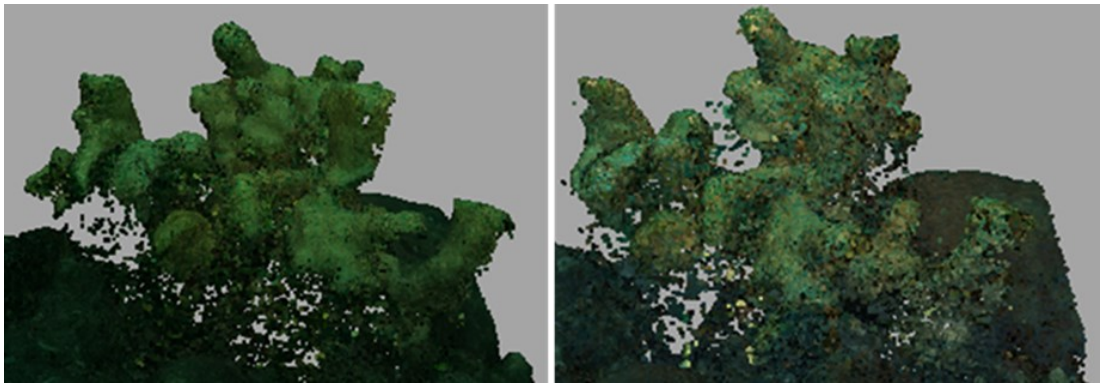

Figure 4.6 Surveys 2 A&B evaluated SfM data quality resulting from handheld underwater photography. Survey 2A utilized a single wide beam dive light - 800 lumens (left) while Survey 2B utilized a single extra-wide beam dive light - 1200 lumens (right). Both resultant models contained a significant number of artefacts on the surface of the glass sponge.

Surveys 1, 4, and 5 produced what appear visually to be high-quality dense point clouds documenting the structure of the surveyed glass sponge. While Survey 2 produced two 3D point clouds, there are noticeable data quality issues with both data sets. These results suggest that, as was revealed during phase one tests, the use of HEXYZ-1 for data capture does improve the quality of the 3D data. However, those early tests also revealed significant differences between the quality of the SfM models derived from photographs and extracted images. This would imply that Survey 4 (photographs) should produce more accurate results than Survey 5 (extracted images). Figure 4.7 provides a side-by-side comparison of the two clouds, and other than the obvious color differences, the dense point clouds appear similar. However, Survey 4 generated a dense point cloud with three times the number of points (2,410,338 versus 754,348) and twice the ground resolution (0.174 mm/pix versus 0.383 mm/pix) of Survey 5 (Figure 4.8).

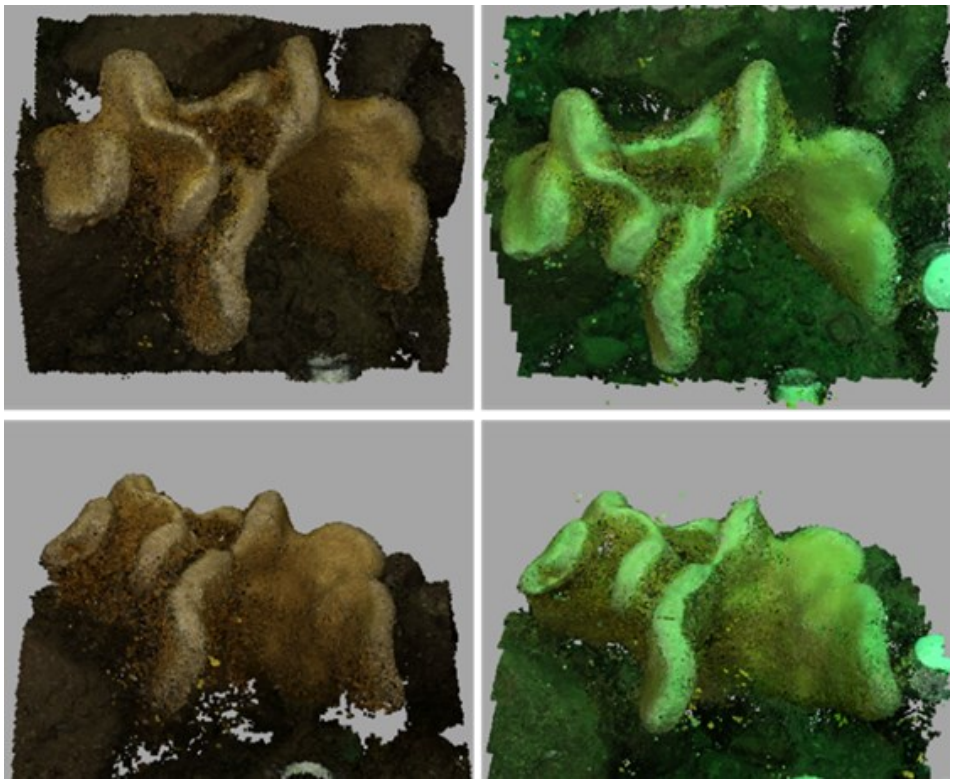

Figure 4.7 **The dense point clouds from Survey 4 (left images) and Survey 5 (right images). Besides the obvious color difference, photographs and extracted images appear to produce point clouds capable of documenting glass sponge morphology.**

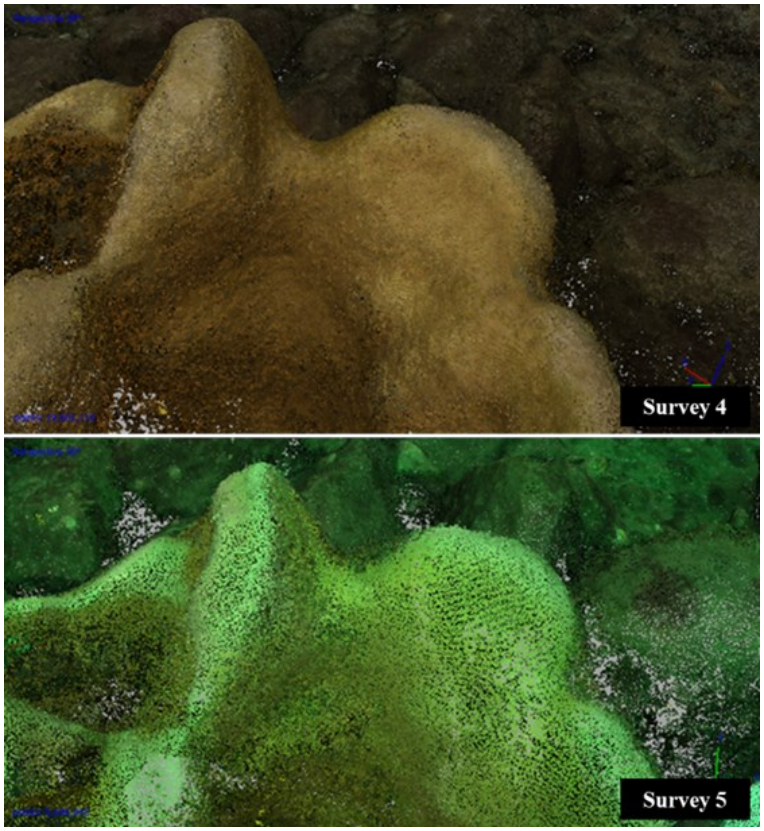

Figure 4.8 The photographs from Survey 4 (top) produced a higher density point cloud than the extracted images from Survey 5 (bottom).

Despite the difference in point density, a cloud-to-cloud distance comparison reveals that the dense point clouds from Survey 4 and 5 have a mean difference of only 2 mm (Figure 9). This minimal mean C2C distance is encouraging for future surveying efforts, as video capture required significantly less time than photographs. A team of two scuba divers were able to capture the three videos within the time that it would have taken them to capture one ring of photographs. More rapid data capture provides an opportunity to conduct successive surveys within the same dive – to ensure survey precision – or more in-depth surveying, moving the camera to additional positions closer to the subject to increase pixel density. Overall, while the video format was not the intended data format, the achieved accuracy is sufficient for monitoring purposes and the more rapid survey logistics greatly assist with data capture.

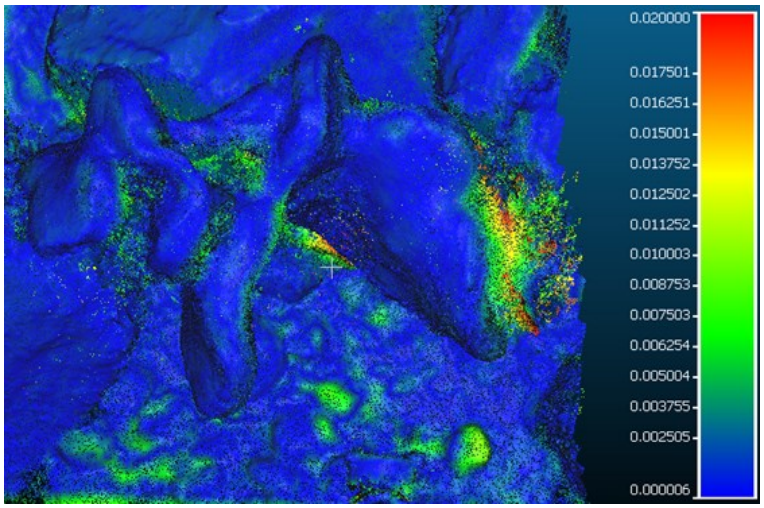

Figure 4.9 The mean cloud-to-cloud distance between the dense point clouds from Survey 4 and Survey 5 was 2 mm (top-down view of the point cloud).

This paper presents a series of field surveys that highlight some of the challenges associated with collecting photographs and videos of benthic species in temperate waters. Survey 5 represents the first of two data sets in a temporal series that will be used to assess morphometric change. While images extracted from video were not the ideal data format, the successive phases of this research project, and the preceding field surveys, provide valuable insight into the quality of this data set. Developing the data science behind our workflow was critical to future analyses of glass sponges, as the ability to generate 3D models of those sponges was never in question, yet the accuracy of the 3D models created by simply collecting and processing photographs or videos was. As illustrated here, subtle changes to lighting schemes, camera settings, and capture strategy can impact 3D model accuracy, and when monitoring millimeter or centimeter scale temporal changes, accuracy is critically important.

Interpreting the subtle changes to 3D morphometry can also be a challenge, as 2D graphical outputs provide a fixed perspective of 3D structures which may exhibit change occluded by the object itself. 3D viewers may help to alleviate the cognitive burden of connecting multiple perspective images, however, the conventional 2D interfaces on which interactive 3D visual analyses are commonly conducted can be awkward and difficult to understand. The 3D visualizations presented in the following

section offer an alternative method of visualization and interaction that is intuitive, tangible, and inherently 3D.

4.3.2. 3D Visualizations

Much of the 3D data generated with SfM programs such as PhotoScan is viewed through a conventional desktop computer or tablet (i.e., in 2D). While the tools contained within these programs allow users to generate numerous 2D and 3D models, and to manipulate the position, scale, and rotation of the displayed content (Figure 4.10), the methods of visualization and interaction create cumbersome and restricted experiences that are limited in their ability to reveal the subtle 3D structural details and relationships of the data itself. One of the primary goals of the 3D visualizations presented in the subsequent sections is to not only provide 3D visuals, but to provide interactivity and additional functionality that allows for visual analyses and scientific inquiry, demonstrating the ability for XR interfaces to overcome the perceptual, cognitive, and collaborative limitations of many conventional visualizations.

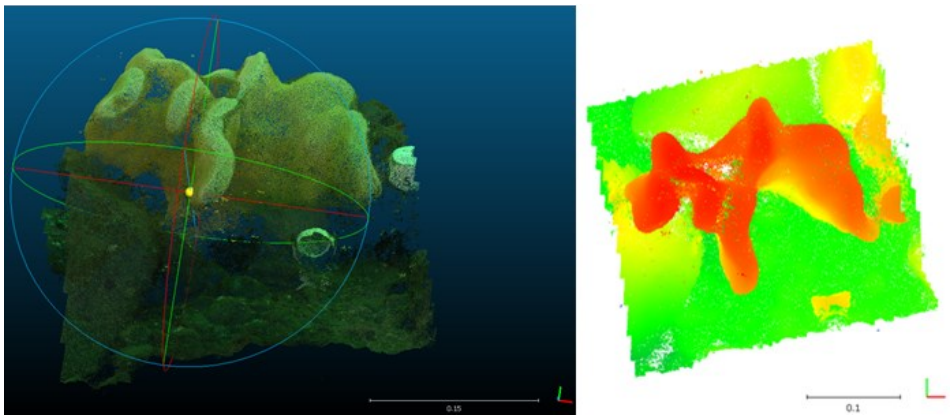

Figure 4.10 Conventional desktop interfaces employ interactive tools (e.g., move, rotate, and scale) that allow the user to manipulate 2D, 2.5D, and 3D content presented to them through a 2D display. In CloudCompare, 3D point clouds can be manipulated using 3D tools (left) and 2D surface models can be viewed in 2D (right).

Mixed Reality

This tangible MR prototype was developed to showcase how the Vancouver Aquarium staff could employ tablet and smartphone-based MR applications to assists with visual analyses of their 3D data sets. The tangible interface provides an intuitive method of inspecting 3D data that is similar to interacting with a real object. The

proprioceptive cues and feedback that are generated by visualizing and interacting with virtual objects in the real world have been shown to hold a cognitive advantage over conventional 2D interfaces (e.g., desktop displays) when it comes to learning (Shelton & Hedley, 2004). In this respect, tangible MR interfaces such as the one presented here (Figure 4.11) could not only be utilized by the researchers collecting and analyzing the data, but as an outreach tool to help educate the public about glass sponges.

Figure 4.11 This tangible MR prototype anchors 3D glass sponge data to the real world using an image target. The proprioceptive cues provided by interfaces such as this one offer cognitive advantages over conventional desktop displays.

This MR prototype was developed for a modern Android-based smartphone or tablet having a touchscreen display and an onboard camera. When the user starts the application a user interface (UI) is presented on the screen allowing them to select which data will be displayed on the devices screen when the camera detects the predefined image target. The UI includes options to switch between different glass sponge point clouds and to activate/deactivate the linear measurement and 3-axis cut-plane tools. The linear measurement tool allows the user to adjust the position two spheres - by either using the touchscreen to drag them into position or by holding a finger on each sphere while adjusting the contextual relationship between the device and the image target – and the distance between those two spheres is presented onscreen. The cut-plane tool is operated using the same combination of touchscreen controls and contextual relationships, allowing the user to position cut-planes anywhere along the X, Y, and Z axes. Screenshots of the functionality provided by the UI are presented in Figure 4.12.

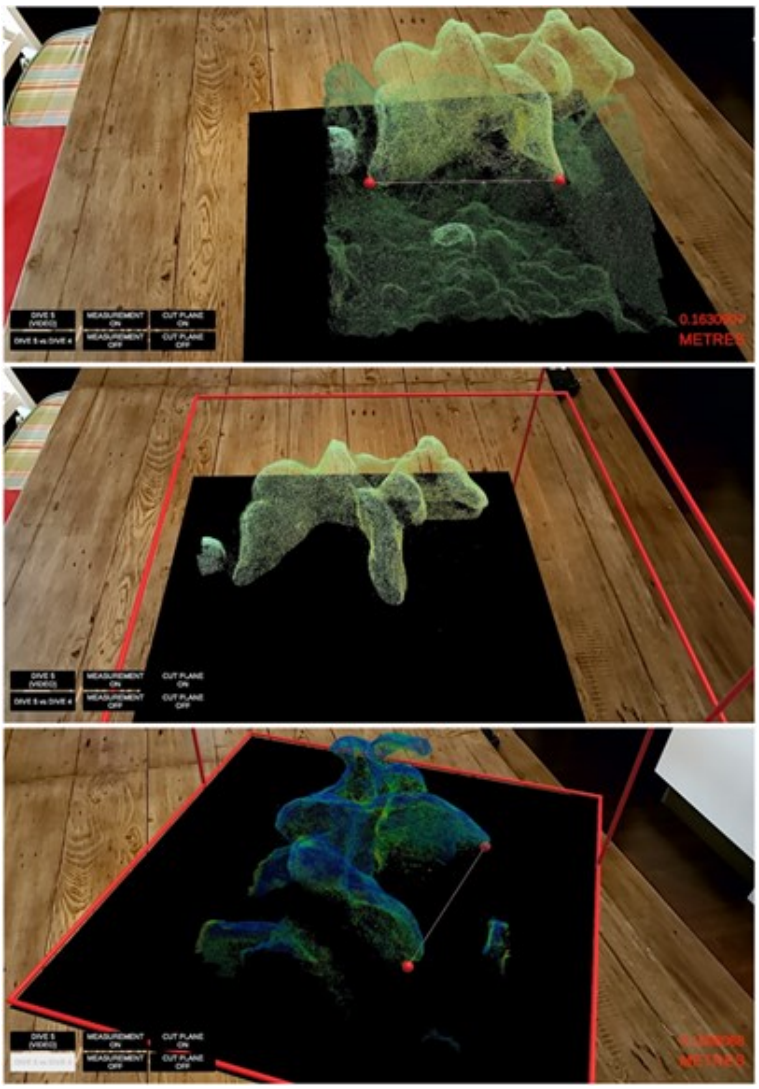

Figure 4.12 The MR prototype was designed to allow the user to make linear measurements by manipulating the position of two spheres (top), to position cut planes that reveal cross sectional structural details (middle), and to alter point cloud textures to display analytical data (bottom). Each image is a screenshot collected from a Samsung Galaxy S10e smartphone.

Virtual Reality

This VR prototype was developed as a virtual data dojo in which individual and collaborative analyses of glass sponge data can be conducted (Figure 4.13). Conventional spaces of data analysis, and the technology used to display those analyses, place restrictions on how data is presented, how much data is presented, where that data is presented, and how people interact with that data. This prototype provides an example of an immersive virtual space that can be customized to include

any number of displays, presenting data of different formats, in different configurations, and offering methods of interaction and inquiry not possible using conventional methods of visualization.

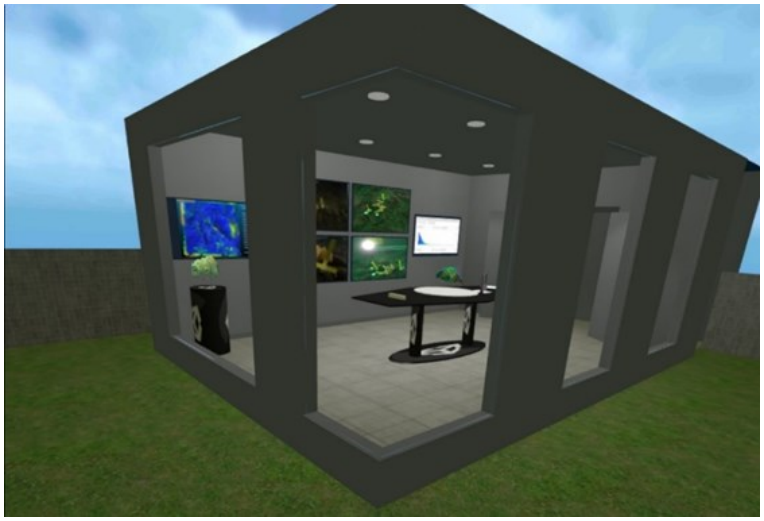

Figure 4.13 This immersive data dojo was designed to showcase how VR can be used to visualize, interact with, and analyze 2D and 3D glass sponge data in a virtual space.

The virtual environment (VE) was designed to simulate a boardroom or other common office space in which data may be analyzed individually or collectively. This virtual boardroom includes a central table, multiple wall mounted display screens, two different 3D point clouds, and two different virtual measurement tools (Figure 4.14). When users entre the VE they are placed near the table so that the display screens are located on the wall opposite them. Displayed on those screens are the images and videos from which the point clouds were created, and a selection of analytical data products generated within PhotoScan and CloudCompare. Users can pick-up manipulate the 3D glass sponge point clouds, as they would any real object, to conduct visual analyses, or they can make linear and volumetric measurements using the virtual tools located on the table. Each of these interactable objects can be picked up and placed anywhere within the VE and will remain in place when the user lets go of them. This allows the user to walk or teleport around the space to inspect the data from different perspectives.

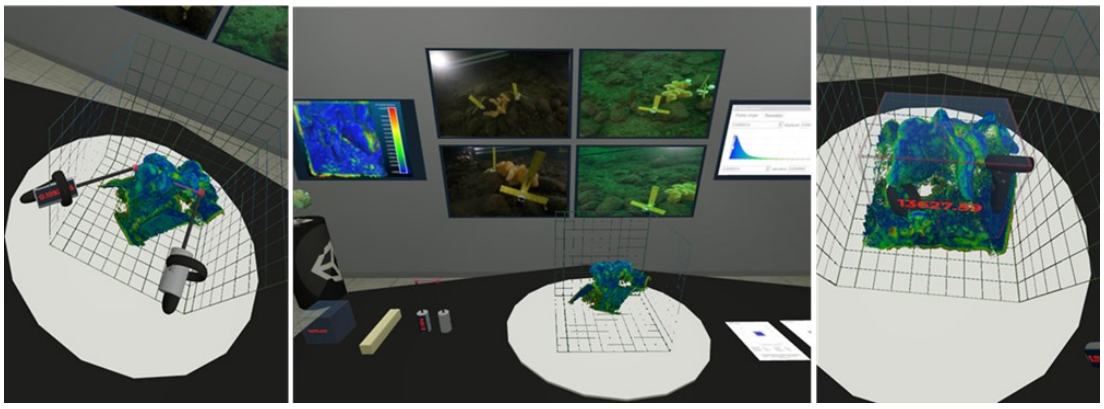

Figure 4.14 The virtual data dojo provides a boardroom-like environment in which 2D and 3D glass sponge data can be visualized and analyzed. Wall mounted display screens present the images and videos used to generate the 3D point clouds, and the products of subsequent data analyses, to users (centre). Linear measurements (left) and volumetric measurements (right) can be made using the included virtual tools.

This VE could support up to 20 concurrent VR users through a cloud-based server (Photon Public Cloud), enabling anyone with the application and an Oculus VR system to access the shared VE. This networking capability would provide an opportunity for researchers, teachers, students, and other stakeholders, located anywhere in the world, to collaborate within the VE, conducting virtual analyses and creating new, collective knowledge about the data presented to them.

4.4. Conclusion

The glass sponge reefs found in the Northeastern Pacific Ocean are the only documented living glass sponge reef structures in the world. It is believed that these unique ecosystems are a key structural habitat, providing refuge to a wide variety of marine fauna. Yet the relative inaccessibility of glass sponge reefs has restricted research on reef function and limited the capacity to monitor reef health. Much of what is known about these reefs is the product of submersible and ROV based exploration projects, limiting research activities to those with significant capital and technological resources. The discovery of glass sponge bioherms in the Strait of Georgia and Howe Sound, B.C. at depths less than 60 m has provided a unique opportunity for SCUBA divers to record, study, and track changes in the 3D structure and complexity of glass sponges over time. However, in situ manual measurements and traditional 2D metrics

are subjective, prone to error, and fail to accurately characterize the 3D structure of these ecosystems. The SfM photogrammetric techniques employed by marine scientists in tropical climates, to both qualify and quantify coral reef ecosystems in 3D, represents a workflow that could transform what is known about the glass sponge ecosystem.

While SfM workflows can provide high-resolution 3D models of the structural characteristics of benthic species and habitats that are critical to the analysis of these ecosystems (J. Burns et al., 2015; Pizarro et al., 2017), much of the published underwater SfM research is restricted to shallow water tropical climates that are considerably different than the coastal waters of the Pacific Northwest. While studies applying the SfM workflow in marine settings have achieved millimeter-scale accuracy, there is a lack of scientific literature documenting the impact that environmental variables such as light, turbidity, salinity, and temperature have on the 3D SfM data, and consequently, the appropriateness of SfM workflows in temperate waters.

The overarching objective of this paper is to share the challenges, strategies, methods, and implications of an applied underwater SfM research project that, in the first instance, sought to develop a rig capable of delivering operational ecological surveying capability. However, rather than simply implementing yet another idiosyncratic marine SfM project, we thought deeply about the need to develop benchmarks for marine SfM more broadly. This led us to develop a rig which could also be used for careful, systematic testing of capture parameters, and their performance in controlled dry and wet-lab conditions with light levels comparable to underwater field sites.

The systematic approach to our SfM research first defined the capacity of our workflow under ideal conditions, and the impact that variable data capture parameters have on SfM data quality in a dry and wet-lab, before attempting to conduct underwater surveys of glass sponges in the field. These preliminary phases provided key data capture and data quality benchmarks that allowed us to adapt to challenging field conditions while understanding the implications that those adaptations would have on the quality of our data. While SfM can be used to generate 3D models of benthic species in temperate marine environments, this research highlights the impact that different capture strategies, different lighting conditions, and different data formats have on the quality of those 3D models. As the published annual growth rate of glass sponges is approximately 1-10 cm/year, those employing SfM to monitor glass sponge

growth and health must acknowledge the subtle yet important role that these differences play if they are to detect real change.

Finally, we introduced a pair of XR prototypes that highlight the potential for VR and MR interfaces as glass sponge visualization interfaces. The complex, 3D structure of glass sponges can be difficult to quantify and comprehend using conventional 2D metrics and interfaces, and these prototypes showcase the ability to explore, interact with, and query the 3D morphology of these organisms. Thees intuitive XR interfaces provide an opportunity for tangible, natural interaction akin to physically handling the glass sponge itself, providing the sensorimotor feedback and proprioceptive cues that are not possible with 2D displays and visualizations, yet are so valuable in helping us understand 3D structures and relationships. These prototypes are a step towards XR enabled visual analytics and research into the cognitive and perceptual affordances of XR enabled scientific analysis and communication.

Acknowledgements: This work was supported by Mitacs - through the Mitacs Accelerate Program - in partnership with Ocean Wise and the Vancouver Aquarium. We would like to acknowledge the SFU Faculty of Science Machine Shop for their help fabricating HEXYZ-1 and the Howe Sound Research Group for their help conducting field activities.

References

Abadie, A., Boissery, P., & Viala, C. (2018). Georeferenced underwater photogrammetry to map marine habitats and submerged artificial structures. The Photogrammetric Record, 33(164), 448–469. https://doi.org/10.1111/phor.12263

Austin, W. C., Conway, K. W., Barrie, J. V., & Krautter, M. (2007). Growth and morphology of a reef-forming glass sponge, Aphrocallistes vastus (Hexactinellida), and implications for recovery from widespread trawl damage. Porifera Research: …, 139–145. http://www.poriferabrasil.mn.ufrj.br/iss/09-book/pdf/Austin et al - Growth and morphology of Aphrocallistes vastus.pdf

Baumeister, J., Sin, S. Y., Elsayed, N. A. M., Dorrian, J., Webb, D. P., Walsh, J. A., Simon, T. M., Irlitti, A., Smith, R. T., Kohler, M., & Thomas, B. H. (2017). Cognitive Cost of Using Augmented Reality Displays. IEEE Transactions on Visualization and Computer Graphics, 23(11), 2378–2388. https://doi.org/10.1109/TVCG.2017.2735098

Bayley, D. T. I., Mogg, A. O. M., Koldewey, H., & Purvis, A. (2019). Capturing complexity: field-testing the use of ‘structure from motion’ derived virtual models to replicate standard measures of reef physical structure. PeerJ, 7, e6540. https://doi.org/10.7717/peerj.6540

Beltrame, C., & Costa, E. (2017). 3D survey and modelling of shipwrecks in different underwater environments. Journal of Cultural Heritage, 3–9. https://doi.org/10.1016/j.culher.2017.08.005

Bennecke, S., Kwasnitschka, T., Metaxas, A., & Dullo, W.-C. (2016). In situ growth rates of deep-water octocorals determined from 3D photogrammetric reconstructions. Coral Reefs, 35(4), 1227–1239. https://doi.org/10.1007/s00338-016-1471-7

Birenboim, A., Dijst, M., Ettema, D., de Kruijf, J., de Leeuw, G., & Dogterom, N. (2019). The utilization of immersive virtual environments for the investigation of environmental preferences. Landscape and Urban Planning, 189(November 2018), 129–138. https://doi.org/10.1016/j.landurbplan.2019.04.011

Burns, J., Delparte, D., Gates, R., & Takabayashi, M. (2015). Integrating structure-from-motion photogrammetry with geospatial software as a novel technique for quantifying 3D ecological characteristics of coral reefs. PeerJ, 3, e1077. https://doi.org/10.7717/peerj.1077

Burns, J. H. R., Delparte, D., Gates, R. D., & Takabayashi, M. (2015). Utilizing underwater three-dimensional modeling to enhance ecological and biological studies of coral reefs. International Archives of the Photogrammetry, Remote Sensing and Spatial Information Sciences - ISPRS Archives, 40(5W5), 61–66. https://doi.org/10.5194/isprsarchives-XL-5-W5-61-2015

Carbonell-Carrera, C., & Saorín, J. L. (2017). Geospatial Google Street View with virtual reality: Amotivational approach for spatial training education. ISPRS International Journal of Geo-Information, 6(9). https://doi.org/10.3390/ijgi6090261

Carbonell Carrera, C., & Bermejo Asensio, L. A. (2016). Landscape interpretation with augmented reality and maps to improve spatial orientation skill. Journal of Geography in Higher Education, 8265(March), 1–15. https://doi.org/10.1080/03098265.2016.1260530

Chu, J. W. F., & Leys, S. P. (2010). High resolution mapping of community structure in three glass sponge reefs (Porifera, Hexactinellida). Marine Ecology Progress Series, 417, 97–113. https://doi.org/10.3354/meps08794

Chu, J. W. F., Maldonado, M., Yahel, G., & Leys, S. P. (2011). Glass sponge reefs as a silicon sink. Marine Ecology Progress Series, 441, 1–14. https://doi.org/10.3354/meps09381

Çöltekin, A., Lochhead, I., Madden, M., Christophe, S., Devaux, A., Pettit, C., Lock, O., Shukla, S., Herman, L., Stachoň, Z., Kubíček, P., Snopková, D., Bernardes, S., & Hedley, N. (2020). Extended reality in spatial sciences: A review of research challenges and future directions. ISPRS International Journal of Geo-Information, 9(7). https://doi.org/10.3390/ijgi9070439

Connell, S. D., & Jones, G. P. (1991). The influence of habitat complexity on postrecruitment processes in a temperate reef fish population. Journal of Experimental Marine Biology and Ecology, 151(2), 271–294. https://doi.org/10.1016/0022-0981(91)90129-K

Conway, K., Barrie, J., Hill, P., Austin, W., & Picard, K. (2007). Mapping sensitive benthic habitats in the Strait of Georgia, coastal British Columbia: deep-water sponge and coral reefs. In Geological Survey of Canada, Current Research (Vols. 2007-A2). https://doi.org/10.1002/9780470344620.fmatter

Conway, K. W., Krautter, M., Barrie, J. V., & Neuweiler, M. (2001). Hexactinellid sponge reefs on the Canadian continental shelf: A unique “living fossil.” In Geoscience Canada (Vol. 28, Issue 2, pp. 71–78).

Conway, Kim W., Barrie, J. V., & Krautter, M. (2005). Geomorphology of unique reefs on the western Canadian shelf: Sponge reefs mapped by multibeam bathymetry. Geo-Marine Letters, 25(4), 205–213. https://doi.org/10.1007/s00367-004-0204-z

Cook, S. E., Conway, K. W., & Burd, B. (2008). Status of the glass sponge reefs in the Georgia Basin. Marine Environmental Research, 66, S80–S86. https://doi.org/10.1016/j.marenvres.2008.09.002

Fisheries and Oceans Canada. (2010). Pacific Region Coral and Sponge Conservation Strategy 2010-2015. In Oceans, Habitat and Species at Risk Oceans Program. Fisheries and Oceans Canada.

Detyna, M., & Kadiri, M. (2020). Virtual reality in the HE classroom: feasibility, and the potential to embed in the curriculum. Journal of Geography in Higher Education, 44(3), 474–485. https://doi.org/10.1080/03098265.2019.1700486

Fukunaga, A., Burns, J., Craig, B., & Kosaki, R. (2019). Integrating Three-Dimensional Benthic Habitat Characterization Techniques into Ecological Monitoring of Coral Reefs. Journal of Marine Science and Engineering, 7(2), 27. https://doi.org/10.3390/jmse7020027

Gratwicke, B., & Speight, M. R. (2005). The relationship between fish species richness, abundance and habitat complexity in a range of shallow tropical marine habitats. Journal of Fish Biology, 66(3), 650–667. https://doi.org/10.1111/j.0022-1112.2005.00629.x

Gutierrez-Heredia, L., Benzoni, F., Murphy, E., & Reynaud, E. G. (2016). End to End Digitisation and Analysis of Three-Dimensional Coral Models, from Communities to Corallites. PLoS ONE, 11(2). https://doi.org/10.1371/journal.pone.0149641

Havenith, H. B., Cerfontaine, P., & Mreyen, A. S. (2019). How virtual reality can help visualise and assess geohazards. International Journal of Digital Earth, 12(2), 173–189. https://doi.org/10.1080/17538947.2017.1365960

Hedley, N. (2017). Augmented Reality. In D. Richardson, N. Castree, M. F. Goodchild, A. Kobayashi, W. Liu, & R. A. Marston (Eds.), International Encyclopedia of Geography (pp. 1–13). John Wiley & Sons, Ltd. https://doi.org/doi:10.1201/9780849375477.ch213\r10.1201/9780849375477.ch213

Jerald, J. (2015). The VR Book: Human-Centered Design for Virtual Reality (T. M. Ozsu & J. Hart (eds.); 1st Edition). Morgan & Claypool. https://doi.org/10.1145/2792790

Kahn, A. S., Vehring, L. J., Brown, R. R., & Leys, S. P. (2016). Dynamic change, recruitment and resilience in reef-forming glass sponges. Journal of the Marine Biological Association of the United Kingdom, 96(02), 429–436. https://doi.org/10.1017/S0025315415000466

Kahn, A. S., Yahel, G., Chu, J. W. F., Tunnicliffe, V., & Leys, S. P. (2015). Benthic grazing and carbon sequestration by deep-water glass sponge reefs. Limnology and Oceanography, 60(1), 78–88. https://doi.org/10.1002/lno.10002

Kharroubi, A., Hajji, R., Billen, R., & Poux, F. (2019). Classification and integration of massive 3D points clouds in a virtual reality (VR) environment. International Archives of the Photogrammetry, Remote Sensing and Spatial Information Sciences - ISPRS Archives, 42(2/W17), 165–171. https://doi.org/10.5194/isprs-archives-XLII-2-W17-165-2019

Krautter, M., Conway, K. W., Barrie, J. V., & Neuweiler, M. (2001). Discovery of a “Living Dinosaur”: Globally unique modern hexactinellid sponge reefs off British Columbia, Canada. Facies, 44, 265–282. https://doi.org/10.1007/BF02668178

Lavy, A., Eyal, G., Neal, B., Keren, R., Loya, Y., & Ilan, M. (2015). A quick, easy and non-intrusive method for underwater volume and surface area evaluation of benthic organisms by 3D computer modelling. Methods in Ecology and Evolution, 6(5), 521–531. https://doi.org/10.1111/2041-210X.12331

Leon, J. X., Roelfsema, C. M., Saunders, M. I., & Phinn, S. R. (2015). Measuring coral reef terrain roughness using “Structure-from-Motion” close-range photogrammetry. Geomorphology, 242, 21–28. https://doi.org/10.1016/j.geomorph.2015.01.030

Levin, E., Shults, R., Habibi, R., An, Z., & Roland, W. (2020). Geospatial Virtual Reality for Cyberlearning in the Field of Topographic Surveying: Moving towards a Cost-Effective Mobile Solution. ISPRS International Journal of Geo-Information, 9(7). https://doi.org/10.3390/ijgi9070433

Leys, S. P., Mackie, G. O., & Reiswig, H. M. (2007). The Biology of Glass Sponges. Advances in Marine Biology, 52(06), 1–145. https://doi.org/10.1016/S0065-2881(06)52001-2

Lochhead, I., & Hedley, N. (in press). Dry-Lab Benchmarking of a Structure from Motion Workflow Designed to Monitor Marine Benthos in Three Dimensions. The Photogrammetric Record.

Lochhead, I., & Hedley, N. (in review). Evaluating the 3D Integrity of Underwater Structure from Motion Workflows. The Photogrammetric Record

Makransky, G., Terkildsen, T. S., & Mayer, R. E. (2019). Adding immersive virtual reality to a science lab simulation causes more presence but less learning. Learning and Instruction, 60(May 2017), 225–236. https://doi.org/10.1016/j.learninstruc.2017.12.007

Marliave, J. B., Conway, K. W., Gibbs, D. M., Lamb, A., & Gibbs, C. (2009). Biodiversity and rockfish recruitment in sponge gardens and bioherms of southern British Columbia, Canada. Marine Biology, 156(11), 2247–2254. https://doi.org/10.1007/s00227-009-1252-8

McCarthy, J. (2014). Multi-image photogrammetry as a practical tool for cultural heritage survey and community engagement. Journal of Archaeological Science, 43(1), 175–185. https://doi.org/10.1016/j.jas.2014.01.010

McCarthy, J., & Benjamin, J. (2014). Multi-image Photogrammetry for Underwater Archaeological Site Recording: An Accessible, Diver-Based Approach. Journal of Maritime Archaeology, 9(1), 95–114. https://doi.org/10.1007/s11457-014-9127-7

Napolitano, R., Chiariotti, P., & Tomasini, E. P. (2019). Preliminary assessment of Photogrammetric Approach for detailed dimensional and colorimetric reconstruction of Corals in underwater environment. 2018 IEEE International Workshop on Metrology for the Sea; Learning to Measure Sea Health Parameters, MetroSea 2018 - Proceedings, 39–45. https://doi.org/10.1109/MetroSea.2018.8657835

Papadopoulou, E. E., Kasapakis, V., Vasilakos, C., Papakonstantinou, A., Zouros, N., Chroni, A., & Soulakellis, N. (2020). Geovisualization of the excavation process in the Lesvos petrified forest, Greece using augmented reality. ISPRS International Journal of Geo-Information, 9(6). https://doi.org/10.3390/ijgi9060374

Piazza, P., Cummings, V., Lohrer, D., Marini, S., Marriott, P., Menna, F., Nocerino, E., Peirano, A., & Schiaparelli, S. (2018). Divers-operated underwater photogrammetry: Applications in the study of Antarctic benthos. International Archives of the Photogrammetry, Remote Sensing and Spatial Information Sciences - ISPRS Archives, 42(2), 885–892. https://doi.org/10.5194/isprs-archives-XLII-2-885-2018

Pizarro, O., Friedman, A., Bryson, M., Williams, S. B., & Madin, J. (2017). A simple, fast, and repeatable survey method for underwater visual 3D benthic mapping and monitoring. Ecology and Evolution, 7(6), 1770–1782. https://doi.org/10.1002/ece3.2701

Raoult, V., David, P. A., Dupont, S. F., Mathewson, C. P., O'Neill, S. J., Powell, N. N., & Williamson, J. E. (2016). GoPros as an underwater photogrammetry tool for citizen science. PeerJ, 4, e1960. https://doi.org/10.7717/peerj.1960

Remondino, F., Pizzo, S. Del, Kersten, T. P., Troisi, S., Metrology, O., Kessler, B., & Fbk, F. (2012). Low-Cost and Open-Source Solutions for Automated Image Orientation – A Critical Overview. In M. Ioannides, D. Fritsch, J. Leissner, R. Davies, F. Remondino, & R. Caffo (Eds.), Progress in Cultural Heritage Preservation 4th International Conference, EuroMed 2012 (pp. 40–54). Springer, Berlin, Heidelberg. https://doi.org/https://doi-org.proxy.lib.sfu.ca/10.1007/978-3-642-34234-9

Shelton, B., & Hedley, N. (2004). Exploring a cognitive basis for learning spatial relationships with augmented reality. Technology, Instruction, Cognition and Learning, 1(4), 323–357. https://doi.org/10.1021/om990262d

Skarlatos, D., Demestiha, S., & Kiparissi, S. (2012). An 'Open' Method for 3D Modelling and Mapping in Underwater Archaeological Sites. International Journal of Heritage in the Digital Era, 1(1), 1–24.

Smith, M. W., Carrivick, J. L., & Quincey, D. J. (2016). Structure from motion photogrammetry in physical geography. Progress in Physical Geography, 40(2), 247–275. https://doi.org/10.1177/0309133315615805

Sutherland, I. E. (1968). Head-Mounted Three Dimensional Display. Fall Joint Computer Conference, 33(pt 1), 757–764.

Thoeni, K., Giacomini, A., Murtagh, R., & Kniest, E. (2014). A comparison of multi-view 3D reconstruction of a rock wall using several cameras and a Laser scanner. International Archives of the Photogrammetry, Remote Sensing and Spatial Information Sciences - ISPRS Archives, 40(5), 573–580. https://doi.org/10.5194/isprsarchives-XL-5-573-2014

Turan, Z., Meral, E., & Sahin, I. F. (2018). The impact of mobile augmented reality in geography education: achievements, cognitive loads and views of university students. Journal of Geography in Higher Education, 42(3), 427–441. https://doi.org/10.1080/03098265.2018.1455174

Valimont, R. B., Vincenzi, D. A., Gangadharan, S. N., & Majoros, A. E. (2007). The Effectiveness of Augmented Reality as a Facilitator of Information Acquisition. Proceedings. The 21st Digital Avionics Systems Conference, 2(2), 7C5-1-7C5-9. https://doi.org/10.1109/DASC.2002.1052926

Van Damme, T. (2015). Computer Vision Photogrammetry for underwater archaeological site recording in a low-visibility environment. International Archives of the Photogrammetry, Remote Sensing and Spatial Information Sciences - ISPRS Archives, 40(5W5), 231–238. https://doi.org/10.5194/isprsarchives-XL-5-W5-231-2015

Wang, X., Van Elzakker, C. P. J. M., & Kraak, M. J. (2017). Conceptual design of a mobile application for geography fieldwork learning. ISPRS International Journal of Geo-Information, 6(11). https://doi.org/10.3390/ijgi6110355

Wedding, L. M., Friedlander, A. M., McGranaghan, M., Yost, R. S., & Monaco, M. E. (2008). Using bathymetric lidar to define nearshore benthic habitat complexity: Implications for management of reef fish assemblages in Hawaii. Remote Sensing of Environment, 112(11), 4159–4165. https://doi.org/10.1016/j.rse.2008.01.025

Westoby, M. J., Brasington, J., Glasser, N. F., Hambrey, M. J., & Reynolds, J. M. (2012). “Structure-from-Motion” photogrammetry: A low-cost, effective tool for geoscience applications. Geomorphology, 179, 300–314. https://doi.org/10.1016/j.geomorph.2012.08.021

Zhang, G., Gong, J., Li, Y., Sun, J., Xu, B., Zhang, D., Zhou, J., Guo, L., Shen, S., & Yin, B. (2020). An efficient flood dynamic visualization approach based on 3D printing and augmented reality. International Journal of Digital Earth, 13(11), 1302–1320. https://doi.org/10.1080/17538947.2019.1711210

Zhao, J., Wallgrün, J. O., LaFemina, P. C., Normandeau, J., & Klippel, A. (2019). Harnessing the power of immersive virtual reality - visualization and analysis of 3D earth science data sets. Geo-Spatial Information Science, 22(4), 237–250. https://doi.org/10.1080/10095020.2019.1621544

Chapter 5.

Designing Virtual Spaces for Immersive Visual Analytics

This paper is published in KN – Journal of Cartography and Geographic Information, Special Issue: Virtual and Augmented Reality in Spatial Visualization. Reproduced with permission from Springer Nature.

Citation Details: Lochhead, I., Hedley, N. (2021). Designing Virtual Spaces for Immersive Visual Analytics. KN – Journal of Cartography and Geographic Information. https://doi.org/10.1007/s42489-021-00087-y

Abstract

Modern virtual reality (VR) technology has garnered significant attention in the geographic visualization community for its ability to immerse users within geospatial data sets. While immersion within one-to-one models of reality offers unique and powerful perspectives from which to view spatial data, VR also allows users to transcend the physical limitations of the real-world, thereby allowing them to visualize, experience, and interact with spatial data at any scale, in any virtual environment, at any time. This paper presents a collection of 3D data-driven geovisualization case studies, implemented in an immersive virtual GIScience data visualization space (IVEVA). IVEVA was purposefully designed and developed to highlight the differences in spatial data type, the challenges associated with spatial data visualization in an immersive virtual environment, and the importance of adhering to the established design heuristics of cartography, human-computer interaction, and extended reality (XR) development. Through this process, we offer our observations on how well each data type fits this medium of visualization and interpretation, and how the design heuristics play out for an immersive virtual environment that extends the practicable space in which GIScience and visual analytics are performed. Finally, we offer our perspectives, from designing and developing this prototype, on the future for immersive interface based GIScience.

Keywords: 3D Geovisualization, Visual Analytics, Virtual Reality, Design Heuristics, GIScience

5.1. Introduction

The potential of extended reality (XR) technology is becoming increasingly visible across a range of geographic information science (GIScience) domains. These technologies allow users to experience, interact with, and immerse themselves within geospatial data in a multitude of new ways, providing the opportunity for alternative perspectives from which to perform scientific inquiry. The value proposition for XR and the future of GIScience resonates deeply with the founding vision for GIScience; where the "S" signifies science and the field itself is legitimized and motivated by scientific questions, is a toolbox that supports scientific practice, and is a domain with an established scientific research agenda that addresses the relationship between GIScience and technology (Goodchild, 1992). In its infancy, it was noted that geographic information systems (GISs) were at times driven by technology that was searching for an application. Today, where the cutting edge in GIScience is no longer defined by primitive 386-based personal computers with limited processing power but by locationally and positionally aware handheld and wearable mobile computers and cloud computing, the relationship between the future of GIScience and XR technology is unclear. Will XR drive the future of GIScience? Could XR fundamentally change GIScience practice and our relationship and understanding of geographic space? As was the case in 1992, technology again appears to be driving current advances. Critical relationships between technology and spatial data collection, analysis, and display must be discussed and demonstrated to illuminate both the potential and implications of XR GIScience.

The proliferation of complex three-dimensional (3D) data sets within modern GIScience requires interfaces that preserve the native dimensionality of spatial data, allowing GIScientists and other stakeholders to visualize, experience, query, and interact with morphological and topological representations that are inherently 3D in analytical visualization environments that can support 3D analyses in space and through time (4D). While conventional GISs do include 3D functionality, the 2D displays and graphical UI metaphors used to overcome the limits of 2D displays add cognitive overhead and prohibit natural physical interactions. As we navigate the transition into increasingly 3D data and displays (and commensurate transducers), it is vital that we address the persistent challenges that plague geovisualization: from the interdisciplinary challenges

facing geovisualization and its relationship with other domains, to the human factors challenges driving cognitive processing and knowledge transfer, and the contextual challenges that must be overcome to develop geovisualizations that match users and use (Çöltekin et al., 2017).

The primary objective of this paper is to unpack some of these issues, presenting and discussing the development of an immersive virtual reality (VR) based virtual environment (VE) prototype designed as a multifunctional environment for geospatial visual analytics (VA) and interpretation of (3D) spatial data sets. This work is informed by design heuristics from cartography, human-computer interaction (HCI), and XR. This multidisciplinary design and development approach accounts for the unique design challenges associated with the VE, the user interface (UI), the user experience (UX), and the representation of geospatial data in VR. While the relationship between XR and GIScience is not new, the democratization of the enabling technologies has presented new opportunities for widespread adoption beyond specialized research labs and could represent a new normal for VA and spatial data science. However, without a practicable set of guidelines from which to base visualization design, inconsistencies between applications and the use/user relationship may hinder the extraction of knowledge from such applications. Here we use five case studies – glass sponge morphometry, human movement, urban development, resource management, and flood risk governance - to highlight how different geospatial phenomena, different data types, scales, and resolutions, and different objectives and analyses demand different design considerations. From these, we discuss a set of design guidelines to support the development of immersive VR-based analytical VEs.

In the following section we provide a brief introduction to geovisualization, XR, and design heuristics from cartography, HCI, and XR development. In section three we outline the development of *IVEVA*, a prototype for an immersive VR-based VE for geospatial VA, focusing on the design of the virtual space, the UI and UX, and the presentation of geospatial data within immersive VEs. In section four we discuss the affordances and limitations of IVEVA, discuss its use in an applied context, and discuss the design heuristics for VR-based VA design. We conclude with some thoughts on the future role of XR in GIScience and the power of XR technology to advance GIScience.

5.2. Background

5.2.1. Geovisualization and Visual Analytics

Geographic visualization, or geovisualization, integrates the approaches from multiple disciplines, cartographic and otherwise, “to provide theory, methods, and tools for visual exploration, analysis, synthesis, and presentation of geospatial data” (MacEachren & Kraak, 2001). Geovisualization, much like scientific visualization, relies on technology to facilitate the development of visualizations that support cognitive processes and knowledge formation (MacEachren & Kraak, 1997). For some time, a community of spatial information visualization researchers have been increasingly exploring the capabilities and potential of immersive and interactive technologies for geographic characterization, interpretation, and communication. This has produced evolving perspectives on these technologies as more than new ways to see, but perhaps new ways to experience; and because of this, new relationships with geographic space mediated by data and interfaces have emerged. A good example of these expert groups, evolving perspectives, and theorizations of emerging interface technologies are the commissions established by the International Cartographic Association (ICA).

Launched in 1995, the Commission on Visualization strived to understand the expanding role of maps (particularly dynamic maps) as decision support tools, and to facilitate the exchange of visualization concepts between disciplines (MacEachren & Kraak, 1997). In 1999, the commission extended its focus to include VEs, as maps were no longer restricted to static, 2D mediums and new challenges emerged for spatial data representation, visualization-computation integration, interfaces, and cognition and usability (MacEachren & Kraak, 2001). By 2007 the ICA pivoted to establish the Commission on Geovisualization, focusing on the use of interactive maps supporting visual analyses of complex, voluminous, and heterogenous data across space and time (Dykes et al., 2010). Finally, in 2015 the ICA formed the Commission on Visual Analytics to address the challenges presented by massive spatio-temporal data sets and to encourage the advancement of visual analytics – “the science of analytical reasoning supported by interactive visual interfaces” (Thomas & Cook, 2005) - in cartography (International Cartographic Association, 2015). Over time, the ICA has shifted its focus to adapt to changes introduced by technology, data, and the use and users of geospatial data products. The democratization of XR technologies and the emergence of

unconventional workflows, such as those using game engines, has enabled new opportunities for explorative visual analyses and has created a new set of challenges for VA.

5.2.2. XR Technology

XR has recently gained traction as a moniker encapsulating all VR, augmented reality (AR), and mixed reality (MR) technologies and experiences. We have, rather reluctantly, adopted 'extended' as the definition for "X" in this manuscript, while others suggest that "X" (or perhaps "x") is simply an undefined variable that could stand for virtual, augmented, or mixed, or that "X" signifies 'cross' reality. Regardless of what "X" represents, XR summarizes a range of emerging technologies under one umbrella. While this may be convenient, there are unequivocal differences between the constituent technologies, how they are used, what they allow users to see, and how they allow them to see it. We reluctantly accepted extended rather than undefined variable or cross as the definition for "X," not because of preference, but because we question the need to amalgamate VR, AR, and MR at the risk of suggesting they are one and the same. There is little doubt that XR technologies are inextricably linked, and there is no harm in referring to them en masse, so long as we recognize, understand, and account for the differences in "X" when designing VA applications.

Conceptualization and differentiation of a range of interface technologies that connect real and virtual worlds have existed for several decades. One that continues to inform developers of VR, AR, and MR (despite the noise created by XR popularity) is the virtuality continuum (Milgram & Kishino, 1994) introduced as a taxonomy for the growing collection of display devices that are now commonly referred to as XR. The continuum extends from entirely real (reality) to entirely virtual (VR), with everything in between the two identified as MR. MR displays combine both virtual and real content, the proportions of which characterized MR displays as being either AR (reality augmented with virtual content) or augmented virtuality (AV) (virtuality augmented with real content). While the continuum considers AR a form of MR, modern discourse views both AR and MR as displays that augment reality with virtual content; where AR simply places virtual content in reality and MR combines virtual content with reality, thereby enabling meaningful interactions between the real and virtual content (Çöltekin, Lochhead, et al., 2020; Hedley, 2017). The capacity for XR technologies to connect users, data, and space is

transforming how we visualize, interact with, and comprehend geospatial data, both within GIScience and beyond.

5.2.3. XR in Visual Analytics

The objective of VA is to combine the powers of human and computer data processing, utilizing visualizations and interactive visual interfaces to establish new approaches tackling the complex spatial problems facing modern society (Gennady Andrienko et al., 2011; Thomas & Cook, 2005). In the simplest sense, XR technologies play into the strengths of visualization, providing additional methods of data visualization and new opportunities for users to detect patterns and anomalies within the data (Çöltekin, Griffin, et al., 2020). At a higher level, XR technologies provide unmatched levels of immersion, presence, and interaction, the benefits of which to human perceptual and cognitive abilities may yet fully be realized.

User studies represent a significant and important piece of the XR research conducted by the geospatial community. The various ICA commissions have regularly identified the major research challenges and set research agendas based on the state of the discipline (see MacEachern and Kraak 1997; G. Andrienko et al. 2007; Virrantaus, Fairbairn, and Kraak 2009). Most recently, Çöltekin et al. (2017) applied a top-down and bottom-up approach to identify the challenges plaguing the discipline and identified interdisciplinarity, human factors, and use/user design challenges have persisted through time. While these are challenges faced by the discipline in general, they are highly relevant to XR technology and the applied research that has been conducted using XR interfaces. This includes research on the use of tangible AR interfaces for face-to-face collaboration (Billinghurst et al., 2002), the impact that AR, proprioception, and sensorimotor function have on spatial knowledge transfer (Shelton & Hedley, 2004), the relationship between spatial presence and mental model formation (Coxon et al., 2016), the perceived spatial relationship between users and spatial AR environments (Schmidt et al., 2016), and the effect that mobile AR has on students' geographic learning (Turan et al., 2018) to name just a few.

While XR technologies come with their own hardware and software related research challenges and priorities (Çöltekin, Lochhead, et al., 2020) - which must be addressed by the greater XR community, and which will arise with each technological

advancement - the geospatial community has continually explored the use of XR technology to address specific geospatial problems. Recent applications include the use of VR to visualize and assess geohazards (Havenith et al., 2019), to evaluate the importance of landmarks in mental map formation (Bruns & Chamberlain, 2019), to assess the effectiveness of VR in topographic survey training (Levin et al., 2020), and as a tool for geographic education (Jong et al., 2020; Lisichenko, 2015; Minocha et al., 2018). Concurrently, AR has also been used in an educational context (Adedokun-Shittu et al., 2020; Al Shuaili et al., 2020; George et al., 2020; Turan et al., 2018; Wang et al., 2017), however, the ability of AR/MR interfaces to connect data and real-world spaces has resulted in several situated, mobile applications. These include landscape orientation (Carbonell Carrera & Bermejo Asensio, 2016), flood risk analyses (Rydvanskiy & Hedley, 2020, 2021) and precipitation simulation (Lonergan & Hedley, 2014), building damage and safety assessment (Imottesjo & Kain, 2018; Liu et al., 2020) and emergency egress analyses (Lochhead & Hedley, 2018), teaching cultural heritage (Han et al., 2019; Panou et al., 2018; Romano & Hedley, 2021), and GIS enabled smart city applications (Yagol et al., 2018). Despite the proliferation of geospatial XR research, there is a lack of theoretical work focused on how and why geospatial XR content is designed a certain way.

5.2.4. Design Heuristics

The multifaceted nature of geovisualization has generated numerous approaches, methods, capabilities, and insights to geovisualization design, as geovisualization itself draws from the scientific visualization, cartography, image analysis, information visualization, exploratory data analysis, and GIS communities (MacEachren & Kraak, 2001). While the goal of any geovisualization is to empower the user(s) with the ability to generate new knowledge through exploration, analysis, synthesis, and communication, the formation of knowledge is mediated by the combined characteristics of the user(s), the interface(s), the data, and the use of the geovisualization as it was designed (Figure 5.1). Therefore, the design process is critically important and must account for these variable differences, identifying the objectives (e.g., perceptual, cognitive, and interactive) of the geovisualization and adopting established design heuristics – guidelines for the evaluation and design of systems – from cartography and geovisualization, HCI, and XR development that

support the defined objectives and maximize the opportunity for knowledge formation through geovisualization use.

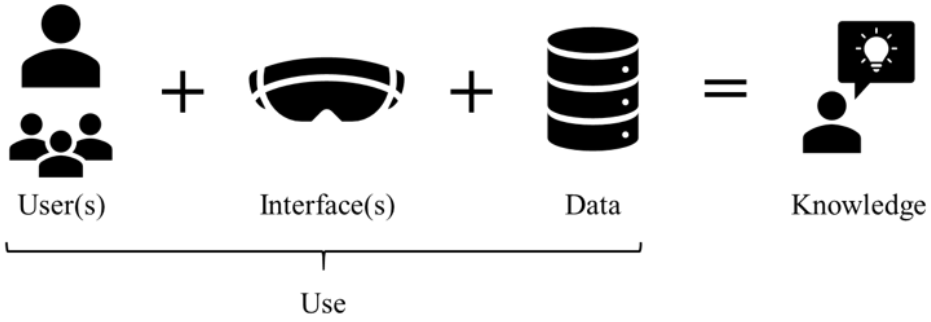

Figure 5.1 The objective of any geovisualization is to generate new knowledge through geovisualization use. However, new knowledge is not simply a product of use, but hinges on the combined characteristics of the user(s), the interface(s), and the data. The challenge is to design geovisualizations which optimally combine the affordances and limitations of the user(s), interface(s), and data in a manner that leads to new knowledge.

Geovisual analysis has always involved technology, the evolution of which has resulted in shifting capabilities and communities of practice. Geovisualization itself emerged as cartography transitioned into the digital era and static maps - designed to communicate specific bits of information - were replaced by dynamic, interactive maps - designed to support exploration, analysis, and decision making (MacEachren & Kraak, 1997). Despite this significant shift in the presentation and consumption of geospatial data, basic cartographic principles remain an integral part of geovisualization design. This includes the use of basic map elements (e.g., legend, source information, scale, direction, and coordinate system) to help the user understand the nature of the data presented to them, and Bertin's graphic variables (shape, size, value, texture, color, orientation, and position) (Bertin, 2011) which inform decisions on graphical representation of geospatial data and which have been adopted as basic tenets of graphical representation across disciplines (e.g., information visualization) (Çöltekin, Griffin, et al., 2020). The digital era also ushered in the need for additional dynamic variables (e.g., duration, order, rate of change, and motion), essential to the visualization of spatio-temporal data (Dibiase et al. 1992; Hedley et al., 1999; Carpendale 2003), as well as those specific to 3D displays and VEs (e.g., perspective height, camera position and orientation) (Rautenbach et al., 2015; Slocum, 2009). While geovisualizations are

more than maps, incorporating emerging technologies and data visualization approaches to address geospatial challenges, the cartographic principles on which maps are designed are essential to effective geovisualization using modern technology.

An effective geovisualization is one that harnesses the power of human perceptual systems while allowing for seamless interaction between people (users) and computers as users pursue new knowledge through geovisualization use. HCI research strives to improve these interactions so that they are user-friendly and adapt to the needs of the user (Kerren et al., 2007). As the user plays a pivotal role in this relationship, a user-centered design (UCD) approach should be adopted to place an early emphasis on the needs of the user, to iteratively address changes to their needs throughout the design process, and to develop useful interfaces (Nielsen, 1993; Roth et al., 2015). Defining the target user is therefore critical to the design and development of a functional prototype from which usability can be evaluated prior to full-scale implementation. Prototypes should be designed following established design heuristics, such as the nine basic usability principles presented by Nielsen and Molich (1990). These usability heuristics, which can be utilized by designers and evaluators when a user study is not feasible (Endsley et al., 2017), state that UIs should use simple and natural dialogue, speak the user's language, minimize the user's memory load, be consistent, provide feedback, provide clearly marked exits, provide shortcuts, provide good error messages, and prevent errors. While these design heuristics are the most well-known, they are often considered to be too general; therefore, it is common to find adaptations that meet the demands of specific applications and domains (Vi et al., 2019).

XR technology has recently entered an era of democratization, whereby increased corporate funding, research, and technological advancement have driven down costs and increased access and availability. This has stimulated an increase in academic, professional, and personal applications, thereby exposing a growing number of novice users to XR interfaces. While Nielsen and Molich's (1990) usability principles do, to some degree, provide a foundation for XR design and development, these heuristics were established while personal computers underwent their own period of democratization, and do not account for the unique design considerations of XR technology. Several heuristics list have been devised to focus on specific applications of AR, VR, and HMD based technologies (e.g., Dünser et al. 2007; Endsley et al. 2017; Vi,

Silva, and Maurer 2019; Tuli and Mantri 2020), addressing considerations such as physical ability, physical effort, user environment, alignment of real and virtual worlds, building upon real world knowledge, and hardware capabilities. While these lists address the basic tenets of Molich and Nielsen (1990) – a system should be easy to learn and remember, effective, and pleasant to use – and focus on the user, they also must account for the fact that the system is no longer restricted to the confines of the 2D display but can encircle the user in both physical and virtual space. As each piece of XR technology and software come with their own idiosyncrasies, a combination of the basic HCI design principles with those specific to the technology, application and domain becomes essential to effective XR-based geovisualization design and development. In the following section we discuss our workflow in the design and development of IVEVA, incorporating design heuristics from multiple sources to create a VR-based interface for VA.

5.3. Design and Development

The IVEVA prototype was designed and developed as an immersive VE that extends the space of everyday GIScience practice to include virtual space, creating a VA experience with alternative perspectives, methods of interaction, and tools for scientific inquiry. IVEVA was developed for the Oculus Quest (www.oculus.com) using Unity (version 2019.2.13f1), a game engine which has gained popularity across academia and industry as a 3D visualization tool. The Oculus Quest is a standalone VR system, comprised of a HMD and two controllers, offering positional tracking with six degrees-of-freedom through internal sensors and cameras. In the following subsections we unpack the design and development of IVEVA.

5.3.1. Designing the UX

As a prototype for an immersive VA tool, IVEVA showcases the power of standalone VR to extend the space of GIScience practice, offering what could be for many users a novel approach to geospatial data visualization and analysis. UX (user experience) design is therefore critical, and emphasis should be placed on creating a positive HCI experience that satisfies more than just the instrumental needs of the user, acknowledging the human-computer relationship as a subjective, situated, complex, and

dynamic encounter that is a product of the user's internal state, the system, and the context in which it is used (Hassenzahl & Tractinsky, 2006). During the development of IVEVA, the UX design process focused not only on the absence of errors, but on creating a pleasurable experience for a specific group of users to explore specific geospatial data in a VE intentionally designed to extend their analytical space and capabilities. The UX design process, while it could not incorporate real-world users, was methodically and iteratively conducted according to the author's own experiences and perspectives, drawing on insight provided by users and user groups from past and present visualization research. While usability and user needs were central to the UX process, it was equally important to create an experience that would be enjoyable and efficient, thereby allowing the user(s) to focus on creating new knowledge.

Traditional UX design principles concentrate on technology and applications utilizing 2D displays and do not properly address the idiosyncrasies of 3D spatial environments and interactions (Vi et al., 2019). These very issues resonate deeply with the challenges faced by mainstream GIS, to reconcile methods and cultures of practice of planar cartography and spatial analysis, with well-established 3D data acquisition, and now, emerging 3D interface platforms. While some design heuristics may be universal in principle - such as using cues to attract the user's attention - in practice, when 2D displays are replaced by 3D VEs, they are not.

In the design and development of IVEVA, UX design principles from multiple sources (including Dünser, Grasset, and Billinghurst 2008; Endsley et al. 2017; Vi, Silva, and Maurer 2019; Tuli and Mantri 2020) were incorporated in the design of a usable and enjoyable UX. This includes the ability to customize the space to match user's needs and preferences (i.e., reposition objects, activate and deactivate objects, change surface textures, and adjust light levels), to attract the user's attention through visual and spatialized audio cues, to make menus available when and where they are needed, to interact with objects at a distance, and to explore the data through trial and error without fear of making irreversible mistakes. Ensuring user comfort and enjoyment also entailed efforts to reduce or prevent motion sickness by avoiding disparity between what users feel and what they expect to feel (Vi, Silva, and Maurer 2019). This included reducing point and polygon counts and baking scene lighting to avoid latency issues, and not introducing user movement not initiated by the user.

5.3.2. Designing a Virtual Space for Multifunctional Visual Analytics

The virtual space within IVEVA is comprised of two adjoining rooms – a larger primary room and a smaller secondary room – in which different yet related spatial data sets can be presented to the user (Figure 5.2). The primary room contains a rectangular data table, on which smaller scale 3D spatial data are presented, and the secondary room is an empty space with a recessed floor, within which larger scale 3D spatial data related to those in the primary space can be rendered. The virtual space was designed and developed within Unity using ProBuilder, a 3D modelling and design package that was imported into the Unity project.

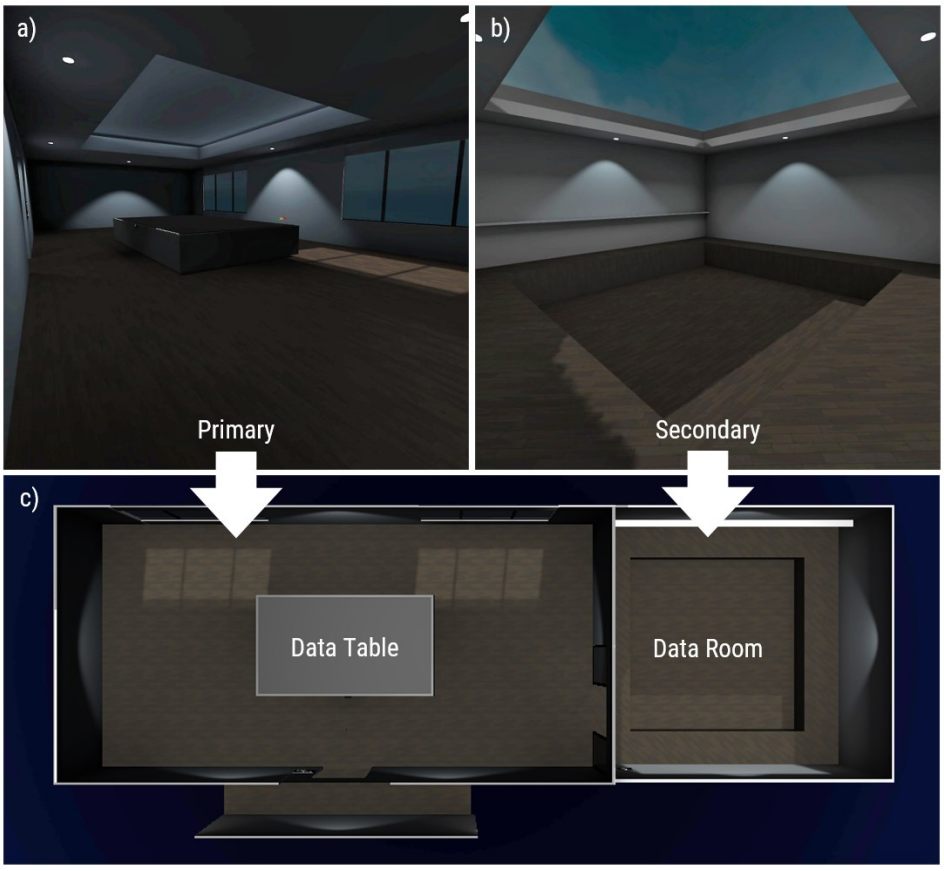

Figure 5.5.2 Virtual Environment Layout. The VE was designed as two distinct spaces of analysis: a) a primary space - built around a central data table - for smaller scale data sets, and b) a secondary space, or data room, designed for larger scale data sets, simulations, and hands on analyses. c) Users can easily move between the primary and secondary spaces.

The virtual space is a simple, empty canvas in which 3D data, tools, and supporting information are presented to the user. The space was designed to be customizable, allowing the user to adjust the color of the walls and floor, change the light level, close the blinds, alter the height of the data table, and reposition supporting documentation (Figure 5.3). These features were designed to promote user comfort through customization, to minimize distraction and not overwhelm the user with unnecessary visual clutter, to be familiar and harness real-world knowledge (e.g., the light panel is in a familiar position near the door), and to be efficient by allowing the user to access supporting documentation when and where it is needed (Endsley et al., 2017; Vi et al., 2019). While the customizability of the virtual space is currently limited to the developed feature set, it was designed to highlight how the user can 'tune' the virtual space to match their everyday workspace, establishing congruence between the virtual and real space of GIScience practice, and could be tailored to the specifications of the user as required. The virtual space also features an isolation dome (Figure 5.4) that can be activated to encapsulate the data, thereby removing all peripheral visuals to allow the user to focus on the data.

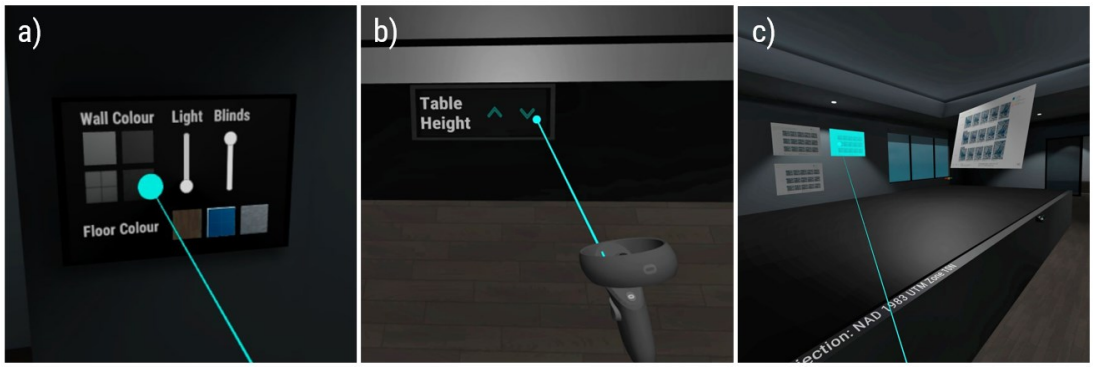

Figure 5.3 IVEVA was designed to allow users to customize the VE. The wall/floor color and light levels (a), data table height (b), and position of supporting information (c) can all be adjusted to suit the user.

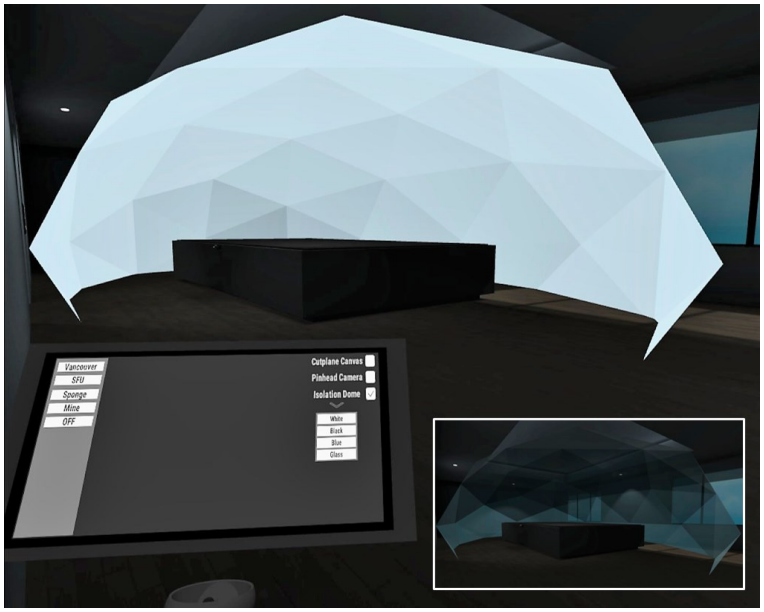

Figure 5.4 **The isolation dome is designed to eliminate peripheral virtual content from the user's view - allowing them to focus their attention on the data. The color of the dome can be changed (inset), thereby allowing the user to control the contrast between the 3D data and the dome.**

5.3.3. Designing the UI

Upon entering the virtual space, users are presented with a tooltips menu that outlines the functionality of each of the controller's buttons (Figure 5.5). This menu is attached to the controllers and can be activated/deactivated, allowing the user to quickly recall or hide the menu as required. This relieves the user of the cognitive overhead necessary to remember the action performed by each button but provides the support necessary for them to learn how to perform those actions. In addition to the tooltips menu, users can activate/deactivate a data menu and a tools menu, both of which are attached to the left-hand (LH) controller.

The data menu is the primary UI in IVEVA (Figure 5.6). This menu appears slightly above the LH controller and allows the user to select which case study is active and which data are displayed. The UI automatically updates as the user selects each case study, thereby ensuring that the UI always matches the active case study and that it is not cluttered with additional irrelevant options. Furthermore, the UI also automatically updates as the user moves between the primary and secondary data space, providing only that functionality which is relevant to their current position in the

VE. The data products of the tools in the 'tools menu' are also presented to the user on the data menu. The tools menu is the secondary UI in IVEVA (Figure 5.7). It is a three-sided UI that is attached to and surrounds the LH controller, allowing the user to select from and operate a suite of tools relevant to each case study. As with the data menu, the tools menu automatically updates as the user activates each case studies.

Figure 5.5 **A tooltips menu is presented to the user upon entering the VE. This menu can be activated/deactivated as required, providing a quick reference without constant visual distraction.**

Figure 5.6 **The data menu is the primary UI through which the user activates a scene and toggles spatial data sets on and off. Realtime data related to the spatial tools are also presented here.**

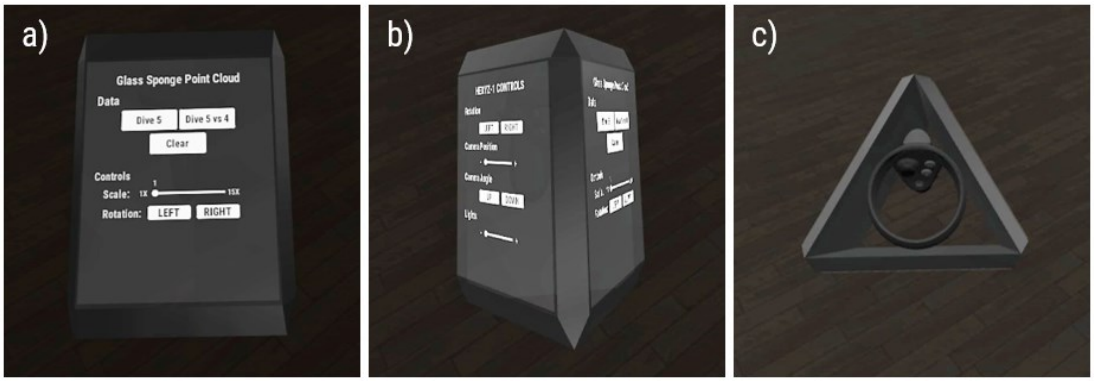

Figure 5.7 The tools menu is a three-sided UI allowing the user to customize and control the tools within each scene. The menu is fixed to the left-hand controller and can be toggled on and off as required. a) front view b) perspective view c) top view.

A collection of spatial tools, beyond the tools within each case study (Figure 5.8), are also available. These tools provide height and scale references, additional visual perspectives, and allow the user to perform simple queries. For example: a cut plane tool can be activated on the data table to create a cross-sectional view of the active data set – this cross-section is displayed on the wall adjacent to the cut plane; a pinhead camera can be placed anywhere within the VE, providing an additional perspective from the camera's position – that perspective view is then displayed on external displays which can be positioned anywhere within the VE, and; a measurement tool can be activated to make distance measurements within each data set.

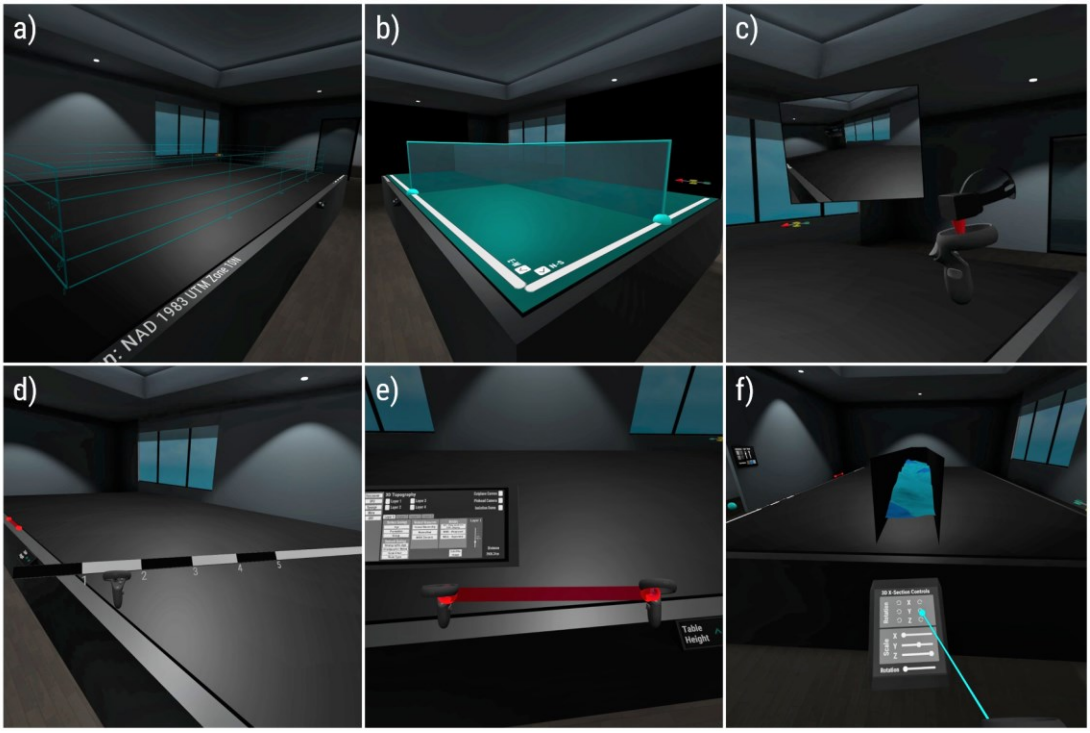

Figure 5.8 A suite of spatial tools are available for spatial reference and inquiry. This includes a) height reference grids, b) cut-planes, c) pinhead cameras, d) scalebars, e) precise measurements, and f) cross-sections.

Interaction with the UI and other 3D content within the VE is provided through the Virtual Reality Toolkit (VRTK) (www.vrtk.io) and the Oculus Integration package for Unity. Users move throughout the scene by either physically walking or by teleporting using the solutions provided by these packages. Additional functionality, such as the ability to grab objects from a distance or spawn and place 3D objects within the scene, was programmed into IVEVA and draws upon the VRTK solutions. Our objective was to create a suite of tools and functionality that gives the user a sense of control that exceeds natural human ability yet feels natural and integral to immersive VA.

5.3.4. 3D Data-driven Case Studies

In this section, we describe the five case studies used within IVEVA. Rather than simply reporting on a single, idiosyncratic applied example, as is common in the literature, our aim was to demonstrate a variety of spatial phenomena represented by a range of data types as exemplars of typical and emerging GIScience – which constantly integrates data of many forms. The following five case studies utilize a combination of

traditional GIS workflows, 3D modelling, and game engine development to produce a collection of 3D assets and 3D visualizations. Digital elevation models (DEMs) were either downloaded from open access databases or were generated from LiDAR point clouds using ArcMap (10.7.1) - the resultant DEMs were converted to 3D assets using Maya 2019. The 3D point clouds in IVEVA were either produced from a collection of photographs using PhotoScan Professional (1.4.0) or were downloaded from open access databases. In either case, point cloud density was reduced within CloudCompare (2.10.1) and ASCII files were converted to OFF files with MeshLab (2016.12), which were then used to create 3D assets within Unity using Point Cloud Viewer – a free Unity asset from the Unity Asset Store. Other 3D assets were generated using a combination of Maya 2019, Blender (2.81a), and SketchUp. Further information about each case study is provided in the following subsections.

Case Study 1: Glass Sponges Morphometry

This case study presents an immersive visualization of 3D glass sponge morphology as an alternative to current practices using 2D photographs (mosaics) and videos, to be utilized by marine ecologists as a VA and communication tool. In this visualization the location of glass sponge bioherms within Howe Sound, BC are presented on the data table against the 3D topography and bathymetry for the region (Figure 5.9) - obtained from the open data repositories of British Columbia, Canada, and the National Oceanic and Atmospheric Administration (NOAA) - and a 3D point cloud representing a glass sponge from that region is presented in the data room (Figure 5.10).

Users can interact with the 3D map on the data table, selecting which data is presented to them and accessing more information about each glass sponge bioherm by highlighting it on the map. Additionally, the location of an underwater SfM survey is provided on the map; that survey corresponds to the 3D point cloud in the data room. By activating the SFM data, users are then able to interact with, manipulate, visually inspect, and query the 3D point cloud. A suite of tools was developed to allow the user to make measurements, visualize cross-sections, observe source data, and even simulate data collection through a working model of the data capture rig. Our objective with this visualization was to create a VE in which marine ecologists can perform

analyses of glass sponge data which has been collected over time, exploring, interacting with, and querying 3D data in 3D space.

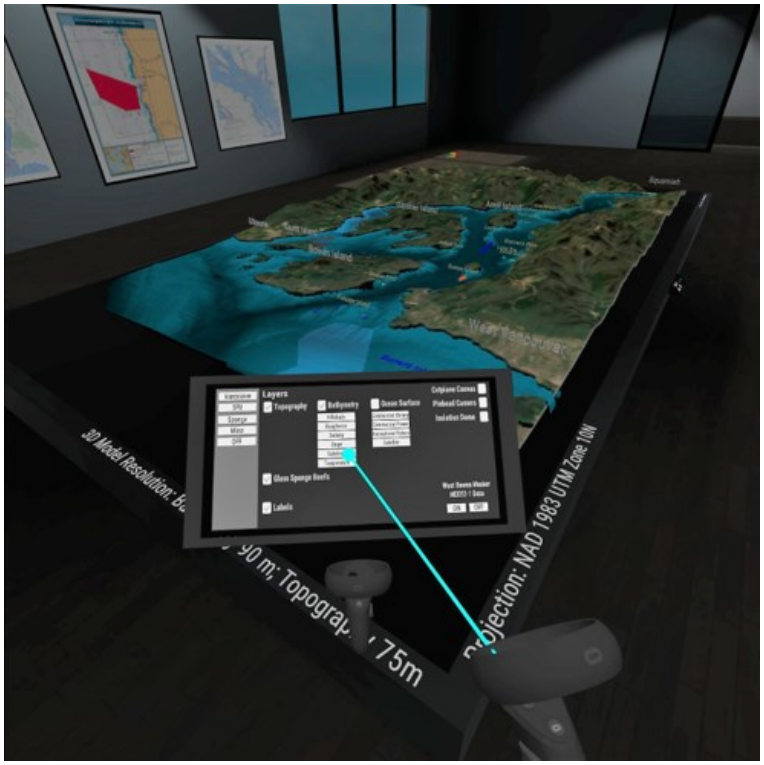

Figure 5.9 An overview of the glass sponge bioherms within Howe Sound, BC is presented to the user on the data table in the primary data space.

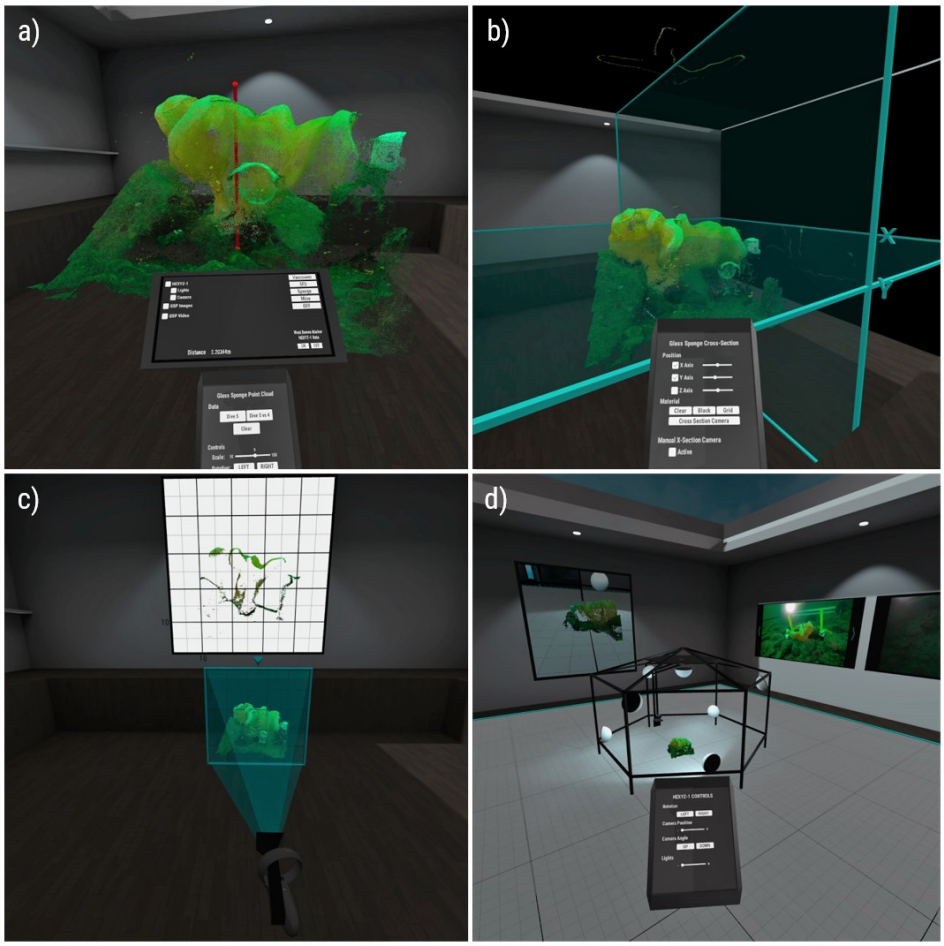

Figure 5.10 A 3D glass sponge point cloud is presented to the user in the secondary data room. Users are able to scale and rotate the model, measure it (a), create cross sections (b and c), and simulate the data collection process (d).

Case Study 2: Human Movement in Built Environments

This case study presents VR as an authoring and visualization tool for human dynamics simulations – in this case, emergency egress and socially distanced movement in a built space. It was designed as a tool allowing emergency management and safety officers to simulate and explore human movement in built environments. This visualization contains a 3D point cloud representing Burnaby Mountain and Simon Fraser University (SFU) (Figure 5.11) and a 3D model of the Academic Quadrangle in which human movement simulations can be created and observed (Figure 5.12).

The primary data space was designed to provide an overview of the campus and the restrictions that are placed on human movement by both the design of the campus

and its location atop Burnaby Mountain. Users can create and observe simulations of human movement within SFU's Academic Quadrangle (AQ). The AQ can be populated with agents (people) of varying speeds that use Unity's NavMesh to navigate from the location at which they are placed to the target location defined by the user. The user can activate trail renderers to observe agent pathways, social distancing buffers to observe the impact that social distancing has on human movement in the AQ, gates to quantify the speed at which those agents move throughout the AQ, and obstacles to explore the impact that potential impedances would have on human movement. Our objective with this visualization was to create an immersive VA tool that can be used to both create and visualize human movement simulations in built environments.

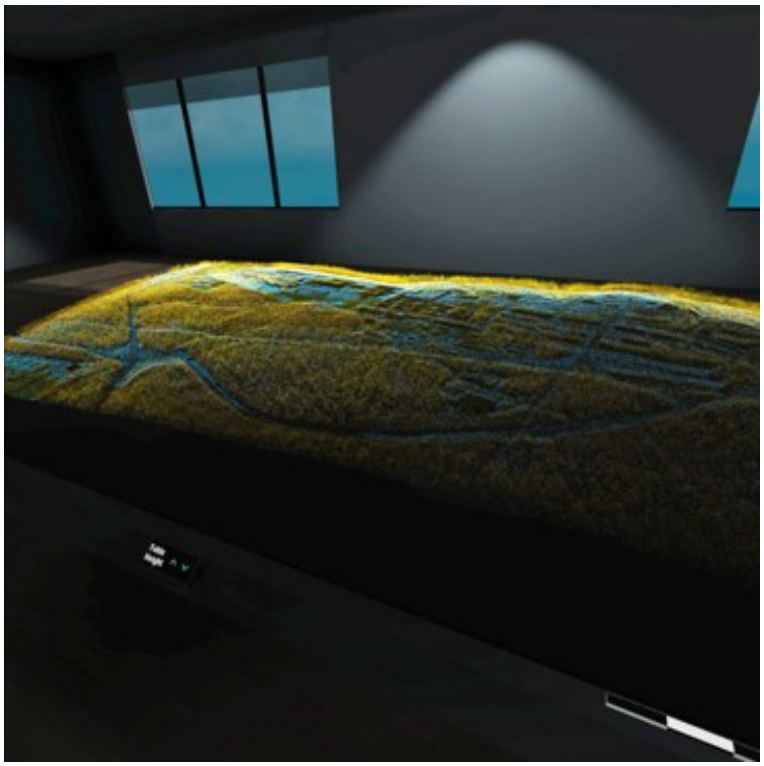

Figure 5.11 A 3D point cloud for Burnaby Mountain and the SFU campus in the primary data space.

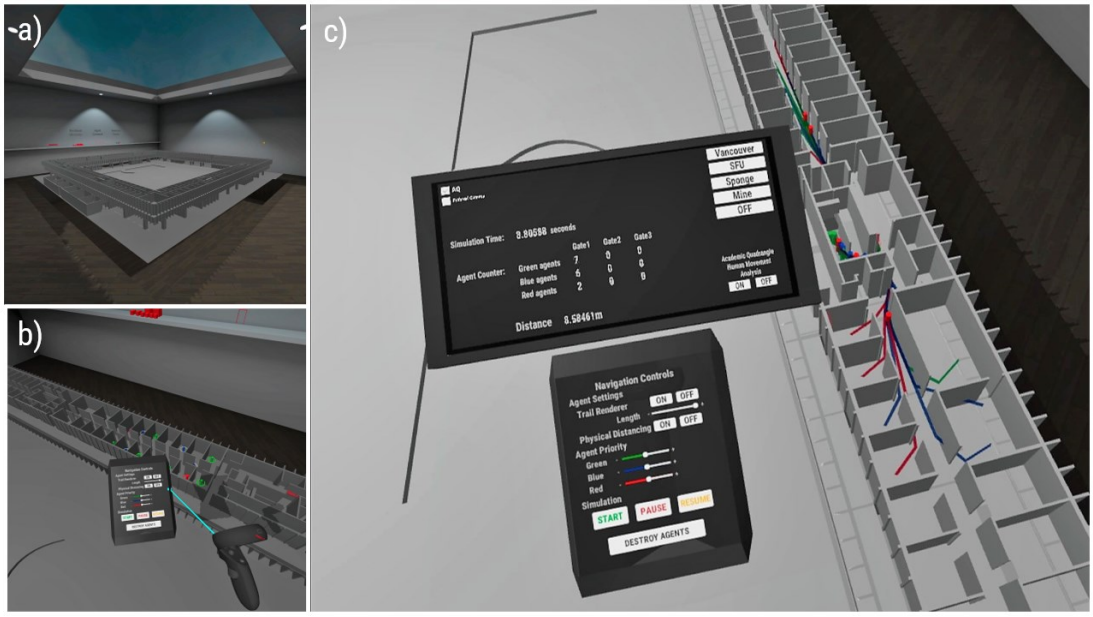

Figure 5.12 a) A 3D model of the Academic Quadrangle is presented in the data room. b) Users can create simulations of human movement during an evacuation or the impact that social distancing has on the flow of people, and c) analyze those simulations in real-time.

Case Study 3: Urban Development

This urban environment case study was designed and developed to allow city officials and community stakeholders to both explore and visualize urban development in Vancouver, BC, and the shadows that that development would cast on the surrounding community. This visualization employs 3D point clouds, to characterize existing buildings and vegetation, and a 3D model of the topography textured with an aerial image (Figure 5.13) – all acquired from the City of Vancouver Open Data Portal.

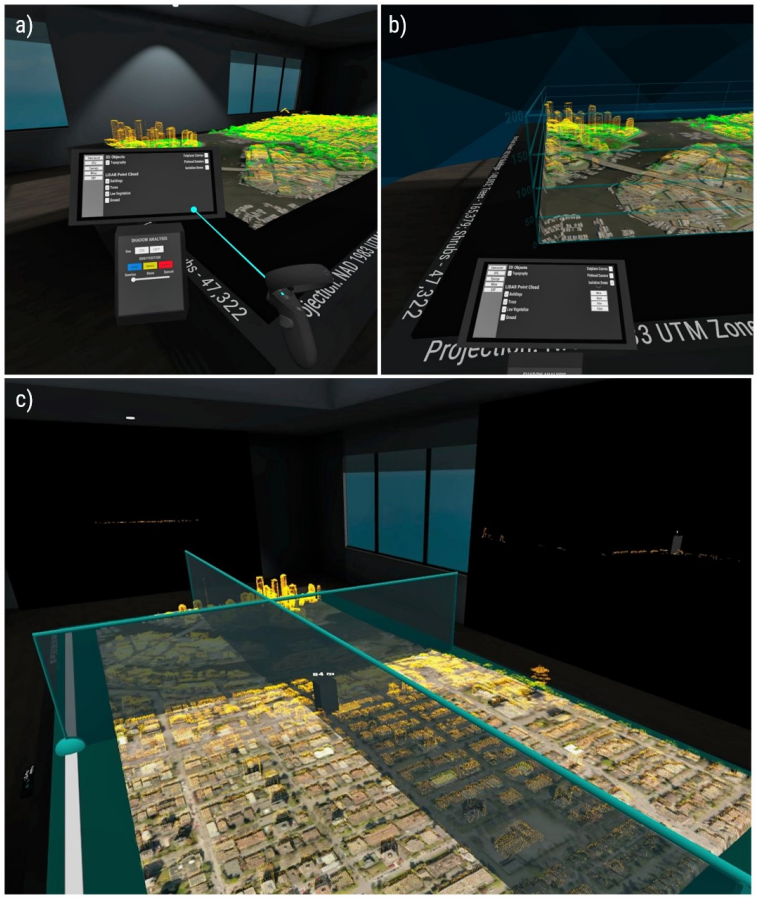

Figure 5.13 This visualization allows stakeholders to visualize urban development and the shadows that would be cast on the surrounding community. a) Users can select which data are visible, b) they can activate reference grids to visualize relative building height, and c) can perform cut-plane analyses to visualize future skylines.

This visualization was designed to utilize the primary data space only, rendering the 3D assets on the data table. Users can select which 3D point clouds are visible, whether the DEM is visible, and can add 3D cubes (buildings) of different heights to perform shadow analyses. The shadow analysis allows the users to activate a virtual sun, set the sun height according to season, and cycle the sun from sunrise to sunset (Figure 5.14). Shadows are updated in real-time so that users can see how each of these changes impacts the size and position of the resultant shadow on the community.

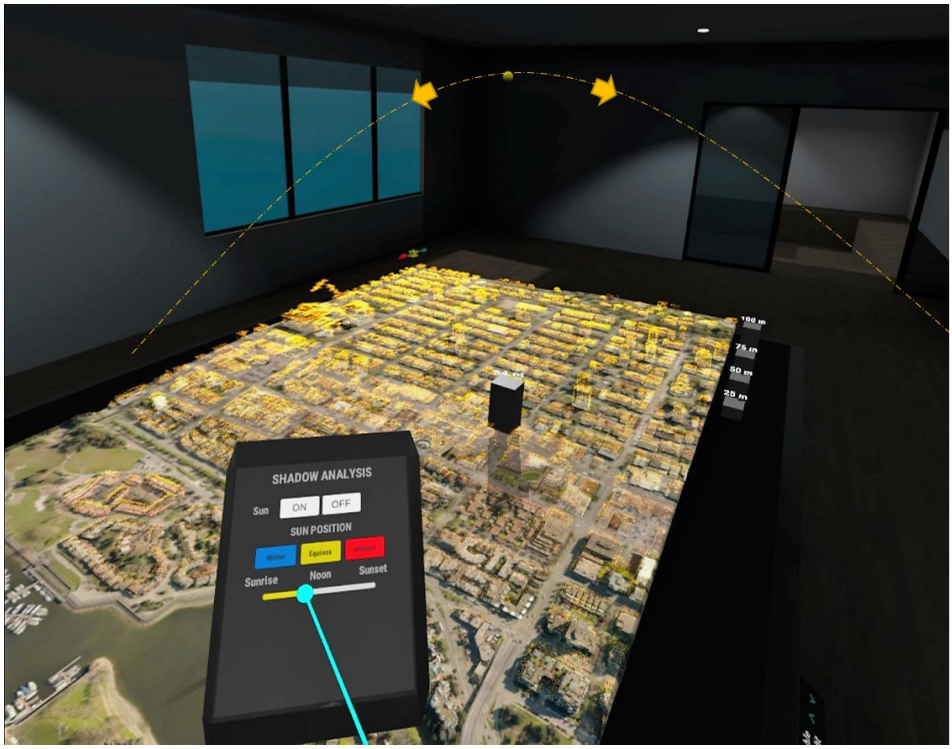

Figure 5.14 A virtual sun, controlled by the user, casts real-time shadows on the surrounding topography. Users can analyze the impact that urban development would have on available sunlight.

Case Study 4: Resource Management

The resource management visualization was designed to highlight the potential for immersive VEs as a VA and communication tool to be used in the analysis of GIS based spatial data layers. This visualization combines multiple data layers - obtained from the British Columbia Open Data Catalogue – and allows users to adjust the position and transparency of those layers to explore the relationships between the presented data (Figure 5.15).

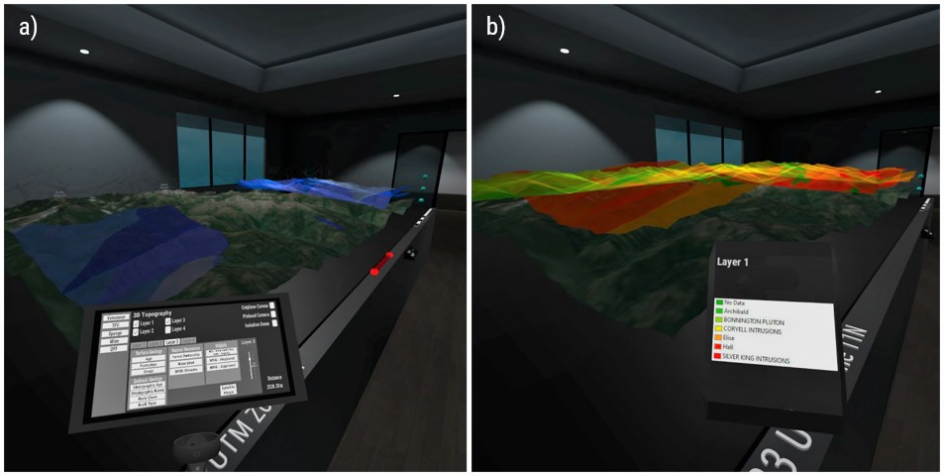

Figure 5.15 This visualization combines multiple spatial data layers in a GIS like interface. a) Multiple data layers can be activated at one time using the data menu, and b) users can analyze that data and its relationship with the surrounding environment.

This visualization was designed only for the primary data space, presenting data on the data table. Users can combine data layers - for surface and bedrock geology, natural resources (e.g., forests, watersheds, and rivers), and wildlife – to explore and visualize the relationships between the data and the surrounding landscape. The user can control the height and transparency of each layer, make measurements, and examine cross-sections in any size and direction. Our objective with this visualization was to showcase an immersive VE that may help to reveal new information by providing new experiences and perspectives.

Case Study 5: Flood Risk Governance

This case study discusses the design and development of an immersive VE for city officials and community stakeholders to explore climate futures and flood risk. This visualization combines topography, LiDAR point clouds, and climate change storm surge data produced by JBA Risk Management - a firm specializing in flood risk modelling - to enable visual analyses of the potential impacts that flooding events could have on the environment and infrastructure (Figure 5.16).

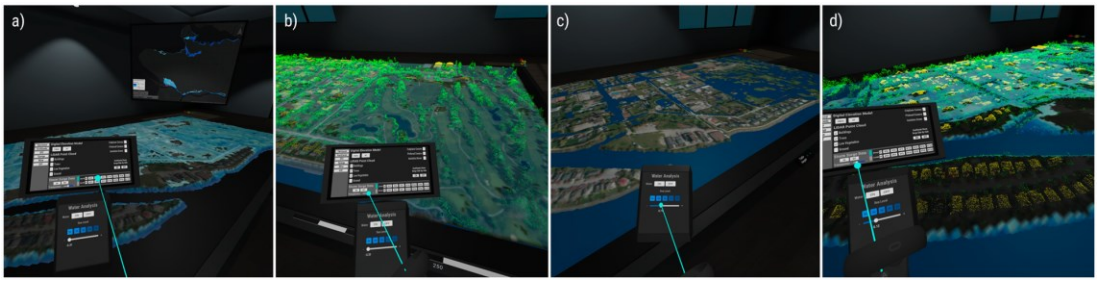

Figure 5.16 Flood risk analyses can be performed in the VE by analyzing a) different climate futures, b) the impact on existing infrastructure, c) sea level rise scenarios, and d) the impact on local communities.

This visualization was designed for both the primary and secondary rooms, allowing users to visualize and explore climate scenarios against 3D models on the data table, and compare multiple climate scenarios against each other in the data room (Figure 5.17). In both cases, users can examine individual flood risk scenarios, or they can observe animated GIFs that cycle through those scenarios. The objective with this visualization was to allow the user to observe the real impact that climate futures would have on the environment and infrastructure by combining modelling data with 3D topography and LiDAR point clouds and integrating interactivity that allows the user to experience the data.

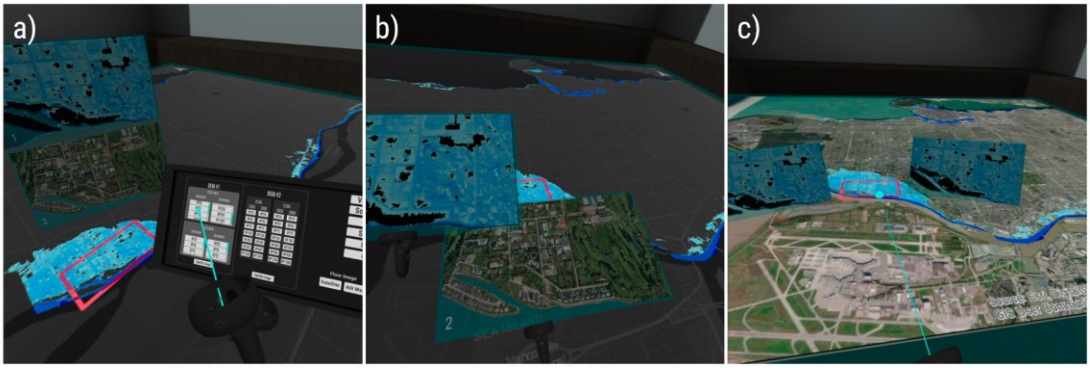

Figure 5.17 The data room allows users to compare multiple flood risk scenarios by a) defining which data appear on which display, b) adjusting those displays to suit their needs, and c) comparing the area of interest to other portions of the city.

5.3.5. Design Considerations

The iterative design process began with careful consideration of the spatial phenomena that would be presented in IVEVA, the user(s) of IVEVA, and how and what they may use IVEVA for. By first developing this contextual foundation, we were able to

gather and process the spatial data and 3D assets necessary for the development of a VE suitable for VA. IVEVA was designed around the users and the data, with use and user at the forefront of the design process. IVEVA and the tools within it were constructed to not only allow the user to see data from a new perspective, but to allow them to interact with and explore the available data in their quest for knowledge.

Testing served an important role throughout the design process, as multiple configurations of each data variable, tool, UI, and interaction method were assessed to achieve the design configuration and customization options necessary to promote usability and usefulness. The IVEVA prototype offers a window into the future of visualization and VA, where a diverse group of users can be immersed in, interact with, and explore 3D spatial data in an analytical VE using accessible modern technology that transforms the relationship between users and spatial data.

5.4. Discussion

IVEVA was developed to highlight the potential for immersive VEs as VA tools and to emphasize the value of a multidisciplinary approach to the design and development process. While geovisualizations are not conventional maps, much can be gained from the principles of cartography; while XR devices are not traditional computers, there are many HCI principles that can be applied to VR; and, while VR does not epitomize XR, VR design can benefit from the lessons learned in the design and development of other XR interfaces. As a VA application, IVEVA draws on the knowledge, experiences, and design heuristics from multiple disciplines to support the development of a VE, spatial data, UI, and UX that promotes knowledge building.

VR-based 3D VEs are popular for their ability to provide realistic experiences that immerse the user in the VE and can promote a sense of presence, or the feeling that they are situated in the VE rather than in the real-world (Edler et al., 2019; Hruby et al., 2019; Keil et al., 2021). Often, immersion and presence are exploited to transport users to virtual copies (digital twins) of real-world environments, allowing them to explore 1:1 representations of those environments for a variety of reasons (for example: simulations, route planning, and training). However, these digital twins are not the only useful application for VR, and IVEVA highlights how VR can be utilized to expand the space for data analysis rather than to replicate the space being analyzed. While the nuance may

be subtle, exploring 3D data in an immersive space is quite different than exploring 3D data spaces.

IVEVA strives to provide a UX that extends the human capacity to perform analytical reasoning through visual representations of spatial data. VA emerged out of the demand for tools and techniques that assist people with the synthesis of information, the quest for insight, the detection and discovery of patterns and relationships, and the assessment and communication of data for effective action (Thomas & Cook, 2005). As the objective of VA is to facilitate human-information discourse using tools that provide innovative interaction techniques and visual representations, the characteristics of the tools and their ability to drive knowledge formation by connecting people and data is critically important. The tool (VR), in and of itself, is just a tool. The usefulness of that tool is determined by its ability to connect people and data in a manner that promotes analytical reasoning and new knowledge.

From a design perspective, IVEVA incorporates cartographic principles for the visualization of spatial data in a 3D living map, liberating the visualization and analytical space of GIScience from the 2D confines of traditional displays, while maintaining the conventions and familiarity of spatial data representation. IVEVA was designed for the user: to provide a compelling data experience that empowers them in their exploration and analysis of spatial data; that is easy to learn, comfortable in use, and does not overwhelm; and to use metaphors and real-world knowledge to provide intuitive functionality. The VE itself is simple; designed as a space for data analysis rather than a space to be analyzed. The VE is customizable, allowing the user to rearrange data elements to suite their physical and cognitive needs, to change the visual characteristics of the space to fit their preferences, and to isolate themselves from the space to focus solely on the data.

The case studies presented in IVEVA were intentionally selected as exemplars of different spatial phenomena and spatial data types with different VA objectives. While VR offers a unique opportunity to immerse users within VEs and spatial data, neither the interface nor the act of immersion guarantees the transfer of knowledge. The interface must be designed to account for the differences in spatial phenomena, how they are characterized, how they can be represented in a VE, and how they are perceived and understood. For IVEVA, this involved careful consideration of the context of each case

study and the data type, extent, resolution, texture, color, transparency, emissivity, occlusion, physics, and the interplay of these variables within and between disparate data sets. Each decision is highly dependent on the relationships between the data, interface, user, and use; therefore, each decision should allow for the contextual variability that defines the *ideal* combination of these variables for effective sense making. The data presented in the IVEVA case studies were intentionally selected to help the user paint a picture, to help them explore and understand the data in the context that it is presented to them. As much as possible, the user should be given agency to make their own decisions concerning what, when, and how those data are presented.

The IVEVA prototype showcases VR as a platform for immersive 3D VA and implements design heuristics from cartography, HCI, and XR development in the design and development process. IVEVA extends both the space in which GIScience can be performed and the ways in which users can visualize, explore, and interact with spatial data. Therefore, the relationship between the user, the interface, and the data is critical to the UX and the knowledge building process. The UX for XR design heuristics published by Vi et al. (2019) provided an excellent foundation for the design and development of IVEVA; these heuristics helped to:

- Maximize efficiency through the organization of the spatial environment – the virtual space is simple and does not contain superfluous content that distracts the user away from the data. The virtual space is divided into two complementary rooms, each serving a different function but both offering a convenient and comfortable data experience.
- Ensure flexible interactions and environments – the virtual space can be customized to match the user's personal preferences: the wall colour, floor material, and light levels in the virtual space can be modified and the position of supplementary data and analytical tools can be rearranged for convenience.
- Design for user comfort – the personal space of the user is respected by not overwhelming them with content in their immediate field of view. The user can adjust the height of the data table so that the data environment matches their physical preferences and visualization and interaction do not require physical strain.
- Focus on simplicity: do not overwhelm the user – the virtual space is clean and simple, and the UI is intuitive and automatically updates to match the data and environment. Users do not have to search for the tools or menus, and both can be hidden to avoid cluttering the user's view.

- Design according to the hardware capabilities and limitations – IVEVA was designed specifically for the Oculus Quest and does not overwhelm the hardware with excessive files sizes, complex processing, or unnatural or complicated commands.

- Guide users throughout the experience using cues – the user's attention is directed towards features of interest using spatialized sound and visual cues.

- Provide a compelling XR experience – supplementary visual elements and audio were included to enhance the experience and to make the user feel comfortable in a virtual space designed to extend their everyday analytical space.

- Leverage real-world knowledge – the design of the virtual space and the presentation of spatial data were intended to be familiar. The virtual space represents a generic office space; control panels were placed near doorways as a light switch would be placed in the real-world; and map marginalia are provided for reference.

- Offer users feedback and consistency – the user's interactions are accompanied by visual or audible feedback that informs them if an action can, cannot, or has been performed.

- Place the user in control of the experience – the user is in control of the experience and the data, allowing them to explore, experiment, and analyze the data as they want.

- Promote unencumbered trial and error – any action performed by the user on the data can be reversed or reset, allowing the user to explore IVEVA without worry.

While the IVEVA prototype was designed to promote human-information discourse there are limitations to IVEVA which hinder this exchange. First, the spatial data presented in IVEVA required significant time and effort to convert from its raw form into one appropriate for Unity. This process reduces the user's ability to quickly import, visualize, and analyze spatial data in applications such as IVEVA; however, the emergence of plugins such as the ArcGIS Maps SDK, bridging the gap between their GIS software and Unity, should improve this process. Second, IVEVA was developed for a single user while analytical reasoning is a process that can involve several different people separated by space and time. This limitation can be overcome through packages such as Photon Unity Networking (PUN), allowing multiple users to collaborate in the same VE.

Further development of IVEVA should adopt a user-centered design approach that directly incorporates the user in the design cycle IVEVA was designed and

developed with the perspective of specific stakeholders (marine ecologists, emergency management personnel, city planners, government officials, community members, and GIScientists) in mind, but without the ability to actively incorporate them in the design cycle. As a VA prototype, designed through heuristic evaluation based on the intuition and knowledge of the developers (Nielsen & Molich, 1990), IVEVA sets the foundation for further design and development with invested stakeholders. Undoubtedly, this would include multiple individuals from diverse backgrounds; therefore, future versions of IVEVA should be developed as a collaborative VA interface, allowing concurrent occupation of the VE by multiple VR users.

5.5. Conclusion

This paper introduced IVEVA, an immersive virtual GIScience data visualization space, and a set of 3D data-driven geovisualization case studies. IVEVA is a VR interface, and while it was designed for VR, design heuristics from cartography, HCI, and XR development played an integral role. However, in adopting design heuristics from disparate fields, careful consideration must be given to the implications that different use, user, data, and technology combinations have on those heuristics in an applied context. For example, a given material, spatial resolution, interaction method, visual cue, or feedback mechanism that is appropriate for one application, spatial phenomena, or data type may not be appropriate for another. These design challenges can be diminished through a proactive and iterative user-centered design and heuristic evaluation process that incorporates, tests, and modifies interface features and functionality to ensure useful, usable, and enjoyable XR interfaces for 3D GIScience and VA.

Emerging XR technologies have the potential to transform the relationship between people and data. As we incorporate these technologies into the social, professional, and academic realms it is important that XR interfaces account for the variability in use, user, data, and technology. In this paper we presented a design and development approach that integrates multiple design heuristics to address the multifaceted challenges associated with creating this immersive VA space. The UX and data were crafted specifically for VR. While our design and development decisions may prove useful for other XR interfaces, they were selected to optimize human-computer-data interaction in VR and promote knowledge formation through immersive visual

analyses. Therefore, the design of VR interfaces for immersive VA should adopt the basic tenets of cartography and HCI, as those are the fundamental building blocks for spatial data visualization using any piece of technology. However, emerging XR interfaces are different from one another and from conventional 2D interfaces, requiring unique heuristic design considerations broadly following those outlined by Vi et al. (2019).

The presented case studies are exemplars for different spatial phenomena and spatial data types presented in VR. Each case study has an overlying objective, and the characterization of the spatial phenomena and the data is driven by the context of that objective. Therefore, it is difficult to say that one data type is better suited for VR than the other without first considering its purpose in the analytical process. While the basic vector and raster files that typify conventional GIS may be extremely useful in VR under certain contexts, VR can provide much more than shapefiles in an immersive 3D VE. For example, an ongoing critique of conventional GIS has been an impeded ability to display topologically 3D data, whereas VR allows the user to transcend the physical limitations of the real-world, to figuratively step into the computer to inhabit the data space, to interact with the data, to experiment with the data, and to experience the data in 3D, which is not possible with conventional 2D interfaces. Therefore, it is not so much the data in and of itself, but the collection of and context in which the data is presented, the spatial tools that are provided to allow users to manipulate and query that data, and the user-data relationship mediated by emerging XR technologies that will drive the future of GIScience and VA. We hope that IVEVA and the presented case studies stimulate further dialogue and collaboration with members of this research community.

Acknowledgements

We acknowledge the support of the Natural Sciences and Engineering Research Council of Canada (NSERC). Portions of this research were also supported by the Mitacs Accelerate Program, in partnership with Ocean Wise, and by the Marine Environmental Observation, Prediction and Response Network (MEOPAR) Canadian Network of Centres of Excellence, Project 1-02-02-032.4— “Coastal Flood Risk Governance in a Changing Climate.”

References

Adedokun-Shittu, N. A., Ajani, A. H., Nuhu, K. M., & Shittu, A. J. K. (2020). Augmented reality instructional tool in enhancing geography learners' academic performance and retention in Osun state Nigeria. Education and Information Technologies, 25(4), 3021–3033. https://doi.org/10.1007/s10639-020-10099-2

Al Shuaili, K., Al Musawi, A. S., & Hi.e.,in, R. M. (2020). The effectiveness of using augmented reality in teaching geography curriculum on the achievement and attitudes of Omani 10th Grade Students. Multidisciplinary Journal for Education, Social and Technological Sciences, 7(2), 20. https://doi.org/10.4995/muse.2020.13014

Andrienko, G., Andrienko, N., Jankowski, P., Keim, D., Kraak, M. J., MacEachren, A., & Wrobel, S. (2007). Geovisual analytics for spatial decision support: Setting the research agenda. International Journal of Geographical Information Science, 21(8), 839–857. https://doi.org/10.1080/13658810701349011

Andrienko, Gennady, Andrienko, N., Keim, D., MacEachren, A. M., & Wrobel, S. (2011). Challenging problems of geospatial visual analytics. Journal of Visual Languages and Computing, 22(4), 251–256. https://doi.org/10.1016/j.jvlc.2011.04.001

Bertin, J. (2011). General Theory, from Semiology of Graphics. In M. Dodge, R. Kitchin, & C. Perkins (Eds.), The Map Reader (First Edit, pp. 8–16). John Wiley & Sons, Ltd. https://doi.org/10.1002/9780470979587.ch2

Billinghurst, M., Kato, H., Kiyokawa, K., Belcher, D., & Poupyrev, I. (2002). Experiments with face-to-face collaborative AR interfaces. Virtual Reality, 6(3), 107–121. https://doi.org/10.1007/s100550200012

Bruns, C. R., & Chamberlain, B. C. (2019). The influence of landmarks and urban form on cognitive maps using virtual reality. Landscape and Urban Planning, 189(May 2018), 296–306. https://doi.org/10.1016/j.landurbplan.2019.05.006

Carbonell Carrera, C., & Bermejo Asensio, L. A. (2016). Landscape interpretation with augmented reality and maps to improve spatial orientation skill. Journal of Geography in Higher Education, 8265(March), 1–15. https://doi.org/10.1080/03098265.2016.1260530

Carpendale (2003). Considering Visual Variables as a basis for Information Visualisation. In Cartographica: International Journal for Geographic Information and Geovisualization (Vol. 43, pp. 175–188).

Çöltekin, A., Bleisch, S., Andrienko, G., & Dykes, J. (2017). Persistent challenges in geovisualization – a community perspective. International Journal of Cartography, 9333, 1–25. https://doi.org/10.1080/23729333.2017.1302910

Çöltekin, A., Griffin, A. L., Slingsby, A., Robinson, A. C., Christophe, S., Rautenbach, V., Chen, M., Pettit, C., & Klippel, A. (2020). Geospatial Information Visualization and Extended Reality Displays. In Manual of Digital Earth. https://doi.org/10.1007/978-981-32-9915-3_7

Çöltekin, A., Lochhead, I., Madden, M., Christophe, S., Devaux, A., Pettit, C., Lock, O., Shukla, S., Herman, L., Stachoň, Z., Kubíček, P., Snopková, D., Bernardes, S., & Hedley, N. (2020). Extended reality in spatial sciences: A review of research challenges and future directions. ISPRS International Journal of Geo-Information, 9(7). https://doi.org/10.3390/ijgi9070439

Coxon, M., Kelly, N., & Page, S. (2016). Individual differences in virtual reality: Are spatial presence and spatial ability linked? Virtual Reality, 20(4), 203–212. https://doi.org/10.1007/s10055-016-0292-x

Dibiase, D., MacEachern, A. M., Krygier, J. B., & Reeves, C. (1992). Animation and the role of map design in scientific visualization. Cartography & Geographic Information Systems, 19(4), 201–214. https://doi.org/10.1559/152304092783721295

Dünser, A., Grasset, R., & Billinghurst, M. (2008). A survey of evaluation techniques used in augmented reality studies. ACM SIGGRAPH ASIA 2008 Courses on - SIGGRAPH Asia '08, June 2014, 1–27. https://doi.org/10.1145/1508044.1508049

Dünser, A., Grasset, R., Seichter, H., & Billinghurst, M. (2007). Applying HCI Principles to AR Systems Design. Proceedings of 2nd International Workshop on Mixed Reality User Interfaces: Specification, Authoring, Adaptation (MRUI '07), March 11, 37–42.

Dykes, J., Andrienko, G., Andrienko, N., Paelke, V., & Schiewe, J. (2010). Editorial - GeoVisualization and the Digital City. Computers, Environment and Urban Systems, 34(6), 443–451. https://doi.org/10.1016/j.compenvurbsys.2010.09.001

Edler, D., Keil, J., Wiedenlübbert, T., Sossna, M., Kühne, O., & Dickmann, F. (2019). Immersive VR Experience of Redeveloped Post-industrial Sites: The Example of "Zeche Holland" in Bochum-Wattenscheid. KN - Journal of Cartography and Geographic Information, 69(4), 267–284. https://doi.org/10.1007/s42489-019-00030-2

Endsley, T. C., Sprehn, K. A., Brill, R. M., Ryan, K. J., Vincent, E. C., & Martin, J. M. (2017). Augmented reality design heuristics: Designing for dynamic interactions. Proceedings of the Human Factors and Ergonomics Society, 2017-October (1990), 2100–2104. https://doi.org/10.1177/1541931213602007

George, R., Howitt, C., & Oakley, G. (2020). Young children's use of an augmented reality sandbox to enhance spatial thinking. Children's Geographies, 18(2), 209–221. https://doi.org/10.1080/14733285.2019.1614533

Goodchild, M. F. (1992). Geographical Information Science. International Journal of Geographic Information Systems, 6(1), 31–45.

Han, D. I. D., Tom Dieck, M. C., & Jung, T. (2019). Augmented Reality Smart Glasses (ARSG) visitor adoption in cultural tourism. Leisure Studies, 38(5), 618–633. https://doi.org/10.1080/02614367.2019.1604790

Hassenzahl, M., & Tractinsky, N. (2006). User experience - A research agenda. Behaviour and Information Technology, 25(2), 91–97. https://doi.org/10.1080/01449290500330331

Havenith, H. B., Cerfontaine, P., & Mreyen, A. S. (2019). How virtual reality can help visualise and assess geohazards. International Journal of Digital Earth, 12(2), 173–189. https://doi.org/10.1080/17538947.2017.1365960

Hedley, N. (2017). Augmented Reality. In D. Richardson, N. Castree, M. F. Goodchild, A. Kobayashi, W. Liu, & R. A. Marston (Eds.), International Encyclopedia of Geography (pp. 1–13). John Wiley & Sons, Ltd. https://doi.org/doi:10.1201/9780849375477.ch213\r10.1201/9780849375477.ch213

Hruby, F., Ressl, R., & de la Borbolla del Valle, G. (2019). Geovisualization with immersive virtual environments in theory and practice. International Journal of Digital Earth, 12(2), 123–136. https://doi.org/10.1080/17538947.2018.1501106

Imottesjo, H., & Kain, J. H. (2018). The Urban CoBuilder – A mobile augmented reality tool for crowd-sourced simulation of emergent urban development patterns: Requirements, prototyping and assessment. Computers, Environment and Urban Systems, 71(October 2017), 120–130. https://doi.org/10.1016/j.compenvurbsys.2018.05.003

International Cartographic Association. (2015). ICA News (I. Drecki (ed.)). https://icaci.org/files/documents/newsletter/ica_news_64_2015_1_lq.pdf

Jong, M. S. Y., Tsai, C. C., Xie, H., & Kwan-Kit Wong, F. (2020). Integrating interactive learner-immersed video-based virtual reality into learning and teaching of physical geography. British Journal of Educational Technology, 51(6), 2063–2078. https://doi.org/10.1111/bjet.12947

Keil, J., Edler, D., Schmitt, T., & Dickmann, F. (2021). Creating Immersive Virtual Environments Based on Open Geospatial Data and Game Engines. KN - Journal of Cartography and Geographic Information, 71(1), 53–65. https://doi.org/10.1007/s42489-020-00069-6

Kerren, A., Ebert, A., & Meyer, J. (2007). Introduction to Human-Centered Visualization Environments. In Human-Centered Visualization Environments (Vol. 4417, pp. 1–9). https://doi.org/10.1007/978-3-540-71949-6_1

Levin, E., Shults, R., Habibi, R., An, Z., & Roland, W. (2020). Geospatial Virtual Reality for Cyberlearning in the Field of Topographic Surveying: Moving towards a Cost-Effective Mobile Solution. ISPRS International Journal of Geo-Information, 9(7). https://doi.org/10.3390/ijgi9070433

Lisichenko, R. (2015). Issues Surrounding the Use of Virtual Reality in Geographic Education. Geography Teacher, 12(4), 159–166. https://doi.org/10.1080/19338341.2015.1133441

Liu, F., Jonsson, T., & Seipel, S. (2020). Evaluation of augmented reality-based building diagnostics using third person perspective. ISPRS International Journal of Geo-Information, 9(1). https://doi.org/10.3390/ijgi9010053

Lochhead, I., & Hedley, N. (2018). Mixed reality emergency management: bringing virtual evacuation simulations into real-world built environments. International Journal of Digital Earth, 0(0), 1–19. https://doi.org/10.1080/17538947.2018.1425489

Lonergan, C., & Hedley, N. (2014). Flexible Mixed Reality and Situated Simulation as Emerging Forms of Geovisualization. Cartographica: The International Journal for Geographic Information and Geovisualization, 49(3), 175–187. https://muse-jhu-edu.proxy.lib.sfu.ca/journals/cartographica/v049/49.3.lonergan.html

MacEachren, A. M., & Kraak, M.-J. (1997). Exploratory cartographic visualization: Advancing the agenda. Computers & Geosciences, 23(4), 335–343. https://doi.org/10.1016/S0098-3004(97)00018-6

MacEachren, A. M., & Kraak, M.-J. (2001). Research Challenges in Geovisualization. Cartography and Geographic Information Science, 28(1), 3–12. https://doi.org/10.1559/152304001782173970

Milgram, P., & Kishino, F. (1994). A Taxonomy of Mixed Reality Visual Displays. IEICE (Institute of Electronics, Information and Communication Engineers) Transactions on Information and Systems, Special Issue on Networked Reality.

Minocha, S., Tilling, S., & Tudor, A.-D. (2018). Role of Virtual Reality in Geography and Science Fieldwork Education. https://doi.org/10.1021/acs.jctc.5b00907

Molich, R., & Nielsen, J. (1990). Improving a Human-Computer Dialogue. Communications of the ACM, 33(3).

Nielsen, J. (1993). Usability engineering. In Cambridge, Mass. AP Professional.

Nielsen, J., & Molich, R. (1990). Heuristic evaluation of user interfaces. Conference on Human Factors in Computing Systems - Proceedings, April, 249–256. https://doi.org/10.1145/97243.97281

Panou, C., Ragia, L., Dimelli, D., & Mania, K. (2018). An architecture for mobile outdoors augmented reality for cultural heritage. ISPRS International Journal of Geo-Information, 7(12). https://doi.org/10.3390/ijgi7120463

Rautenbach, V., Çöltekin, A., & Coetzee, S. (2015). Exploring the impact of visual complexity levels in 3D city models on the accuracy of individuals' orientation and cognitive maps. ISPRS Annals of the Photogrammetry, Remote Sensing and Spatial Information Sciences, 2(3W5), 499–506. https://doi.org/10.5194/isprsannals-II-3-W5-499-2015

Romano, S., & Hedley, N. (2021). Daylighting Past Realities: Making Historical Social Injustice Visible Again Using HGIS-Based Virtual and Mixed Reality Experiences. Journal of Geovisualization and Spatial Analysis, 5(1). https://doi.org/10.1007/s41651-021-00077-8

Roth, R. E., Ross, K. S., & MacEachren, A. M. (2015). User-centered design for interactive maps: A case study in crime analysis. ISPRS International Journal of Geo-Information, 4(1), 262–301. https://doi.org/10.3390/ijgi4010262

Rydvanskiy, R., & Hedley, N. (2020). 3d geovisualization interfaces as flood risk management platforms: Capability, potential, and implications for practice. Cartographica, 55(4), 281–290. https://doi.org/10.3138/CART-2020-0003

Rydvanskiy, R., & Hedley, N. (2021). Mixed Reality Flood Visualizations: Reflections on Development and Usability of Current Systems. ISPRS International Journal of Geo-Information, 10(2), 82. https://doi.org/10.3390/ijgi10020082

Schmidt, S., Bruder, G., & Steinicke, F. (2016). Illusion of depth in spatial augmented reality. 2016 IEEE VR 2016 Workshop on Perceptual and Cognitive Issues in AR, PERCAR 2016, 1–6. https://doi.org/10.1109/PERCAR.2016.7562417

Shelton, B. E., & Hedley, N. R. (2004). Exploring a cognitive basis for learning spatial relationships with augmented reality. Technology, Instruction, Cognition and Learning, 1, 323–357. http://digitalcommons.usu.edu/itls_facpub/92/

Shuaili, Khalfan Al, Ali Sharaf Al Musawi, and Raja Muznah Hussain. 2020. "The Effectiveness of Using Augmented Reality in Teaching Geography Curriculum on the Achievement and Attitudes of Omani 10th Grade Students." Multidisciplinary Journal for Education, Social and Technological Sciences 7 (2): 20. https://doi.org/10.4995/muse.2020.13014.

Slocum, T. A. (2009). Virtual Environments. In T. A. Slocum, R. B. McMaster, F. Kessler, & H. H. Howard (Eds.), Thematic Cartography and Geovisualization (3rd ed., pp. 460–477). Pearson.

Thomas, J., & Cook, K. A. (2005). Illuminating the path: the R&D agenda for visual analytics. National Visualization and Analytics Center, Institute of Electrical and Electronics Engineers, January 2005.

Tuli, N., & Mantri, A. (2020). Usability principles for augmented reality based kindergarten applications. Procedia Computer Science, 172(2019), 679–687. https://doi.org/10.1016/j.procs.2020.05.089

Turan, Z., Meral, E., & Sahin, I. F. (2018). The impact of mobile augmented reality in geography education: achievements, cognitive loads, and views of university students. Journal of Geography in Higher Education, 42(3), 427–441. https://doi.org/10.1080/03098265.2018.1455174

Vi, S., Silva, T. S. da, & Maurer, F. (2019). User Experience Guidelines for Designing HMD Extended Reality Applications. In D. Lamas, F. Loizides, L. Nacke, H. Petrie, M. Winckler, & P. Zaphiris (Eds.), Human-Computer Interaction -- INTERACT 2019 (pp. 319–341). Springer International Publishing. https://doi.org/10.1007/978-3-030-29390-1

Virrantaus, K., Fairbairn, D., & Kraak, M. (2009). ICA Research Agenda on Cartography and GIScience. Cartography and Geographic Information Science, 36(2), 209–222. https://doi.org/10.1559/152304009788188772

Wang, X., Van Elzakker, C. P. J. M., & Kraak, M. J. (2017). Conceptual design of a mobile application for geography fieldwork learning. ISPRS International Journal of Geo-Information, 6(11). https://doi.org/10.3390/ijgi6110355

Yagol, P., Ramos, F., Trilles, S., Torres-Sospedra, J., & Perales, F. J. (2018). New trends in using augmented reality apps for smart city contexts. ISPRS International Journal of Geo-Information, 7(12). https://doi.org/10.3390/ijgi7120478

Chapter 6.

The Immersive Mental Rotations Test: Evaluating Spatial Ability in Virtual Reality

This paper is published in *Frontiers in Virtual Reality*.

Citation Details: Lochhead, I., Hedley, N., Çöltekin, A., & Fisher, B. (2022). The Immersive Mental Rotations Test: Evaluating Spatial Ability in Virtual Reality. Frontiers in Virtual Reality, 3(January), 1–19. https://doi.org/10.3389/frvir.2022.820237

Abstract

Advancements in extended reality (XR) have inspired new uses and users of advanced visualization interfaces, transforming geospatial data visualization and consumption by enabling interactive 3D geospatial data experiences in 3D. Conventional metrics (e.g., mental rotations test (MRT)) are often used to assess and predict the appropriateness of these visualizations without accounting for the effect the interface has on those metrics. We developed the Immersive MRT (IMRT) to evaluate the impact that virtual reality (VR) based visualizations and 3D virtual environments have on mental rotation performance. Consistent with previous work, the results of our pilot study suggest that mental rotation tasks are performed more accurately and rapidly with stereo 3D stimuli than with 2D images of those stimuli.

Keywords: spatial ability; mental rotation; virtual reality; 3D geovisualization; spatial knowledge

6.1. Introduction

Recent advances in extended reality (XR) technology have sparked renewed interest in, and new opportunities for, visualizing three-dimensional (3D) spatial data with virtual reality (VR), mixed reality (MR), and augmented reality (AR) interfaces. Concurrently, access to and the production of 3D spatial data has undergone a significant transformation, empowering those with common consumer electronics (e.g., smartphones and computers) with an ability to generate what once required significant

capital expenditures and highly specialized equipment. In the realm of geographic visualization (or *geovisualization*) these advancements have led to new forms of data exploration and interaction, allowing users to immerse themselves within spatial data for the purposes of visualization, analysis, collaboration, and communication (e.g., Çöltekin et al., 2020; Devaux et al., 2018; Filho et al., 2020; Hruby et al., 2019; Lochhead & Hedley, 2018; Pulver et al., 2020; Rydvanskiy & Hedley, 2021; Zhao et al., 2019).

Geovisualizations such as these will become more numerous as the popularity of XR technology and 3D geospatial content creation continues to evolve. As new technologies and methods emerge, new geovisual analytical capabilities and experiences also emerge, raising questions regarding accuracy, utility, and the optimal interface, data, application, user, and venue combination(s). While there is no guarantee that any given combination is ideal, future advancements in artificial intelligence and information science may deliver software-based solutions that optimize these combinations for geospatial knowledge transfer (Çöltekin et al., 2017). However, the success of such solutions ultimately hinges on our ability, as a research community, to answer some of the persistent challenges that have plagued geovisualization (see Çöltekin et al., 2017; Laramee & Kosara, 2006; MacEachren & Kraak, 1997; Slocum et al., 2001), including: a need to better understand geovisualization's place in the broader research community, an actionable set of guidelines that match geovisualization type with use and user, and a greater understanding of the human factors which dictate cognitive processes and geospatial knowledge transfer.

In this paper we address spatial ability – one of the many human factors challenges faced by the geovisualization community – and the role it plays in an era of 3D data and XR technology. While spatial ability has long been recognized as an important component of geovisualization use, impacting the degree to which one is able to generate knowledge from different types of geovisualizations, there has yet to be a consensus as to whether those with low or high spatial ability are better positioned to benefit from (3D) geovisualizations (Çöltekin et al., 2016). On one hand, it is argued that low spatial ability learners benefit more from graphical presentations – the ability-as-compensator hypothesis (Hegarty and Sims 1994; Hays 1996; Huk 2006) – and on the other, that high spatial learners stand to benefit more – the ability-as-enhancer hypothesis (Mayer, Richard E. and Sims 1994; Huk 2006). Part of the challenge in determining which hypothesis holds true is that spatial ability itself is a general construct

encapsulating a variety of skills and processes (Hinze et al. 2014) that themselves are malleable (i.e. our spatial abilities can change over time) (Uttal et al. 2013; Newcombe 2014).

Built on one of the most popular measures of spatial ability called the Mental Rotations Test (MRT) (Shepard & Metzler, 1971; Vandenberg & Kuse, 1978), here we introduce the Immersive Mental Rotations Test (IMRT), a modified version of the MRT adapted to explore the effect that immersive technologies (i.e., VR) have on our ability to mentally rotate assemblages of cubes presented as 2D images and as 3D objects (Figure 6.1). While the works of Shepard & Metzler (1971), Vandenberg & Kuse (1978), and Peters et al. (1995) have been fundamental in spatial ability (specifically, mental rotations) studies, arguably, the ability to mentally rotate 2D images of hypothetical 3D objects to quantify spatial abilities seems to be a poor fit for modern immersive display technologies – which do not require the same cognitive operations as 2D representations. Given the lack of spatial ability tests that are specifically developed for XR displays, here we explore an adaptation of the MRT that we hope will help translate the bedrock methods of existing MRT work into the contexts of contemporary and emerging 3D interfaces. Furthermore, we explore whether solving the MRT tasks in stereo 3D vs. 2D will lead to new knowledge in this domain by answering the question of how important is the 'imagining 3D shapes from 2D projections' *vs.* actual mental *rotations* in the MRT.

While some may argue that this 3D adaptation of the MRT subverts the objective of the long established MRT – and we do not object to this discussion – that is precisely the point of this test. The classic MRT implicitly measures two things: 1) can people imagine the 3D shapes from 2D drawings, and 2) can people mentally rotate these imagined objects and tell the difference among apparently similar options. We tease apart the two here. From an applied perspective, especially in the domain of geovisualization, classical MRT has many conceptual links to map reading (from printed or digital 2D maps). However, modern data formats and display technologies have changed the way that we represent, visualize, and experience geospatial phenomena. Thus, our objectives with this initial IMRT study are to examine whether MRT performance (score and time) is impacted by 1) the spatial dimensionality of the MRT stimuli (2D vs stereo 3D) in an immersive virtual environment (VE), and 2) the background complexity of the VE (simple vs complex). Furthermore, we conduct

additional exploratory analyses to examine the relationship between MRT/IMRT performance and participant movement and the angular difference between stimuli (difficulty).

6.2. Background

Spatial ability is an important component of our general intelligence, relied upon for everyday spatial reasoning, and is strongly correlated with success across several STEM (science, technology, engineering, and math) majors and professions (Casey, 2013; Johnson & Bouchard, 2005). STEM disciplines commonly use visualizations to communicate the complex concepts and relationships behind imperceptible or abstract phenomena and accurate interpretations of these visualizations are therefore critical (Hinze et al. 2014). However, despite our reliance on visualizations, questions concerning for whom and when visualizations prove most effective remain unanswered (Hinze et al. 2014) due to the complex relationship between spatial ability and learning from visualizations.

While evidence supports both the ability-as-compensator hypothesis and the ability-as-enhancer hypothesis, these two hypotheses contradict each other. Hinze et al (2014) posit that learning from visualizations is a function of visualization design, task demands, prior knowledge, and processing strategy – not simply the learner's spatial ability, which includes a variety of separable spatial skills that are each indicative of a unique cognitive process best suited for specific spatial tasks (Casey, 2013; Newcombe, 2014). Therefore, for any given visualization, learners with a deficiency in one spatial skill may not realize a negative learning outcome, as non-spatial skills may be relied upon to overcome those limitations. Nevertheless, formal taxonomies of spatial skills have been developed to help connect the task demands of the visualization with the spatial skills of the learner (Hinze et al. 2014).

Research on individual and group differences in spatial abilities commonly addresses the object-based spatial skills (Casey, 2013). Linn & Petersen (1985) categorized these skills as spatial perception, spatial visualization, and mental rotation. Spatial perception tasks involve determining spatial relationships relative to one's own body (e.g. Rod-and-Frame test or Water Levels test), spatial visualization tasks require complex, multistage manipulation of spatial information (e.g. Embedded Figures or

mazes), and mental rotation tasks involve the ability to observe an object, or picture of an object, and imagine how it may appear when rotated in 3D space (e.g. Mental Rotation Test or Card Rotation Test) (Casey, 2013; Linn & Petersen, 1985; Uttal et al., 2013). Of all the object-based tests, mental rotations tests, and in particular the Vandenberg & Kuse MRT (1978), are the most common – in part because of the strong performance difference between sexes that are absent with other tests (Casey, 2013).

6.2.1. The MRT

The Vandenberg & Kuse MRT (1978) is a paper-and-pencil test based on the computer generated 2D images of 3D objects developed by Shepard & Metzler (1971). Shepard & Metzler (1971) presented 1600 paired stimuli to eight adult subjects, asking them to determine whether each pair contained the same, albeit rotated, stimuli. The Vandenberg & Kuse MRT (1978) is a 20-question test, wherein each question contains one standard stimulus and four rotated alternatives (two of which are the same as the standard and two which are not), in which respondents must select the two stimuli that are rotated versions of the standard (Figure 6.1). As the physical quality of the Vandenberg MRT deteriorated over time, Peters et al. (1995) developed a 24-question, redrawn version of the MRT.

Shepard & Metzler (1971) found a near perfect correlation between the angular disparity of pairs of stimuli and the amount of time required for respondents to identify matching pairs, and Vandenberg & Kuse (1978) as well as Peters et al. (1995) observed clear and replicable performance differences between sexes, where males outperform females. This performance difference has made the MRT one of the more popular tests of spatial skill and it has been argued that these types of image rotation tasks are a critical component of our general intelligence and STEM achievements (Casey, 2013; Johnson & Bouchard, 2005; Wai et al., 2009).

6.2.2. Applied Use of the MRT

The connection between spatial ability and visualization comprehension is apparent, yet the exact nature of that connection remains unclear (i.e., whether different types of visualization better assist those with low or high spatial ability remains unestablished). Spatial ability tests, such as the MRT, are commonly incorporated in

visualization research as researchers attempt to connect spatial ability with performance metrics relevant to their visualization and its objective. Examples include: the relationship between spatial abilities (including MRT performance), mental model formation, and a sense of presence in an immersive VE (IVE) (Coxon, Kelly, and Page 2016), the importance of spatial ability (measured through MRT performance) for spatial knowledge acquisition through AR interface use (Hedley 2003), the role that mental rotation skills play in real-world wayfinding (Malinowski 2001) and map-based route learning (Çöltekin et al., 2018), the importance of spatial ability (mental rotation) and visuospatial memory in virtual navigation (Lokka and Çöltekin 2019), and the impact that spatial abilities (including MRT performance) have on map learning (Sanchez and Branaghan 2009). Outside the realm of geovisualization, the MRT has been applied in a similar fashion to: evaluate the role of spatial thinking in STEM fields (Hegarty, Stieff, and Dixon 2014), to study the importance of spatial ability in learning from 3D cell biology models (Huk 2006), and to explore the relationship between biological sex and mental rotation ability (Casey & Brabeck, 1989; Collins & Kimura, 1997; Debelak et al., 2014; Hoyek et al., 2012; Moè, 2012).

6.2.3. Beyond the MRT

The Vandenberg MRT has inspired further studies, employing the original MRT stimuli and others, that explore the idiosyncrasies of mental rotation performance. Some have altered how the test was administered: Parsons et al. (2004) developed the Virtual Reality Spatial Rotation (VRSR) test for the ImmersaDesk, Monahan, Harke, & Shelley (2008) built a computerized, touchscreen version of the MRT, and McWilliams, Hamilton, & Muncer (1997) constructed tangible 3D models of the MRT stimuli out of balsa wood. Others have altered the difficulty of the test: Datta & Roy (2016) used fewer, colored and shaded stimuli, in each question. While others recognized the MRT as a tool to develop spatial skill: Marusan, Kulistak, & Zara (2006) built a web application for visuospatial rehabilitation following traumatic brain injury, and Alqahtani, Daghestani, & Ibrahim (2017) used a semi-immersive Virtual Mental Rotation Training (VMRT) system to develop mental rotation skills in engineering students. Additionally, the Dynamic Spatial Test in Augmented Reality (DSTAR) – effectively non-immersive VR (not AR) since the see-through functionality of the HMD was disabled – tested participants' ability to

mentally rotate, remember, and then reconstruct 3D objects in a 4 x 4 grid (Kaufmann et al. 2008).

6.2.4. The Importance of Mental Rotation Ability

These studies reported mental rotation ability to have varying levels of importance and an in-depth review of the results is beyond the scope of this manuscript. This is not to suggest that the results from each study are not interesting or important (they are), but rather that when these results are considered individually, they are somewhat insignificant; the results from one test may argue that spatial abilities are highly important for visualization, while the next may suggest the alternative if the prescribed task does not require the spatial ability being tested. When considered collectively, mental rotation ability (and spatial ability in general) is highly dependent on the idiosyncrasies of the prescribed task, and everyone may draw upon several abilities (spatial and otherwise) to perform that task. In other words: is spatial ability important? Many would argue that *it depends*.

The ability to mentally transform and manipulate images is an important skill for many disciplines. However, the MRT may not measure one's 'mental rotation' ability as such, but rather a process of figure perception, identification, and comparison – something that is significantly more difficult to accomplish when the objects in the MRT are homogenous rather than heterogenous and the individual segments of those objects cannot be counted to discern their orientation (Caissie, Vigneau, and Bors 2009). Regardless of which strategy is employed, the ability to perform these 'mental rotations' is very important in an academic or professional environment that requires visual analyses and comprehension of 2D images representing 3D phenomena.

Studies employing the MRT have consistently produced results replicating the significant sex effect noted by Vandenberg & Kuse (1978). The performance difference between males and females has been central to much MRT research (e.g. Collins & Kimura, 1997; Debelak et al., 2014; Moè, 2012) and it was found that the average effect size was 0.94 (using Cohen's $d = (M_1 – M_2)/ \sigma$) – or that on average males outperform females by almost one standard deviation (Voyer, Voyer, and Bryden 1995). Contrary to these findings are those of McWilliams et al. (1997), Parsons et al. (2004), and Monahan et al. (2008) who reported no significant gender effect when MRTs were conducted

using real 3D models, an ImmersaDesk, or a touchscreen device respectively. These results support the notion that the sex effect is not a function of mental rotation ability per se but of how the stimuli in the MRT are represented.

6.2.5. Technology, Geovisualization, and Spatial Ability

Representation has played a critical role in discussions outlining the geovisualization research agenda, from the cartographic visualization agenda of MacEachren & Kraak (1997) to the research communities perspective on persistent challenges within the field (Çöltekin et al., 2017) three decades later. As the objective of any geovisualization is to "facilitate(s) knowledge construction through visual exploration and analysis of geospatial data" (MacEachren and Kraak 2001), the way geospatial data are represented plays an influential role in the transfer of knowledge through geovisualization use. Representation is therefore a fundamental issue within the field of geovisualization, as both the data representing the geospatial phenomena and the display technology through which they are presented must be considered concurrently during the geovisualization design process.

As powerful XR display technologies have advanced into the realm of consumer level electronics, discussions about the use of 3D and VR (or XR) are no longer predicated on their *potential* to change how we consume geospatial data. Digital cartography transformed cartography by changing what is visible, how we think, and how maps work (MacEachren and Kraak 1997) and now XR technologies are changing how we consume geospatial data, how we think about geospatial data, and how geovisualizations work. While there is tremendous potential for XR technology within geovisualization, change in and of itself is not inherently positive and many questions about the design and use of XR-based geovisualizations must be answered. For example: how do immersion, interactivity, information intensity, and object intelligencer (MacEachren et al. 1999), both individually and collectively, impact knowledge construction? How does this differ for each use, user, and venue? While XR enables immersive experiences in information rich VEs, there is a risk that the complexity and richness of these VEs could overwhelm the working memory capacity of the user, thereby negatively impacting the effectiveness of the geovisualization itself.

XR technologies are redefining what is possible for geovisualization and may also redefine our understanding of effective geovisualization use and the role that human factors, such as spatial ability, serve in defining geovisualization effectiveness. This research presents a pilot study of the IMRT as a contemporary measure of mental rotation ability commensurate with modern spatial data representation. Here we explore the relationship between 3D data, spatial ability (specifically mental rotation ability), and VR – examining the impact that stimuli dimensionality and VE complexity have on metal rotation task performance.

6.3. Materials and Methods

6.3.1. Experimental Design

The IMRT experiment was designed to explore the effect that stimuli dimensionality (2D vs. 3D) and VE (background) complexity (simple vs. complex) have on IMRT performance (score and time). The dependent variables (score and time) are evaluated in a repeated measures experiment, with participants as a random factor and dimensionality, VE complexity, biological sex, and start room as fixed factors. Further exploratory analyses evaluated the relationship between IMRT performance and participant movement and the angular difference between MRT stimuli (difficulty).

Based on the research cited above, we propose the IMRT as a contemporary test of mental rotation ability. We hypothesize that:

- Participants' IMRT performance (score and time) will be greater with 3D stimuli than with 2D pictures of those 3D stimuli
- Participants' IMRT performance (score and time) will be greater when the IMRT is completed in the simple VE than in the complex VE.

The 3D IMRT alleviates the cognitive burden imposed by dimensionality crossing, thereby allowing participants to focus on the mental rotation task rather than on imagining 3D shapes from 2D pictures. While it is possible that the peripheral visual cues of the complex VE could allow participants to anchor their mental rotations, the absence of peripheral visuals in the simple VE reduces the overall mental load placed on participants, thereby allowing them to focus solely on the IMRT stimuli.

This study was approved by the institutional Research Ethics Board (20200129).

6.3.2. Materials

The IMRT is a 54-question (30 stereo 3D questions and 24 2D questions) MRT designed exclusively for VR. The test is conducted within one of two unique VEs, both of which contain questions with the same set of 2D and 3D stimuli. The development of this test is outlined in the following subsections.

3D Stimuli Development

The stimuli utilized in the IMRT are based on the 2D line drawings of 3D cubes used by Peters et. al. (1995) in their redrawn version of the Vandenberg & Kuse MRT (1978). We reconstructed the 3D structure of the standard stimuli from the original MRT in Autodesk Maya 2019, and each of the reconstructed stimuli were assigned an X, Y, and Z rotation value (0 - 359 degrees) defined by a random number generator (Microsoft Excel - RANDBETWEEN). The resultant stimuli were exported as 3D models in the OBJ file format.

The 3D models were then imported into Unity (Version 2019.2.13f1), a popular game engine for 2D and 3D multiplatform game and interactive experience development[1], where 30 MRT questions were designed using the developed 3D stimuli. Each question, like the original MRT, consists of a standard stimulus (i.e., criterion figure or target) and four reference stimuli (i.e., alternatives or samples) – two of which match the standard and two which are isomers (mirror-images) of the standard (Figure 6.1). However, unlike the original MRT, the reference stimuli in each question are homogenous and not heterogenous (i.e., distractor stimuli were not included); while this deviates from the traditional MRT (Peters et al. 1995; Vandenberg and Kuse 1978), distractor stimuli were omitted so as to encourage mental rotation rather than the pursuit of distinct features across the stimuli (Shepard and Metzler 1971).

The rotation of the stimuli around the vertical axis was defined by a random number generator, and a combination of that random number generator and sorting were used to determine which of the two reference stimuli in each question would become the mirror-images of the standard stimuli. Additionally, a rotation around the horizontal axis, defined using the random number generator, was applied to six of the 30

[1] www.unity3d.com

3D stimuli. These six (dual rotation) extra stimuli were included in the 3D IMRT (questions 25-30), in accordance with the *very difficult* MRT(C) administered by Peters et al. (1995), but are not included in the performance analyses presented in this manuscript, as our analyses focus only on the 24 single rotation 2D and 3D questions. Nevertheless, the set of 30 questions were exported as a Unity Package to be imported during VR test development.

2D Stimuli Development

The 2D stimuli are orthographic images (as per Peters & Battista, 2008), generated from within Unity, of the 24 single rotation 3D stimuli in the developed set of 30 MRT questions (i.e., excluding the 6 *very difficult stimuli* introduced in the previous section). Orthogonal images were captured of the 3D stimuli that were rotated around the vertical axis only, and each image was captured from the perspective of an orthographic camera positioned directly in-front of each stimulus. All images were saved as PNG files to be imported during VR test development.

IMRT Development

The IMRT was developed for the Oculus Quest[2], a standalone VR system developed by Facebook that operates on the Android OS, using Unity (Version 2019.2.13f1). Several assets from the Unity Asset Store were installed during development - including the Oculus Integration, Virtual Reality Tool Kit (VRTK) (Version 3.3), and Photon Unity Networking (PUN 2) packages.

A graphical user interface (GUI) was designed to resemble the MRT layout of Peters et al. (1995) and Vandenberg and Kuse (1978) (Figure 6.1). The standard stimulus was clearly labeled, to the left of the four reference stimuli, and each reference stimulus was encircled by a black border that functioned to both create separation between the stimuli and served as a button allowing users to submit their answers. Users progress through each of the MRT questions using the Back and Next buttons located below the stimuli, which also serve as the stop and start buttons recording the amount of time users spend on each question. The reference stimuli are enclosed within a circular border, as in Shepherd and Metzler (1971) and Vandenberg and Kuse (1978),

[2] www.oculus.com/quest/

rather than the square border used by Peters et al (1995), to avoid hard points of reference from which users could anchor their rotation of each reference stimulus.

As explained above, the 54-question IMRT is comprised of two separate tests; a 30-question test containing the 3D stimuli (we refer to this as Room A in the VR application) and a 24-question test containing 2D images of the 3D stimuli (Room B in the VR application) (Figure 6.1). While the stimuli in Room B are the same as those contained within the first 24-questions in Room A, following standard experimental procedures, both the order in which the stimuli appear within each question, and the order of the questions themselves, were randomized during development to counter for possible learning and fatigue effects. As such, participants completing all questions in Room A and Room B would effectively answer the same question twice – once in 3D and once in 2D.

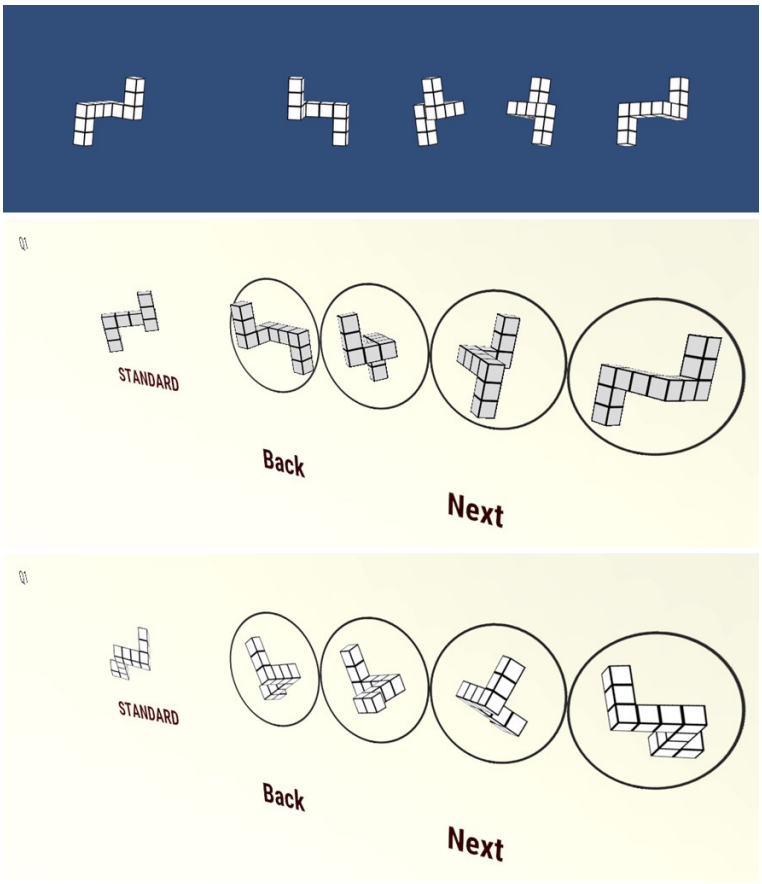

Figure 6.1 **(top) A screenshot from the IMRT question development in Unity. Each question contains a standard stimulus (left) and four reference stimuli (right). These stimuli became the 3D stimuli in Room A (middle) and the 2D stimuli in Room B (bottom). Perspective view provided here to highlight the difference between the 3D and 2D stimuli (i.e., this is not how the stimuli were shown to participants, they always had the same perspective).**

Furthermore, because it has been shown that information processing in 'clean' vs. cluttered (i.e., simple vs. complex) environments may lead to differences in participant performance (e.g., Schnürer et al., 2020), *and* most, if not all MRT studies have been conducted with a 'clean' background, we generated two unique VEs for the IMRT (Figure 6.2) to examine the possible effect of background complexity. The first VE surrounds the user with a perceptually limitless, off-white sphere (simple VE) – developed with the original paper and pencil version of the MRT in mind. The second VE places the user in a furnished, virtual living room (complex VE) – affording visual cues absent from the original MRT and increasing the information intensity of the VE. The scale and design of the virtual living room are a generic representation of a space in which VR may be used, but more importantly, as a space containing objects of varying

size, depth, color, light, and shadow that creates visual complexity contrasting the simple VE. The more complex background represents the *information intensity* of the VE, a defining feature of VEs according to MacEachren et al. (1999). In both VEs, the user remains seated at the centre of the VE, with the GUI appearing directly in front of them at a distance of 1.75 meters (Figure 6.3).

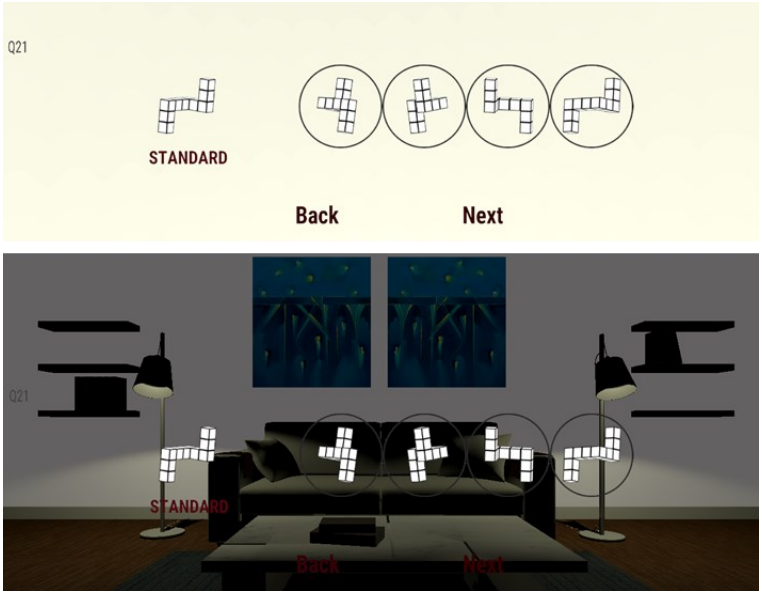

Figure 6.2 **Two unique VEs were developed for the IMRT: (top) a simple, off-white space devoid of visual cues (Test 1); (bottom) a more complex virtual room providing several visual cues (Test 2). Both Test 1 and Test 2 (simple vs complex backgrounds) are conducted in Room A and Room B (2D vs 3D stimuli) shown in Figure 6.1.**

Figure 6.3 A third-person perspective of an IMRT participant (illustrated by the HMD) seated at the centre of the VE with the test stimuli appearing directly in front of them.

Two separate Android Packages (APKs), or Android Apps, were developed for the Oculus Quest using the questions and VEs discussed above. The first, referred to as Test 1, contains 54-questions located within the simple VE; and the second, known as Test 2, consists of the same set of 54-questions, this time situated within the more complex VE (Table 6.1). These APK files were distributed to each of the study participants as assigned.

Table 6.1 Summary of IMRT APKs

		Questions	
APK	**Virtual Environment**	**Room A**	**Room B**
Test 1	Simple - off-white sphere	30-questions (3D stimuli)	24-questions (2D images of 3D stimuli)
Test 2	Complex – furnished virtual room	30-questions (3D stimuli)	24-questions (2D images of 3D stimuli)

Participants

Participants were recruited through followers of the distributed-VR3DUI Slack channel[3] to take part in a one-time study of spatial abilities. Participants were advised that the study would be conducted remotely – mediated over Skype (or similar) – and that they must have access to an Oculus Quest. These prerequisites were necessitated by the ongoing COVID-19 pandemic and restrictions surrounding in-person research. Participants were not offered any incentive for their participation. In total, 29 participants (12 female), ranging in age from 22 to 64 years (M = 33 years, SD = 10.13 years), participated in the study.

Procedure

We sent the participants an email the day before their study date containing a link to the appropriate APK file and instructions regarding APK installation through SideQuest.[4] Participants were each given a unique Participant ID, and while all 29 participants solved all tasks with 2D and 3D conditions in rotated order (Rooms A vs. B), we split them into groups for the simple vs. complex backgrounds (Test 1 vs. Test 2) to keep the experiment duration reasonable (i.e., under one hour). They were, thus, randomly assigned to either Test 1 (14 participants) or Test 2 (15 participants), within which the order was counterbalanced so that they started with either Room A (Test 1: 7 participants, Test 2: 7 participants) or Room B (Test 1: 7 participants, Test 2: 8 participants). On the day of the experiment, upon connecting with each of the study participants via private video conference, consent to participate was confirmed, and we asked participants to complete two online surveys: a personality type survey (Locus of Control) and a demographics survey (Pre-Experiment Questionnaire) which included questions about their color and stereo vision. Participants were then asked about their level of familiarity with the Oculus Quest and, if required, were given a brief introduction to the device. After that, they put their HMD on and launched either Test 1 or Test 2 depending on which version of the IMRT they were assigned. In either of these two tests, participants first enter a virtual lobby where they are introduced to the controls.

---

[3] distributed-vr3dui.slack.com

[4] SideQuest is a third-party application allowing users to install VR content directly to their Oculus Quest via PC, Mac, or Linux (sidequestvr.com)

They are then asked to confirm their connection to the internet and are reminded to remain seated throughout the test.

After selecting the designated room and submitting their participant ID number, we provided the participants with an introduction to the IMRT. Onscreen text, as well as verbal instructions delivered by the moderator, provided an overview of the controls and a detailed explanation of the objective. In short, for each question, they were instructed to select the two reference objects that they believed are rotated versions of the standard. At this stage, participants completed five sample questions, allowing them to familiarize themselves with both the GUI and their objective. Finally, an overview of the procedure for each test room (outlined below) was provided before participants began the test.

Following the procedure by Peters et al. (1995), in Room A (stereo 3D stimuli), participants had up to seven-and-a-half minutes to answer as many questions as possible from a total of 30-questions. The questions were arranged into two sets of 12-questions and one set of six-questions, with a one-minute break in between each set. Participants had up to three-minutes to answer each set of 12-questions and one-and-a-half minutes for the remaining six-questions. In Room B (2D stimuli), participants had up to six-minutes to answer 24-questions, arranged as two sets of 12-questions with a one-minute break in between each set. Again, participants had up to three-minutes to complete each 12-question set. Participants were then informed that a pop-up message would appear should they exceed any of the allotted time limits, thereby ending that round of questions and advancing them to the next stage of the test.

As a final step prior to beginning the test, the moderator reiterated the objective, asked the participants if they understood the objective, and asked if they had any questions. The participants were then advised that they could begin the test when ready and the moderator initiated a recording of the video conference to document the participants as they completed the IMRT. Upon reaching the conclusion of a test room, participants submitted their answers and proceeded to the next test room (i.e., Room A if they started with Room B, and vice versa). Participants then proceeded through the examples and the test procedure overview before completing the second test room. At the conclusion of both test rooms, participants were asked to remove the HMD and complete a third online survey, the Post-Experiment Questionnaire. Participants were

then thanked for their time and were asked if they had any questions, comments, or concerns with the test procedure. Each study sessions required approximately 45-60 minutes, of which 15-20 minutes were necessary for the IMRT itself. Participants were not offered any compensation.

Data Analysis

Each completed IMRT generated a dataset documenting the participants' response to each of the 2D and 3D IMRT questions and the amount of time required to provide that response. The test number, test room, responses, and time data were compiled within the IMRT application, and upon the completion of each test, were automatically submitted online. Each submitted dataset was then recorded and scored in Microsoft Excel. Time is reported as the mean time per question (time per question / the number of questions answered) for each participant.

As an additional post-hoc analysis, we analyzed each video documenting study participants as they completed the IMRT and quantified participants' head and body movements. While participants were instructed to remain seated, they were not limited in their ability to change their perspective by moving their head or body in any direction. For this analysis, movement was defined as "purposeful head or body movements – beyond simply looking back and forth – performed to modify the user's perspective in an effort to collect additional information about the reference objects." Movements in the left-right, forward-back, and up-down directions were recorded, and the sum of all recorded movements provided an overall movement score for each participant. Movement was only documented for the 3D IMRT, as movement during the 2D IMRT would not yield additional information about the structure of the objects

6.4. Results and Discussion

The 2D and 3D IMRTs were each scored out of 24 points, following the 1-point for two correct answers scoring methodology (see Peters 2005); the six *difficult* dual rotation questions in the 3D IMRT (i.e., questions 25-30 in Room A) were not included in the participants' 3D IMRT scores for a balanced and fair comparison between 2D and 3D versions of the test. Participant performance was evaluated using a mixed model analysis of variance with either score or time (average time per question) as the dependent variable, participants as a random factor, and biological sex, VE complexity

(Test 1 or Test 2), start room (2D or 3D first), and dimensionality as fixed factors. Additional exploratory analyses examined how participant movement and the angular difference between stimuli (difficulty) interact with IMRT performance. The effect size for each of these analyses was calculated as Cohen's *d* ($d = M_1 - M_2 / SD_{pooled}$) or Hedges' *g* ($g = M_1 - M_2 / SD^*_{pooled}$) and a correction factor was applied for samples <50. The results of these analyses are presented in the following subsections and an overview is presented in Figure 6.4.

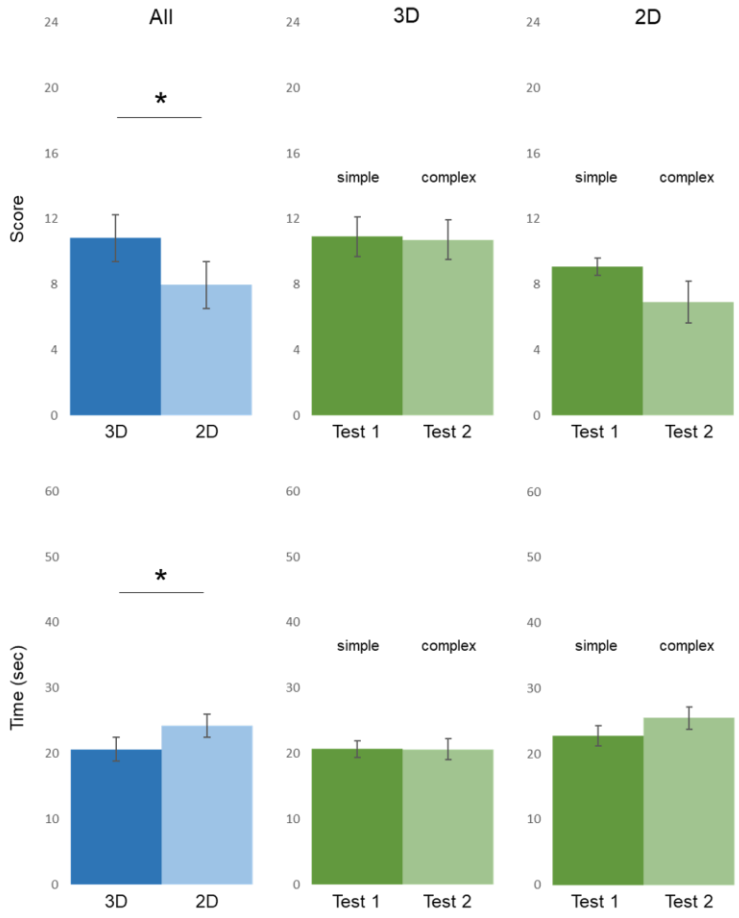

Figure 6.4 **Main effects of dimensionality for test score (top left) and time (bottom left) for all participants, and main effects of VE complexity (3D: middle top and bottom; 2D: right top and bottom) on IMRT performance (score and average time per question).**

* p < .05. Error bars: SEM.

6.4.1. Main Effects and Interactions

The IMRT score analysis revealed a significant main effect of dimensionality, $F(1,21) = 13.54$, $p < 0.01$, $d = .58$, indicating that 3D IMRT score (M = 10.83, SE 0.90) was significantly greater than 2D IMRT score (M = 7.96, SE = 0.88). There was not a statistically significant effect of biological sex, VE complexity, or start room on IMRT score, nor were there statistically significant interactions between effects. The results of the fixed effect tests are presented in Table 6.2. The REML variance component estimates indicate that the variance component associated with participants accounts for 71.57% of the variation in the IMRT score data (Table 6.3).

Table 6.2 IMRT Score Fixed Effect Tests

Source	DF	DFDen	F Ratio	Prob > F
Biological Sex	1	21	2.1266	0.1596
VE Complexity	1	21	0.017	0.8974
Start Room	1	21	1.0137	0.3255
Dimensionality	1	21	13.5425	0.0014
Biological Sex*VE Complexity	1	21	0.0354	0.8526
Biological Sex*Start Room	1	21	0.0247	0.8767
Biological Sex*Dimensionality	1	21	0.0014	0.97
VE Complexity*Start Room	1	21	1.3703	0.2549
VE Complexity*Dimensionality	1	21	1.2661	0.2732
Start Room*Dimensionality	1	21	0.0014	0.97
Biological Sex*VE Complexity*Start Room	1	21	1.2488	0.2764
Biological Sex*VE Complexity*Dimensionality	1	21	0.4045	0.5317
Biological Sex*Start Room*Dimensionality	1	21	2.3664	0.1389
VE Complexity*Start Room*Dimensionality	1	21	0.0003	0.9871
Biological Sex*VE Complexity*Start Room*Dimensionality	1	21	3.1595	0.09

Table 6.3 IMRT Score REML Variance Component Estimates

Random Effect	Var Ratio	Var Component	Std Error	95% Lower	95% Upper	Wald p-Value	Pct of Total
Participant	2.517	15.863	5.948	4.205	27.522	0.0077	71.567
Residual		6.302	1.945	3.730	12.871		28.433
Total		22.165	5.948	13.936	40.659		100

The IMRT time analysis also revealed a significant main effect of dimensionality, $F(1,21) = 4.95$, $p < 0.05$, $d = .52$, indicating that 3D IMRT time (M = 20.65, SE 1.08) was

significantly less than 2D IMRT time (M = 24.20, SE = 1.36). There was not a statistically significant effect of biological sex, VE complexity, or start room on IMRT score; however, there was a significant interaction between biological sex and VE complexity, $F(1,21) = 4.36$, $p < 0.05$. There were no other statistically significant interactions between effects. The results of the fixed effect tests are presented in Table 6.4. The REML variance component estimates indicate that the variance component associated with participants accounts for 61.17% of the variation in the IMRT time data (Table 6.5).

Table 6.4 IMRT Time Fixed Effect Tests

Source	DF	DFDen	F Ratio	Prob > F
Biological Sex	1	21	0.3689	0.5501
VE Complexity	1	21	0.2902	0.5958
Start Room	1	21	0.3773	0.5456
Dimensionality	1	21	4.9529	0.0371
Biological Sex*VE Complexity	1	21	4.3658	0.049
Biological Sex*Start Room	1	21	0.0014	0.9708
Biological Sex*Dimensionality	1	21	0.1404	0.7117
VE Complexity*Start Room	1	21	0.3459	0.5627
VE Complexity*Dimensionality	1	21	2.1922	0.1536
Start Room*Dimensionality	1	21	3.8712	0.0625
Biological Sex*VE Complexity*Start Room	1	21	1.5039	0.2337
Biological Sex*VE Complexity*Dimensionality	1	21	3.9097	0.0613
Biological Sex*Start Room*Dimensionality	1	21	0.5676	0.4596
VE Complexity*Start Room*Dimensionality	1	21	0.0769	0.7842
Biological Sex*VE Complexity*Start Room*Dimensionality	1	21	0.9132	0.3501

Table 6.5 IMRT Time REML Variance Component Estimates

Random Effect	Var Ratio	Var Component	Std Error	95% Lower	95% Upper	Wald p-Value	Pct of Total
Participant	1.575	23.102	9.662	4.166	42.039	0.0168	61.166
Residual		14.667	4.526	8.682	29.954		38.834
Total		37.770	9.662	24.208	67.068		100

Dimensionality

As shown in Figure 6.4 and 6.5, participants' average IMRT scores are higher overall with the 3D version and participants took less time to complete the mental rotation tasks. These results clearly demonstrate that mental rotation task performance (score and average time per question) is affected by the dimensionality of the stimuli,

thus our main working hypothesis is retained. The size of the dimensionality effect was medium for both score (d = .60) and time (d = .54).

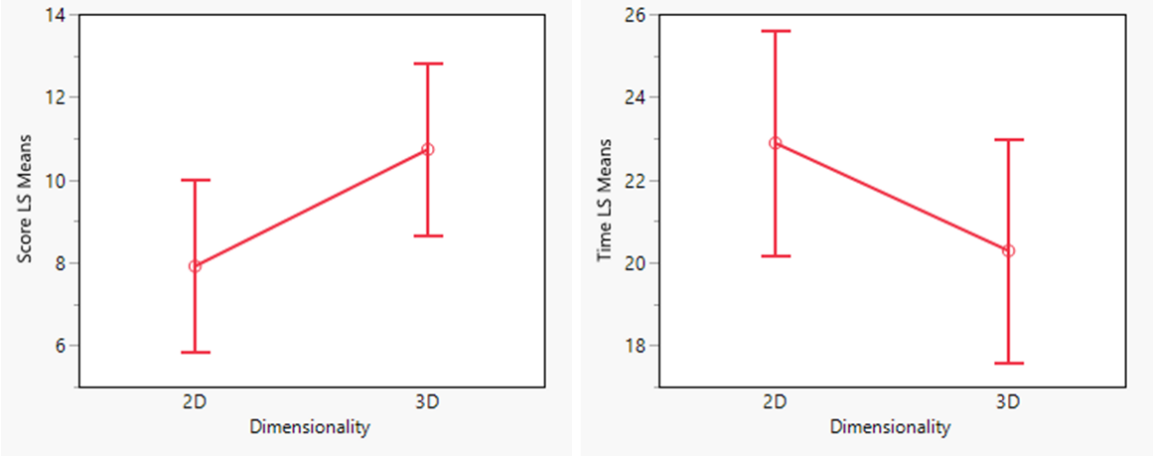

Figure 6.5 LS means plots of score (left) and time (right) for the 2D and 3D IMRT.

The inclusion of 3D objects rather than 2D images of those objects in the IMRT resulted in higher mean scores and lower average time per question; however, this does not necessarily prove that mental rotations are performed more accurately or more rapidly with 3D objects, but that our ability (spatial or otherwise) to comprehend the overall 3D structure of the 3D object is greater when it is perceived as a 3D object rather than as a 2D image of a 3D object. As the 3D IMRT alleviates the need for dimensionality crossing, or the mental processing required to transform a spatial problem presented in 2D into a 3D solution (Voyer, Voyer, and Bryden 1995), this improved performance was expected.

VE Complexity

The complexity of the background (i.e., varying visual cues and information intensity) on which the cubes were displayed did not have a statistically significant effect on IMRT score or time (see Figure 6.4). However, the interaction between VE complexity and biological sex did have a statistically significant effect on IMRT time; female participants required more time per question in the complex VE (Test 2) than the simple VE (Test 1) and the opposite interaction was noted for male participants (Figure 6.6). While the three-way interaction between VE complexity, biological sex, and dimensionality was not statistically significant, $F(1,21) = 3.91$, $p = .06$, male and female participants' 3D IMRT time was less than their 2D IMRT time in the complex VE (Test 2)

but not in the simple VE (Test 1), where female and not male participants required more time for the 3D IMRT than the 2D IMRT (Figure 6.6). These interactions suggest VE complexity has a differential impact on males and females completing mental rotations tasks and that more data should be collected to verify that this pattern is stable.

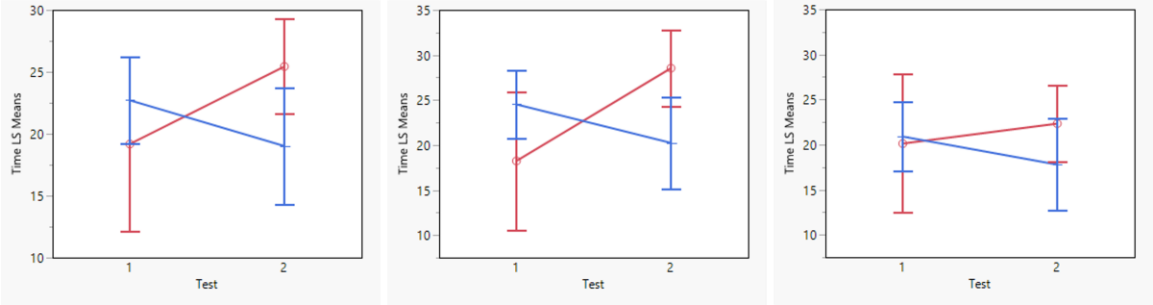

Figure 6.6 LS means plots of overall (left), 2D (middle), and 3D (right) IMRT time for male (blue) and female (red) participants completing Test 1 (simple VE) and Test 2 (complex VE).

The VE complexity effect size was greater for 2D IMRT score (g = .43) and time (g = .34) than 3D IMRT score (g = .04) and time (g = .004). This difference is notable and suggests that background does affect mental rotation task performance when those mental rotations are performed with 2D images. While Peters & Battista (2008) offer a library of MRT figures with both black and white backgrounds – suggesting that this choice of backgrounds is inconsequential – they provide no guidance regarding the geometry of the shape surrounding each MRT stimuli, although Peters et al. (1995) opted for a square rather than a circle as per Shepard & Metzler (1971) and Vandenberg & Kuse (1978). Despite the apparent fastidiousness, small details such as these, and by extension the details of a 3D VE, might be important to consider and further research on the design of VR visualization environments is necessary to better understand the implications of the context in which mental rotations must be conducted.

Biological Sex

The study was not designed to examine sex differences in the sense that we did not control for all possible confounding factors between our male and female participants. However, since many previous MRT studies have reported differences based on biological sex, *and* it has been shown in one study that the stereoscopic versions of the MRT might reduce gender differences, we present an exploratory analysis here. Biological sex did not have a statistically significant effect on IMRT score

or time. On average, males (M_{3D} = 19.85, M_{2D} = 22.79, *g* = .21) and females (M_{3D} = 21.79, M_{2D} = 26.20, *g* = .21) required less time per question for the 3D IMRT than the 2D IMRT, and males (M_{3D} = 11.88, M_{2D} = 9.35, *g* = .47) and females (M_{3D} = 9.33, M_{2D} = 6.00, *g* = .79) scored higher on the 3D IMRT than the 2D IMRT.

The results of the 2D IMRT nearly replicate the sex effect reported throughout the conventional MRT literature (see McWilliams et al., 1997; Parsons et al., 2004; Peters et al., 1995), where the corrected effect size recorded here (*g* = .70) falls just below the expected range (0.75 – 1.12) for MRTs scored using the one point for both correct answers rubric (Voyer, Voyer, and Bryden 1995; Linn and Petersen 1985). However, the corrected sex effect was smaller (*g* = .50) for the 3D IMRT, supporting the notion that the sex effect can be reduced by eliminating the processing demands of dimensionality crossing (McWilliams, Hamilton, and Muncer 1997). While this effect size is not negligible, and is greater than the *d* = .05 reported by Parsons et al. (2004) in their VRSR study, it is clear that the 3D IMRT does not produce the same sex effect as the traditional MRT and that female participants realized greater performance gains when the test was performed with 3D objects.

Start Room

To counterbalance against a possible learning effect, we presented the 2D and 3D stimuli in rotated order; those that started in Room A completed the 3D IMRT first, while those that started in Room B completed the 2D IMRT first. According to our analysis, start room did not have a statistically significant effect on IMRT score or time, nor were there statistically significant interactions. However, the mean 3D IMRT scores (M_{RoomA} = 11.21, M_{RoomB} = 10.47, *g* = .14) and 2D IMRT scores (M_{RoomA} = 9.14, M_{RoomB} = 6.87, *g* = .46) were higher for those starting in Room A (3D) than those starting in Room B (2D). While the effect sizes are small, the start room effect was three times greater when participants started in Room A (3D) than Room B (2D).

The learning effect, or the element of practice, is well documented in the MRT literature. In a four week long study in which the MRT was administered weekly, Peters et al. (1995) found that the mean MRT performance (score) of both male and female participants increased with each successive test, with the largest performance gain occurring between weeks one and two. Casey & Brabeck (1989) reported a similar effect when administering the MRT twice, with only a five-minute break between each

test. In the IMRT, in which the tests were administered with less than five-minutes between each test, the learning effect did not play a significant role, as there was not a statistically significant difference between 2D or 3D IMRT results based on test order. This could be a function of the different order in which the questions were presented and arranged (i.e., while the questions are identical between 2D and 3D conditions, the question order within each test is randomized), but it is more likely a function of the dimensionality difference between the two tests. The IMRT results show a greater effect size for those participants starting with the 3D objects than those that started with the 2D images. This would suggest that by first working with 3D objects, participants were better equipped to work with 2D images of those 3D objects, perhaps by improving their ability to visualize 3D structures and perform dimensionality crossing tasks.

6.4.2. Exploratory Analyses

Participant Movement

When presented in stereo 3D, head and body movements made by the participants during the 3D IMRT offer an opportunity to gather additional information about the structure of the 3D objects in the 3D IMRT, which might have a potentially confounding effect. While participants were seated during the experiment, their ability to move was not restricted. We conducted a post-hoc analysis of their movements to better understand how often participants attempted to gather additional information about the cubes by looking at them from slightly different perspectives. A movement score was established for 23 of the 3D IMRT participants ($\mu = 22.5$, $\sigma = 18.7$). A linear regression analysis revealed that movement did not have statistically significant effect on 3D IMRT score ($F(1,21) = 0.005$, $p = 0.94$) or time ($F(1,21) = 2.67$, $p = 0.12$), suggesting that the additional information gained, or that was at least sought out, did not translate to higher 3D IMRT performance.

Angular Difference

Similarly, as in the movement analysis presented above, how *much* the test cubes are rotated can affect their level of difficulty and it is interesting, and arguably necessary, to control for this. Our analysis (Figure 6.7) yielded that the near linear relationship that Shepard & Metzler (1971) observed between reaction time and the angular difference between pairs – calculated here as the net absolute value of the

smallest angular difference between each reference object and the standard – was not present for the IMRT. The average time per question did increase as the total angular difference increased, but the relationship was not linear. The total angular difference also impacted the accuracy of responses, as the correct answer was provided less frequently as the total angular difference increased. A mixed model analysis of variance revealed that total angular difference had a statistically significant effect on both time (p = .01) and the accuracy of responses (p = .0002), but that there was not a statistically significant difference between 2D and 3D time (p = .29) or accuracy of response (p = .32) based on these angular differences. Therefore, our findings confirm that those questions with a greater total angular difference were more difficult, as they required more time and were answered correctly less frequently in both 2D and 3D.

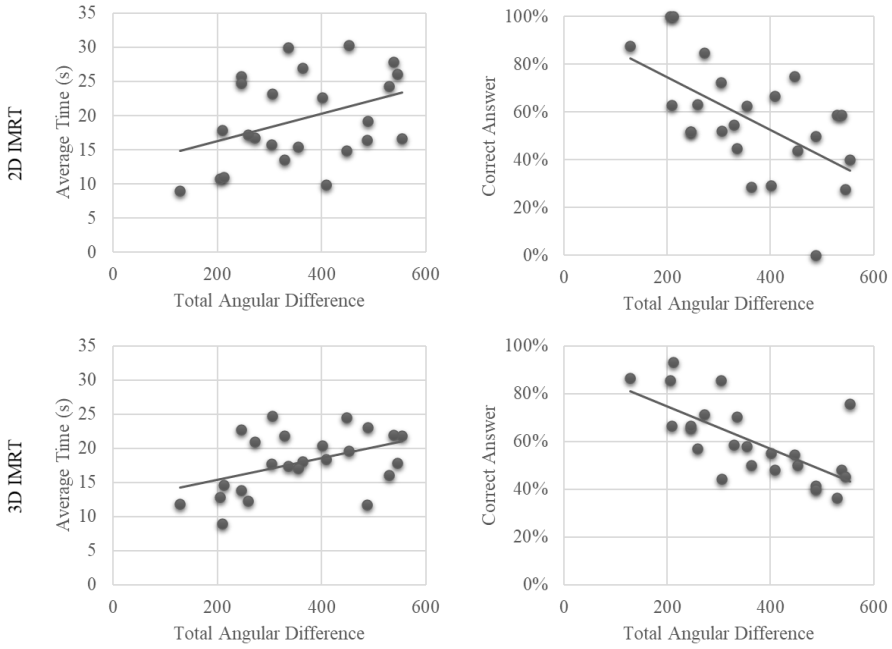

Figure 6.7 **The total angular difference was calculated as the net absolute value of the smallest angular difference between each reference object and the standard. (top left and right) The average time per question increased as the total angular difference increased. (bottom left and right) The accuracy with which participants answered questions decreased as the total angular difference increased.**

6.4.3. Meta Factors

Speed vs Accuracy

As explained in the Procedure section, participant performance was limited by the 3-minute time constraint placed on each 12-question set and many participants expressed their frustration that time had expired prior to them answering all questions. Peters et al. (1995) note that their MRT may be performed with either a 3-minute or 4-minute time constraint (per 12-question set), and others have conducted the MRT without a time constraint. While removing the time constraint may reduce the established MRT sex effect, this adaptation challenges the ecological validity of the MRT as a test of spatial abilities, which have naturally evolved under the confines of time (Peters 2005). The effect of the time constraint on IMRT performance is evident in Figure 6.8, where the percent of answered questions are shown for females and males. The 2D IMRT graphs in this figure resemble those of Peters (2005), indicating that males attempted more questions than females, and that both sexes saw an increase in attempted questions for the second set of 12-questions, which Peters attributed to a “mini practice effect”. However, for the 3D IMRT the male and female graphs are similar, with both sexes attempting a similar number of questions and the practice (learning) effect being less pronounced.

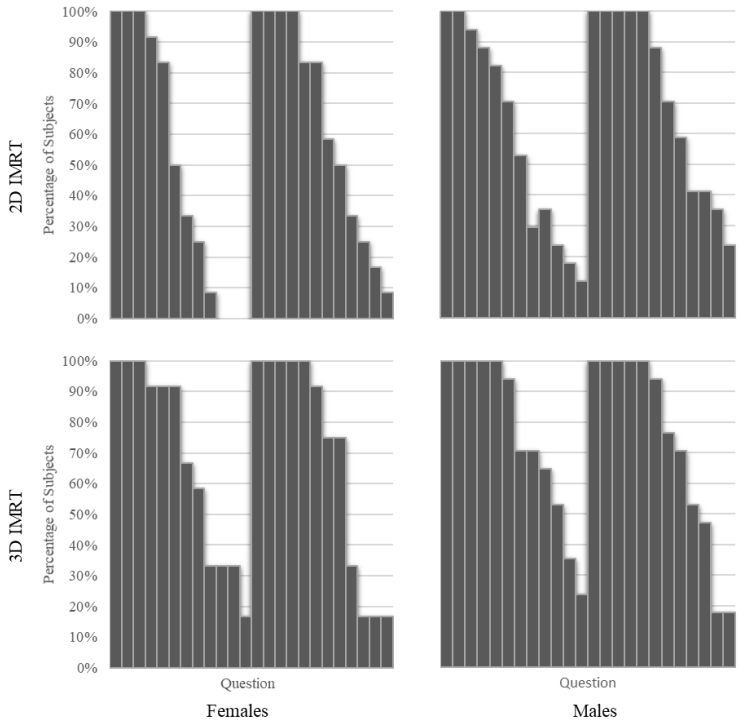

Figure 6.8 The percent of participants answering a question as a function of question order. 2D IMRT scores are presented for females (top left) and males (top right) and 3D IMRT scores are presented for females (bottom left) and males (bottom right).

While time constraints play a vital role in determining the number of questions that can be answered, IMRT performance is also a function of accuracy. With time constraints in place, the only path to obtaining a higher score is to decrease the amount of time spent on each question - at the risk of decreasing accuracy - or to increase accuracy - at the risk of decreasing overall speed. The speed (average time per question) and accuracy (score) of male and female participants are plotted against each other in Figure 6.9 to examine the possible speed-accuracy trade-off.

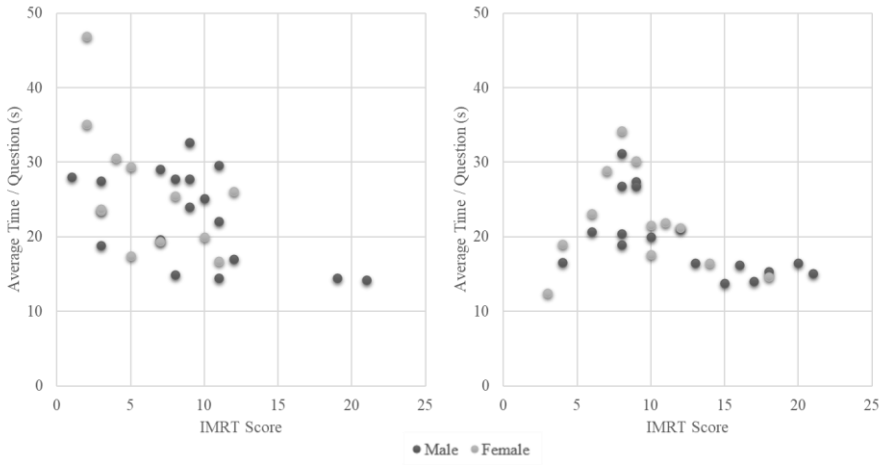

Figure 6.9 Comparing the relationship between speed (average time/question) and accuracy (score) for the (left) 2D IMRT and (right) 3D IMRT.

The two distributions in Figure 6.9 are quite dissimilar, with the 2D IMRT data points being more randomly distributed than the 3D IMRT data points. For the 3D IMRT, those that spent less time per question tended to achieve a higher score, whereas for the 2D IMRT, a relationship between speed and time was less apparent. This raises questions about the speed-accuracy trade-off and its relationship to mental rotation ability and IMRT performance in 2D and 3D. Scali, Brownlow, & Hicks (2000) found that men outperformed women on the MRT only when scored in a particular manner and when explicit instructions were provided to focus on accuracy, and not when participants were explicitly instructed to focus on speed or were not given explicit instructions either way. IMRT participants were not given explicit instructions either way, nor was a relationship between speed and accuracy implied. Further research into the speed-accuracy trade-off for the IMRT may provide valuable insight into the mental rotation ability of males and females in 2D and 3D, as the observed performance differences are more likely the product of nurture differences than nature differences and warrant further evaluation.

An Element of Luck

As with any multiple-choice question, it is possible that respondents provide a correct answer based on a lucky guess. For the IMRT, the 1-point for two correct answers scoring method was selected, as it both discourages guessing and has proven to yield a larger sex-effect (Peters 2005). While the probability of participants receiving one point based on two lucky guesses was minimal (8.3%), we felt it was pertinent to

assess the IMRTs for unusual responses. This assessment was conducted using the Student-Problem (SP) chart originally created by Takahiro Sato (Mok et al., 2012).

The SP chart is a student-item response matrix – students in this case are the IMRT participants – where rows represent student responses and columns represent items (questions). One point is awarded for a correct response and no points for an incorrect response, and the row and column totals are then calculated. These totals are then used to sort the rows and columns in descending order and either a student curve (S-Curve) or item curve (P-Curve) can be constructed to reveal student performance or item responses that deviate from the expectation. From this, a student (participant) type and item type can be determined using a Modified Caution Index (MCI) calculation (see Mok et al., 2012) that identifies students and items that warrant careful consideration.

Figure 6.10 presents the participant type and item type charts, in which the MCI values are plotted against score (questions answered correctly / questions answered) for the 2D and 3D IMRT. A vertical line is drawn at an MCI value of 0.3 and a horizontal line is drawn at a score of 0.5, providing four quadrants distinguishing the student and item types. Ideally, all participant type data points would fall in the upper left quadrant (satisfactory performance) and few points in the lower right quadrant (unsatisfactory and unstable performance), and all item type data points in the upper left quadrant (fair question) with few points in the lower quadrants (unfair, too difficult).

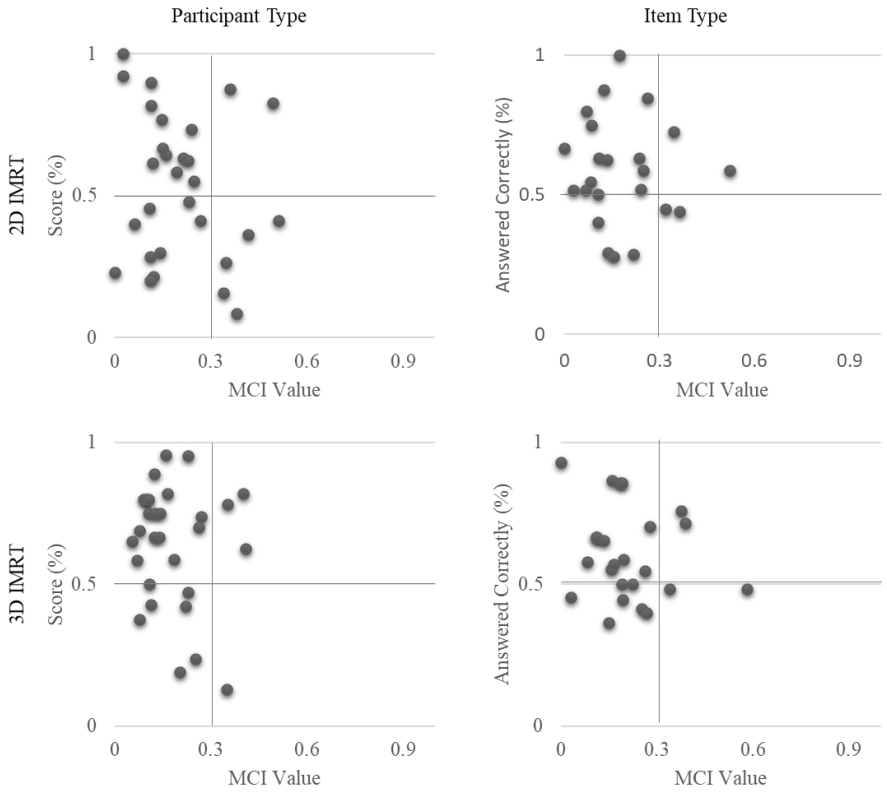

Figure 6.10 The Participant Type and Item Type charts plot score (questions answered correctly / questions answered) against MCI value to classify student (participant) performance and item (question) difficulty. A vertical line at MCI = 0.3 and a horizontal line at score = 0.5 divide the chart into four quadrants. Ideally, all data points should fall in the upper left quadrant.

Based on the SP analyses, more participant type data points fall in the upper left quadrant for the 3D IMRT (17) than the 2D IMRT (13) and fewer data points fall in the lower right quadrant for the 3D IMRT (1) than the 2D IMRT (5). Participant performance could therefore be interpreted as better overall on the 3D IMRT than the 2D IMRT. The item type data points tend to cluster between the upper left and lower right quadrant for the 3D IMRT and are more dispersed between these two quadrants for the 2D IMRT, indicating greater parity in question difficulty in 3D than in 2D. However, when score is a function of overall performance and not simply performance on the questions answered, the participant and item types are drastically different, where >50% of the participant and item type data points are in the lower left quadrant.

Overall, the SP chart and participant and item type analyses suggest that luck was not a factor in the IMRT scores, and that participant performance and item

responses did not deviate from what would be expected. These analyses also suggest that 3D IMRT performance was less erratic than 2D IMRT performance and that there was greater parity between participants when IMRT questions were presented in 3D.

6.5. Overall Discussion

We developed the IMRT as a tool to explore the effect that emerging XR technologies have on mental rotation ability. While it may be true that the IMRT subverts the intended objective of the original MRT by offering 3D rather than 2D stimuli, thus alleviating the cognitive burden of dimensionality crossing, this is precisely what XR technology has done to geovisualization; XR has changed the way we perceive and process spatial data. With XR, we no longer read a 2D map, at least not always. If we are going to gauge the utility of XR-based geovisualizations based on users' individual differences defined through traditional metrics (e.g., the MRT) which do not properly account for the impact XR technologies may have on those metrics, then we are going to misjudge the utility of those geovisualizations. By exploring how XR technologies change our ability to perceive or comprehend certain 3D phenomena, we can begin to purposefully apply these technologies to address the individual differences and limitations which impact our ability to perform certain visualization-based tasks.

The primary objectives of this study were to assess the differences in mental rotation ability based on dimensionality and VE complexity. Our data show that when mental rotation tests are performed in immersive VR there are significant differences in both score and time when those tests contain 3D versus 2D stimuli. Also, importantly, the dimensionality effect was strong for female participants, whose mean 3D score was 0.79 standard deviations above their mean 2D score. There were clear differences in 2D IMRT performance between males and females, and those differences *(g* = .70) aligned with the expected MRT sex-differences reported in the literature (d = .75 – 1.12) (Voyer, Voyer, and Bryden 1995; Linn and Petersen 1985). However, the sex effect was reduced for the 3D IMRT *(g* = .50), suggesting that females benefited more than males in the transition from 2D to 3D. These findings, even though they may be considered preliminary, are an interesting contribution to the debate regarding biological sex and MRT, as well as the nature of the MRT tasks themselves. The narrowing gap between the two sexes in the stereo 3D condition confirms the findings of Peters et al. (1995) and suggests that the different MRT scores between men and women are at least partially

explained by the ability to visualize the 2D shapes in 3D in mind, and not only about the ability to *rotate* them. This 2D-3D transition also appears to have lessened the influence of VE complexity, which negatively impacted 2D IMRT performance, as the VE complexity effect size was greater for 2D IMRT scores *(g* = .43) than it was for 3D IMRT scores *(g* = .04).

In a series of secondary analyses, we explored various post-hoc hypotheses and controlled for possible confounding effects of participant *movemen*t and *angular disparity* (i.e., question difficulty), on IMRT performance. While each of these analyses provided interesting insights into their effect on mental rotation ability, they also raised some interesting questions concerning mental rotation ability, spatial abilities in general, and immersive geovisualizations that warrant further study, such as; *how is learning impacted by dimensionality crossing (2D to 3D and 3D to 2D)*? *what are users looking at and looking for when they change their perspective in an immersive VE?* and, *does a low score reflect a lack of ability or a lack of time?* These questions can be investigated as follow-up questions in future research to better establish our understanding of the IMRT and similar solutions.

Nonetheless, our study establishes the merit of the IMRT, the results of which suggest that the IMRT has a significant effect on the quantification (or classification) of mental rotation ability compared to conventional (pen and paper, or on screen 2D) tests. It is our hope that this IMRT implementation lays the initial groundwork for others to expand upon it. It is important to note that we did not have the option to control for all possible variables (e.g., age, education, XR experience) in our sample population due to the limitations imposed by the global COVID-19 pandemic as well as due to the scope of the study. A natural next step for future research could be to consider variables such as these and explore interactions between them.

6.5.1. Limitations

While this research represents a step forward in the analysis of human factors and geovisualization, it is not without its limitations. The primary limitation of this study is the sample size (n = 29) and the population from which this sample was drawn. Restrictions addressing the COVID-19 pandemic prohibited in-person research, thereby forcing data collection from a population owning, or having access to, an Oculus Quest.

This requirement both reduced the population from which our sample could be drawn and introduced a bias towards those with established 3D skills and VR experience. The small sample size also impacted our ability to explore interactions between variables.

Additionally, the remote method of data capture reduced our ability to control the study environment. Of the 29 IMRT participants, 11 participated from work or school and 18 participated from home. While participants were asked to ensure a quiet and disturbance free environment, and most did, there is inherent variability across the range of environments that may have influenced individual IMRT performance. Arguably, such variability is not as critical as in other studies given that the participants are wearing a headset that shuts any contact to the actual room they are in, however, it is nonetheless important to note as it might still have an impact in the way people feel when they are at home vs. at the office.

6.5.2. Future Research

Future research expanding on this study should first address the sample and environment limitation to ensure the repeatability of the IMRT. Second, the IMRT only evaluates mental rotation performance in VR, leaving the impact of other XR display devices yet to be studied. The IMRT has been adapted for HoloLens2 and Android-based mobile devices and future research efforts will evaluate the impact that MR and AR have on mental rotation task performance.

6.6. Conclusion

The results from this study suggest that MRT performance (score and average time per question) is greater when mental rotations are performed with stereo 3D objects rather than 2D images of those 3D objects. Overall, the 3D IMRT scores were greater than the 2D IMRT scores and the average 3D IMRT time per question was less than the average 2D IMRT time per question. This does not confirm that mental rotations are performed more accurately or more rapidly with stereo 3D objects but suggests that our ability (spatial or otherwise) to understand and compare the 3D structure of 3D objects is greater when they are perceived in 3D, thereby alleviating the cognitively challenging task of dimensionality crossing imposed by 2D representations of 3D structures.

Our results suggest that this 3D performance advantage was greater for females (g = .79) than males (g = .47). The biological sex effect for the 2D IMRT *(*g = .70) falls just short of the expected gender effect values reported by Voyer et al. (1995) and others. However, the biological sex effect for the 3D IMRT *(*g = .50) was less than the expected effect range, but not as low as reported by those using real 3D objects and other immersive interfaces (McWilliams, Hamilton, and Muncer 1997; Parsons et al. 2004). Our results also suggest that the physical characteristics of the VE (i.e., the visual complexity of the background when solving the MRT tasks) have a greater impact on mental rotation performance when those mental rotations are performed with 2D images rather than 3D objects. It is possible that the design of the peripheral elements of a VE have minimal impact on our ability to perceive and comprehend 3D data.

Our study contributes to the assessment of human factors and their impact on geovisualizations designed for VR interfaces. These results suggest that there is value in developing VR interfaces for visual analyses of 3D data, and that with the opportunity for natural data interaction, the performance advantage over conventional 2D mediums could be even greater. However, this study does not prove that visualizing 3D data in VR is superior to other interfaces (desktop, tablet, AR etc.) and further research comparing these interfaces is required. Overall, we hope that this study highlights the importance of performance metrics that account for the effect that emerging technologies have on those metrics, taking us one step closer to understanding the data, use, and user combinations that maximize the transfer of knowledge.

Acknowledgements

We thank Dr. Ortega for piloting the distributed-VR3DUI Slack channel that allowed us to recruit participants remotely during the global pandemic, and all those who participated in this research.

Funding

We acknowledge the support of the Natural Sciences and Engineering Research Council of Canada (NSERC), [PGSD3-518954-2018].

Cette recherche a été financée par le Conseil de recherches en sciences naturelles et en génie du Canada (CRSNG), [PGSD3-518954-2018].

References

Alqahtani, Asmaa Saeed, Lamya Foaud Daghestani, and Lamiaa Fattouh Ibrahim. 2017. "Semi-Immersive Virtual Reality for Improving the Mental Rotation Skill for Engineering Students: An Experimental Study." *Computer Engineering & Information Technology* 06 (04). https://doi.org/10.4172/2324-9307.1000180.

Caissie, Andre F., Francois Vigneau, and Douglas A. Bors. 2009. "What Does the Mental Rotation Test Measure? An Analysis of Item Difficulty and Item Characteristics." *The Open Psychology Journal* 2 (1): 94–102. https://doi.org/10.2174/1874350100902010094.

Casey, Beth M. 2013. "Individual and Group Differences in Spatial Ability." In *Handbook of Spatial Cognition.*, 117–34. Washington: American Psychological Association. https://doi.org/10.1037/13936-007.

Casey, M. Beth, and Mary M. Brabeck. 1989. "Exceptions to the Male Advantage on a Spatial Task: Family Handedness and College Major as Factors Identifying Women Who Excel." *Neuropsychologia* 27 (5): 689–96. https://doi.org/10.1016/0028-3932(89)90113-9.

Collins, David W., and Doreen Kimura. 1997. "A Large Sex Difference on a Two-Dimensional Mental Rotation Task." *Behavioral Neuroscience* 111 (4): 845–49. https://doi.org/10.1037/0735-7044.111.4.845.

Çöltekin, A, I Lokka, and M Zahner. 2016. "On the Usability and Usefulness of 3D (Geo)Visualizations - A Focus on Virtual Reality Environments." In *International Archives of the Photogrammetry, Remote Sensing and Spatial Information Sciences - ISPRS Archives*, 41:387–92. https://doi.org/10.5194/isprsarchives-XLI-B2-387-2016.

Çöltekin, Arzu, Susanne Bleisch, Gennady Andrienko, and Jason Dykes. 2017. "Persistent Challenges in Geovisualization – a Community Perspective." *International Journal of Cartography* 9333: 1–25. https://doi.org/10.1080/23729333.2017.1302910.

Çöltekin, Arzu, Rebecca Francelet, Kai Florian Richter, John Thoresen, and Sara Irina Fabrikant. 2018. "The Effects of Visual Realism, Spatial Abilities, and Competition on Performance in Map-Based Route Learning in Men." *Cartography and Geographic Information Science* 45 (4): 339–53. https://doi.org/10.1080/15230406.2017.1344569.

Çöltekin, Arzu, Amy L. Griffin, Aidan Slingsby, Anthony C. Robinson, Sidonie Christophe, Victoria Rautenbach, Min Chen, Christopher Pettit, and Alexander Klippel. 2020. *Geospatial Information Visualization and Extended Reality Displays*. *Manual of Digital Earth*. https://doi.org/10.1007/978-981-32-9915-3_7.

Coxon, Matthew, Nathan Kelly, and Sarah Page. 2016. “Individual Differences in Virtual Reality: Are Spatial Presence and Spatial Ability Linked?” *Virtual Reality* 20 (4): 203–12. https://doi.org/10.1007/s10055-016-0292-x.

Datta, Sumona, and Debdulal Dutta Roy. 2016. “Construction of Test Measuring Mental Rotation Ability of Adolescent High School Students.” *The International Journal of Indian Psychology* 3 (2): 91–100.

Debelak, Rudolf, Georg Gittler, and Martin Arendasy. 2014. “On Gender Differences in Mental Rotation Processing Speed.” *Learning and Individual Differences* 29: 8–17. https://doi.org/10.1016/j.lindif.2013.10.003.

Devaux, A., C. Hoarau, M. Brédif, and S. Christophe. 2018. “3D Urban Geovisualization: In Situ Augmented and Mixed Reality Experiments.” *ISPRS Annals of the Photogrammetry, Remote Sensing and Spatial Information Sciences* 4 (4): 41–48. https://doi.org/10.5194/isprs-annals-IV-4-41-2018.

Filho, Jorge A.Wagner, Wolfgang Stuerzlinger, and Luciana Nedel. 2020. “Evaluating an Immersive Space-Time Cube Geovisualization for Intuitive Trajectory Data Exploration.” *IEEE Transactions on Visualization and Computer Graphics* 26 (1): 514–24. https://doi.org/10.1109/TVCG.2019.2934415.

Hays, Timothy A. 1996. “Spatial Abilities and the Effects of Computer Animation on Short-Term and Long-Term Comprehension.” *Journal of Educational Computing Research* 14 (2): 139–55. https://doi.org/10.2190/60Y9-BQG9-80HX-UEML.

Hedley, N R. 2003. “Empirical Evidence of Advanced Geographic Visualization Interface Use.” *21st International Cartographic Conference Cartographic Renaissance*, no. August: 10–16. http://icaci.org/documents/ICC_proceedings/ICC2003/Papers/052.pdf.

Hegarty, Mary, and Valerie K. Sims. 1994. “Individual Differences in Mental Animation during Mechanical Reasoning.” *Memory & Cognition* 22 (4): 411–30. https://doi.org/10.3758/BF03200867.

Hegarty, Mary, Mike Stieff, and Bonnie Dixon. 2014. “Reasoning with Diagrams: Toward a Broad Ontology of Spatial Thinking Strategies.” In *Space in Mind*, edited by Daniel R. Montello, Karl Grossner, and Donald G Janelle, 75.98. The MIT Press. https://doi.org/10.7551/mitpress/9811.003.0005.

Hinze, Scott R, Vickie M Williamson, Mary Jane Shultz, Ghislain Deslong-, Kenneth C. Williamson, and David N. Rapp. 2014. “Spatial Ability and Learning from Visualizations in STEM Disciplines.” In *Space in Mind: Concepts for Spatial Learning and Education*, edited by Daniel R Montello, Karl Grossner, and Donald G Janelle, 99–118. MIT Press.

Hoyek, Nady, Christian Collet, Patrick Fargier, and Aymeric Guillot. 2012. “The Use of the Vandenberg and Kuse Mental Rotation Test in Children.” *Journal of Individual Differences* 33 (1): 62–67. https://doi.org/10.1027/1614-0001/a000063.

Hruby, Florian, Rainer Ressl, and Genghis de la Borbolla del Valle. 2019. "Geovisualization with Immersive Virtual Environments in Theory and Practice." *International Journal of Digital Earth* 12 (2): 123–36. https://doi.org/10.1080/17538947.2018.1501106.

Huk, T. 2006. "Who Benefits from Learning with 3D Models? The Case of Spatial Ability." *Journal of Computer Assisted Learning* 22 (6): 392–404. https://doi.org/10.1111/j.1365-2729.2006.00180.x.

Johnson, Wendy, and Thomas J. Bouchard. 2005. "The Structure of Human Intelligence: It Is Verbal, Perceptual, and Image Rotation (VPR), Not Fluid and Crystallized." *Intelligence* 33 (4): 393–416. https://doi.org/10.1016/j.intell.2004.12.002.

Kaufmann, Hannes, Mathis Csisinko, Irene Strasser, Sabine Strauss, Ingrid Koller, and Judith Gluck. 2008. "Design of a Virtual Reality Supported Test for Spatial Abilities." *Proceedings of the International Conference on Geometry and Graphics*, 2008. https://publik.tuwien.ac.at/files/PubDat_170660.pdf.

Laramee, Robert S., and Robert Kosara. 2006. "Challenges and Unsolved Problems." In *Human-Centered Visualization Environments*, edited by Andreas Kerren, Achim Ebert, and Jörg Meyer, 1st ed., 231–54. Springer-Verlag Berlin Heidelberg. https://doi.org/10.1007/978-3-540-71949-6.

Linn, Marcia C, and Anne C Petersen. 1985. "Emergence and Characterization of Sex Differences in Spatial Ability : A Meta-Analysis Author (s): Marcia C . Linn and Anne C . Petersen Published by : Wiley on Behalf of the Society for Research in Child Development Stable URL : Http://Www.Jstor.Org/St." *Child Development* 56 (6): 1479–98.

Lochhead, Ian, and Nick Hedley. 2018. "Communicating Multilevel Evacuation Context Using Situated Augmented Reality." *ISPRS Annals of the Photogrammetry, Remote Sensing and Spatial Information Sciences* IV-4/W6 (13th 3D GeoInfo Conference): 33–40.

Lokka, Ismini E., and Arzu Çöltekin. 2019. "Toward Optimizing the Design of Virtual Environments for Route Learning: Empirically Assessing the Effects of Changing Levels of Realism on Memory." *International Journal of Digital Earth* 12 (2): 137–55. https://doi.org/10.1080/17538947.2017.1349842.

MacEachren, Alan M., and Menno-Jan Kraak. 2001. "Research Challenges in Geovisualization." *Cartography and Geographic Information Science* 28 (1): 3–12. https://doi.org/10.1559/152304001782173970.

MacEachren, Alan M, Robert Edsall, Daniel Haug, Ryan Baxter, George Otto, Raymon Masters, Sven Fuhrmann, and Liujian Qian. 1999. "Virtual Environments for Geographic Visualization : Potential and Challenges." *Proceedings of the 1999 Workshop on New Paradigms in Information Visualization and Manipulation in Conjunction with the Eighth ACM Internation Conference on Information and Knowledge Management*, 35–40.

MacEachren, Alan M, and Menno-Jan Kraak. 1997. “Exploratory Cartographic Visualization: Advancing the Agenda.” *Computers & Geosciences* 23 (4): 335–43. https://doi.org/10.1016/S0098-3004(97)00018-6.

Malinowski, Jon C. 2001. “Mental Rotation and Real-World Wayfinding.” *Perceptual and Motor Skills* 92 (1): 19–30. https://doi.org/10.2466/pms.2001.92.1.19.

Marusan, M., P. Kulistak, and J. Zara. 2006. “Virtual Reality in Neurorehabilitation: Mental Rotation.” *Third Central European Multimedia and Virtual Reality Conference*, 77–83. https://www.researchgate.net/profile/Jiri_Zara/publication/268355077_Virtual_Reality_in_Neurorehabilitation_Mental_Rotation/links/551a7a740cf244e9a4587832.pdf.

Mayer, Richard E. and Sims, Valerie K. 1994. “For Whom Is a Picture Worth a Thousand Words? Extensions of a Dual-Coding t...: EBSCOhost.” *American Psychological Association, Inc* 86 (3): 389–401. http://libproxy.library.unt.edu:2067/ehost/pdfviewer/pdfviewer?vid=1&sid=cacecf36-cd5b-4ffe-9996-9b0332df5fb7%40pdc-v-sessmgr05.

McWilliams, W., C. J. Hamilton, and S. J. Muncer. 1997. “On Mental Rotation in Three Dimensions.” *Perceptual and Motor Skills* 85 (1): 297–98. https://doi.org/10.2466/pms.1997.85.1.297.

Moè, Angelica. 2012. “Gender Difference Does Not Mean Genetic Difference: Externalizing Improves Performance in Mental Rotation.” *Learning and Individual Differences* 22 (1): 20–24. https://doi.org/10.1016/j.lindif.2011.11.001.

Mok, Magdalena Mo Ching, Sze Ming Lam, Ming-Yan Ngan, Jing Yao, Michael Ying Wah Wong, Jacob Kun Xu, and Stephen Yin Chuen Ting. 2012. “Student-Problem Chart: An Essential Tool for SLOA.” In *Self-Directed Learning Oriented Assessments in the Asia-Pacific*, edited by Mo Ching Mok, 203–21. Dordrecht: Springer Netherlands. https://doi.org/10.1007/978-94-007-4507-0_11.

Monahan, John S., Maureen A. Harke, and Jonathon R. Shelley. 2008. “Computerizing the Mental Rotations Test: Are Gender Differences Maintained?” *Behavior Research Methods* 40 (2): 422–27. https://doi.org/10.3758/BRM.40.2.422.

Newcombe, Nora S. 2014. “Teaching Space: What, How, and When.” In *Space in Mind: Concepts for Spatial Learning and Education.*, edited by Daniel R. Montello, Karl Grossner, and Donald G. Janelle, 323–34. MIT Press. http://ovidsp.ovid.com/ovidweb.cgi?T=JS&PAGE=reference&D=psyc11&NEWS=N&AN=2015-20750-016.

Parsons, Thomas D., Peter Larson, Kris Kratz, Marcus Thiebaux, Brendon Bluestein, J. Galen Buckwalter, and Albert A. Rizzo. 2004. “Sex Differences in Mental Rotation and Spatial Rotation in a Virtual Environment.” *Neuropsychologia* 42 (4): 555–62. https://doi.org/10.1016/j.neuropsychologia.2003.08.014.

Peters, M., Laeng, B., Latham, K., Jackson, M., Zaiyouna, R., & Richardson, C. 1995. “A Redrawn Vandenberg and Kuse Mental Rotations Test.” *Brain and Cognition*. https://doi.org/https://doi.org/10.1006/brcg.1995.1032.

Peters, Michael. 2005. “Sex Differences and the Factor of Time in Solving Vandenberg and Kuse Mental Rotation Problems.” *Brain and Cognition* 57 (2): 176–84. https://doi.org/10.1016/j.bandc.2004.08.052.

Peters, Michael, and Christian Battista. 2008. “Applications of Mental Rotation Figures of the Shepard and Metzler Type and Description of a Mental Rotation Stimulus Library.” *Brain and Cognition* 66 (3): 260–64. https://doi.org/10.1016/j.bandc.2007.09.003.

Peters, Michael, Bruno Laeng, Kerry Latham, Marla Jackson, Raghad Zaiyouna, and Chris Richardson. 1995. “A Redrawn Vandenberg and Kuse Mental Rotations Test. Different Versions and Factors That Affect Performance.” *Brain and Cognition* 28: 39–58.

Pulver, Y., C. Merz, K. Koebel, J. Scheidegger, and A. Çöltekin. 2020. “Telling Engaging Interactive Stories with Extended Reality (Xr): Back to 1930s in Zurich’s Main Train Station.” *ISPRS Annals of the Photogrammetry, Remote Sensing and Spatial Information Sciences* 5 (4): 171–78. https://doi.org/10.5194/isprs-Annals-V-4-2020-171-2020.

Rydvanskiy, Ruslan, and Nick Hedley. 2021. “Mixed Reality Flood Visualizations: Reflections on Development and Usability of Current Systems.” *ISPRS International Journal of Geo-Information* 10 (2): 82. https://doi.org/10.3390/ijgi10020082.

Sanchez, Christopher A., and Russell J. Branaghan. 2009. “The Interaction of Map Resolution and Spatial Abilities on Map Learning.” *International Journal of Human Computer Studies* 67 (5): 475–81. https://doi.org/10.1016/j.ijhcs.2008.12.003.

Scali, Robyn M., Sheila Brownlow, and Jennifer L. Hicks. 2000. “Gender Differences in Spatial Task Performance as a Function of Speed or Accuracy Orientation.” *Sex Roles* 43 (5–6): 359–76. https://doi.org/10.1023/A:1026699310308.

Schnürer, Raimund, Martin Ritzi, Arzu Çöltekin, and René Sieber. 2020. “An Empirical Evaluation of Three-Dimensional Pie Charts with Individually Extruded Sectors in a Geovisualization Context.” *Information Visualization* 19 (3): 183–206. https://doi.org/10.1177/1473871619896103.

Shepard, Roger, and Jacqueline Metzler. 1971. “Mental Rotation of Three-Dimensional Objects.” *Science* 171 (3972): 701–3.

Slocum, Terry A., Connie Blok, Bin Jiang, Alexandra Koussoulakou, Daniel R. Montello, Sven Fuhrmann, and Nicholas R. Hedley. 2001. “Cognitive and Usability Issues in Geovisualization.” *Cartography and Geographic Information Science* 28 (1): 61–75. https://doi.org/10.1559/152304001782173998.

Uttal, David H., Nathaniel G. Meadow, Elizabeth Tipton, Linda L. Hand, Alison R. Alden, Christopher Warren, and Nora S. Newcombe. 2013. “The Malleability of Spatial Skills: A Meta-Analysis of Training Studies.” *Psychological Bulletin* 139 (2): 352–402. https://doi.org/10.1037/a0028446.

Vandenberg, Steven G, and Allan R Kuse. 1978. “Mental Rotations, a Group Test of Three-Dimensional Spatial Visualization.” *Perceptual and Motor Skills* 47 (2): 599–604. https://doi.org/10.2466/pms.1978.47.2.599.

Voyer, Daniel, Susan Voyer, and M P Bryden. 1995. “Magnitude of Sex Differences in Spatial Abilities.” *Psychological Bulletin* 117 (March): 250–70.

Wai, Jonathan, David Lubinski, and Camilla P. Benbow. 2009. “Spatial Ability for STEM Domains: Aligning Over 50 Years of Cumulative Psychological Knowledge Solidifies Its Importance.” *Journal of Educational Psychology* 101 (4): 817–35. https://doi.org/10.1037/a0016127.

Zhao, Jiayan, Jan Oliver Wallgrün, Peter C. LaFemina, Jim Normandeau, and Alexander Klippel. 2019. “Harnessing the Power of Immersive Virtual Reality - Visualization and Analysis of 3D Earth Science Data Sets.” *Geo-Spatial Information Science* 22 (4): 237–50. https://doi.org/10.1080/10095020.2019.1621544.

Chapter 7.

Conclusion

7.1. Summary

The collection of research presented within this dissertation explored SfM and XR as EGTs for 3D spatial data capture, visualization, and analysis. This research aims to strengthen the foundation supporting EGT use in 3D GIScience by documenting experiences applying them to focused geospatial problems, and through an empirical study evaluating individuals' spatial ability, as the discipline potentially transitions from conventional to immersive and mixed-reality GIScience. As the popularity of 3D data production methods such as SfM, and 3D interface technologies of XR, have increased significantly in academia, industry, and society over the past decade – stimulated by improved ease-of-use and access to these technologies – so too has the need for GIScience research that legitimizes these EGTs as useful 3D GIScience tools. Despite the compelling photorealistic 3D models and novel visual experiences that SfM and XR can deliver, respectively, their usefulness as GIScience technologies demands commensurate data science, theory, design, and empirical research supporting their use. The five manuscripts within this dissertation explored workflows representative of applied 3D geospatial data acquisition, visualization, and analysis. They provided an in-depth assessment of an emerging data acquisition workflow (SfM) and the veracity of its data products, discussed the design and development of immersive visualization environments as geovisual analytical interfaces through applied spatial data case studies, and presented a new approach to the assessment of spatial cognitive outcomes in immersive spaces and empirical evidence that immersive spaces do impact spatial performance and reasoning. Collectively, this research demonstrates that SfM and XR can be useful EGTs for 3D GIScience.

The first manuscript presents the dry-lab phase in a systematic, multiphase (dry-lab, wet-lab, and field) assessment of SfM workflow performance and 3D data quality. As a user-friendly 3D photogrammetric processing method, SfM has experienced a meteoric rise in popularity across many spatial data domains. The applied context of this research was a project designed to enable temporal analyses of dynamic glass sponge

morphology in Howe Sound, BC. While glass sponges constitute the subject of study, this research and the two subsequent manuscripts constitute a detailed multi-part study of SfM-based surveying and the veracity of the 3D data products, from a GIScience perspective. These dry-lab tests provided a critical set of data quality benchmarks regarding the impact that light levels, capture strategy, camera equipment, and camera settings have on SfM derived 3D data quality. They also established an ideal SfM workflow and objectively defined data accuracy thresholds – which were critical to the wet-lab and field-based phases of this project – and demonstrated that SfM can accurately capture small scale (mm to cm) changes over time. However, this manuscript also demonstrates that subtle changes to the workflows (that are being adopted across GIScience, and in many related spatial-data-reliant fields) can have a measurable impact on 3D data quality and that simply capturing photographs or videos for an SfM-based survey may not produce 3D data that accurately characterizes the morphometry of the spatial phenomenon of interest. This in turn has extremely significant implications for the interpretation (and potential misinterpretation) of phenomena and processes, for which we rely on data through which to understand them.

The second manuscript documents the wet-lab phase of the SfM research, building upon the dry-lab phase to identify the impact that temperate marine environments and underwater photography have on SfM-based 3D data quality. The wet-lab tests provided a controlled, simulated temperate marine environment from which the veracity of 3D data could be measured, but also from which alternative data capture strategies could be evaluated to identify an SfM workflow that balances data accuracy and survey pragmatism. As data capture efforts were restricted by the amount of time divers could safely spend underwater, it was critical that the wet-lab phase of this research identified a workflow that achieved the necessary 3D data accuracy while ensuring the safety of the divers. These wet-lab tests were an essential component of this SfM research, identifying both what is possible given the SfM workflow and what is practical given the context in which that workflow is applied. This research revealed that many different SfM workflows can successfully produce 3D data, yet that data may not successfully capture the 3D morphometry of the survey subject. For applied studies of SfM in challenging, unproven environments, value is derived from knowing precisely what is possible with any given workflow, knowing how the workflow and the environment impact an ability to achieve what is possible, and knowing what the

resultant 3D data product represents. The systematic exploration of these factors and their influence on the veracity of resulting 3D data products in manuscripts one and two, provides hard evidence with which to strengthen principles that should underpin future 3D data generation in GIScience.

The third manuscript presents the field-based phase of the 3D data capture workflow and introduces a set of XR interfaces for data visualization, connecting the two research efforts (3D data capture and 3D visualization/analysis) presented within this dissertation. The results of the field-based research are documented, showcasing the accuracy of the 3D data obtained in the field and highlighting the challenges associated with field-based data capture. The 3D data sets that were generated provide a temporal snapshot of 3D glass sponge morphology that, in conjunction with subsequent data sets, provides an opportunity for temporal analyses of morphometric change and therefore new knowledge about the dynamic and complex structures of these organisms. The XR interfaces were introduced as an ancillary method of data visualization and analysis, forgoing conventional 2D interfaces for virtual and augmented reality interfaces that enable immersive, interactive, and analytical 3D data experiences. However, the bigger picture is that in conjunction with the HEXYZ-1 workflow these interfaces elucidate an entire 3D workflow for applied geospatial surveying, characterization, visualization, and analysis that may unlock the potential for the future of 3D data and 3D GIScience.

The fourth manuscript focuses on the design and development of an immersive virtual environment for visual analytics (IVEVA). IVEVA was developed following a multidisciplinary set of design heuristics and demonstrates a VR interface as an extension to the space in which 3D GIScience and visual analytics are performed. Five case studies are presented in IVEVA, highlighting both what can be done with purposefully designed analytical VEs and tools, and the challenges associated with incorporating different spatial phenomena and spatial data formats. While novel XR interfaces have gained attention across academia, industry, and society, it is not the interfaces themselves nor the 3D data within them that makes them useful, but the ability of the interface to connect users and data in meaningful ways – providing new opportunities for spatial data sense making and knowledge formation. The intention of this manuscript, and the IVEVA prototype it introduced, was to illustrate the development of purposefully designed XR interfaces for 3D GIScience – not simply combining 3D data

and XR because we can or to create XR-based GIS, but to harness the power of XR to change how 3D spatial data are experienced, analyzed, and understood.

Finally, the fifth manuscript examines the extent to which immersive geovisual interfaces may empower users as they engage with 3D data. This manuscript documents the design, development, and execution of a VR-based immersive mental rotations test (IMRT). While the traditional paper and pencil MRT may be included in geovisualization research to characterize the spatial ability (mental rotations ability) of research participants, it did not seem appropriate to include the MRT in a study of XR-based geovisualizations. Where the traditional MRT measures an ability to imagine 3D objects from 2D images, and then mentally rotate those imagined objects, VR-based geovisualizations relieve users of the cognitively demanding dimensionality crossing task (imagining 2D from 3D and vice versa). Thus, the IMRT teases apart these two tasks, focusing solely on the ability to mentally rotate 3D objects. As XR-based visualizations of 3D glass sponge data (and other 3D phenomena) may draw upon a similar ability, and therefore influence an ability to perceive and comprehend the complex 3D structures within these visualizations, the IMRT seemed a more appropriate test. Furthermore, this research explored the impact that information intensity, or the complexity of VE backgrounds, has on mental rotations task performance, suggesting that the design of VEs does have an impact on performance. This work delivered a new spatial ability assessment workflow (the IMRT) rooted in the multi-decadal psychometric tradition yet aimed to manifest it in a form pertinent to the contemporary modes of experience offered by immersive 3D visual interfaces. Such basic empirical works are going to be crucial to underpin our understanding and development of EGT-based interfaces across many sectors of spatial data infrastructure and use in the coming years.

Collectively, this dissertation evaluates the utility of SfM and XR for 3D GIScience. Whether or not these technologies could be used to create 3D spatial data and 3D spatial data visualizations was never in question. Rather, the focus of this dissertation and its components, were explorations of what data captured using 3D methods can capture, and how well they are able to characterize complex spatial objects, how visualizations using these data can be designed (for anticipated user outcomes with data), and what these forms of visualizations enable us to do as geospatial practitioners.

If we revisit the expressed objective of the original MITACS proposal (the basis of the 3D glass sponge survey project) – to implement an SfM workflow in a temperate marine environment – the quality of the resultant data and how that data could be visualized and analyzed were not acknowledged or requested. More importantly, the true objective of that research proposal was not simply to apply SfM in a temperate marine environment, but to use SfM as a tool to help marine ecologists improve their ability to understand changing glass sponge health over time.

While the ability to accurately characterize 3D glass sponge morphometry, as well as to visualize and analyze dynamic morphometry, were critical to support characterization and interpretation of glass sponges and to assess their health - the work to critically assess and validate these methods and technologies was not part of the original initiative. Monitoring the dynamic, complex 3D structure of glass sponges is undoubtedly a spatial problem that requires accurate spatial data and an effective approach to 3D data visualization and analysis. The omission of plans or methods to build rigorous data science to support this initiative is not at all unusual or isolated.

As new 3D spatial data acquisition technologies/methods have gained traction in industry and academia, they have been adopted and used headlong, with far less (or often, no) attention being paid to the quality and integrity of the spatial data they produce or the analyses they can support. Ongoing and evolving 3D geographic information science and geovisualization approaches provide critical lenses through which to enrich and improve the integration of these technologies/methods into society – by being able to: document, evaluate and interpret spatial data quality; assess and quantify representational veracity; rationalize intentional geovisual design and information experience design (tuned to the logic of spatial representation, and intended users); and gather empirical evidence for the cognitive outcomes of users of new 3D data.

The manuscripts in this dissertation, therefore, systematically approach this problem from a 3D GIScience perspective, assessing SfM and XR as EGTs for such spatial problems; not simply applying SfM to produce 3D spatial data and XR to visualize that data, but unpacking the capabilities and implications of applied SfM workflows, designing and developing XR interfaces to encourage spatial knowledge transfer, and evaluating the impact that emerging interfaces (VR) have on individual spatial ability. The first manuscript establishes a set of performance benchmarks for spatial data

acquisition workflows in a controlled dry-lab. Those benchmarks were then used to inform wet-lab tests identifying the impact that a simulated temperate marine environment has on 3D data quality. The results of the field research presented in manuscript three can then be interpreted and understood with respect to the performance benchmarks established in manuscripts one and two. Without this succession of research, it would have been difficult to establish whether the data captured in the field were impacted by changing workflows, whether the results were the best that could be expected, and precisely how the temperate marine environment was impacting data quality. Manuscript three also presented a collection of XR interface prototypes for data visualization and analysis, which were further explored in manuscript four through a discussion of multidisciplinary design heuristics applied to a collection of spatial data case studies. Manuscript five then evaluates the impact that VR and information intensity may have on our ability to formulate new knowledge through immersive interface use, presenting the immersive mental rotations test as a contemporary test of spatial ability commensurate with modern spatial data and interface technologies.

The collective objective of the research presented in this dissertation is to help establish SfM and XR as useful 3D GIScience tools for visual analyses of spatial data and the acquisition of knowledge about the spatial phenomena that data represents. If we are to encourage the development of spatial knowledge concerning the location, size, distance, direction, shape, connectivity, overlap, dimensionality, or hierarchy of spatial phenomena then it is essential that our spatial data acquisition workflows accurately capture those spatial data characteristics. If we are to implement emerging interface technologies for visual analyses, then we must design interfaces that offer user experiences conducive to spatial data exploration and sense making. Without an understanding of EGT based data quality, the design of immersive visual analytics interfaces, or the affordances and limitations of emerging interface use then the acquisition of spatial knowledge may either be impeded by inaccurate spatial data, inefficient or incomplete interface design, or misguided interface use. Under the context of the MITACS project, SfM represents an opportunity for 3D spatial data acquisition regarding the dynamic spatial complexity of glass sponge ecosystems. XR interfaces then allow for visual analyses affording the perceptual-motor experiences akin to direct real-world interaction (Montello & Raubal, 2012), or even exceeding what is possible in

the field by allowing direct interactions that would otherwise impact real-world spatial phenomena.

7.2. Research Contributions by Research Questions and Objectives

This dissertation contributes to the future of SfM and XR as EGTs for 3D GIScience by advancing the 3D data science, empirical assessment, and design theory which supports these EGTs as legitimate 3D GIScience tools. This dissertation takes a holistic approach to EGT use in 3D GIScience, focusing not only on one EGT or aspect of 3D GIScience but on establishing 3D data workflows that incorporate multiple EGTs to capture, visualize, and analyze 3D spatial data. However, EGT use in and of itself does not constitute usefulness. While SfM workflows can produce compelling 3D data sets, and XR interfaces can offer unique visual experiences, their usefulness hinges on the quality of the 3D data produced and the impact that those interfaces have on our ability to derive new knowledge from spatial data. Without answers to critical questions concerning the usefulness of these EGTs for spatial data science, the use of these EGTs is simply use for the sake of technology itself. SfM and XR can be used for many spatial applications – the objective of this dissertation was to strengthen the foundation supporting why SfM and XR should be used for 3D GIScience.

The research questions presented in this dissertation challenge SfM and XR as EGTs, questioning not whether they can be used but how they should be used and what their use enables. The contributions that this dissertation makes to the research community, specific to each of the research questions raised, are presented below.

Emerging data collection workflows and their implications

- *How accurately can terrestrial SfM workflows characterize the morphology of discrete phenomena?*

  The HEXYZ-1 workflow was designed to address the challenging underwater conditions typical of temperate marine environments. The terrestrial SfM tests presented in Chapter 2 were conducted to provide a set of performance benchmarks informing subsequent phases of this research. Linear

measurements of the resultant 3D data sets were accurate to within 3.17% – 8.83% (1.09 mm – 3.07 mm) of real-world measurements.

- *How accurately can underwater SfM workflows characterize the morphology of discrete phenomena?*

The terrestrial SfM performance benchmarks provided a performance standard for the HEXYZ-1 workflow. The marine SfM tests presented in Chapter 3 were performed to evaluate the impact that temperate marine conditions and underwater camera housings have on SfM performance. Linear measurements of the 3D data characterizing the morphology of an ornamental coral were accurate to within 0.6% - 5.07% (0.1 mm – 2.06 mm) of real-world measurements. The HEXYZ-1 workflow proved to be as accurate in a simulated temperate marine environment as it was in a terrestrial setting.

- *What implications do SfM workflow parameters (e.g., camera, camera settings, camera position/configuration, and lighting) have for the accuracy of the 3D data product?*

The terrestrial and marine tests in Chapters 2 and 3 prove that the HEXYZ-1 workflow can produce highly accurate 3D data and demonstrate that SfM workflow parameters do have a measurable impact on data accuracy. The variability in terrestrial and marine SfM accuracy is primarily a function of different workflow parameters and not the precision of any given workflow. Therefore, SfM workflow development should systematically evaluate these workflow parameters, as high-accuracy SfM surveying is more nuanced than simply capturing a collection of images.

Emerging data display and analysis technologies and their implications

- *How can XR technology be leveraged to help visualize the structure of complex 3D phenomena?*

The virtual, mixed, and augmented reality prototypes presented within this dissertation demonstrated how XR technology can be utilized for 3D geovisualization and visual analytics. These XR prototypes were developed to supplement contemporary 3D data workflows, offering alternative data exploration and sense making opportunities in 3D.

- *Are mental rotation tasks performed more accurately and/or more rapidly with stereo 3D stimuli than with 2D images of those 3D stimuli?*

The results of the IMRT research presented in Chapter 6 suggest that mental rotation tasks performed in VR are performed more rapidly and more accurately with 3D stimuli than when those tasks are performed with 2D images of 3D stimuli.

- *What impact does background complexity (i.e., information intensity) have on mental rotation task performance?*

The results of the IMRT research presented in Chapter 6 suggest that background complexity does not have a significant impact on mental rotation task performance. However, the impact that background complexity had on 2D and 3D IMRT performance of male and female participants did show some variability, suggesting that background complexity may have a greater impact on females than males, and more so with 2D stimuli than 3D stimuli.

- *What is the relationship between XR technology and the human factors which dictate geovisualization use and usefulness?*

The research presented in Chapter 6 challenges the use of conventional human factors metrics for applications involving contemporary visual interfaces. These advanced interfaces offer alternate methods of visualization that change the relationship between people and 3D data. Therefore, the characterization of human factors as an indicator of XR-based geovisualization use and usefulness must account for the effect that these interfaces have on our ability to perform the tasks that those conventional metrics measure, as a failure to do so may result in misconceptions regarding what is useful to whom.

- *What impact does XR technology have on the characterization of spatial ability (specifically mental rotation task performance)?*

Research shows that the mental rotation task performance of males and females is not equal, and that males typically outperform females on these tasks. However, the research presented in Chapter 6 suggests that this gender effect is reduced when mental rotations are performed in VR with 3D stimuli. While the IMRT alleviates the cognitive demand of imagining 3D form from 2D images, and thus does not replicate the conventional MRT as it measures spatial ability, this is

not necessarily a negative. XR technologies have the power to change how we visualize spatial data, and the metrics used to evaluate the suitability of those interfaces and visualizations should be consistent with the demands. In the age of 3D data and interfaces the ability to imagine 3D form may be less important. The improved mental rotation task performance and reduced the gender effect suggests that this type of visualization may be better suited for a greater portion of the general population completing this type of task and suggests that conventional spatial ability metrics may not be a good indicator of XR-based geovisualization usefulness.

- *What impact does XR technology have on (geo)visualization use and usefulness?*

XR technology changes the relationship between the data presented within geovisualizations and the users of those visualizations. The ability to occupy the data space and physically interact with the data provides an opportunity for new perspectives and sense making. While the results of the IMRT research presented in Chapter 6 are too limited to make broad claims about the use and usefulness of XR-based geovisualizations, this research confirms that XR (namely VR) does have an impact on the human factors that are used to characterize geovisualization use and usefulness.

- *What role do multidisciplinary design heuristics serve in the development of XR-based visual analytics applications?*

The research presented in Chapter 5 incorporates design heuristics from cartography, HCI, and XR in the design and development of IVEVA, an immersive visual analytics prototype. The design heuristics from each of these fields were essential, as IVEVA is a tool for the visualization and analysis of 3Dspatial data, developed using the Unity game engine for VR. The five case studies presented in IVEVA highlight how different uses, users, spatial phenomena, data formats, and interface technologies require design heuristics that account for the multidisciplinary nature of contemporary visual analytics design.

These research questions addressed the use and usefulness of SfM and XR as EGTs for the characterization of 3D spatial phenomena and the visualization and

analysis of 3D spatial data. In addressing these questions, this research served the overarching objective of this dissertation, building the empirical foundation supporting the use of SfM and XR for 3D GIScience. This research achieved the stated objectives of this dissertation:

- Studying the evolving practice of 3D spatial data acquisition, analysis, and visualization as enabled by EGTs (SfM and XR) – and their implications for modern 3D GIScience.
- Exploring SfM workflows for morphometric monitoring in terrestrial and temperate marine environments.
- Designing, developing, and systematically evaluating a SfM workflow for characterizing discrete phenomena in temperate marine environments.
- Exploring the capabilities of emerging interface technologies (i.e., XR) and demonstrating how they can transform the spaces in which we conduct 3D GIScience.
- Designing, developing, and deploying an immersive mental rotations test (IMRT) to examine the effect that emerging interface technologies (VR) have on mental rotations task performance.
- Assessing the perceptual and experiential implications of emerging 3D interface technologies for applied geospatial research, practice, and social integration.
- Curating and demonstrating a multidisciplinary set of design heuristics through the design and development of an VR-based visual analytics environment.

The research associated with these research objectives represents an advancement for the use of SfM and XR in 3D GIScience. The specific contributions of each chapter are discussed below.

7.3. Research Contributions by Chapter

Chapters 2 and 3 explored questions concerning the veracity of terrestrial and marine SfM workflows and the impact that variable workflow parameters have on 3D data accuracy. The developed data capture strategy was designed to provide a controlled, repeatable approach for capturing photographs and videos in a challenging underwater environment, and to emphasize the variability that results from simply capturing photographs for the purpose of SfM-based 3D modelling. For the glass sponges featured in this research, subtle variations in 3D data accuracy resulting from

variations in capture strategies, cameras and camera settings, and lighting choices have a measurable impact on data quality that affects marine ecologists' ability to monitor changing glass sponge morphology. This research builds upon other SfM studies (e.g., Lavy et al., 2015; Raoult et al., 2017) exploring SfM accuracy in marine environments, contributing a unique approach to underwater SfM surveying, 3D data quality benchmarks for temperate marine environments, and contemporary methods of 3D data visualization. This 3D data workflow stresses the importance of data representation, both in defining precisely what the 3D data capture strategy represents and how that data can be visually represented. Representation is a fundamental issue for GIScience and geovisualization, and as technology changes how geospatial phenomena are represented, both in how they are modelled and how they are presented, conventional knowledge and methods of representation may prove to be inadequate and new research supporting contemporary approaches is required (Dykes et al., 2005; Fairbairn et al., 2001).

Chapter 4 presents the results of the field-based SfM research and introduces a collection of XR interfaces for 3D data visualization and analysis. This research makes two important contributions to the research community. The first, that field-based research is unpredictable and understanding the capabilities of your data capture workflow is critical to understanding the quality of your data. The research conducted in the dry-lab and wet-lab was essential to understanding the value of the 3D data product derived from extracted video frames. Without these benchmarks it would have been difficult to know whether the 3D data product was sufficient, whether it was the best that could be expected, and what could have been done to improve data quality and how much improvement could have been achieved. In a remote and challenging environment, it is essential that the performance of the data capture workflow, especially if its performance is unproven, be thoroughly evaluated. This research builds upon the work of others (e.g., Kahn et al., 2016) applying SfM workflows to monitor glass sponge morphology, introducing a strategic, substantiated approach to temperate underwater SfM surveying. The second contribution is that SfM and 3D data are not the ultimate objective, but rather an integral piece of a 3D data workflow that involves data capture, visualization, and analysis. While the marine ecologists involved in this study were interested in 3D data, XR interfaces offered a significant opportunity to advance their 3D data visualization, analysis, and communication efforts. The presented prototypes

explore how XR technology can be leveraged to create interactive and experiential methods of 3D data visualization that offer proprioceptive and sensorimotor cues to support visual learning (Shelton & Hedley, 2004), ease data measurement through immersive data exploration (Zhao et al., 2019), and provide an opportunity for learning through virtual 'visits' to field sites (Minocha et al., 2018). This research stresses that there is value in not just capturing 3D data but harnessing the power of XR interfaces for data exploration and analysis.

Chapter 5 explores questions concerning the design and development of XR interfaces for visual analytics and the role served by multidisciplinary design heuristics. This research contributes to the advancement of VR design for immersive visual analytics through a discussion and demonstration of the challenges associated with incorporating disparate spatial data types and the importance of multidisciplinary design heuristics in the context of the IVEVA prototype. The five case studies presented within IVEVA highlight the challenges associated with incorporating spatial data of different formats and representing different spatial phenomena, and in doing so, the opportunity presented by developing interactive and exploratory visual analytics interfaces that are not VR-based reproductions of conventional GIS. IVEVA demonstrates how human-information discourse can be stimulated by providing interactive techniques for analytical reasoning and thereby promoting a 'science of interaction' for immersive (geo)visual analytics (Thomas & Cook, 2005). Critical in the process of analytical reasoning are the users themselves, who invariably define the usability of an interface and the knowledge that can be gained through interface use. While the ultimate objective may be to find the ideal representation or method of interaction, the inherent variability in data, interfaces, users, and uses necessitates an approach to design that accounts for variability and allows the user to determine the ideal combination for their own sense making efforts. This aligns with the human-centered design and human-factors challenges (see Çöltekin et al., 2017; Dykes et al., 2005; Virrantaus et al., 2009) that have persisted within geovisualization, and which require empirical evaluation to determine the ideal design choices. While this research does not provide that empirical evaluation, it does present these considerations in the context of immersive visual analytics design and encourages future research on informed design.

Finally, Chapter 6 addresses questions regarding the relationship between XR and the human factors that influence geovisualization use and usefulness; namely, the

characterization of mental rotation ability (a spatial ability and human factor), the effect that 3D stimuli and stereo 3D displays have on mental rotation task performance, and the impact that information intensity (i.e., virtual environment complexity) has on mental rotation task performance. This research introduced the IMRT, a contemporary alternative to established MRTs (i.e., Peters et al., 1995; Vandenberg & Kuse, 1978), which was designed to explore the effect that emergent immersive display technologies have on our ability to mentally rotate 3D objects and 2D images of those 3D objects. This research suggests that IMRT performance is improved when the test contains 3D objects rather than 2D images and that this performance advantage is greater for females than males. Furthermore, this research also suggests that the design of the virtual environment does have an impact on IMRT performance. This research contributes to the assessment of human factors as they pertain to VR-based geovisualization use and usefulness and suggests that similar relationships may exist with AR and MR interfaces, as they too alleviate the process of dimensionality crossing (Horan & Rosser, 1984). While the sample size may limit the strength of this study, the IMRT itself represents a step forward; towards thinking about the impact that contemporary interfaces have on the conventional metrics used to assess geovisualization use and usefulness. This research contribution would suggest that immersive 3D geovisualizations are better suited for a greater portion of the general population and contemporary methods of assessing human factors warrant further evaluation.

7.4. Inspiring Future Research

The research presented in this dissertation explores contemporary topics grounded in the roots of GIScience. When Goodchild (1992) first suggested that the “S” in GIS should be recognized as the science of GIS he also set the stage for what that science could entail, incorporating everything from data collection to analysis. He also noted that emerging data capture trends were leading to a shift away from traditional map documents and that electronic displays enabled much more than conventional cartography could ever achieve. This digital transformation inspired geovisualization (or visual analytics) as a subfield of GIScience that has invariably explored issues concerning spatial data, interfaces, and the uses and users of geovisualizations in their

many forms (see Andrienko et al., 2007; Çöltekin et al., 2017; Dykes et al., 2005; Fairbairn et al., 2001; Virrantaus et al., 2009).

This dissertation addresses some of these challenges, exploring contemporary 3D GIScience as a process of capturing, visualizing, and analyzing spatial data using EGTs – namely SfM and XR. An empirical evaluation of SfM as a method of 3D data capture was presented, demonstrating the impact that idiosyncratic sets of variables have on data quality and that a successful SfM data capture strategy for 3D GIScience involves more than just collecting photographs. A set of XR prototypes were then developed to showcase how AR and VR interfaces can be used to visualize that 3D data, and an immersive MRT (the IMRT) was developed to evaluate the impact that VR has on mental rotation task performance. The IMRT study and the IVEVA VR prototype address some of the human challenges of geovisualization, exploring for whom VR based geovisualizations may be most useful and how those geovisualizations should be designed for effective use. While Goodchild recognized the influential role that technology would have in his proposed scientific field, technology has maintained if not accelerated its role driving that science forward and a massive transformation in geospatial technology has been predicted to occur over the next few years (Dangermond & Goodchild, 2020).

The future of GIScience will be determined by innovative technologies that enhance or transform GIScience processes. The EGTs discussed in this dissertation represent a monumental leap forward from those that Goodchild (1992) discussed when he proposed GIScience, and it is therefore not impractical to imagine another monumental leap forward over the next 30 years. As technology evolves, miniaturizes, and increasingly closes the gap between human and machine, it is highly likely that future of GIScience is one that involves spatial data cyborgs. The interfaces we know today, the connections between human and machine, will disappear as they are simplified and become more natural (Clark, 2003), and the technologies of XR interfaces, like the powerplants of vehicles, will be subsumed into spatial information tools and take on appliance-level convenience (Hedley et al., 2002). The EGTs presented in this dissertation will effectively become part of us, empowering humans (i.e., cyborgs) with an ability to generate spatial data through sight, to perform complex spatial data operations on command, to visualize and analyze complex multidimensional spatial data sets without the need for visual displays, and to collaborate through a

network of connected thoughts. While this future may at first appear farfetched, Mojo Vision has already produced contact lenses embedded with microelectronics and displays and Neuralink is developing brain interfaces that connect mind and machine. Technological advancements such as these will change the GIScience landscape but will not negate the need for research that defines spatial data best practices, 3D interfaces design, or the impact that 3D data and has on human perception and cognition – although what it means to know something may be redefined by the speed of the connection between our brain and internet. Nevertheless, the presented EGT research contributes even to this far off future of GIScience.

However, this research is not without its limitations, and I consider these limitations an opportunity for future academics. The study of SfM-based data capture was unable to produce temporally disparate data sets for morphometric change detection. This was not a function of the research design, but rather the pending end of the internship and changes in personnel. Additionally, while the colony-scale research conducted here was critical to understanding the capacity for SfM workflows to produce accurate 3D data in temperate marine environments, reef-scale surveying and monitoring are ultimately a better indicator of ecosystem health and were not completed. There were also limitations associated with the IMRT and IVEVA. For the IMRT, the global pandemic constrained the number of participants (n =29). The limited N and the decision to split participants between the simple and complex VE inhibited the ability to compare interactions between variables. Furthermore, while the IMRT was developed for MR and AR interfaces – to compare mental rotation task performance across interfaces – IMRT performance using these interfaces was not evaluated. Finally, IVEVA was designed for different spatial phenomena and spatial data types with specific user groups in mind, however user studies were not completed because of challenges presented by the pandemic. While users are essential to user centered design and are necessary for a thorough analysis of design choices and user preferences, design heuristics and an iterative design approach were utilized to adapt to the challenging circumstances and to ensure that purposeful and useful design choices were made.

7.5. Final Comments

The presented research supports SfM and XR as legitimate 3D GIScience tools and provides several opportunities for future scholars to continue where this research

left off. This research suggests that SfM and XR can be effective 3D GIScience tools: SfM can produce high-accuracy 3D spatial data characterizing complex 3D phenomena and XR interfaces are an effective method for visualizing 3D (spatial) data. However, the research in this dissertation also suggests that SfM and XR cannot simply be applied to geospatial problems with the expectation of effective outcomes. In other words, use does not guarantee usefulness. SfM workflows and XR interfaces must be designed intentionally to account for the contextual challenges presented by factors such as the environment, the technology, and the user(s). Further research should explore these factors, examining SfM based data capture in other complex environments, using different equipment, and for different purposes. Additionally, XR research should explore mental rotation task performance using other XR interfaces, a larger and broader sample, and should incorporate eye-tracking data to study where people look while performing prescribed tasks.

While my work is clearly focused on unpacking the implications of emerging data collection, production, visualization, and interaction, it also has a resonance with the broader discipline of Geography, and key theoretical frameworks that underpin it. Data, visualizations, and interfaces all have the potential to mediate the realities we aim to document, observe, interpret, or detect change in. This theoretical perspective is fundamental to contemporary GIScience, but also has deeper conceptual roots in Chrisman's Transformational GIScience (1999), and Waldo Tobler's (1979) Transformational Cartography.

The way in which we conduct GIScience data collection and use, but especially in how we experience and engage spatial phenomena through new technologies, also intersect meaningfully with other discourses. For example, scholars of the Geoweb might engage some of my work as geographic reality characterized and mediated by specific assemblies of sensors, data, processes, algorithms, visualizations, and interfaces.

The emerging interface parts of my work might lead us to consider, at a more philosophical level, what fundamental geographic concepts, such as place (Tuan, 1975) become - as reality and virtuality collide, mix, and combine, into many new environments (and experiences with them).

These questions are beyond the intended design of this thesis but do further underscore the significance of this work in emerging 3D GIScience data acquisition technologies and geovisual interfaces to be far more significant to Geography than simply as novel technologies.

It is my hope that this research helps others take a pragmatic look at EGT use in 3D GIScience. As EGTs, SfM and XR hold tremendous potential to influence the future of 3D GIScience. That future will be determined by our ability, as a research community, to develop the science that further legitimizes their use as useful scientific tools and not just as novel technology.

References

Andrienko, G., Andrienko, N., Jankowski, P., Keim, D., Kraak, M. J., MacEachren, A., & Wrobel, S. (2007). Geovisual analytics for spatial decision support: Setting the research agenda. International Journal of Geographical Information Science, 21(8), 839–857. https://doi.org/10.1080/13658810701349011

Chrisman, N. (1999). A transformational approach to GIS operations, International Journal of Geographical Information Science, 13:7, 617-637, DOI: 10.1080/136588199241030

Clark, A. (2003). Cyborgs Unplugged. In Natural Born Cyborgs. Oxford University Press. https://doi.org/10.1002/9781118922590.ch14

Çöltekin, A., Bleisch, S., Andrienko, G., & Dykes, J. (2017). Persistent challenges in geovisualization – a community perspective. International Journal of Cartography, 9333, 1–25. https://doi.org/10.1080/23729333.2017.1302910

Dangermond, J., & Goodchild, M. F. (2020). Building geospatial infrastructure. Geo-Spatial Information Science, 23(1), 1–9. https://doi.org/10.1080/10095020.2019.1698274

Dykes, J., MacEachren, A. M., & Kraak, M.-J. (2005). Exploring Geovisualization. In J. Dykes, A. M. MacEachren, & M.-J. Kraak (Eds.), Exploring Geovisualization (1st Edition, pp. 3–19). Pergamon.

Fairbairn, D., Andrienko, G., Andrienko, N., Buziek, G., & Dykes, J. (2001). Representation and its Relationship with Cartographic Visualization. Cartography and Geographic Information Science, 28(1), 13–28. https://doi.org/10.1559/152304001782174005

Goodchild, M. F. (1992). Geographical Information Science. International Journal of Geographic Information Systems, 6(1), 31–45.

Hedley, N. R., Billinghurst, M., Postner, L., May, R., & Kato, H. (2002). Explorations in the Use of Augmented Reality for Geographic Visualization. Presence: Teleoperators and Virtual Environments, 11(2), 119–133. https://doi.org/10.1162/1054746021470577

Horan, P. F., & Rosser, R. A. (1984). A Multivariable Analysis by Sex. Developmental Review, 4, 387–411.

Kahn, A. S., Vehring, L. J., Brown, R. R., & Leys, S. P. (2016). Dynamic change, recruitment and resilience in reef-forming glass sponges. Journal of the Marine Biological Association of the United Kingdom, 96(02), 429–436. https://doi.org/10.1017/S0025315415000466

Lavy, A., Eyal, G., Neal, B., Keren, R., Loya, Y., & Ilan, M. (2015). A quick, easy and non-intrusive method for underwater volume and surface area evaluation of benthic organisms by 3D computer modelling. Methods in Ecology and Evolution, 6(5), 521–531. https://doi.org/10.1111/2041-210X.12331

Minocha, S., Tilling, S., & Tudor, A.-D. (2018). Role of Virtual Reality in Geography and Science Fieldwork Education. https://doi.org/10.1021/acs.jctc.5b00907

Peters, M., Laeng, B., Latham, K., Jackson, M., Zaiyouna, R., & Richardson, C. (1995). A Redrawn Vandenberg and Kuse Mental Rotations Test. Different Versions and Factors That Affect Performance. Brain and Cognition, 28, 39–58.

Raoult, V., Reid-Anderson, S., Ferri, A., & Williamson, J. (2017). How Reliable Is Structure from Motion (SfM) over Time and between Observers? A Case Study Using Coral Reef Bommies. Remote Sensing, 9(7), 740. https://doi.org/10.3390/rs9070740

Shelton, B. E., & Hedley, N. R. (2004). Exploring a cognitive basis for learning spatial relationships with augmented reality. Technology, Instruction, Cognition and Learning, 1, 323–357. http://digitalcommons.usu.edu/itls_facpub/92/

Thomas, J., & Cook, K. A. (2005). Illuminating the path: the R&D agenda for visual analytics. National Visualization and Analytics Center, Institute of Electrical and Electronics Engineers, January 2005.

Tobler, Waldo. (1979). A Transformational View of Cartography. Cartography and Geographic Information Science - CARTOGR GEOGR INF SCI. 6. 101-106. 10.1559/152304079784023104.

Tuan, Yi-Fu. (1975). Place: An Experiential Perspective. Geographical Review 65, no. 2: 151–65. https://doi.org/10.2307/213970.

Vandenberg, S. G., & Kuse, A. R. (1978). Mental rotations, a group test of three-dimensional spatial visualization. Perceptual and Motor Skills, 47(2), 599–604. https://doi.org/10.2466/pms.1978.47.2.599

Virrantaus, K., Fairbairn, D., & Kraak, M. (2009). ICA Research Agenda on Cartography and GIScience. Cartography and Geographic Information Science, 36(2), 209–222. https://doi.org/10.1559/152304009788188772

Zhao, J., Wallgrün, J. O., LaFemina, P. C., Normandeau, J., & Klippel, A. (2019). Harnessing the power of immersive virtual reality - visualization and analysis of 3D earth science data sets. Geo-Spatial Information Science, 22(4), 237–250. https://doi.org/10.1080/10095020.2019.1621544